UAB
Universitat Autònoma de Barcelona

ELUCIDATING THE ROLE OF NATURAL KILLER CELLS IN HIV CONTROL AND EVALUATION OF A BISPECIFIC ANTIBODY TO ENHANCE THEIR FUNCTION

Nerea Sánchez Gaona

ADVERTIMENT. L'accés als continguts d'aquesta tesi queda condicionat a l'acceptació de les condicions d'ús establertes per la següent llicència Creative Commons:  https://creativecommons.org/licenses/?lang=ca

ADVERTENCIA. El acceso a los contenidos de esta tesis queda condicionado a la aceptación de las condiciones de uso establecidas por la siguiente licencia Creative Commons:  https://creativecommons.org/licenses/?lang=es

WARNING. The access to the contents of this doctoral thesis it is limited to the acceptance of the use conditions set by the following Creative Commons license:  https://creativecommons.org/licenses/?lang=en

Universitat Autònoma de Barcelona

Department of Biochemistry and Molecular Biology

Faculty of Biosciences

ELUCIDATING THE ROLE OF NATURAL KILLER CELLS IN HIV CONTROL AND EVALUATION OF A BISPECIFIC ANTIBODY TO ENHANCE THEIR FUNCTION

Nerea Sánchez Gaona

Vall d'Hebron Research Institute (VHIR)

Hospital Universitari Vall d'Hebron

Barcelona, June 2024

Doctoral thesis to obtain the PhD degree in Biochemistry, Molecular Biology and Biomedicine of the Universitat Autònoma de Barcelona

Director: Dr. Maria José Buzón

Tutor: Dr. Ibane Abasolo Oloartua

The Spanish Ministry of Science, Innovation and Universities supported the research performed in this thesis through the grant PRE2019-087393 (Project RTI2018-101082-B-100).

Table of contents

Abbreviations 1

1 Introduction 7

1.1 Human Immunodeficiency Virus 7

1.1.1 History and origin 7

1.1.2 State-of-the-art in HIV infection 7

1.2 HIV virus biology 8

1.2.1 HIV classification 8

1.2.2 HIV structure and genome 9

1.2.3 HIV replication cycle 11

1.3 HIV pathogenesis 14

1.3.1 Transmission 15

1.3.2 Primoinfection or acute phase 15

1.3.3 Chronic infection 16

1.3.4 AIDS 17

1.4 Antiretroviral treatment 17

1.5 HIV latency, reservoir, and persistence 20

1.5.1 Cellular reservoirs 21

1.5.2 Anatomical reservoirs 24

1.5.3 Reservoir establishment and maintenance 25

1.5.4 Mechanisms of reservoir maintenance 28

1.5.5 Measuring the HIV reservoir 29

1.6 Immune responses against HIV infection 31

1.6.1 Innate immunity 31

1.6.2 Adaptive immunity 32

1.7 Natural Killer cells 33

1.7.1 Definition 33

1.7.2 Development 34

1.7.3 Classification 35

1.7.4 NK cell receptors 37

1.7.5 NK cell effector mechanisms 40

1.8 NK cells in HIV infection 41

1.9 HIV controllers 42

1.9.1 Genetic factors 43

1.9.2 Adaptive immune responses 43

1.9.3 Innate immune responses 44
1.9.4 Viral reservoir configuration 45
1.9.5 Non-immunological factors 45
1.10 HIV cure strategies 45

2 Hypothesis and objectives 51

3 Results 55
3.1 Chapter 1 55
3.1.1 Title 55
3.1.2 Abstract 55
3.1.3 Graphical Abstract 56
3.1.4 Introduction 57
3.1.5 Materials and methods 59
3.1.6 Results 64
3.1.7 Discussion 80
3.1.8 Supplementary Data 85
3.2 Chapter 2 105
3.2.1 Title 105
3.2.2 Abstract 105
3.2.3 Introduction 106
3.2.4 Materials and methods 109
3.2.5 Results 118
3.2.6 Discussion 133
3.2.7 Supplementary Data 137

4 Discussion 149

5 Conclusions 163

6 References 169

7 Publications 209

Abbreviations

AC	Aborted Control
ADCC	Antibody-Dependent Cell-Cytotoxicity
AIDS	Acquired Immune Deficiency Syndrome
ART	Antiretroviral Therapy
AZT	Zidovudine
BiAbs	Bispecific Antibodies
bNAbs	Broadly Neutralizing Antibodies
caHIV-1 RNA	Cell-associated HIV-1 RNA
cART	Combined Antiretroviral Therapy
CCL3	C-C Motif Ligand 3
CCL4	C-C Motif Ligand 4
CCL5	C-C Motif Ligand 5
CCR5	CC Chemokine Receptor type 5
CDC	Centers for Disease Control
cDNA	Complementary DNA
CLPs	Common Lymphoid Progenitor Cells
CMV	Cytomegalovirus
CSF	Cerebrospinal Fluid
CTL	Cytotoxic T lymphocyte
CXCR4	CXC Chemokine Receptor type 4
DC	Durable Control
ddPCR	Droplet Digital PCR
DNA	Deoxyribonucleic Acid
dsDNA	Double-stranded DNA
EC	Ellite Controllers
ELISA	Enzyme-Linked ImmunoSorbent Assay
EMA	European Medicines Agency
Env	Envelope
EPV	Epstein-Barr virus
FACS	Fluorescence-Activated Cell Sorting
FBS	Fetal Bovine Serum
FDA	US Food and Drug Administration
FDC	Follicular Dendritic Cells
FISH	Fluorescence *In Situ* Hybridization
Gag	Group Specific Antigen
GALT	Gut Associated Lymphoid Tissue
HAART	Highly Active Antiretroviral Therapy
HD	Healthy Donors
HDAC	Histone Deacetylase
HESN	HIV-Exposed Seronegative Individuals
HIV	Human Immunodeficiency Virus
HLA	Human Leukocyte Antigens

HPCs	Hematopoietic Progenitor Cells
HPV	Human Papillomavirus
HSCs	Hematopoietic Stem Cells
HTLV	Human T-cell Leukemia Virus
IFI16	Interferon Inducible Protein
IFN	Interferon
IL	Interleukin
ILCs	Innate Lymphoid Cells
iNKs	Immature NK cells
iNKTs	Invariant Natural Killer T cells
IPDA	Intact Proviral DNA Assay
IQR	Interquartile Range
ISG	Interferon-stimulated genes
ITAMs	Immunoreceptor Tyrosine-Based Activation Motifs
ITIMs	Immunoreceptor tyrosine-Based Inhibition Motifs
KIRs	Killer Cell Immunoglobulin-like Receptors
LN	Lymph Nodes
LPS	Lypopolysaccharides
LRA	Latency Reversal Agents
LTR	Long Terminal Repeat
MHC	Major Histocompatibility Complex
MPPs	Multipotential Progenitors
mRNA	Messenger RNA
MS	Multiple Spliced
mVOA	Murine Viral Outgrowth Assay
NC	Natural Cytotoxicity
NCR	Natural Cytotoxicity Receptors
Nef	Negative factor
NFkB	Nuclear Factor Kappa-Light-Chain Enhancer of Activated B cells
NK	Natural Killer
NKPs	NK cell progenitors (NKPs)
NNRTI	Non-nucleoside Reverse Transcriptase Inhibitors
NRTIs	Nucleoside Reverse Transcriptase Inhibitor
PAMPs	Pathogen-Associated Molecular Patterns
PBMCs	Peripheral Blood Mononuclear Cells
PBS	Phosphate-Buffered Saline
PCR	Polymerase Chain Reaction
PD-1	Programmed Cell Death Protein 1
pDCs	Plasmacytoid Dendritic Cells
PIC	Pre-Integration Complex
PIs	Protease Inhibitors
POL	Polymerase
PRRs	Pattern Recognition Receptors
PWH	People with HIV

qPCR	Quantitative PCR
qVOA	Quantitative Viral Outgrowth Assay
Rev	Regulator of Expression of Virion Proteins
RNA	Ribonucleic Acid
RNAPII	RNA Polymerase II
RPMI	Rowell Park Memorial Institute
RT	Reverse Transcriptase
RT-qPCR	Reverse Transcription Quantitative PCR
SCA	Single Copy Assay
SCM	T Stem Cell Memory
SIMOA	Single-Molecule Array
SIV	Simian Immunodeficiency Virus
SLO	Secondary Lymphoid Organs
ssRNA	Single-Stranded RNA
STD	Sexually Transmitted Diseases
Tat	Trans-activating Regulatory Protein
TCM	T Central Memory
TEFb	Positive Transcription Elongation Factor B
TEM	T Effector Memory
TFH	T Follicular Helper
Th	T helper
TILDA	Tat/Rev Induced Limiting Dilution Assay
TLR	Toll Like Receptor
TNA	T Naive
TNF	Tumor Necrosis Factor
TREG	T Regulatory
TRM	Tissue Resident Memory
TTD	T Terminally Differentiated
TTM	T Transitional Memory
UNAIDS	Joint United Nations Programme on HIV/AIDS
US	Unspliced
VC	Viremic Controllers
VIF	Virion Infectivity Factor
VIR	Viremic
VPR	Viral Protein R
VPU	Viral Protein U

1. INTRODUCTION

1 Introduction

1.1 Human Immunodeficiency Virus

1.1.1 History and origin

In the early 1980s, the Center for Disease Control and Prevention (CDC) reported the first cases of Acquired Immune Deficiency Syndrome (AIDS), initially associated with an unknown virus later identified as Human Immunodeficiency Virus (HIV)[1]. AIDS was characterized by severe immunosuppression and opportunistic infections, notably affecting men who have sex with men, intravenous drug users, hemophiliacs, and blood transfusion recipients[2]. The transmission routes identified included sexual, bloodborne, and vertical transmission[3,4].

The epidemic garnered increasing global attention over preceding years, but it achieved worldwide recognition in 1983 when researchers definitively identified a retrovirus as the causative agent of pathological syndromes, notably AIDS[5]. HIV was initially designated as Human T-cell Leukemia Virus (HTLV), and was subsequently isolated by research groups affiliated with the National Institute of Health (NIH, USA) and the University of California (USCF, USA)[6–8]. In 1986, the International Committee of the Taxonomy of Viruses formally classified the virus as HIV[9]. The groundbreaking discovery of HIV was acknowledged with the Nobel Prize of Physiology or Medicine in 2008[10].

The development of the first diagnostic tools in 1985, the approval of the first antiretroviral drug in 1987 (zidovudine, AZT), and the later approval and optimization of a diverse spectrum of antiretroviral drugs represented a shift in the HIV infection management[3]. In 1997, empirical evidence substantiated that the combination of diverse antiretroviral drugs could effectively suppress HIV viremia below clinically detectable levels[11]. Current antiretroviral therapy (ART) regimens demonstrate efficacy in suppressing HIV replication in the majority of patients, yet complete eradication of the virus remains elusive.

1.1.2 State-of-the-art in HIV infection

Two decades ago, the global HIV/AIDS pandemic presented an alarming challenge, with over 2.5 million new HIV infections annually, and an associated mortality rate of 2 million lives per year. The HIV/AIDS pandemic has been responsible for nearly 76 million infections and 33 million people have died due to HIV/AIDS related complications since the start of the pandemic.

Currently, HIV infection persists globally. According to the United Nations Programme on HIV/AIDS (UNAIDS) data, 39 million [33.1 million-45.7 million] people are living with HIV infection (PWH) globally, from which 29.8 million are receiving treatment[12]. Despite the progress made, about 9.2 million PWH were not receiving treatment and about 2.1 million people were getting treatment but were not virally suppressed.

HIV infection prevalence varies globally, with East and Southern Africa being most affected, where 43% of all new worldwide infections take place[12]. Particularly, in Southern Africa, the epidemic has caused a reversal of life expectancy gains achieved over decades. Effective treatment has reduced AIDS-related deaths by 52% globally since 2010[12]. Access to ART has expanded notably in sub-Saharan Africa and Asia, with approximately 82% of the HIV-positive population residing there[12]. Improved access to treatment has averted an estimated 20.8 million deaths globally[12]. Almost 71% of PWH had suppressed viral loads in 2022, enabling them to live long, healthy lives with no risk of sexually transmitting HIV[13].

Although effective treatments have been developed, their accessibility is hindered by expensive costs, limiting its use to a privileged minority. Furthermore, the lack of effective vaccines and awareness among certain populations impede efforts to curtail HIV expansion. Achieving viral suppression is crucial, as evidence shows that it renders the virus non-transmissible[13]. Despite novel ART regimens reducing mortality rates and leading to chronicity, HIV infection remains a significant global health issue.

1.2 HIV virus biology

1.2.1 HIV classification

HIV belongs to the *Retroviridae* family, *Orthoretrovirinae* subfamily, and *Lentivirus* genus[14]. Retroviruses are found in a wide variety of vertebrate hosts and can cause various diseases, including cancer, immunodeficiencies, and neurological disorders[15].

HIV can be classified into two subtypes: HIV type 1 (HIV-1) and type 2 (HIV-2). Both types present similar transmission mechanisms and clinical outcomes, potentially progressing to the development of AIDS[16]. Predominantly, HIV infections are attributed to HIV-1. In contrast, the less virulent HIV type (HIV-2), more prevalent in West Africa, exhibits limited transmission capacity and infection rates[17,18]. Plasma viral load and levels of immune cell activation are reduced in HIV-2 infection, suggesting an enhancement of more potent and multifunctional antiviral cellular responses[19]. Both HIV-1 and HIV-2 trace their origins to the simian variant of HIV, known as simian immunodeficiency virus (SIV), primarily infecting non-human primates that serve as natural hosts to SIV[20].

Specifically, HIV-1 is reported to have originated from SIVcpz, originating in common chimpanzees, while HIV-2 demonstrates phylogenetic homology with SIVsmm, the simian immunodeficiency virus found in sooty mangabeys[21]. Extensive phylogenetic investigations have established that SIV likely persisted in non-human primates, including chimpanzees, for over 32,000 years, with multiple independent transmissions to humans[21–23]. Intriguingly, SIV, despite extensive virus replication in its natural host, such as sooty mangabeys, typically does not induce pathogenic effects. However, when present in a non-natural host, such as rhesus macaques, SIV often leads to immunodeficiency and heightened immune activation, events paralleling AIDS in HIV-1 infection[24,25]. In the context of this thesis, the usage of the term "HIV" refers to HIV-1, unless explicitly specified otherwise.

1.2.2 HIV structure and genome

HIV virions exhibit a spherical morphology with a diameter ranging from 119 to 207 nm, wrapped with an envelope formed by a lipid bilayer derived from the host cell[26] (**Figure 1**). Enclosed within the envelope are the matrix, a conically shaped-capsid core, and the nucleocapsid[27].

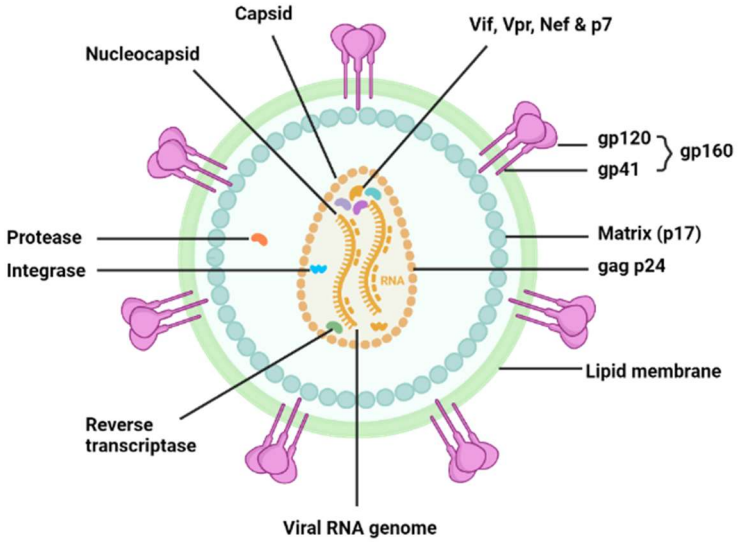


Figure 1 Schematic structure of the HIV virion. Adapted from: https://www.eenzyme.com/HIV-research-tools.aspx

The envelope contains embedded trimers of the envelope glycoproteins, encoded by the *env* gene (gp160), representing the only virus-encoding determinants on the viral surface. Gp160 comprises a gp120 surface protein tethered to the membrane by the gp41 transmembrane protein, facilitating attachment and fusion to the host cell, as well as interaction with CD4 molecules[28]. Furthermore, the envelope contains host-derived proteins, including cellular receptors, actin, ubiquitin, and MHC proteins.

The matrix provides structural and mechanical support to the virion, and surrounds the conically-shaped capsid core and the nucleocapsid. The nucleocapsid harbors two copies of positive single-stranded RNA molecules (ssRNA), each approximately 9.88 kb in length, flanked by repetitive sequences identified as long terminal repeats (LTR)[29]. The non-coding LTR regions, comprised of U3, R, and U5 regions, serve as pivotal sites for viral integration, packaging, and transcriptional regulation[30]. These regions play a critical role in establishing latency, with the 5'LTR region serving as a transcriptional regulator for various transcription factors, including C-Myc, NFkB, USF, AP1, COUP, TCF-1a, and SP1. These factors collectively regulate HIV transcription[31]. For instance, SP1 recruits C-Myc to the 5'LTR, leading to the subsequent recruitment of histone deacetylation 1 (HDAC1). This recruitment prompts chromatin remodeling, ultimately suppressing viral gene expression.

The HIV genome encodes nine genes: three major genes responsible for structural proteins (*gag, pol*, and *env*), two regulatory genes (*tat* and *rev*), and four accessory genes (*vif*, *vpr*, *vpu*, and *nef*), that determine the synthesis of regulatory and accessory proteins essential for the viral life cycle[32,33] (**Figure 2**).

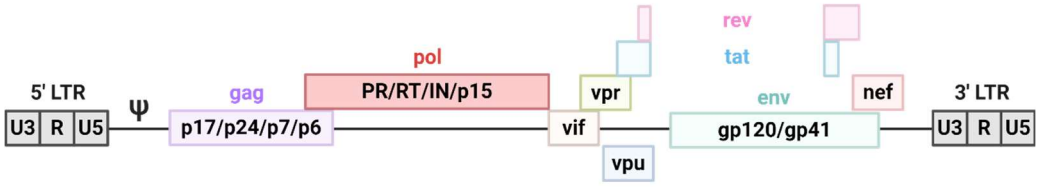


Figure 2. Schematic structure of the HIV genome. Adapted from [34].

- Major structural genes:
    - *Gag* (Group Specific Antigen). Encodes for the Gag polyprotein, processed during maturation to yield structural proteins p17, p24, p7 and p6.
    - *Pol* (Polymerase). Encodes for viral enzymes, including reverse transcriptase (transcribes DNA from RNA), integrase (integrates double-stranded RNA into the host genome), and protease (cleaves the precursor Gag polyprotein to produce structural proteins).
    - *Env* (Envelope). Encodes gp160, the precursor of gp120 and gp41 proteins embedded in the viral envelope.
- Regulatory genes:
    - *Tat* (Trans-Activating Regulatory Protein). Codifies for the Tat protein, which positively regulates the reverse transcription of viral RNA.

- *Rev* (Regulator of Expression Proteins): Encodes the Rev protein, that regulates the export of non-spliced and partially spliced viral transcripts between the nucleus and the cytoplasm.

- Accessory genes:
  - *Vif* (Virion Infectivity Factor). Encodes the Vif protein, which is critical for the infectious virus production.
  - *Vpr* (Viral Protein R). Encodes the Vpr protein, that facilitates the nuclear import of cDNA, transactivates HIV promoters, inhibits cellular growth, induces cellular differentiation, and has been described to counteract the host's antiviral response[28,35,36].
  - *Vpu* (Viral Protein U). Encodes the Vpu polypeptide, that induces virion release from the infected cell surface, and participates in CD4 degradation. Along with Vif, Vpu interacts with the restriction factors APOBEC3G and Tetherin, counteracting their antiviral effects and promoting HIV expansion[37].
  - *Nef* (Negative Factor Nef). Encodes the Nef protein, which has influence on HIV replication by downregulating CD4 on target cells and enhancing infectivity by negatively regulating MHC class I molecule expression.

1.2.3 HIV replication cycle

The HIV replication cycle encompasses a series of sequential steps in which both viral components and cellular host elements synergistically contribute. The explanation of each step is detailed as follows (**Figure 3**):

1. Binding and fusion. The viral glycoprotein gp120 binds to CD4, which is the primary cellular receptor for HIV, expressed on the surface of target cells. CD4 is predominantly found on circulating T lymphocytes and, occasionally, on macrophages[38,39]. The interaction between the viral protein and the target receptor facilitates the binding, but alone is insufficient for infection, necessitating additional co-receptors to facilitate membrane fusion. This binding event induces a conformational change in gp120, exposing the co-receptor binding site (V3 loop), enabling interaction with either CCR5 or CXCR4 as co-receptors[40–42]. Of note, the specific co-receptor employed for cellular entry determines the virus tropism, classified as R5-, X4-, or dual-tropic[43]. The binding of gp120 to CD4 and the co-receptor induces a conformational change in gp41, initiating fusion between the viral and cellular membranes, resulting in the release of the viral capsid into the cytoplasm. Subsequently, the viral capsid enters the nucleus, and uncoats in close proximity to the integration site[44].

2. Reverse transcription. Despite the traditional consensus in the field that reverse transcription occurred in the cytoplasm, recent discoveries indicate that this process occurs within the nucleus. During this step, the reverse transcriptase enzyme switches templates between the two co-packaged ssRNA strands, leading to the synthesis of one double-stranded DNA molecule (dsDNA)[45]. Due to the absence of proofreading mechanisms, this process introduces high rates of DNA base pair mutations, contributing to the rapid viral evolution[46,47]
3. Integration. Following reverse transcription, the dsDNA is integrated into the host cell genome through the action of the viral enzyme integrase in a two-step process[48]. During the initial step, referred to as 3' end processing, the integrase primes the viral DNA by removing two nucleotides from both 3' ends of the viral DNA. Subsequently, the viral DNA binds to integrase complexes, involving other host cell and viral proteins, forming the viral pre-integration complex (PIC). Then, the viral enzyme integrase catalyzes the second step of the integration process, termed "strand transfer". This step involves the ligation of the processed DNA into the host chromosome. Viral genome integration can occur in distinct genome regions, including regions characterized by lower transcriptional activity, allowing the virus to persist in a latent state within the host cell. However, integration is not entirely random, as certain studies suggest a tendency for the virus to integrate into regions of high genetic activity[49–51]. Once integrated into the host genome, the HIV DNA is referred to as provirus, and the host cell undergoes permanent and irreversible infection.
4. Transcription and translation. Upon receiving an activation signal, the host cell undergoes transcription of the provirus into mRNA utilizing the host cellular RNA polymerase II (RNAPII). Viral gene transcription is initiated at the U3 promoter of the LTR region, with the initial synthesis of the Tat protein, crucial for elongation and subsequent protein production[52]. Subsequently, HIV transcripts undergo multi-splicing to generate mature mRNA for *Tat*, *Rev*, and *Nef*. Smaller mRNAs are directly transported to the cytoplasm for translation into viral proteins Tat and Rev. By contrast, unspliced and single spliced forms require Rev function for transport to the cytoplasm[52]. Once a sufficient quantity of protein is produced, Tat and Rev return to the nucleus. Tat enhances the transcription rate by recruiting TEFb (Positive Transcription Elongation Factor B) and promoting elongation[53]. The accumulation of Rev in the nucleus induces the transcription of single and unspliced mRNAs of *Gag*, *Pol*, *Env*, *Vif*, *Vpr*, and *Vpu*.

Once the mRNAs are obtained, all transcripts are transported to the cytoplasm, processed, and translated into viral proteins[54]. Env proteins are directed to the plasma membrane, while *Gag* and *Pol* products are directed to the cell membrane.

5. Viral assembly and budding. The assembly of new HIV virions takes place at specialized plasma membrane microdomains of the host cell[55]. The env precursor is processed by cellular proteases, leading to the generation of gp41 and gp120 proteins. Simultaneously, the Gag precursor within the nucleocapsid domain promotes the formation of an immature capsid. The immature capsid recruits newly synthesized viral RNA genome molecules and viral enzymes, including reverse transcriptase, integrase, and protease, facilitating virion assembly. The matrix domain of the immature virion directs Gag to the plasma membrane, promoting the incorporation of Env glycoproteins into the forming virions, a process known as budding[56]. To enable viral assembly and budding, the levels of CD4 expression at the cellular surface must decrease, in order to prevent new virions from re-infecting the same cell through gp120 interaction. To achieve this, the Nef accessory protein downregulates CD4 levels, accelerating its endocytosis and subsequent degradation[57].
6. Maturation. The viral particles released by infected cells undergo a maturation step to become infectious viruses[58]. This maturation process is orchestrated by the viral protease, which processes the Gag and Gag-Pol polyprotein precursors, yielding the matrix, capsid, nucleocapsid, p6, protease, reverse transcriptase, and integrase viral enzymes[56,59].

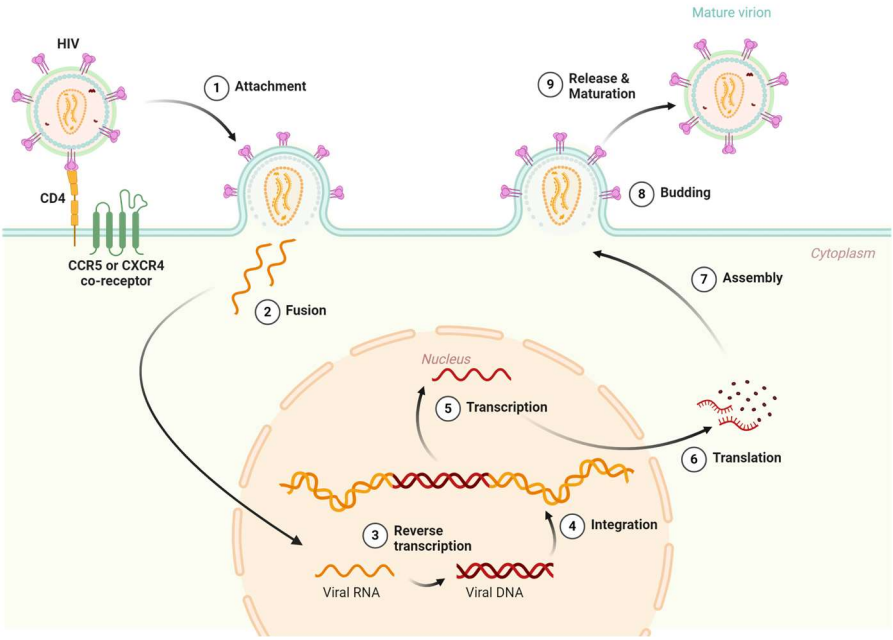


Figure 3. Schematic overview of the HIV replication cycle. The figure depicts the main steps in the HIV life cycle comprising: (**1**) initial attachment of the viral particle to the target cell facilitated by CD4 and co-receptor CCR5 or CXCR4 interaction; (**2**) fusion with the host cell membrane, subsequent uncoating of the viral capsid, and release of HIV RNA genome and proteins into the nucleus; (**3**) reverse transcription of the viral RNA genome into dsDNA, followed by(**4**) integration into the host cell genome; (**5**) transcription of the proviral DNA into new viral RNA, followed by (**6**) translation to generate viral proteins, which then translocate to the cell surface and (**7**) assemble in the cell membrane to produce new viruses. Finally, the newly formed viral particles are (**8**) released and undergo maturation until they attain the status of mature virions. Adapted from: https://www.niaid.nih.gov/diseases-conditions/hiv-replication-cycle

1.3 HIV pathogenesis

The natural course of HIV infection is characterized by three distinct stages: 1) the acute phase or primoinfection, 2) the chronic phase, and 3) AIDS (**Figure 4**).

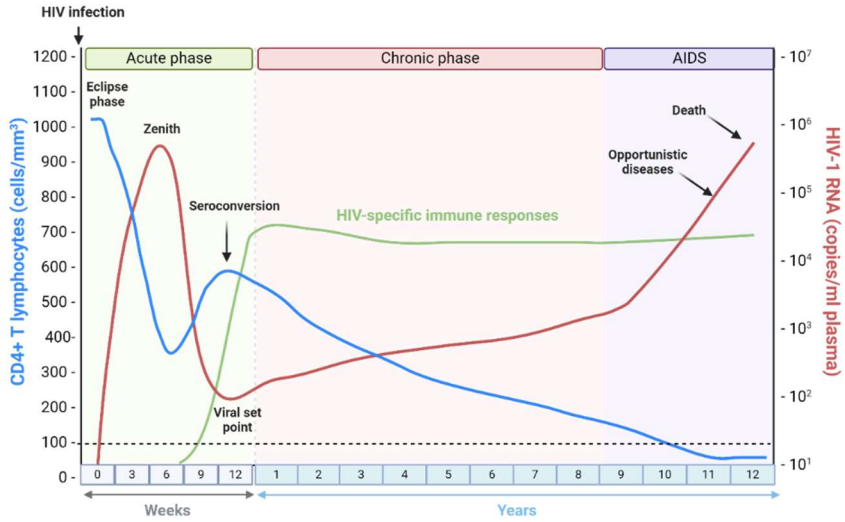


Figure 4. Schematic representation of the natural course of HIV infection in the absence of ART. $CD4^+$ T lymphocyte counts are shown in blue, HIV-RNA copies/ml in red, and HIV-specific immune responses in green. Adapted from[60].

Typically, during the acute phase, HIV infection induces a progressive decline in the number of $CD4^+$ T cells (<200 cells/mm^3), concomitant with an elevation in HIV viral load and immune cell activation. Subsequent to this phase, there is a partial recovery in $CD4^+$ T cell counts, and HIV viral load decreases due to the active engagement of the immune system. After an asymptomatic period lasting 8 to 10 years, there is a gradual decline in $CD4^+$ T cell numbers over time, leading to infection chronicity and progression to AIDS[60]. AIDS is characterized by a significant reduction in $CD4^+$ T lymphocyte counts, fostering the development of opportunistic infections and cancers, ultimately resulting in death. HIV pathogenesis and the progression to AIDS are contingent upon the infecting viral strain and the host immune response against the virus. Monitoring HIV infection involves clinical tests, the assessment of parameters such as $CD4^+$ T cell counts, viral RNA plasma concentration, the assessment of clinical manifestations, and the emergence of opportunistic infections, among other factors.

1.3.1 Transmission

HIV transmission occurs through the exchange of body fluids containing the virus, including blood, semen, vaginal secretions, and breast milk, primarily originating from infected individuals[61]. Additionally, vertical transmission, from an infected mother to her child during pregnancy or childbirth, constitutes another mode of transmission[62]. The risk of infection is contingent upon various factors, including the specific route of transmission, the viral concentration within the exposed body fluid, the presence of other sexually transmitted diseases (STD), and the susceptibility of the recipient.

1.3.2 Primoinfection or acute phase

The primary mode of HIV transmission is sexual, initiating viral spread from the anal or vaginal mucosa through the monocyte/macrophage system and lymphatic tissue, where it encounters its target cells, primarily $CD4^+$ T lymphocytes. Dendritic cells, also susceptible to infection, are capable of capturing the virus on their surface via lectins and other binding molecules, migrating to secondary lymphoid organs (SLOs) and facilitating viral dissemination to regional lymph nodes (LNs) and blood, aided by $CD4^+$ T cells[63–65]. HIV disrupts gut-associated lymphoid tissue (GALT), leading to an increase of bacterial products, such as lipopolysaccharides (LPS), in mesenteric LNs, thereby inducing chronic inflammation[66,67].

The initial days following HIV infection constitute the “eclipse phase”, which is characterized by viral replication and dissemination through various tissues and organs without detectable viremia in plasma or clinical symptoms[68].

Approximately 10-12 days post-infection, viral loads become detectable in blood, indicating the onset of acute infection, which persists for 2 to 9 weeks[69,70]. During this phase, significant viral replication occurs in mucosal lymphatic tissue and regional LNs, leading to a peak in plasma viremia around day 18-21 (10^5-10^9 HIV RNA copies/ml plasma), accompanied by a marked decrease in $CD4^+$ T cells[70]. During this phase, PWH may manifest a virus-like illness characterized by fever, pharyngitis, lymphadenopathy, and rash[71]. Some individuals experiencing severe symptoms may progress rapidly to AIDS in the absence of ART[72,73].

Elevated viral load levels are transient as the host mounts humoral and cellular immune responses that partially control HIV replication. Following the peak of plasma viremia, the immune system produces antibodies -a process termed seroconversion- against HIV viral proteins, leading to a substantial decrease in HIV viremia over two weeks[74]. Seroconversion occurs between 3 to 9 weeks post-infection and marks the end of the acute phase, where immune responses reduce plasma viremia, establishing a virologic set point predictive of disease progression, alongside an increase in $CD4^+$ T cell counts. The period from infection initiation to antibody detection is known as the “window period” (**Figure 5**).

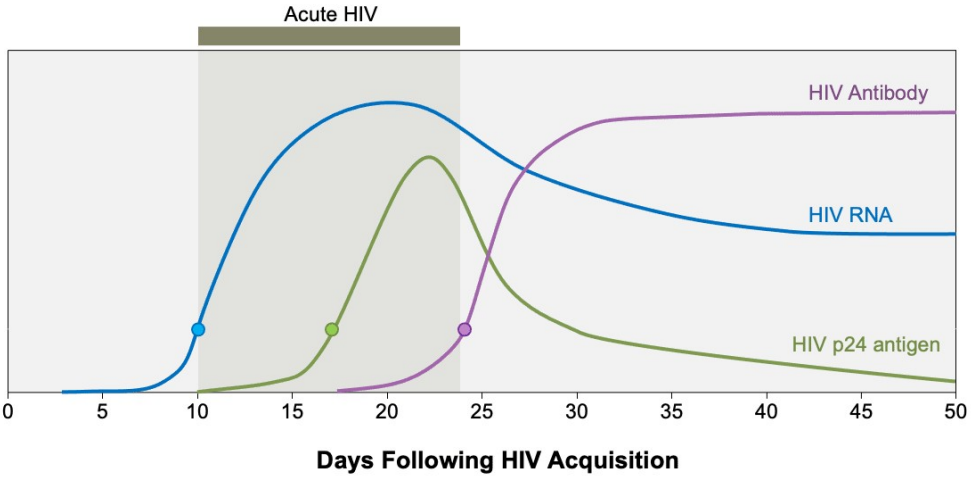


Figure 5. Diagram illustrating the acute phase of HIV infection. The acute phase, formerly referred to as primary HIV infection, denotes the period following HIV acquisition, characterized by the emergence of detectable HIV RNA and HIV p24 antigen in the absence of anti-HIV antibodies. Extracted from: https://www.hiv.uw.edu/go/screening-diagnosis/acute-recent-early-hiv/core-concept/all.

1.3.3 Chronic infection

Following acute infection, HIV enters a chronic, typically asymptomatic phase, termed clinical latency[75]. Stable $CD4^+$ T cell levels characterize this stage, with decreased viral load due to effective cellular and humoral immune responses[76].

$CD8^+$ T cells recognize viral antigens on infected cells and elicit cytotoxic responses, contributing to viral containment, while antigen-specific antibodies neutralize viral particles and induce cytotoxic responses, including Natural Killer (NK) cell recruitment and antibody-dependent cell cytotoxicity (ADCC) responses[77–80].

Despite lacking clinical symptoms, constant immune stimulation occurs from persistent viral antigen exposure. Continuous viral replication and active viral dissemination into new cells sustain this immune activation. Reservoir cells harbor integrated viral copies, known as provirus, with low or absent antigen levels[81]. Within this phase, HIV establishes a state of low yet persistent viral replication, contributing to immune activation and systemic chronic inflammation. The duration of these responses eventually leads to immune system exhaustion and an inability to control viral replication, resulting in a gradual decline in peripheral $CD4^+$ T cell counts, marking the end of the chronic phase[76]. In the absence of treatment, clinical latency may persist for 7 to 10 years, varying among individuals.

1.3.4 AIDS

Persistent antigen exposure and sustained immune activation lead to alterations in regulatory and effector immune responses, culminating in the emergence of opportunistic infections during the later stage, AIDS. AIDS is characterized by uncontrolled HIV replication, a sharp increase in viral load, and $CD4^+$ T cell decline below 200 cells/mm^3. $CD4^+$ T cell levels during this phase determine the onset of AIDS-defining illnesses, including opportunistic infections, HIV-associated cancers, and kidney failure, often leading to death within 11 years in the absence of treatment[82].

1.4 Antiretroviral treatment

The development of ART has modified the natural course of HIV infection, achieving one of the major breakthroughs in the field. The introduction of the first antiretroviral drug, zidovudine (AZT), in 1987 transformed the course of HIV infection from a potentially fatal disease to a manageable condition capable of achieving a chronic phase, accompanied by a significantly elevated survival rate[83,84]. Over 40 antiretroviral drugs have been developed and approved by regulatory organizations such as the US Food and Drug Administration (FDA) and the European Medicines Agency (EMA) for the management of HIV (**Figure 6**).

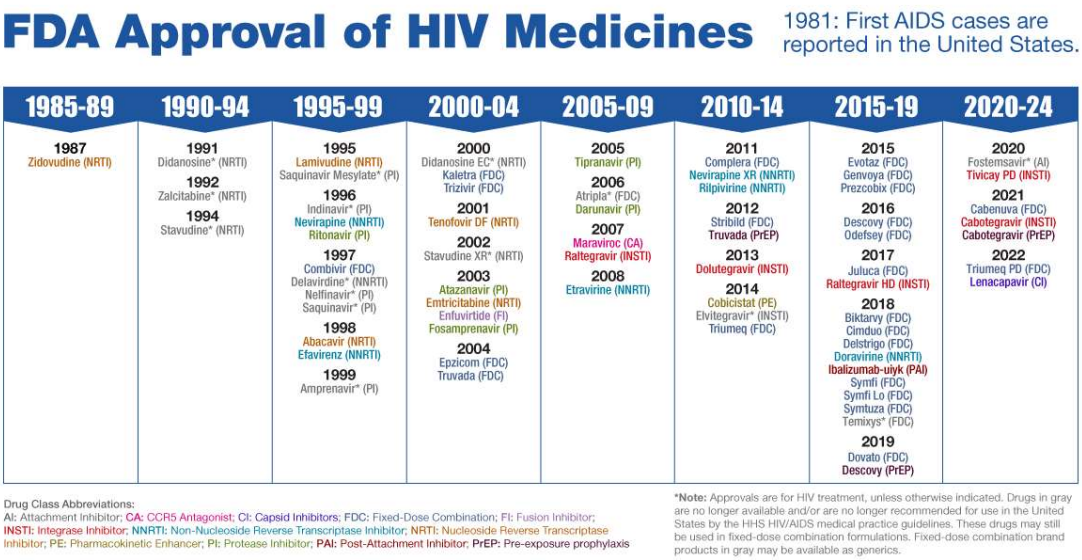


Figure 6. Temporal overview of FDA-approved drugs for HIV. Obtained from: https://hivinfo.nih.gov/understanding-hiv/infographics/fda-approval-hiv-medicines.

To date, five distinct families of antiretroviral drugs have been described, designed to target specific stages in the viral replication cycle (**Figure 7**)[58,85].

1) Integrase inhibitors (INIs). Prevent integration of viral DNA into the host genome.
2) Reverse transcriptase inhibitors.
    - Nucleoside/nucleotide-analog reverse transcriptase inhibitors (NRTIs). Defective nucleotides that are incorporated into viral DNA, inhibiting viral transcription.
    - Non-nucleoside reverse transcriptase inhibitors (NNRTIs). Block the reverse transcriptase activity by binding to its active site and inducing a conformational change, thus inhibiting their DNA polymerase activity.
3) Protease inhibitors (PIs). Inhibit the protease enzyme, impeding the splicing of the Gag and Gag-Pol precursor polyproteins, resulting in defects in viral particle maturation.
4) Fusion inhibitors. Interfere with HIV binding, fusion, and entry into host cells.
5) Entry inhibitors. Block HIV binding to the co-receptor CCR5 or CD4 receptor.

In addition, ongoing clinical trials are evaluating the efficacy of a novel ART family, capsid inhibitors[86,87].

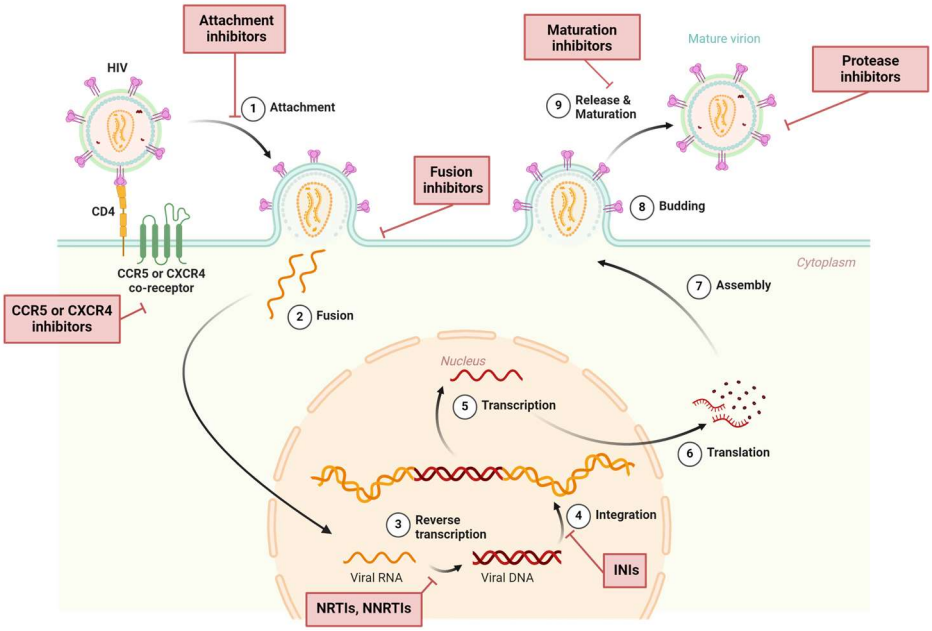


Figure 7. Antiretroviral therapy (ART) targets. Each step of the HIV life cycle, including entry, reverse transcription, integration, and viral protein maturation, can be targeted by several families of antiretroviral drugs. *NRTIs, Nucleoside/nucleotide-analog reverse transcriptase inhibitors; NNRTIs, Non-nucleoside reverse transcriptase inhibitors; INIs, Integrase inhibitors*.

Initially, mono or dual therapies for HIV led to drug resistance due to reverse transcriptase mutations[88]. Consequently, triple-drug therapy, termed highly active ART (HAART) or combined ART (cART) since 1996, achieved prolonged HIV suppression[89,90]. Current regimens involve a combination of three drugs from two families, thus reducing viral replication to undetectable levels and restoring $CD4^+$ T cell counts in most PWH. Subsequently, ART partially counteracts the immunological damage and lowers the risk of progressing to AIDS, thereby extending the life expectancy of PWH to levels near that that of the general population[91,92]. In addition, adherence to daily therapy is crucial, as highly adherent individuals exhibit negligible levels of viral transmission[93].

Starting ART immediately upon diagnosis is associated with improved outcomes, while early initiation during acute infection provides additional benefits, including lower disease progression, preserved $CD4^+$ T cell counts, and reduced lymphoid tissue destruction[89,94]. However, ART is unable to cure HIV due to the establishment of viral reservoirs, requiring lifelong treatment administration and exploration of new strategies[95–97]. Additionally, ART is associated with several comorbidities, including hypertension and neuropsychiatric conditions[98].

1.5 HIV latency, reservoir, and persistence

ART effectively suppresses HIV replication, reducing HIV RNA levels below detection limits, and bolstering immune system reconstitution, thereby resulting in a decrease in viral transmission[92,93]. Despite these advancements, HIV infection remains incurable. The discovery in 1995 of integrated HIV DNA within resting $CD4^+$ T cells marked a pivotal moment in understanding the persistent nature of the virus[99]. Latent infection represents a non-productive state characterized by the presence of transcriptionally inactive cells capable of inducible replication-competent virus production. The cellular or anatomical compartments that contain such replication-competent viruses for prolonged periods of time are designated as reservoirs (**Figure 8**)[100]. Reservoirs can persist for longer periods within the host relative to cells undergoing active replication, and constitute the primary causative factor for viral rebound following the interruption of antiretroviral therapy, thereby representing the main obstacle for HIV cure[101,102].

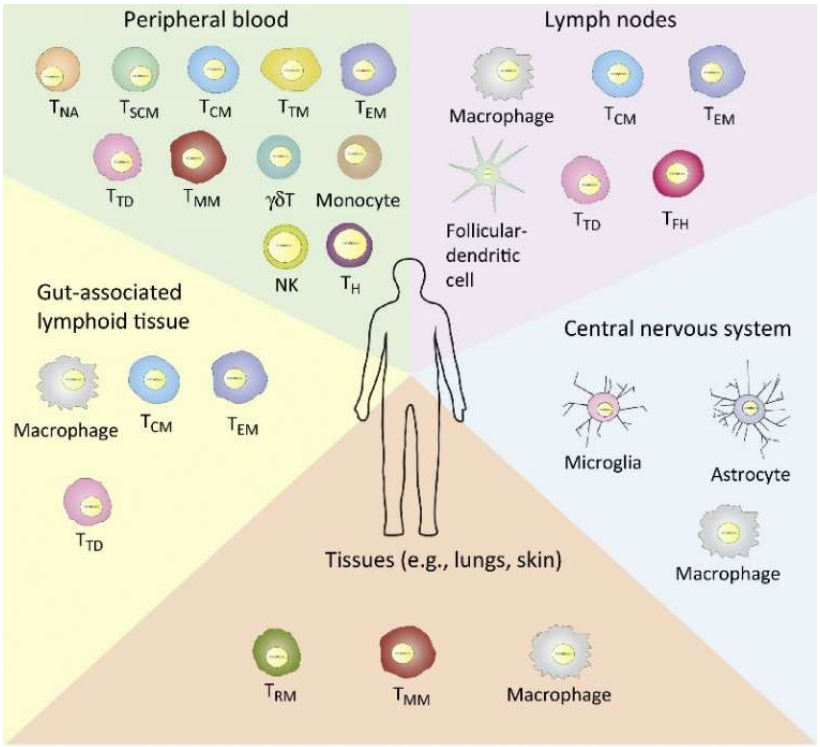


Figure 8. Latent HIV poses a multifaceted challenge, involving various factors. A schematic depiction is provided illustrating the diverse cells and tissues that contribute to HIV persistence during ART. Extracted from [103].

Reservoir dynamics vary throughout the course HIV infection. Although reservoirs are detectable early post-infection, their reduction in blood occurs upon ART initiation, yet heterogeneity exists among individuals[104–106]. Recent advances in measurement and characterization techniques have enhanced comprehension of HIV reservoirs and their inherent diversity.

Two primary reservoir categories exist:

- Latent. Integrated within the host genome, dormant proviruses remain transcriptionally inactive but capable of viral production upon stimulation, rendering resistant to the effects of ART or the immune system[97,107,108].
- Transcriptionally active. Involve active viral transcription, resulting in the production of viral RNA and proteins, thereby being susceptible to therapeutic interventions[109–111].

1.5.1 Cellular reservoirs

The primary cellular target and reservoir for HIV infection are CD4⁺ T lymphocytes, due to the need of specific interaction of the viral glycoprotein gp120 with the CD4 receptor during viral entry. Notably, distinct subpopulations, particularly memory CD4⁺ T lymphocytes, significantly contribute to the persistence of HIV in PWH[112].

1.5.1.1 CD4⁺ T cell classification by differentiation and memory status

Memory CD4⁺ T lymphocytes are a subject of extensive research due to their ability to foster latent HIV and establish long-term resistant viral niches[99,113]. Studies in the late 90s demonstrated the activation of replication-competent HIV in CD4⁺ T lymphocytes from long-term treated individuals[95–97]. Subsequently, the quantitative viral outgrowth assay (QVOA) was developed to measure the length of the replication-competent viral reservoir in peripheral blood from PWH[114]. Memory CD4⁺ T cells are highly heterogeneous, with distinct subpopulations distinguished by marker expression, maturation state, activation, differentiation, function, and half-life (**Figure 9**).

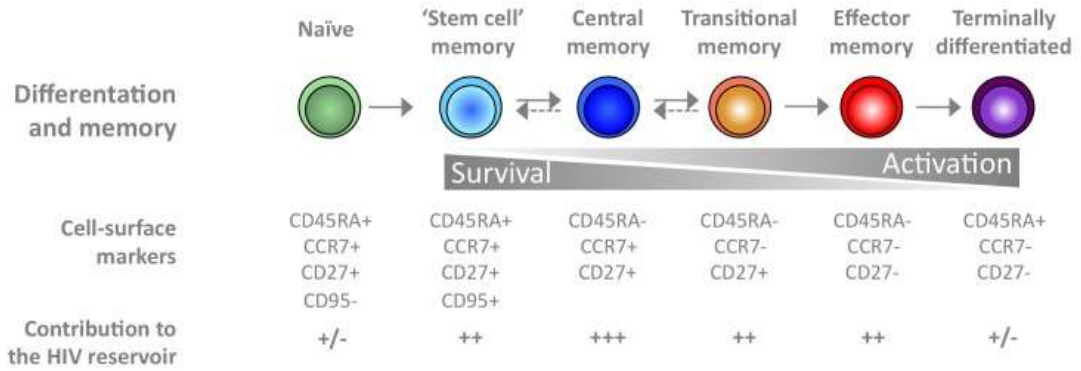


Figure 9. Contribution of CD4⁺ T cell subsets to the HIV reservoir during ART. CD4⁺ T cell subsets can be classified according to their differentiation and memory status. Extracted from[115].

Studies have revealed that different CD4⁺ T cell subsets harbor distinct amounts of latent HIV proviruses, and the mechanisms supporting viral persistence may differ.

Central memory (T_{CM}), transitional memory (T_{TM}), and effector memory (T_{EM}) populations in peripheral blood exhibit the highest proportions of HIV DNA. T_{CM} and T_{EM}, as primary memory subpopulations, can be differentiated based on several criteria:

- Immediate effector functions. Upon antigenic stimulation, T_{EM} exhibit immediate effector functions, in contrast to T_{CM}, which lack such immediate responses.
- Chemokine expression. T_{CM} express migration receptors such as CCR7 and CD62L, facilitating migration to SLO, whereas T_{EM} lack the expression of these receptors.
- Cytokine production. T_{CM} can produce IL-2 in response to antigenic stimulation, while T_{EM} produce IFN_{γ}.
- Intracellular signaling. T_{CM} exhibit pro-survival signals, whereas T_{EM} display pro-apoptotic markers.

Upon antigenic stimulation, T_{CM} differentiate into T_{EM}, which present a long half-life in blood and self-renewal abilities, contributing significantly to the pool of total infected cells[113,116]. By contrast, T_{EM} exhibit higher proliferative capacity and intact viral genomes but contribute less to the total pool of infected cells[117,118]. Additionally, naïve (T_{NA}) and terminally differentiated (T_{TD}) $CD4^+$ T cells contain HIV DNA, although at lower frequencies than the other mentioned T cell subsets. Of note, recent studies underscore the importance of T_{NA} as a significant viral reservoir for HIV[119,120]. These cells contain infectious viral sequences, express elevated levels of the CXCR3 coreceptor, making them susceptible to HIV infection, and display high survival rates[113,121,122]. Additionally, they possess the ability to generate diverse memory subpopulations, thereby representing a significant obstacle to HIV eradication.

Transitional memory (T_{TM}) cells represent an intermediate between T_{CM} and T_{EM}, and contribute substantially to the total viral reservoir[113]. $CD4^+$ T stem cell memory (T_{SCM}) represent a minor population with stem-cell-like properties and contribute significantly to the viral reservoir, although present lower levels of HIV DNA compared to other memory $CD4^+$ T cell subsets[105]. By contrast, tissue-resident memory (T_{RM}) cells, are non-circulating lymphocytes that express CD69 and are found in various tissues, and play a key role in the immune response against invading pathogens[123]. Of note, in women with HIV, T_{RM} cells in cervical mucosa have been identified as preferential targets for HIV and represent the primary cellular reservoir in this tissue[124].

1.5.1.2 CD4⁺ T cell classification by function

CD4⁺ T cell subpopulations are traditionally defined based on their migratory potential to SLO and effector functions. However, post-activation, they exhibit distinct effector functions, leading to an alternative classification based on the cytokine profile produced and the expressed chemokine receptors[125,126] (**Figure 10**):

- T helper cells (Th). Includes several types of cells:
    - *Th1*. These cells contribute to HIV persistence through antigen-induced proliferation, harboring intact viral genomes[127].
    - *Th2*. During HIV infection, a reported shift from Th1 to Th2 occurs. Th2 cells are associated with anti-inflammatory cytokines and play a role in the altered immune response observed[128].
    - *Th9*. Specialized in antitumoral responses, Th9 cells are enriched in viral genomes with X4 tropism[129].
    - *Th17*. These cells present certain stem cell properties, including long-life, self-renewal, and survival, and may serve as long-lived reservoirs[130].
    - *Th22*. Playing a protective role in HIV infection, the proliferation of circulating Th22 cells after successful ART suggests potential immunological advantages for suppressing HIV infection[131].
- T regulatory cells (T_{Reg}). These cells are crucial in the control of immune activation during HIV infection, but their expansion may weaken HIV-specific responses, potentially contributing to viral persistence[132,133].
- T follicular helper cells (T_{FH}). Identified as viral reservoirs, these cells are localized in B follicles of SLO, where they promote B cell maturation. Of note, T_{FH} cells are highly enriched in HIV, and constitute one of the cellular compartments with heightened permissiveness for viral replication and particle production, which establishes them as a significant obstacle for HIV eradication[134,135].

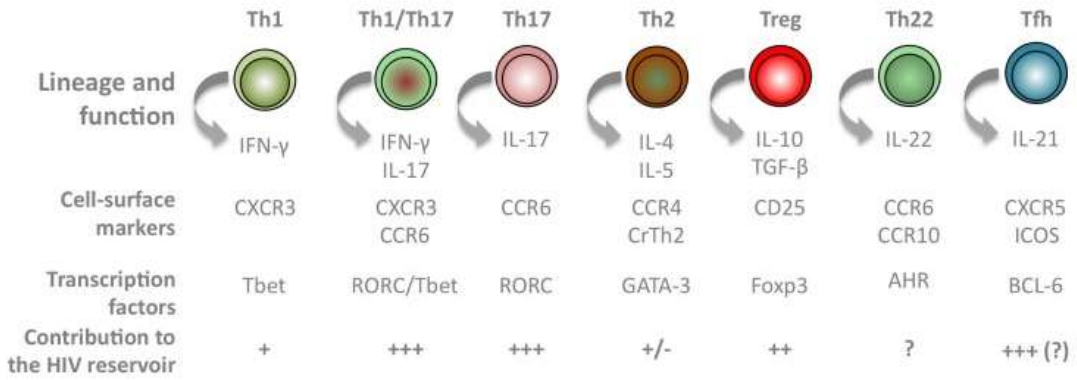


Figure 10. Classification of CD4⁺ T cell subsets based on their effector functions. The relative contribution of each subset to the HIV reservoir is indicated. Extracted from[125].

1.5.1.3 Other cellular reservoirs

Additionally, cells of the myeloid lineage, including monocytes, macrophages, and dendritic cells, have been suggested to be permissive to HIV infection despite their lower CD4 receptor expression compared to $CD4^+$ T lymphocytes[136–138]. Monocytes, originating from myeloid progenitors in the bone marrow, rarely host HIV in peripheral blood but can disseminate into various tissues and differentiate into macrophages[139]. Macrophages, particularly those residing in tissues such as the lung, central nervous system, intestine, and male reproductive system, have been implicated in the viral reservoir[140–143]. Notably, urethral tissue macrophages in ART-treated individuals have been identified as an important HIV reservoir, harboring replication-competent virus[144]. On the contrary, minimal quantities of proviral DNA have been detected in dendritic cells in vivo. However, the main impact of dendritic cells on the HIV reservoir appears to lie in their ability to capture HIV virions and facilitate their transmission to $CD4^+$ T cells[145].

1.5.2 Anatomical reservoirs

HIV reservoirs have been extensively investigated in peripheral blood; however, it is imperative to recognize that circulating $CD4^+$ T lymphocytes constitute less than 2% of the total lymphocyte population within the human body[146]. Consequently, distinct dynamics may be occurring in various tissues, underscoring the importance of examining the HIV reservoir across diverse anatomical compartments. Several studies have identified specific tissues as preferential sites for HIV persistence, including LNs, the intestinal tract, and the genital tract, where elevated frequencies of cells containing HIV genomes have been documented[124,147]. Notably, intact viral genomes with potential infectivity have been detected in up to 28 distinct anatomical compartments, emphasizing the need to eliminate all these reservoirs for a successful cure due to their high viral load levels[148].

SLOs, including the spleen, LNs, and GALT, serve as pivotal sites for viral replication during active HIV infection, with detectable HIV DNA persisting even after years of ART[149,150]. Secondary lymphoid tissues contain cells harboring competent viral reservoirs, particularly within B cell follicles, that exhibit heightened viral RNA production, playing a crucial role in sustaining HIV persistence[151,152]. Several factors contribute to the increased viral transcription within B cell follicles, including:

1) Permissiveness of T_{FH} cell populations. T_{FH} cells, including T follicular regulatory cells, are highly permissive to viral infection compared to other extra-follicular cell populations[153].

2) Presence of extracellular HIV virions on follicular dendritic cells (FDC). In the B cell follicle, extracellular HIV virions constitute a significant reservoir, accumulating on the surface of FDCs within germinal centers. These virions retain their infectious potential and can persist for long periods of time[68].
3) Immune privilege partially evading cytotoxic T lymphocyte (CTL) control. The B cell follicle serves as an immune-privileged site for HIV due to reduced immune surveillance by CTLs, partially attributed to decreased expression of the follicular migratory receptor CXCR5[154]. This leads to lower frequencies of HIV-specific CTLs within follicles compared to extrafollicular regions. Additionally, CTLs within follicles may exhibit compromised functionality, further impairing immune surveillance[155,156].
4) Potential deficiencies in drug penetration. Some studies have suggested that these compartments may present a less efficient drug penetration[157].

In addition to LNs, the GALT experiences significant alterations during early HIV infection, serving as a major primary site for viral replication and latent $CD4^+$ T cell reservoirs. The intestinal tract, rich in lymphoid tissue and susceptible target cells expressing high levels of CCR5, undergoes considerable T cell depletion upon HIV infection, resulting in damage, microbial translocation, and sustained immune activation, persisting despite ART[158,159]. In treated individuals, viral DNA and RNA persist in intestinal $CD4^+$ T cells, myeloid cells, and macrophages, with higher levels compared to circulating lymphocytes even after years of ART[143,160,161].

Further, the central nervous system has been described as a site for HIV persistence, with viral DNA and RNA detected in macrophages, microglia, and astrocytes of ART-treated individuals[162,163]. Additionally, studies have reported the presence of virus in the brain and cerebrospinal fluid (CSF) with drug-resistant mutations, suggesting HIV persistence in the brain, which is implicated in PWH experiencing neurological symptoms associated with a viral rebound from CSF[164].

1.5.3 Reservoir establishment and maintenance

1.5.3.1 Generation and establishment of latently infected reservoir cells

Viral latency is defined as a reversible non-productive infectious state that allows HIV to establish latent infection within specific cell types, leading to the formation of reservoirs that facilitate their indefinite maintenance within the host[107,165]. The establishment of HIV reservoirs occurs during the initial days of infection[166]. Consequently, treatment administered during acute HIV infection fails to preclude their emergence.

The precise mechanisms responsible for the establishment of the HIV reservoir are not completely clear yet. Two primary latency models have been delineated[167,168]:

1) Post-activation latency. This model is based on the concept that latently infected cells originate from previously productively infected cells undergoing a transition to a resting state associated with viral silencing[169,170]. Within the context of an immune response, as antigen levels decrease, a contraction phase is initiated leading a subset of cells to transition from an effector phenotype to a memory phenotype, which manifest heightened CCR5 expression, rendering them highly permissive to HIV infection. Additionally, they undergo transcriptional reprogramming towards a quiescent state, fostering viral latency[170].
2) Pre-activation latency. In this model, resting memory $CD4^+$ T cells are directly infected, leading to the immediate establishment of latency. Due to the quiescent state of the resting cell, the virus remains unintegrated in the cell cytoplasm[171]. Activation of the resting cell enables the integration of these DNA forms into the host genome, facilitating productive infection. Although the contribution of this model to viral persistence is limited due to the short lifespan of unintegrated forms in the cytoplasm, factors like chemokines and cytokines can modulate the susceptibility of resting cells to HIV infection and latency establishment[172].

Following establishment via either mechanism, the reservoir of latently infected cells demonstrates remarkable stability, with an estimated median half-life of 3.7 years in PWH under ART[112,173]. It is estimated that it would take more than 60 years of ART treatment to achieve eradication of the infection. Several mechanisms contribute to the establishment of HIV latency, primarily encompassing:

- Epigenetic mechanisms. Chromatin condensation modulates RNA transcription. In the euchromatin state, chromatin is less condensed, facilitating the accessibility of transcription factors and promoting transcriptional activity. Conversely, in the heterochromatin state, chromatin is more compacted, limiting access to the transcriptional machinery, thereby restricting transcription. Dynamic histone modifications contribute to the removal of signals required for transcription, establishing a repressive environment for RNA transcription and promoting latency[174,175].
- Transcription factor and Tat protein levels. Resting $CD4^+$ T cells exhibit high levels of densely compacted heterochromatin, resulting in limited viral expression, thereby fostering latency[176]. However, several studies have indicated that most integration events occur in actively transcribed gene introns, suggesting the involvement of additional mechanisms in latency maintenance[177].

Evidence suggests that repressive epigenetic elements govern HIV promoter activity during latency, impeding viral transcription or elongation, often associated with diminished levels of Tat protein and the transcription factor P-TEFb[178,179]. Epigenetic regulation of the HIV promoter during latency involves DNA methylation and histone modifications[180–183].

- Integration sites and transcriptional interferences. The location of viral genome integration significantly impacts latency maintenance. Studies have shown that preferential integration of HIV in centromeric and heterochromatin regions leads to deep-latency viral reservoirs associated to HIV control[184]. In addition, transcriptional interferences during viral transcription initiation and elongation that hinder productive infection can occur[185,186]. Numerous studies have reported that proviral HIV DNA tends to integrate within transcriptionally active host genome regions, with intact proviruses often integrating in opposing orientations to host genes, thereby leading to transcriptional silencing of HIV and latency establishment[186–188].
- Cellular transcription repressors and restriction factors. While certain restriction factors, including NFkB and NFAT, play pivotal roles in initiating HIV transcription, inhibitors such as IKBα can impede the binding of these factors, thereby promoting transcriptional inhibition and the induction of latency.
- RNA splicing and exportation defects. HIV has evolved to exploit weak splice sites, facilitating the export of unspliced and partially spliced RNA molecules. However, this adaptation can lead to aberrant virus-host splicing events, potentially affecting cellular genes linked to proliferation and promoting HIV persistence within cellular clones[189,190]. Aberrant splicing can also suppress the production of MS-RNA, inducing a state of deep latency characterized by viral transcriptional silence[191]. Proper splicing is crucial for the generation of regulatory proteins like Tat and Rev, essential for viral replication and RNA export. Splicing defects can reduce the levels of these proteins, impeding the transition from latency to active viral replication.

Moreover, stochasticity in HIV transcription, influenced by cellular factors such as metabolic state and cell cycle phase, adds another layer of complexity to latency maintenance[192]. Understanding these diverse mechanisms is imperative for developing effective strategies to eliminate HIV infection and achieve a cure.

1.5.3.2 Active reservoirs

While the majority of HIV-infected cells remain in a latent state, a subset of cells, comprising 2-18% of all infected cells, actively transcribe HIV and produce viral proteins during ART, forming the active viral reservoir[109,193,194]. Their contribution to long-term HIV persistence has been inadequately characterized, primarily due to their exclusion from reservoir studies based on assumptions of a limited lifespan and anticipated immune-mediated clearance[99]. However, several studies have indicated that cells exhibiting a quiescent or resting phenotype are also capable of HIV transcription[195]. Furthermore, cell clones harboring intact HIV genomes with ongoing viral transcription have demonstrated persistence over years[193,196]. Active reservoirs may contribute to residual viremia during suppressive ART, highlighting their importance in eradication strategies and the need for targeted interventions aimed at its elimination[196].

1.5.4 Mechanisms of reservoir maintenance

The maintenance of the HIV reservoir in individuals undergoing ART can be attributed to several factors:

- Persistence of latently infected cells. The latent reservoir is sustained over time through several mechanisms:
    - *Clonal expansion*. This process involves the transmission of identical proviral copies from dividing cells to their progeny, occurring frequently in cells with defective HIV genomes and replication-competent provirus[197–200].
    - *Homeostatic proliferation*. Driven by cytokines like IL-7 or IL-15, this process promotes the proliferation of latently infected $CD4^+$ T cells while maintaining latency[113].
    - *Antigen-driven proliferation*. This process leads to the expansion of latently infected $CD4^+$ T cells in response to tumor antigens or antigens derived from coinfections with CMV, EPV or HPV[198,201].
    - *Immune system evasion*. Latently-infected cells evade the effects of ART and the immune system, while retaining the capacity for reactivation and subsequent infection of new cells, thereby perpetuating the HIV reservoir.
- Incomplete reservoir elimination by ART. ART effectively suppresses viral loads to undetectable levels[202]. However, the HIV reservoir remains resilient to eradication, resulting in residual viral replication. Highly sensitive PCR tests have identified residual viremia in the plasma of ART-suppressed individuals[203].

Factors contributing to low-level replication include insufficient drug penetration in tissues like LNs, cell-to-cell transmission, suboptimal treatment adherence, or the presence of pharmacological barriers hindering ART efficacy[157,204].

- Immunological dysfunctions. Persistent dysfunctions in immunological mechanisms hinder their ability to control residual viral replication and the reactivation of latently infected cells in HIV infection. These dysfunctions manifest at various levels, including impaired recognition of HIV-infected cells, diminished effector responses due to prolonged antigen exposure, and restricted access to HIV sanctuaries like lymph nodes. CTLs play a critical role in HIV infection[205]. Studies have reported the presence of escape mutations in dominant viral epitopes, significantly impeding the recognition of infected cells by CTLs[206,207]. Further, ART fails to fully restore dysfunctional immune responses mediated by CD4, CD8, or NK cells[208–210].

1.5.5 Measuring the HIV reservoir

In HIV-infected individuals, latent infection occurs in approximately 1 in 10^4 to 10^7 $CD4^+$ T cells, depending on the time of ART initiation and the HIV viral load set point[211,212]. Assays quantifying HIV reservoirs require sensitivity, specificity, ability to distinguish replication-competent proviruses, and precision for assessing eradication strategies. Assays measure:

1) Cell-free virus. These assays encompass the quantification of viral load via quantitative PCR in body fluids, including CSF and plasma, of ART-treated PWH. While cell-free viruses are not considered part of the latent HIV reservoir, they indicate residual viral production[213]. Clinical assays detect viremia down to 20 HIV-1 RNA copies/ml, but lack sensitivity to detect low-level persistent viremia (<20 HIV-1 RNA copies/ml)[202]. The Single-Copy Assay (SCA) detects minimal plasma HIV-RNA levels[202]. Derived assays aim to enhance automation but require substantial fluid volumes, target conserved viral genomes regions, and have a limit of detection of 1 copy of HIV-1 RNA/ml[214–216].
2) Cell-associated HIV DNA. Quantifying the HIV reservoir traditionally involves PCR-based assessment of total, integrated, and episomal HIV-DNA.
    - *Total HIV DNA*. Despite challenges in interpretation due to differential decay rates and the prevalence of defective proviral DNA, total HIV-DNA quantification offers valuable insights into HIV persistence[217,218]. RT-qPCR or Droplet Digital PCR (ddPCR) are used for total HIV-DNA measurement[219,220]. While ddPCR enables absolute quantification without a standard curve, it has a narrower dynamic range than RT-qPCR, increasing the risk of false positives[221,222].

Both methods target specific genome regions and require normalization to a housekeeping gene[223]. However, PCR-based quantification tends to overestimate the competent reservoir length as the majority of quantified viral genomes are not replication-competent[224].

- *Episomal HIV-DNA*. These forms are predominant in ART-naïve PWH, and are quantified using primers targeting the 2-LTR circle junction, employing both qPCR and ddPCR methodologies[219,225].
- *Integrated HIV-DNA*. Levels of integrated HIV-DNA are considered a more precise indicator of reservoir size compared to total HIV DNA. The Alu-gag PCR method is frequently used to detect integrated HIV-DNA, and comprises two sequential PCR steps: a conventional PCR targeting the Alu region in the host genome and the viral gag gene, followed by a RT-qPCR using primers for the LTR region[226,227].
- *Intact HIV-DNA*. Although PCR techniques offer sensitivity and cost-effectiveness, they tend to overestimate the competent reservoir due to the predominance of defective viral genomes, and lack information on viral genome integrity[228]. In this regard, the Intact Proviral DNA Assay (IPDA) distinguishes intact genomes from those with deletions or hypermutations, eliminating the need for viral sequencing[229]. However, it presents limitations, including that approximately 30% of PWH may present sequence polymorphisms in proviral genomes, resulting in amplification failure[229,230].

3) Transcription-competent reservoirs. Quantification of HIV-1 RNA involves cell RNA extraction followed by RT-qPCR, with results normalized to a standard curve. Cell-associated HIV-RNA indicates active viral transcription but does not reflect the size of the viral reservoir[231]. The Tat/Rev Induced Limiting Dilution Assay (TILDA) quantifies the frequency of peripheral $CD4^+$ T cells expressing cell-associated HIV-RNA[232]. Alternative methods to quantify the transcription-competent reservoir include RNAscope and RNA Fluorescence in Situ Hybridization (FISH)-Flow, enabling visualization of individual HIV-RNA molecules in cells by microscopy or flow cytometry[117,233]. These techniques offer cell-type specificity and high throughput but are labor-intensive and require substantial cell input.
4) Translation-competent reservoirs. Several assays have been employed to quantify the HIV reservoir capable of both RNA transcription and protein translation. The digital p24 Single Molecule Array Technology (SIMOA) enables the direct quantification of viral antigen from individual HIV^+ cells[234,235].

However, it may lead to an overestimation of the replication-competent reservoir due to its heightened sensitivity. Of note, a recent optimization of the SIMOA assay has been devised to detect p24 in plasma at concentrations 1000 times lower than previous assays[236]. Furthermore, RNA FISH-flow can be combined with anti-p24 antibodies, allowing the simultaneous assessment of HIV transcription and translation within individual cells[237]. Flow cytometry-based assays offer simplicity, higher throughput, and sensitivity, but measure the frequency of cells capable of ex vivo induction to produce provirus and/or HIV protein, irrespective of harboring defective or replication-competent virus.

5) Replication-competent reservoirs. The QVOA is currently considered the gold standard for measuring the replication-competent HIV reservoir[238,239]. It involves stimulating infected cells and co-culturing them with cells from an HIV-negative donor susceptible to infection. After 14 or 21 days, p24 gag levels are measured in the culture supernatant via ELISA[240]. QVOA quantifies cells capable of producing infectious virus upon stimulation. However, it is labor-intensive and costly, and potentially underestimates the reservoir size[241]. The Murine Viral Outgrowth Assay (MVOA) detects replication-competent HIV in individuals with low viral levels[242]. Cells from these individuals are transferred to NSG mice and monitored for viremia over time. Nonetheless, MVOA is laborious, expensive, and time-consuming.

1.6 Immune responses against HIV infection

Both innate and adaptive immunity play a significant role in controlling HIV infection through diverse mechanisms.

1.6.1 Innate immunity

Innate immunity serves as the initial defense barrier against viral and microbial infections and comprises physical barriers (i.e. skin, mucus), blood proteins (i.e. complement), soluble factors (i.e. cytokines, chemokines), antigen-presenting cells (dendritic cells, macrophages), neutrophils, phagocytes, NK cells and NKT cells. Pattern Recognition Receptors (PRRs) detect Pathogen-Associated Molecular Patterns (PAMPs), initiating signaling cascades that activate the transcription of antiviral and immune regulatory genes, thereby limiting viral replication and modulating adaptive immunity[243,244]. Notably, all nucleated cells possess PRRs like RIG-1-like receptors (RLR) and toll-like receptors (TLR), enabling the recognition of viral components[245–247]. For instance, intracellular PRRs such as Interferon Inducible Protein 16 (IFI16) and Cyclic GMP-AMP Synthase (cGAS) are able to detect products of the HIV genome[248,249].

Upon recognition of viral products by PRRs, signaling pathways are initiated to induce the production of IFNs, which subsequently stimulate the transcription of Interferon-Stimulated Genes (ISGs), facilitating the establishment of an antiviral cellular state and activate adaptive immunity[250–252]. For instance, IFI16 can induce the production of IFN type I, facilitating the elimination of HIV-infected $CD4^+$ T cells, a key characteristic of HIV infection[253]. Of note, plasmacytoid dendritic cells (pDCs) play a critical role in antiviral responses by serving as key producers of interferon (IFN) upon recognition of ssDNA viral genomes through stimulation of TLR7 and TLR9[254,255].

Consequently, HIV infection triggers innate immune activation through detection of viral products by PRRs, resulting in the production of proinflammatory cytokines and chemokines. Dendritic cells are among the first responders to infection, and secrete type I IFNs such as IFN- α and IL-15, leading to NK cell activation[256,257]. Thus, subsequent to viral stimulation, monocytes, macrophages and NK cells become activated and release immune-mediators such as IFN_γ, tumor necrosis factor α (TNF-α), and various chemokines, aiming to restrict HIV infection and initiate the adaptive immune response[258].

1.6.2 Adaptive immunity

Adaptive immunity comprises humoral and cellular responses. The activation of these responses occurs within days to weeks after the peak of viremia during the early stages of HIV infection, subsequent to the innate immune response generated in diverse mucosal tissues such as GALT and LNs[259]. Notably, the quality of initial innate immune responses closely correlates with and can predict the efficacy of subsequent adaptive immune responses to HIV infection. This interplay between innate and adaptive immunity is essential for effective immune control of HIV.

1.6.2.1 Humoral response

Following the onset of innate responses, diverse cellular populations undergo expansion, giving rise to a multicellular response characterized by T and B cell interactions[260]. These interactions induce robust production of specific antibodies by B cells, targeting a wide spectrum of viral antigens. While some of these antibodies present neutralizing activity against the virus, the majority exhibit non-neutralizing properties, inducing effector responses such as phagocytosis or ADCC[261]. However, HIV presents a high mutation rate, facilitating the evasion of these immune responses[78]. Studies employing B cell depletion in macaques described no alterations in viral clearance, indicating that initial control of HIV replication is not significantly influenced by the production of neutralizing antibodies[262].

1.6.2.2 Cellular response

The cellular antiviral response against HIV involves $CD4^+$ and $CD8^+$ T lymphocytes[263]. $CD4^+$ T lymphocytes, the primary targets of the virus, suffer a substantial depletion throughout the course of infection. Particularly, specific $CD4^+$ T cell populations, such as α4β7-expressing cells in the gut, and Th1/Th17 subsets produce IL-17, IFN_γ and IL-2, thereby contributing to antiviral responses[264,265].

Furthermore, HIV-specific $CD8^+$ T cells undergo clonal expansion and exhibit cytotoxic responses against HIV-infected cells, leading to a systematic viral load reduction[266–268]. These cells also present the ability to migrate to anatomical sites where viral persistence has been described, including LNs, spleen, peripheral blood, CSF, vaginal mucosa, and GALT[78]. Initial CTL responses target epitopes within the viral proteins nef and env, while subsequent responses are directed against other viral proteins, such as p24, and play a pivotal role in controlling viral load during the set point phase, characterized by a stabilization of plasma viremia levels[269]. Additionally, these CTLs exhibit the ability to secrete cytokines (i.e. IFN_γ, TNF-α) and chemokines (i.e. MIP-1α (CCL3), MIP1β (CCL4), and RANTES (CCL5)), which serve to inhibit viral replication and impede viral entry into $CD4^+$ T cells[270].

Despite the capacity of the immune system to combat infections, it is not able to control HIV infection effectively. One major obstacle is that HIV can establish a latent infection in $CD4^+$ T cells and render invisible to CTL activity, while concurrently infecting other cells within immunological sanctuaries. Moreover, certain CTL responses intended to eliminate HIV may elicit other effects, such as IL-10 production by B cells, which inhibits CTL responses, or the induction of a dysfunctional state in CTLs resulting from both reduced numbers of helper $CD4^+$ T cells and sustained antigenic exposure[271,272].

1.7 Natural Killer cells

1.7.1 Definition

NK cells are classically defined as effector lymphocytes from the innate immune system capable of killing target cells “naturally”, that is, in a spontaneous fashion that does not require prior sensitization[273,274]. These cells demonstrate inherent cytolytic activity against stressed, tumoral, or infected cells, thereby playing pivotal roles in immune responses against diverse pathogens and tumors. NK cells typically constitute 5-20% of circulating lymphocytes in humans and are also distributed in various tissues and organs, including lymphoid organs, lung, liver, uterus (during pregnancy), and gut[275].

NK cells belong to the family of innate lymphoid cells (ILCs), characterized by their lymphoid morphology, absence of rearranged antigen receptors akin to T and B cells, and expression of specific phenotypic markers. ILCs are widely distributed throughout various tissues but are particularly abundant at barrier surfaces, where they modulate immune responses to infection, chronic inflammation, and tissue homeostasis[276]. They are categorized into five groups based on their developmental and effector programs defined by lineage-specifying transcription factors: NK cells, ILC1s, ILC2s, ILC3s, and lymphoid tissue inducer (LTi) cells, each exhibiting distinct functions and cytokine profiles. Both NK cells and ILCs originate from $CD34^+$ hematopoietic progenitor cells (HPCs)[273]. NK cells, the oldest members of the ILC family, represent the sole cytotoxic ILC subset and express the lineage-specifying factor Eomesodermin (Eomes). Non-cytotoxic ILCs, comprising ILC1, ILC2, and ILC3, contribute to type 1, type 2, and type 3 immune responses, respectively. Although NK cells and ILC1s exhibit overlapping surface markers (i.e. CD56, NKp46) and can occupy similar compartments, they diverge in the expression of lineage-specifying factors, notably T-bet (expressed exclusively by ILC1s) and their cytotoxic capabilities (ILC1s lack perforin-dependent cytotoxicity)[275–277].

NK cells have been described to have a relatively short lifespan, with an estimated circulating population exceeding 2 billion in adults at any given time[278]. In contrast to T cells, NK cells lack antigen-specific receptors and are identified phenotypically by the absence of T cell markers such as CD3, along with the expression of characteristic NK cell markers including CD56 and CD16. Of note, a minor subset (<5%) of normal peripheral blood lymphocytes co-expresses CD56 and CD3 and is capable of non-MHC-restricted cytotoxicity. These cells, termed invariant natural killer T cells (iNKTs), possess both innate and adaptive immune properties, and contribute significantly to immune regulation and antimicrobial defense[279].

1.7.2 Development

Human NK cells can develop not only within the bone marrow but also within extramedullary tissues like tonsils and LNs[274,280]. The prevailing model suggests that human NK cells develop along a continuum, starting with hematopoietic stem cells (HSCs), which differentiate into multipotential progenitors (MPPs), which then transition into common lymphoid progenitor cells (CLPs) with the capacity to commit to various cell lineages including pro-B cells, pre-T cells, NK progenitors (NKPs), and other ILC progenitors (**Figure 11**)[281,282]. CLPs gradually downregulate CD34 expression and upregulate CD56 expression. Additionally, the expression of IL-1R and CD122 characterizes the early stages of committed NKPs, thus indicating the irreversible lineage specification of NK cells originating from CLPs[281,282].

NKPs undergo differentiation into immature NK cells (iNKs), characterized by elevated expression of IL-1R and the emergence of activating receptors such as NKG2D, NKp46, NKp30, and CD161[281–283].

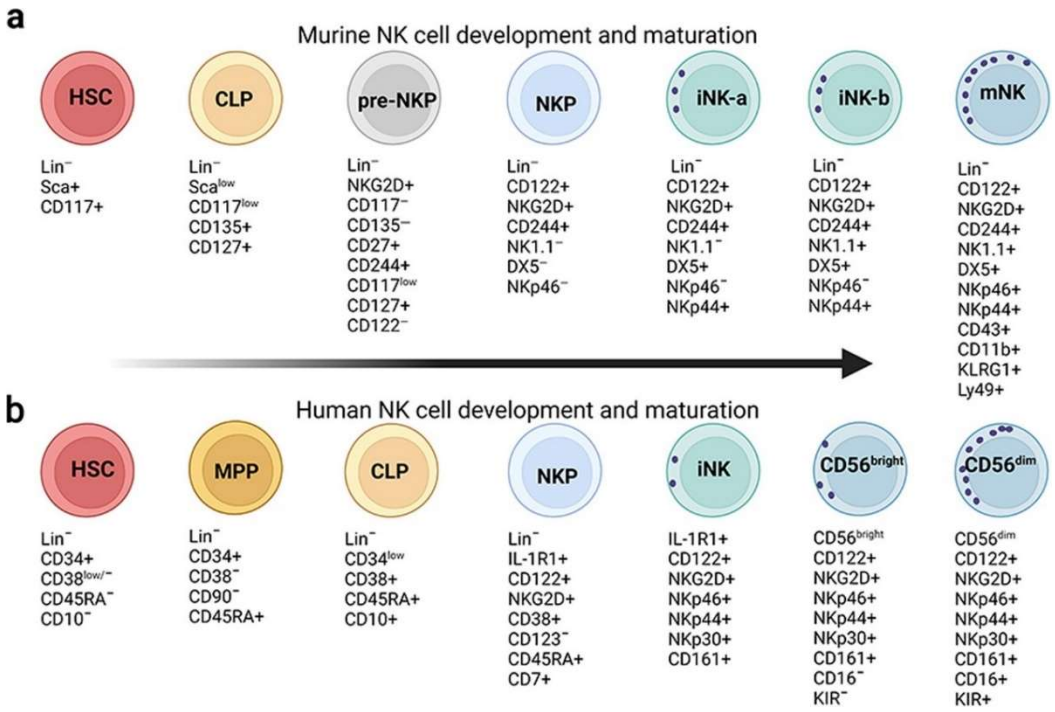


Figure 10. Schematic illustration delineating the cellular intermediates involved in a) murine and b) human NK cell development. Surface antigens serve as crucial markers for discerning the distinct intermediate populations during NK cell ontogeny. + (expression), - (no expression), hi (high expression), low (low expression). Extracted from[283].

Subsequently, iNKs transition into CD56^{bright} NK cells, which exhibit heightened CD56 expression along with maximal expression of NKG2D, NKp46, NKp30, and CD161[281–283]. Finally, CD56^{bright} NK cells progress to CD56^{dim} NK cells, distinguished by reduced CD56 expression, enhanced CD16 expression, and the appearance of various subtypes of killer cell immunoglobulin-like receptors (KIRs)[281–283].

1.7.3 Classification

CD56 is ubiquitously expressed on human PBMCs capable of non-MHC-restricted cytotoxicity. NK cells are typically categorized into two primary subpopulations based on CD56 expression levels, which differ in their homing, proliferation, and cytotoxic activity[274]:

- CD56^{bright} NK cells. Primarily found in SLO such as LNs and tonsils, constitute approximately 10% of peripheral blood NK cells[284]. These cells originate from CD34^{+} HSCs through phenotypically identified stages and express CCR7, CXCR3 and CD62L, facilitating their migration to SLO.

CD56^{bright} NK cells are characterized by low or absent CD16 expression and the presence of CD25, the low-affinity IL-2 receptor. Notably, CD56^{bright} NK cells are the primary producers of cytokines such as IFN$_\gamma$, TNF-α, and GM-CSF in response to IL-2, IL-15, or IL-18 stimulation, and lack perforin expression[285,286].

- CD56^{dim} NK cells. Constitute approximately 90% of the NK cells in peripheral blood, and express CD16, a low-affinity receptor for the Fc region of IgG, together with CD122, the intermediate-affinity IL-2 receptor. These cells preferentially migrate to inflamed peripheral tissues via CXCR1, CX3CR1, and ChemR23 expression. CD56^{dim} NK cells express perforin and are primarily responsible for cytolytic activity and target cell killing, although they can also produce IFN$_\gamma$ and other cytokines upon activation[287,288].

CD56^{bright} NK cells are considered the precursors of CD56^{dim} cells, based on their appearance after HSC transplantation and in cytokine-driven models of NK cell in vitro differentiation[288,289]. Some studies identified CD94 and CD62L surface expression density as a marker delineating functional intermediates between CD56^{bright} and CD56^{dim} human NK cell subsets, supporting the notion that, in vivo, human CD56^{bright} NK cells may undergo progressive differentiation towards a CD56^{dim}CD62L^{neg} phenotype. This transition entails the loss of NKG2A expression and the expression of receptors such as CD16, KIRs, and CD57 (**Figure 12**)[288].

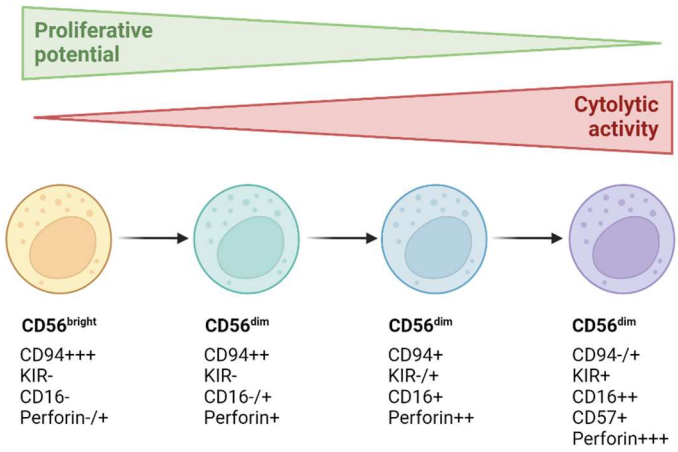


Figure 11. Schematic representation delineating the distinct NK cell subpopulations based on CD56 expression levels, proliferative potential, and cytotoxic responses. Adapted from[288].

In addition to this classification, the NK cell repertoire exhibits remarkable diversity. Studies utilizing mass cytometry have identified up to 30,000 distinct phenotypic NK cell subpopulations in peripheral blood from healthy donors[290]. These subsets encompass developmental intermediates along pathways of maturation and differentiation, as well as different types of effector NK cells.

1.7.4 NK cell receptors

NK cell functions are regulated by a detection system comprising diverse cell surface activating and inhibitory receptors (**Figure 13**)[274]. Upon interaction with their ligands expressed by neighboring cells, these receptors lead to the transmission of activating and inhibitory signals. The integration of these antagonistic pathways modulates the dynamic balance regulating NK cell activation, determining whether NK cells are activated to eliminate target cells[274].

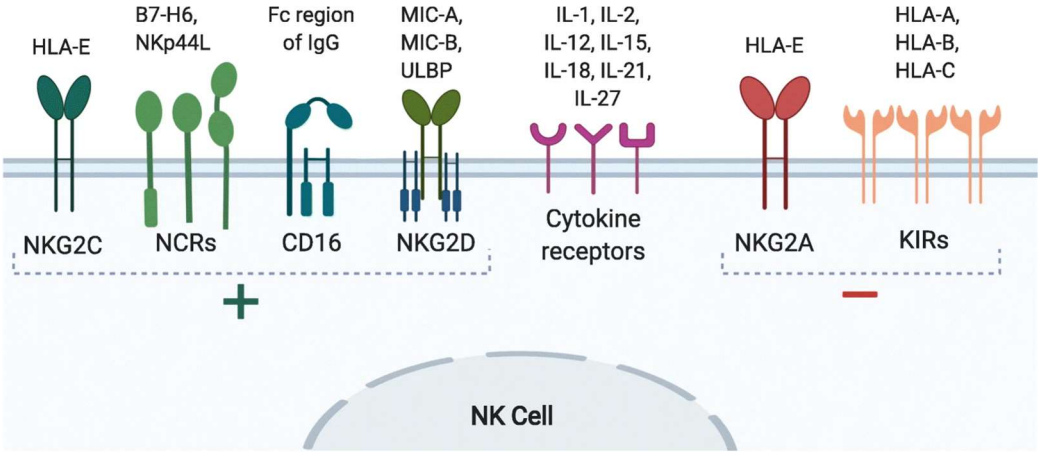


Figure 12. Primary NK cell receptors and their corresponding ligands. NK cells exhibit an array of activating ("+") receptors, including NKG2C, NCRs, CD16, NKG2D, along inhibitory ("-") receptors such as NKG2A and KIRs on their cell membrane. Extracted from[291].

1.7.4.1 Activating receptors

Activating receptors on NK cells recognize ligands that are upregulated or expressed de novo upon cell stress, viral infection, or tumor formation, and play a critical role in facilitating the NK-mediated elimination of these cells[292,293]. Some of these receptors initiate protein tyrosine kinase (PTK)-dependent signaling pathways by forming noncovalent associations with transmembrane signaling adaptors containing intracytoplasmic ITAMs (Immunoreceptor Tyrosine-based Activation Motifs). Key activating receptors in humans include:

- CD16 (also known as FcgRIIIA) mediates ADCC by binding to the Fc portion of IgG antibodies attached to target cells, leading to the exocytosis of cytotoxic granules containing perforin and granzyme, and the production of IFN_{γ}, contributing to the elimination of the target cell[294].
- NKG2D is a type II transmembrane receptor with C-type lectin-like characteristics expressed on cytotoxic T cells. Its ligands are stress-induced self-ligands that include UBLPs along with MICA/B molecules, which are upregulated in infected, stressed, and tumor cells[274,293].

- NKG2C is an activating receptor specific to HLA-E, which, upon engaging its ligand, triggers NK cell cytotoxic responses[295]. Its expression is observed in the most mature stages of NK cell development. Several studies have indicated that NKG2C^{+} NK cells exhibit adaptive traits, such as recognizing CMV peptides bound to HLA-E and expanding selectively in response to specific peptide combinations[295,296]. This selective expansion suggests a memory-like function of these cells, enabling rapid control of CMV reactivation[293]. Memory-like NK cells can emerge following exposure to specific antigens, viral infections, or stimulation with cytokines like IL-12, IL-15, and IL-18, and exhibit enhanced responses upon re-exposure to the activating stimuli[297].
- Natural Cytotoxicity Receptors (NCRs) are type I transmembrane molecules that belong to the immunoglobulin-like family, and include NKp46, NKp44, and NKp30[293]. NCRs play crucial roles in eliciting NK cell cytotoxicity against both tumor cells and infected cells. While NKp46 and NKp30 are expressed constitutively on nearly all resting human NK cells and are further upregulated upon NK cell activation, NKp44 is primarily found on CD56^{bright} NK cells but it is acquired by essentially all NK cells following cytokine-induced activation[293]. Different molecules can engage with the extracellular domains of NCRs, including viral components like the hemagglutinin (HA) of Influenza virus, which can activate NK cell function through recognition by NKp46 or NKp44[293]. Additionally, other NCR ligands encompass intracellularly located proteins such as BAT3/BAG6 (the ligand for NKp30), MLL5 (the ligand for NKp44), and PCNA (also a ligand for NKp44), which can translocate to the cell surface under stress conditions or during tumorigenesis[293].

Finally, other molecules, including 2B4, NTB-A, DNAM-1, CD59, and NKp89, serve as coreceptors, augmenting NK cell activation initiated by other activating receptors[293].

1.7.4.2 Inhibitory receptors

Throughout evolution, the development of cellular cytotoxicity has been linked to the emergence of intricate and robust regulatory mechanisms governing the initiation of cytolytic processes, thereby preventing tissue damage. NK cells undergo maturation through interactions with self-molecules, which educate them to recognize aberrant cells while preserving self-tolerance towards healthy tissues[290]. The array of inhibitory NK cell receptors is shaped during NK cell maturation, a process termed NK cell “licensing” or “education”[287,298]. Consequently, only NK cells expressing receptors for self HLA-class I molecules attain full functional capability, while others are either eliminated or rendered anergic[274].

Human NK cells feature two distinct categories of inhibitory receptors: those specific to HLA molecules and those non-specific to HLA. Within the HLA-specific category, two classes of inhibitory receptors are recognized, which possess Immunoreceptor Tyrosine-based Inhibition Motifs (ITIMs) in their cytoplasmic tails to mediate inhibitory signals[274]:

- KIR/CD158. KIRs are type I transmembrane receptors with specificity for polymorphic HLA-A, B, and C molecules[293,299]. Each KIR consists of two of three extracellular Ig domains, denoted as "KIR2D" or "KIR3D" based on the number of Ig domains, respectively[300]. Furthermore, KIRs are classified as "L" (long) or "S" (short) based on the length of their cytoplasmic tail[300]. Two types of KIR2D can be distinguished based on their extracellular Ig domain composition: 1) those comprising D1 and D2 domains, which encompass the majority of KIRs (i.e. KIR2DL1/L2/L3 and KIR2DS1/S2/S3/S4/S5), and 2) those comprising D0 and D2 domains, which include KIR2DL4/L5[301]. Importantly, both HLA class I molecules and KIRs exhibit high levels of polymorphism, influencing their interactions[302].
- CD94/NKG2A (CD94/CD159a). NKG2A is a type II transmembrane receptor that is expressed earlier in NK cell maturation compared to KIRs, and binds HLA-E, a non-classical HLA molecule, with higher affinity than NKG2C[303]. Primarily, NKG2A is observed in immature NK cells within peripheral blood, and together with KIRs, contributes to the suppression of responses against cells expressing self-HLA class I molecules[293,304].

In addition to HLA-class I-specific inhibitory receptors, additional inhibitory checkpoints, crucial for maintaining immune cell homeostasis, have been identified in NK cells, including PD-1, TIGIT, CD96, TIM-3, and KLRG1[274]. These receptors are not expressed on resting NK cells, but their expression can be induced under pathological conditions, thereby influencing NK cell function.

1.7.4.3 Homing receptors

NK cell trafficking in the circulation and towards tissues and lymphoid organs is governed by a complex interplay of various molecular mechanisms, including: integrins, selectins, chemokine receptors, as well as their respective ligands, cytokine-induced signals, sphingosine-1-phosphate (S1P), and the cellular microenvironment. Integrins and chemokine receptors serve as important biomarkers for characterizing different subsets of circulating and tissue-resident NK cell subsets[283].

- Integrins. NK cells express a diverse array of integrins, a class of transmembrane receptors that mediate interactions with the extracellular matrix (ECM) and other cells, guiding their migration and residency within tissues[283,305].

For instance, β2 integrins such as LFA-1, Mac-1, CR4, and αDβ2 mediate NK cell migration, adhesion, and immune synapse formation during target cell lysis by binding to CAMs within the ECM or non-lymphocytic cells[283,305,306].

- Chemokine receptors. These receptors belong to the family of G-protein-coupled seven-transmembrane receptors and are pivotal in regulating integrin activation and modulating NK cell migration patterns[283,305]. Chemokine receptors are classified into four structural types: 1) C-X-C chemokine receptor (CXCR), 2) C-C chemokine receptor (CCR), 3) C-X3-X chemokine receptor (CX3XR), and 4) XCR[283,305]. Several chemokine receptors including CXCR1, CXCR3, CXCR4, CXCR6, CCR7, CCL3/4, CCL5, and CXCL1 are implicated in NK cell trafficking and function[283,305].

Notably, the expression of CD62L, CXCR3, and CCR7 guides $CD56^{bright}$ NK cells to SLO in response to CCL19 and CCL21, whereas the expression of Chemerin R, CXCR1, CXCR2, and CX3CR1 directs $CD56^{dim}$ NK cells to inflammatory peripheral tissues in response to their respective chemokine ligands (Chemerin, IL-8, and Fraktalkine)[274].

1.7.5 NK cell effector mechanisms

NK-mediated killing of target cells is finely regulated by the balance of activating and inhibitory signals through surface receptors, and can be influenced by multiple factors, such as interactions with dendritic cells and other myeloid cells, and the stimulation by cytokines such as IL-12, IL-15, and IL-21, which can enhance their cytotoxicity and pro-inflammatory cytokine production[258,307]. Additionally, IL-15 and TGF-β promote a tissue-resident phenotype in NK cells, sustaining heightened effector functions[308]. Activated NK cells initiate apoptosis in target cells through distinct signal transduction pathways:

- Granule secretion. Involves the intracellular delivery of granule-associated serine proteases, activating caspase-independent (Granzyme A) and dependent (Granzyme B) death programs. The entry of granzymes into target cells is facilitated by perforins, which are molecules that form pores in the target cell membrane[309]. In addition, lysosome-associated membrane protein-1 (LAMP-1 or CD107a) has a critical role in the trafficking of perforin to lytic granules, since it protects cytotoxic NK cells from damage during degranulation[310,311]. Of note, CD107a is widely used as a degranulation marker[312].

- Cytokine secretion. NK cell activation also triggers the secretion of cytokines and chemokines, including IFNɣ, TNF-α, CCL3, CCL4, and CCL5[313].
    - IFNɣ plays a key role in activating macrophages, enhancing antigen presentation, and promoting immune responses against intracellular pathogens[313].
    - CCL3 and CCL4, along with CCL5, function as type 1 cytokines that, together with IFNɣ, contribute to the inflammatory process and the recruitment and activation of immune cells.
- Apoptotic ligand expression. Moreover, NK cells can induce cell death by expressing apoptotic ligands like TNF and Trail, which bind to the TNF receptor (TNFR) and Fas, respectively, initiating apoptosis upon ligand binding[314].

Despite historically being considered innate immune cells, NK cells exhibit memory responses, including antigen-specific memory and adaptive features, which can be: 1) hapten-induced long-lived memory NK cells, 2) virally-induced, which includes $NKG2C^+$ NK cells expanded in response to human CMV infection, and 3) cytokine-induced, with enhanced IFNɣ production upon re-stimulation[315,316]. The diverse and potent immune responses mediated by NK cells underscore their potential as candidates for immunotherapeutic strategies.

1.8 NK cells in HIV infection

NK cells exert a pivotal role in the host immune response against HIV infection through diverse mechanisms, such as direct lysis of HIV-infected cells via ADCC or cytokine secretion of CC chemokines such as CCL3, CCL4, and CCL5, which act as ligands for CCR5, thereby impeding the entry of R5-tropic viruses into target cells[317–319]. In addition, specific genotypes of NK cells have been described to influence HIV control, such as the KIR allele KIR3DS1 or the KIR ligand HLA-Bw4, which have been linked to delayed progression to AIDS[320,321]. However, HIV infection induces phenotypic and functional abnormalities in NK cells, which include[317]:

- Altered expression of NK cell receptors. Individuals with HIV viremia exhibit heightened frequencies of inhibitory NK cell receptors, such as CD94 and LIR1, and downregulation of NCRs[322–324].
- Expansion of defective $CD56^-CD16^{high}$ NK cells. This subset is expanded in untreated PWH and presents defective cytotoxic activity and cytokine production[325].

- Impaired non-cytolytic suppression of HIV. NK cells from individuals with HIV viremia demonstrate markedly reduced secretion of CC-chemokines, resulting in decreased suppression of endogenous HIV replication[326].
- Dysfunctional ADCC activity. Several studies have reported impairments in NK cell cytolytic activity during HIV infection, including ADCC[80,327,328]. Further, viral escape from HIV-specific non-neutralizing ADCC antibodies may contribute to defects in ADCC[329].
- Impaired NK cell responses to cytokines. Various studies have highlighted the reduced responsiveness of NK cells to cytokines as a contributing factor to NK cell dysfunction in PWH[322].

Although improvements in NK cell function upon ART initiation have been observed, complete restoration of NK cell function remains elusive[209,330].

1.9 HIV controllers

While the natural course of HIV infection typically follows the trajectory described previously, a small subset of PWH (<1%), termed HIV controllers, exhibit the remarkable ability to maintain viral loads below detectable levels for prolonged periods in the absence of treatment[331]. HIV controllers can be categorized into two distinct groups[332]:

- Elite Controllers (EC). Maintain undetectable viral loads over time (below the detection limit, typically <40 copies HIV-1 RNA/ml of plasma).
- Viremic Controllers (VC). Exhibit low but detectable HIV viremia (ranging from 40 to 2,000 copies of HIV-1 RNA/ml of plasma).

Although EC cannot eliminate HIV infection, their immune system demonstrates exceptional ability in controlling viral replication without the aid of ART[333,334]. This characteristic has positioned EC individuals as a focal point of interest in HIV research, as they hold potential as a model for achieving a functional cure[335]. The mechanisms underlying the antiviral immunity observed in EC remain incompletely understood. Multiple factors have been described to be implicated in their natural ability to control HIV infection, including genetic determinants, innate and adaptive immune responses, viral reservoir dynamics, and other non-immunological factors. However, elucidating the precise interplay of these factors in EC individuals remains a subject of investigation, and will be addressed in **Chapter 1** of this thesis.

1.9.1 Genetic factors

Certain EC exhibit genetic variations that may predispose them to heightened immune responses against HIV. Notably, specific T-cell responses restricted to HLA class I molecules have been associated with superior HIV control in these individuals[336]. Genome-wide association studies (GWAS) have identified polymorphisms within the HLA class I binding pocket that are correlated with natural HIV control[337]. These amino acid variations delineate distinct HLA class I alleles, such as HLA-B*57, HLA-B*52, and HLA-B*27, which facilitate the presentation of HIV-derived peptides on infected cells for recognition by the T cell receptors of HIV-specific $CD8^+$ T cells[337,338].

However, genetic associations within the HLA class I gene locus account for less than 25% of the observed variability in host immune control[337]. Furthermore, a topological network analysis has suggested that HIV-specific $CD8^+$ T cells in EC individuals target epitopes that are highly interconnected within the viral proteome, irrespective of the presence of protective HLA alleles[339]. Further research is needed to comprehensively understand the intricate genetic and immunological determinants underlying the remarkable immune control observed in EC.

1.9.2 Adaptive immune responses

EC exhibit robust virus-specific T cell responses mediated by both CD8 and CD4 T cells, which are pivotal in restraining HIV replication[331]:

- $CD8^+$ T cell responses. HIV-specific $CD8^+$ T cells are recognized as the primary effectors responsible for sustaining durable viral suppression in EC[340]. While the presence of protective alleles contributes to this phenomenon, recent studies suggest that effective $CD8^+$ T cell responses in EC may also stem from enhanced effector functions, strategic localization, and optimized immunometabolic activities[331]. Indeed, accumulating evidence indicates increased functionality of $CD8^+$ T cells in EC[341–343]. Notably, HIV-specific $CD8^+$ T cells from EC demonstrate the capacity to recognize and eliminate resting HIV-infected $CD4^+$ T cells in the absence of viral reactivation[344]. Moreover, viral control in EC has been linked to the presence of polyfunctional memory $CD8^+$ T cells within LNs, which actively suppress viral replication[345]. Furthermore, persistent EC individuals exhibit metabolic plasticity characterized by increased fatty acid uptake and heightened effector gene expression compared to ART-treated individuals, which present a metabolic profile largely dependent on glycolysis and elevated glucose uptake[346].

- CD4⁺ T cell responses. EC have been described to exhibit superior preservation of the central memory compartment within CD4⁺ T cells expressing the chemokine receptor CCR7[347]. These cells possess the capacity for migration to lymphoid organs and display higher levels of activation compared to non-controllers. In addition, CD4⁺ T cells derived from EC exhibit heightened affinity for Gag antigens along with robust effector functions[348,349]. Notably, downregulation of the CCR5 marker has been observed in HIV-specific CD4⁺ T cells from EC, which correlates with reduced susceptibility to CCR5-dependent viral entry[350]. While CD4⁺ T cells are also suggested to harbor effector functions that support CD8⁺ T cell responses, further research is needed to validate and elucidate the specific roles of CD4⁺ T cells in this context[351].

1.9.3 Innate immune responses

The majority of studies conducted in EC have reported correlations between HIV-specific T cell responses and superior viral control during HIV disease progression. Nevertheless, recent studies have also highlighted the potential involvement of innate immune cells in the natural control of HIV:

- Dendritic cells. Myeloid dendritic cells derived from EC individuals exhibit enhanced abilities to detect HIV via cytosolic pathways, thereby augmenting the activation of CD8⁺ T cells[352]. In addition, these cells show increased immune activation and metabolic functionality, which is associated with distinct epigenetic profiles that result in enhanced antigen presentation[331,353].
- NK cells. Reduced expression levels of exhaustion markers such as LAG3, TIGIT, and CXCR6 have been observed in NK cells from EC[354]. Notably, a distinct population of NK cells characterized by expressing CD16, CD11b, CD161, and Siglec-7, while showing lack of CD57 expression, appears to be more abundant in EC and exhibits enhanced functionality, evidenced by increased IFN_{γ} production and cytotoxic degranulation[354]. Additionally, ADCC represents a crucial mechanism of EC viral control. Multiple studies have demonstrated elevated levels of anti-Env/gp120-specific non-neutralizing antibodies in the plasma of EC individuals compared to other groups of PWH[355,356]. However, the specific contribution of NK cells limiting HIV infection via the ADCC mechanism remains incompletely understood in EC. The in-depth identification of ADCC-mediating NK cells in HIV-EC will be addressed in **Chapter 1** of this thesis.

1.9.4 Viral reservoir configuration

The natural control of HIV infection in EC has been associated with a unique landscape of proviral reservoirs, characterized by the preferential integration of intact proviruses into centromeric satellite DNA or regions containing zinc finger genes, which are associated with heterochromatin features[357]. Consequently, EC individuals maintain a reservoir of infected cells harboring intact HIV proviruses that are more frequently integrated into non-permissive regions, potentially leading to a state of deep latency[184,331]. This observation suggests that immune-mediated selection mechanisms in EC may drive the formation of this distinct viral reservoir configuration by preferentially eliminating proviruses that are more susceptible to reactivation signals. Furthermore, some studies indicate limited proviral evolution over time in EC individuals[358–360].

1.9.5 Non-immunological factors

Mutations in viral regulatory proteins such as Vif or Nef have been documented in EC[361]. The loss of Nef's ability to downregulate HLA class I expression would heighten susceptibility to cytotoxic $CD8^+$ T cell targeting[362]. Additionally, cells derived from EC individuals reportedly express intracellular proteins, including APOBEC3G, Tetherin, and SAMHD1, which serve to counteract viral replication[363,364]. Moreover, prior studies have indicated that T cells from EC exhibit a differently regulated FOXO3a apoptosis pathway, characterized by an enhanced capacity for sustained activation compared to non-controllers, suggesting an inherent resistance to apoptosis[365].

1.10 HIV cure strategies

Several strategies are currently focused on the elimination or reduction of the latent reservoir associated with HIV infection. Among these strategies, one of the most widely discussed, the shock and kill approach, involves the use of latency reversing agents (LRAs) to induce viral gene expression, thereby rendering infected cells susceptible to immune-mediated clearance[366]. However, a significant challenge lies in the identification of LRAs with consistent efficacy, as many exhibit incomplete penetrance and considerable variability in their capacity to reactivate latent proviruses, both at the individual and cellular levels[366–372]. Furthermore, LRAs that demonstrate robust activity in vitro or ex vivo often trigger downstream pathways associated with T cell receptor activation, raising concerns regarding their potential toxicity[373]. Several LRAs capable of inducing proviral expression are accompanied by widespread immune activation or severe adverse effects, rendering them unsuitable for clinical applications. However, for LRAs that avoid T cell activation, the proportion of proviruses induced may be insufficient, further impeding significant reductions in the viral reservoir.

Of note, a recent study delineated that blockade of IFN-β signaling via anti-IFN-β antibodies reactivated the HIV reservoir during ART in HIV-infected BLT humanized mice[374]. However, no discernible changes in viral rebound post-ART cessation were observed between experimental groups[374]. Nevertheless, even if a method were devised to safely activate all replication-competent proviruses, ensuring the elimination of all infected cells poses a formidable challenge exacerbated by issues such as immune exhaustion and the emergence of viral escape mutations.

An alternative approach for reducing the HIV reservoir, termed the “functional cure”, aims to elicit immune responses capable of effectively suppressing viral replication to levels undetectable by clinical assays, thereby ensuring sustained viral control. Despite the persistence of the reservoir in this scenario, disease progression and viral transmission are mitigated. Insight into this strategy is gleaned from HIV controllers. HIV controllers typically exhibit minimal HIV reservoir levels, underscoring the importance of reservoir reduction in the pursuit of an HIV cure[375]. While extensive research suggests that HIV-specific CTLs play a central role in mediating viral control, several studies suggest that innate immune responses may also be important for HIV control[376,377].

In this regard, numerous studies present compelling evidence of NK cells playing a pivotal role in the elimination of HIV-infected cells and the attainment of HIV control. Of note, NK cells have been shown to display heightened functional responses in HIV-exposed seronegative individuals (HESN) compared to HIV-infected individuals[378]. Specifically, NK cells derived from HESN demonstrate elevated production of IFNɣ and increased degranulation capacity[378]. Further, the presence of specific KIR haplotypes, along with highly polyfunctional and cytotoxic NK cell responses, has been linked to slower HIV disease progression and reduced viral loads[379]. Other studies have underscored the involvement of NK cells in the configuration of HIV reservoirs. Specifically, one study showed that the inducible production of IFNɣ and expression of specific NCRs in a distinct subset of NK cells correlated with HIV reservoir control[380]. Moreover, two studies examining the impact of pegylated IFN-α2a (PEG-IFN-α2a) in combination with ART on HIV infection revealed an increase in innate immune activity and NK cell cytotoxicity, which was associated to PEG-IFN-α2a -mediated HIV control[381,382].

Additionally, several studies offer compelling evidence regarding the importance of ADCC responses in the context of both HIV and SIV infections[80]. ADCC has been linked to vaccine efficacy in various human and animal vaccine trials[80,383–385].

Notably, the RV144 clinical trial conducted in Thailand stands out as the first trial to demonstrate an estimated efficacy of 30% for a vaccine regimen against HIV[383]. This study generated hypotheses suggesting that V1V2 antibodies may contribute to protection against HIV infection, along higher ADCC responses in the presence of low levels of Env-specific IgA antibodies[386]. Moreover, several studies have identified a correlation between ADCC responses and reduced viral loads, protection from infection, and enhanced clinical outcomes in linked transmission[387–389]. These studies position NK cells as promising candidates for immunotherapeutic interventions aimed at targeting the HIV reservoir.

In this regard, **Chapter 2** of the present thesis endeavors to evaluate, a novel bispecific antibody, both in vitro and in vivo, intended to enhance the NK-mediated immune clearance of HIV-infected cells.

2. HYPOTHESIS AND OBJECTIVES

2 Hypothesis and objectives

The development of ART represents a significant milestone in HIV research, successfully suppressing HIV viremia to undetectable levels in the majority of PWH. Nonetheless, despite its notable efficacy, ART fails to achieve complete elimination of HIV. Cessation of ART is followed by a rebound in viral load, primarily attributed to the establishment of latent HIV reservoirs shortly after infection, which persists within the body over prolonged periods. Furthermore, the prevalence of HIV infections has reached a plateau in recent years, increasing the number of people that require therapeutic interventions for life. The convergence of adverse effects and limited accessibility for ART in some populations highlights the need for the development of innovative therapeutic approaches aimed at achieving a cure for HIV infection.

Our hypotheses are the following:

1) Given the capability of HIV EC to manage HIV infection without ART, they may harbor distinct innate immunological characteristics that facilitate either the elimination or containment of HIV upon infection.
2) The induction of targeted NK cell responses, along the enhancement of NK-mediated clearance of HIV-infected cells, may contribute to the reduction of the viral reservoir.

The global objectives of this thesis encompass, first, the characterization of the NK cell repertoire linked to HIV control in EC, alongside an examination of their functional activity compared to diverse cohorts of PWH. Second, this study aims to devise and assess a novel immunotherapeutic approach centered on employing a bispecific antibody designed to target both NK cells and HIV-infected cells, with the goal to enhance NK-mediated responses directed at eliminating HIV-infected cells.

The specific objectives of this doctoral thesis are as follows:

1) To characterize the phenotype, activation, and ADCC responses within the NK cell repertoire of HIV EC.
2) To identify and investigate the phenotype and transcriptional profile of NK cells that mediate ADCC responses in HIV EC.
3) To evaluate, in vitro, a novel bispecific antibody targeting CD16 expressed by NK cells, and gp120 present on HIV-infected cells, and to assess its efficacy in promoting the elimination of HIV-infected cells in the context of diverse HIV infection settings.
4) To conduct the preclinical assessment of the bispecific antibody in a humanized mice model of HIV infection.

3. RESULTS

3 Results

3.1 Chapter 1

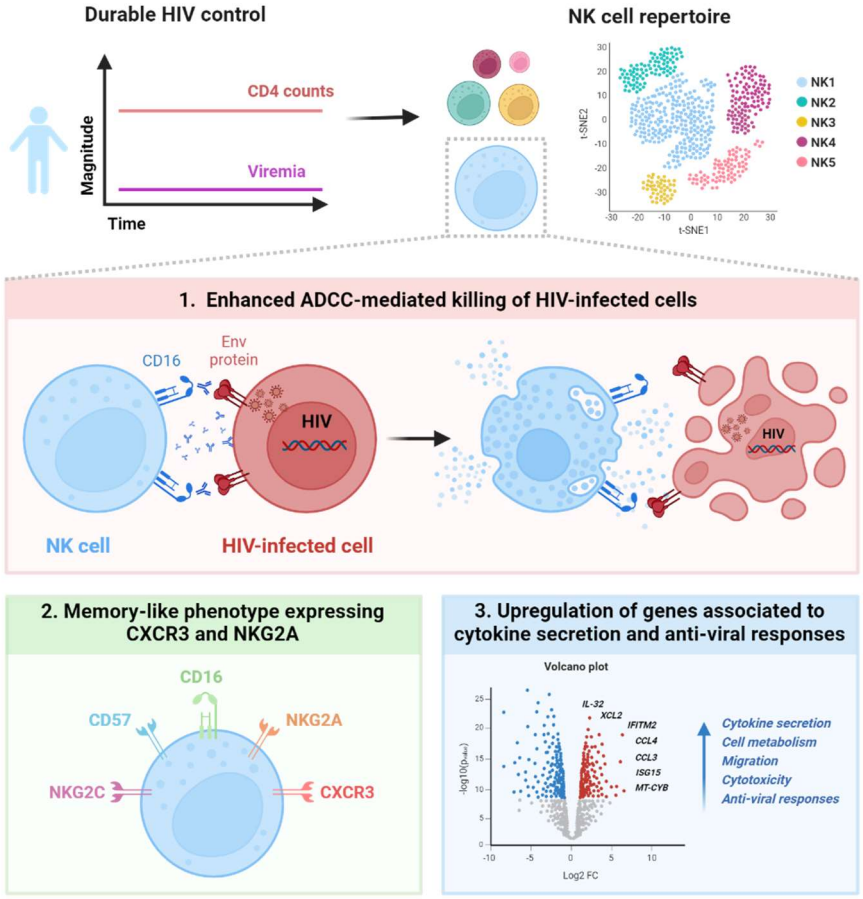
3.1.1 Title

Co-expression of NKG2C and NKG2A Defines a Highly Functional Antiviral NK Population in Spontaneous HIV Control

3.1.2 Abstract

Elite controllers (EC), a unique group of people with HIV (PWH), exhibit remarkable control of viral replication in the absence of antiretroviral therapy. In this study, we comprehensively characterized the NK cell repertoire in EC after long-term viral control. Phenotypic profiling of NK cells revealed profound differences compared with other PWH, but marked similarities to uninfected individuals, with a distinctive prevalence of $NKG2C^{+}CD57^{+}$memory-like NK cells. Functional analyses indicated that EC had limited production of functional molecules upon NK stimulation and consequently reduced natural cytotoxicity against non-HIV target cells. Importantly, EC showed an exceptional ability to kill primary HIV-infected cells by the Antibody-dependent cell cytotoxicity (ADCC) adaptive mechanism, which was achieved by a specific memory-like NK population expressing CD16, NKG2A, NKG2C, CD57 and CXCR3. In-depth single-cell RNA sequencing unveiled a unique transcriptional signature in these NK cells linked to increased cell metabolism, migration, chemotaxis, effector functions, cytokine secretion, and antiviral response. Our findings underscore a pivotal role of NK cells in the immune control of HIV and identify specific NK cells as new targets for immunotherapies.

3.1.3 Graphical Abstract



3.1.4 Introduction

Elite controllers (EC) are extraordinary people with HIV (PWH) who maintain undetectable HIV viremia in the absence of antiretroviral therapy (ART)[390,391]. Although EC cannot eliminate the HIV infection, their immune system presents a remarkable ability to control viral replication, representing a model for a functional cure[333,334,184,335]. Fundamental to this exceptional control, there are different genetic, immunological, and virological factors that contribute to their ability to maintain viral suppression[392,393]. These factors vary among EC cohorts, indicating heterogeneity in the mechanisms underlying viral control. The establishment of viral control after acute infection is also not uniform across all EC and depends on both viral and host factors. This suggests that effective host mechanisms from the beginning of infection are essential to achieve rapid suppression of viral replication[394–396]. Furthermore, the duration of spontaneous control, once established, can differ significantly, ranging from a few months to more than a decade. Only a small proportion (around 0.15%) can maintain replication control for long periods (longer than 10 years)[375,397]. Additionally, some studies have found the existence of residual plasma viremia in the majority of EC individuals (<2 copies HIV-1 RNA/ml), which may be associated with both immunological and/or virologic progression[398,399].

Genetic polymorphisms in the human HLA class I locus, particularly the overrepresentation of alleles including HLA-B*57, HLA-B*27, HLA-B*13, and HLA-B*58-01, are strongly associated with HIV control[400,401]. Some studies have demonstrated the association of these protective MHC alleles with a robust cytotoxic CD8 T cell response in EC[336,402]. Nonetheless, a considerable proportion of EC that lack protective MHC alleles may control HIV infection through non-CTL mechanisms, pointing out that MHC alleles are neither necessary nor sufficient for HIV control[403]. While studies on EC have intensively focused on adaptive immunity due to the association with MHC-I alleles[404,405], it is possible that innate immune responses are also important in HIV control[406,407].

Natural killer (NK) cells are critical effector cells from the innate immunity that play an important role in HIV infection since they recognize and respond to HIV-infected cells from the earliest infection stages[274]. NK cell activation state is contingent upon the signaling received through a broad set of cell surface receptors. When these receptors bind to their cognate ligands, they promote either activating or inhibitory signals. Therefore, the balance between these opposing signals dictates the functional status of NK cells[408]. Activating receptors such as NKG2C, NKp30 and NKG2D facilitate target cell recognition and cytotoxicity, while inhibitory receptors such as KLRG1, NKG2A and Killer Immunoglobulin-like Receptors (KIRs) help fine-tune NK cell responses by counteracting excessive activation[409].

This balance, maintained through interactions with MHC-I antigens, serves to educate NK cells, promoting tolerance to healthy cells while priming them to respond to infected cells with reduced MHC class I antigen expression levels[410]. In HIV infection, certain genetic combinations, such as KIR3DS1 with its ligand HLA-Bw4-08I, and KIR3DL1 with HLA-B*57, have been associated with lower viral loads and reduced risk of progression to AIDS, emphasizing the importance of NK cell genetics in HIV control[411,412]. Importantly, during viral infections, such as human cytomegalovirus (CMV), the virus can imprint the NK cell receptor repertoire, leading to the expansion of diverse, long-lived, and highly functional NK cells[413]. These expanded NK cells, characterized by the expression of the NKG2C and CD57, have the potential to mediate immune memory[414].

In addition, NK cells mediate antibody-dependent cellular cytotoxicity (ADCC), an adaptive immune mechanism implicated in protection against HIV[356]. ADCC is triggered when NK cells, via CD16, recognize the constant fraction (Fc) of IgG antibodies bound to aberrant targets. Antibodies form a bridge between NK and target cells, promoting CD16 cross-linking, which triggers NK cell activation and degranulation, leading to the cytolysis of target cells. In this regard, several studies have shown that PWH present an altered NK cell phenotype and decreased cytotoxic activity compared to healthy individuals[354,415,416]. Other studies have reported elevated levels of anti-Env/gp120 antibodies in EC compared to other groups of PWH[356]. However, the specific contribution of NK cells in HIV control via the ADCC mechanism remains unclear in these individuals. Taken together, these studies provide strong evidence that NK cells influence disease progression, and therefore, represent a new target to explore in the context of HIV control.

Here, to identify NK-cell factors associated with HIV control, we investigated the phenotypic, functional and transcriptional profiles of NK cells from 4 cohorts of PWH: ART-suppressed (ART), ART-naïve viremic (VIR), and EC with durable HIV control (DC), or immunological aborted HIV control (AC), compared to uninfected individuals (HD). In-depth characterization indicated that DC-individuals present a unique NK cell repertoire associated to a robust ADCC response against HIV-infected cells. Our work shows important aspects of the NK cell phenotype and function in EC that may contribute to the long-term HIV control, and which might have important implications for the development of new NK-targeted anti-HIV immunotherapies.

3.1.5 Materials and methods

Sex as a biological variable

Cisgender women and men were included in the study.

Ethics statement and study samples

Blood samples from n=25 healthy donors (HD) were obtained from the Blood and Tissue Bank, Barcelona, Spain (register number C.0003590). Collected samples were anonymous and untraceable. Blood samples from two cohorts of people with HIV (PWH, n=66) were obtained from the HIV unit of the Hospital Universitari Vall d'Hebron (Institutional Review Board numbers PR(AG)270/2015, PR(AG)192/2018, and PR(AG)476-2018): ART-suppressed PWH (ART, n=24, 2-4 years undetectable viral load) and recently diagnosed ART-naïve viremic participants with immunological factors compatible with chronic infection (VIR, n=18, HIV-1 RNA=30,000-900,000 copies/ml, $CD4^+$ T cell counts=300-1,400). PBMC samples from n=35 HIV EC were obtained from the Spanish AIDS Research Network (RIS) cohorts of HIV Controllers Study Group (ECRIS) database. Viral load and complete blood count records were obtained from healthcare providers with subject consent (**Supplementary Figure 1**).

EC samples were selected and classified in two different EC phenotypes according to their ability to maintain long-term viral and immunological control. Aborted immunological control (AC, n=14) was defined as five to ten years of documented HIV control to viral loads below 40 HIV-1 RNA copies/ml and stable $CD4^+$ T cell counts in absence of ART prior to a progressive but significant $CD4^+$ T cell decline during the patient's follow-up period, evaluated by linear regression (negative slope, $p<0.05$) without subsequent return to stable control. Durable control (DC, n=21) was defined by maintenance of viral loads below 40 HIV-1 RNA copies/ml and stable $CD4^+$ T cell counts over time. All participants provided written informed consent prior to study participation. Subject characteristics are summarized in **Table 1**.

Due to sample accessibility, phenotypic analysis was conducted on all available samples, while functional analyses were restricted to a subset: n=14 HD, n=14 DC, n=10 AC, n=8 ART, and n=7 VIR.

Cells lines and reagents

PBMCs were obtained from peripheral blood samples using density-gradient centrifugation with Ficoll-Hypaque (Lymphoprep; Stemcell technologies).

Cells were then cryopreserved in liquid nitrogen in fetal bovine serum (FBS; Gibco, Life Technologies, Inc) containing 20% dimethyl sulfoxide (DMSO; Thermo Fisher Scientific) and stored until required for functional studies. The human lymphoblastic leukemia ACH-2 cell line (RRID:CVCL_0138) was obtained through the NIH AIDS Reagent Program, Division of AIDS, NIAID, NIH, from Dr. Thomas Folks. The human myeloid leukemia K562 cell line (RRID:CVCL_0004) was purchased from Sigma-Aldrich. Cells were cultured in RPMI 1640 medium supplemented with 10% fetal bovine serum (FBS; Gibco, Life Technologies, Inc), 100 U/ml penicillin, and 100 µg/ml streptomycin (Life Technologies, Inc.) (R10; control medium), and maintained at 37ºC in a 5% CO_2 incubator. NK cells were isolated from PBMCs using a commercial kit (MagniSort™ Human NK cell Enrichment; eBioscience). Two rounds of cell separation were performed to maximize the purity of the cells (overall purity >70%). Recombinant human interleukin-15 (IL-15) was purchased from Miltenyi Biotec.

Flow cytometry phenotyping

PBMCs were stained with a viability dye (LIVE/DEAD Fixable Aqua dead cell stain; Thermo Fisher) for 20 min at RT. After washing twice with PBS, cells were incubated with anti-CXCR3-BV650 (G025H7; Biolegend) for 30 min at 37ºC. Cells were then washed with staining buffer and stained with anti-CD57-PerCP-Cy5.5 (HNK-1; Biolegend), anti-CD56-FITC (B159; Becton Dickinson), anti-CD3-PE-Cy7 (SK7; Becton Dickinson), anti-NKp30-PE-CF594 (P30-15; Biolegend), anti-NKG2C-PE (134591; R&D Systems), anti-NKG2D-APC-Cy7 (1D11; Biolegend), anti-CD4-AF700 (RPA-T4; Becton Dickinson), anti-NKG2A-APC (Z199; Beckman Coulter), anti-CD16-BV786 (3G8; Becton Dickinson), anti-CD158b-BV605 (CH-L, Becton Dickinson), and anti-KLRG1-BV421 (14C2A07; Biolegend) for 20 min at RT. After washing, cells were then fixed with PFA (1%) and acquired on an LSR Fortessa flow cytometer (Becton Dickinson). Data was analyzed using OMIQ software from Dotmatics (www.omiq.ai, www.dotmatics.com). Gating was performed according to the different FMO controls.

NK cell functional activity assays

NK cell activation and natural cytotoxicity was measured by the detection of CD69, HLA-DR, CD107a and IFN_{γ} by flow cytometry in unstimulated NK cells and after co-culture with K562 cells or primed with IL-15. Briefly, NK cells were isolated from cryopreserved PBMCs using a commercial kit (MagniSort Human NK cell enrichment; eBioscience).

Then, NK and K562 cells were mixed at 1:1 ratio and cultured in R10 medium in the presence or absence of 25 ng/ml IL-15 (Miltenyi Biotec) for 4.5h in U-bottom 96-well plates at 37ºC and 5% CO_2. CD107a-PE-Cy5 (H4A3; Becton Dickinson), BD GolgiPlug Protein Transport Inhibitor (Becton Dickinson) and BD GolgiStop Protein Transport Inhibitor containing monensin (Becton Dickinson) were also added to each well at the recommended concentrations. Cells were then washed and stained with a viability dye (LIVE/DEAD Fixable Aqua dead cell stain; Thermo Fisher). To measure the activation markers HLA-DR and CD69, cells were stained with anti-CD56-FITC (B159; Becton Dickinson), anti-CD3-PE-Cy7 (SK7; Becton Dickinson), anti-HLA-DR-SB600 (LN3; eBioscience) and anti-CD69-PE-CF594 (FN50; Becton Dickinson) antibodies for 20 mins at RT. Cells were then fixed and permeabilized with Fixation/Permeabilization Solution (Becton Dickinson) for 20 mins at 4ºC, washed with BD Perm/Wash buffer and stained with anti-IFN_γ AF700 (Life Technologies) for 30 min at RT. After washing, cells were fixed with PFA (1%) and acquired on an LSR Fortessa flow cytometer (Becton Dickinson). Data were analyzed using FlowJo V10 software and OMIQ software from Dotmatics (www.omiq.ai, www.dotmatics.com).

Antibody-dependent cell-mediated cytotoxicity (ADCC) assays

ADCC was measured as described by others with some modifications[417]. Briefly, ACH-2 cells (used as target cells) were plated in round bottom 96 well plates and incubated for 15 mins with plasma (1:1.000 dilution) from a viremic HIV^+ PWH containing a mix of antibodies targeting different HIV epitopes. NK cells were isolated from PBMCs using magnetic beads (MagniSort™ Human NK cell Enrichment Kit, eBioscience) and added at 1:10 target/effector ratio. Plates were centrifuged at 400g for 3 minutes and incubated for 4 hours at 37ºC and 5% CO_2. After the co-culture, cells were washed and stained with a viability dye (LIVE/DEAD Fixable Violet dead cell stain; Thermo Fisher). Then, cells were stained with anti-CD56-FITC (B159; Becton Dickinson) and anti-CD3-PE-Cy7 (SK7; Becton Dickinson) for 20 min at RT. Cells were then fixed and permeabilized with Fixation/Permeabilization solution (Becton Dickinson) for 20 mins at 4ºC, washed with BD Perm/Wash buffer and stained with anti-p24-PE (KC57-RD1; Beckman Coulter) for 30 min at 4ºC and 30 min at RT. After washing, cells were fixed with PFA (2%) and acquired on an LSR Fortessa flow cytometer (Becton Dickinson). Data were analyzed using Flowjo V10 software. Reduction of the p24 marker was used to determine the percentage of target cell killing.

Fluorescence Activated Cell Sorting (FACS) of selected NK cell subsets from EC

For cell sorting, NK cells from EC were isolated from PBMCs using a commercial kit (MagniSort™ Human NK cell Enrichment; eBioscience). After enrichment, NK cells were stained with a viability dye (LIVE/DEAD Fixable Aqua Dead Cell stain; Thermo Fisher) for 20 min at RT in the dark. After, cells were washed with 1X PBS and stained with anti-CXCR3-BV650 (G025H7; Biolegend) for 30 min at 37ºC. Then, cells were washed with staining buffer and stained with anti-CD57-PerCP-Cy5.5 (HNK-1; Biolegend), anti-CD56-FITC (B159; Becton Dickinson), anti-CD3-PE-Cy7 (SK7; Becton Dickinson), anti-NKG2C-PE (134591; R&D Systems), anti-CD4-AF700 (RPA-T4; Becton Dickinson), anti-NKG2A-APC (Z199; Beckman Coulter), and anti-CD16-BV786 (3G8; Becton Dickinson) for 20 min at RT. Cells were then washed with staining buffer and immediately sorted using the Cytek Aurora Cell Sorter. We sorted live NK cell populations ($CD3^-CD4^-CD56^+$). Then, $CD16^+$ cells derived from $CD56^+$ NK cells were classified based on the expression of NKG2A, NKG2C, CD57 and CXCR3. NK cell classification included: NKA ($NKG2A^+$ $NKG2C^+$ $CD57^+$ $CXCR3^+$), NKB ($NKG2A^-$ $NKG2C^+$ $CD57^+$ $CXCR3^+$), NKC ($NKG2A^+$ $NKG2C^-CD57^+$ $CXCR3^+$), and NKD ($NKG2A^-NKG2C^-$ $CD57^+$ $CXCR3^+$). CD16- NK cells were designated as NKE. Cell numbers obtained after sorting of selected NK cell populations are shown in **Supplementary Table 2**.

Dimensionality Reduction Analysis

Dimensionality reduction analysis (opt-SNE) of flow cytometry data was performed in OMIQ (www.omiq.ai, www.dotmatics.com). All events within pre-gated $CD56^+$ NK cells were concatenated for each group per group and culture condition and analyzed. Clustering analysis was performed via Flow-Self Organizing Maps (FlowSOM) artificial intelligence algorithm on equal samples of randomly selected 7 x 10^5 cells from each group. For phenotypic characterization, clustering was performed based on the expression of the markers: CD57, NKp30, NKG2C, NKG2D, NKG2A, CD16, CXCR3 and CD158b and KLRG1. Marker expression was normalized and represented as Archsinh-transformed medians within heatmaps generated via optSNE analysis[418].

Gene expression analysis by single-cell RNA sequencing

NK cell samples enriched in specific receptors were obtained through FACS, as described in the previous section. A total of 529.800 cells were isolated from the NKA subset, 170.000 from the NKB subset, and 370.000 from the NKC subset.

Subsequently, RNAseq libraries were prepared at the Josep Carreras Institute using the Chromium single-cell RNA sequencing (scRNAseq) 3' protocol and were subjected to sequencing on the NovaSeq PE150 platform at Novogene. The Cell Ranger pipeline was employed for read alignment to the human genome, cell calling, and generation of the raw counts matrix. Quality controls were conducted using FastQC v0.11.9 to ensure data was appropriate for downstream analyses. Based on the quality control outcomes, a conservative filtering approach was applied, considering the number of features per cell and mitochondrial/ribosomal counts, to exclude cells of low quality. Subsequent to alignment and quantification of reads to annotated mRNAs using the Cell Ranger count tool, data normalization was executed using SCTransform. Dimensionality reduction was achieved through Principal Component Analysis (PCA) based on the top 3000 most variable features, and the first 30 principal components (PCs) were retained for subsequent analyses. Cell clustering was performed using a shared nearest neighbor (SNN) modularity optimization-based clustering algorithm. Visualization of cell distribution based on sample type was accomplished through Uniform Manifold Approximation and Projection (UMAP). Cluster marker identification and Differential Expression Analyses (DEA) were conducted using the FindMarkers function from the Seurat package. The assessment of biological significance was conducted through enrichment analysis utilizing the Gene Ontology Biological Process category database. Additionally, differentiation trajectory analysis was carried out using the Slingshot package. Bioinformatics analysis was carried out in the Statistics and Bioinformatics Unit (UEB) at Vall d'Hebron Research Institute (VHIR).

Quantification and statistical analyses

Number of individuals per group are described in the figure legends. All figure panels include data sets obtained from individual samples. All graphing and statistical analyses were performed using GraphPad Prism 8.3. Significance of differences between all experimental groups was determined using a 1-way or 2-way ANOVA followed by a Dunn's multiple-comparisons test or Tukey's multiple-comparisons test, and are reported within each figure legend. A *P* value of less than 0.05 was considered significant: *P<0.05, **P<0.01, ***P<0.001, ****P<0.0001. Data is shown as median ± interquartile range (IQR). Tables were prepared using Microsoft Word and Excel.

3.1.6 Results

Cohort characteristics

PBMCs from 35 EC were obtained from the Spanish AIDS Research Network (RIS) cohort of HIV Controllers Study Group (ECRIS). Within this cohort, 21 participants demonstrated durable control (DC) over HIV infection, maintaining viral loads below 40 HIV-1 RNA copies/ml and stable $CD4^+$ T cell counts for a period ranging from 5 to 20 years (median 7.25 years). Conversely, 14 individuals experienced a loss of immunological control (aborted control, AC), as evidenced by a progressive and statistically significant decline in $CD4^+$ T cell count over the follow-up period ($p<0.05$, determined by simple linear regression). The longitudinal profiles of $CD4^+$ T cell counts and HIV-1 RNA levels for EC participants are depicted in **Supplementary Figure 1**. Two additional cohorts were included in the study: samples from 2 to 4 years of ART-suppressed PWH (ART, n=24), and samples from treatment-naïve viremic participants recently diagnosed and with immunological factors indicative of chronic infection (VIR, n=17). Samples from uninfected donors (HD, n=24) served as controls. The clinical characteristics of HIV^+-individuals included in the study are summarized in **Supplementary Table 1**.

No significant differences in sex distribution were observed among the study groups (**Supplementary Table 1**). However, the median ages of DC (55 years) and AC (58 years) subjects were higher than that of ART (44 years) and VIR (39 years) groups ($p<0.05$, Kruskal Wallis test followed by Dunn's multiple comparisons test). These findings are consistent with the increased time since HIV diagnosis observed in the DC and AC groups compared to VIR ($p_{DC}=0.07$, $p_{AC}<0.001$, Kruskal Wallis test followed by Dunn's multiple comparisons test). Furthermore, significant differences in transmission routes were observed among all groups ($p<0.0001$, Fisher's exact test). $CD4^+$ T cell counts were also higher in DC, AC, and ART groups compared to VIR ($p<0.05$, Kruskal Wallis test followed by Dunn's multiple comparisons test). While DC, AC, and ART groups exhibited effective viral suppression (HIV-1 RNA<40 copies/ml), VIR participants demonstrated viral loads ranging between 60,000 and 800,000 copies/ml ($p<0.0001$, Kruskal Wallis test followed by Dunn's multiple comparisons test). Despite having HLA typing data available for only 22 out of 35 participants within the EC group, protective HLA-B alleles (HLA-B57, B52, B27, and B14), identified through genome-wide association studies in spontaneous HIV controllers[337], were found at comparable frequencies in both AC and DC subjects (**Supplementary Table 1**).

These findings suggest similarities in clinical, genetic, and virologic parameters within HIV$^+$ individuals with spontaneous HIV control while confirming the anticipated differences between these groups and viremic individuals.

NK cell phenotypes with memory-like attributes distinguish individuals with durable control

We first studied the overall frequencies of NK cells, the prevalence of the primary NK cell subsets based on CD56 and CD16 expression, and the percentage of memory-like NK cells characterized by the presence of NKG2C and CD57 markers across all study groups[419–421]. An example of the gating strategy and a representative flow cytometry plot delineating the distinct NK cell subsets studied are shown in **Supplementary Figure 2** and **Figure 1A**, respectively. All groups exhibited comparable frequencies of total and CD56^{bright} NK cells (**Figure 1B**). However, higher proportion of CD56^{dim}CD16^{high} NK cells were observed in ART individuals (**Figure 1B**). Interestingly, all PWH exhibited higher frequencies of memory-like NKG2C$^+$CD57$^+$ NK cells, although significance was only reached for DC, ART, and VIR, compared to HD (**Figure 1C**). These cells are more likely to represent expanded adaptive NK cells, as previously reported in CMV[422], and lately, in HIV infection[423].

Next, we studied if NK cells from DC presented a different expression pattern of important receptors for NK activity. For these analyses, we included NK receptors with activating or inhibitory potential upon interaction with ligands found on HIV-infected cells (KIR2DL2/L3 (CD158b), KLRG1, NKG2A, NKG2D, NKp30, and NKG2C), the chemokine receptor CXCR3, and the maturation marker CD57. Expression of selected markers in HD were concordant with previous studies[424]. We observed higher expression of the negative receptors CD158b and KLRG1 in ART and VIR groups relative to HD, DC, and AC in total CD56$^+$ and CD56^{dim}CD16^{high} NK cells (**Figure 1D**, **Supplementary Figure 3A**). By contrast, higher frequencies of NKG2A$^+$ and NKp30$^+$ NK cells were observed in HD, and AC, in both total CD56$^+$ and CD56^{dim}CD16^{high} NK cell subsets, compared to ART and VIR groups (**Figure 1D, Supplementary Figure 3A**). While NK cells from DC generally presented similar receptor expression patterns relative to those from HD and AC groups, DC displayed higher expression of the activating receptor NKG2C in all three NK cell subsets (**Figure 1D, Supplementary Figure 3A-B**). No remarkable differences were observed in the expression of CXCR3, NKG2D, and CD57 receptors among DC and other groups in both total CD56$^+$ and CD56^{dim}CD16^{high} NK cells (**Figure 1D**, **Supplementary Figure 3A**).

By contrast, increased CXCR3 expression was observed in ART compared to DC and VIR groups in $CD56^{bright}$ NK cells (**Supplementary Figure 3B**).

Next, we focused on the memory-like $NKG2C^{+}CD57^{+}$ NK cell population. For consistency, only samples with expanded $NKG2C^{+}CD57^{+}$ NK cells (>5% frequency) were analyzed. Comparative analysis revealed no statistical differences in the expression levels of CD158b, CXCR3, NKG2D, and NKp30 across the distinct study cohorts (**Figure 1E**). Consistent with the other NK cell subsets, a trend towards elevated frequencies of $KLRG1^{+}$ memory-like NK cells was observed in ART and VIR groups compared to HD, DC, and AC (**Figure 1E**). Furthermore, within the DC group, heightened frequencies of $NKG2A^{+}$ memory-like NK cells were found compared with ART (**Figure 1E**).

Overall, our study reveals two important aspects; the first is that distinct phenotypic variations are observed within NK cell populations among different PWH groups, underscoring the heterogeneity of the NK cell repertoire during HIV infection. Second, the expression of the different NK cell receptors within the distinct NK cell subsets observed in DC was similar to those observed in AC, and in healthy controls, except for the memory-like $NKG2C^{+}CD57^{+}$ subset of cells, which was enriched in NK from the DC cohort. Moreover, within the memory-like NK cell subset, the expression of NKG2A was elevated compared to other groups, indicating their potential to regulate their functional responses[425]. These identified markers of NK cell populations represent a distinctive hallmark of EC who spontaneously control HIV for prolonged periods without virological and immunological progression.

Figure **1**

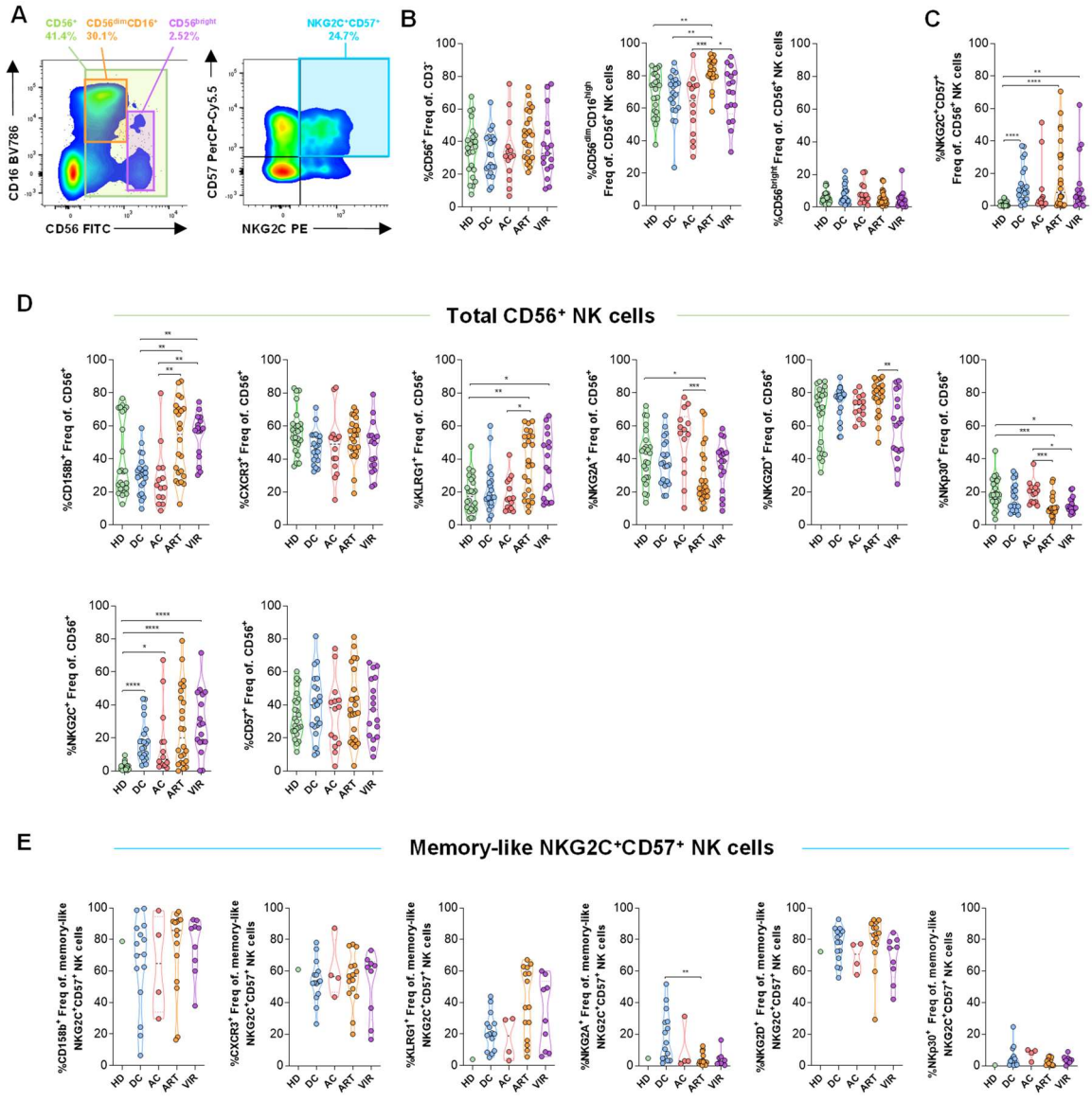


Figure 1. Phenotypic characterization of NK cells in EC. The expression of different NK markers was quantified by flow cytometry in different study groups: healthy donors (HD, n=25), EC with durable HIV control (DC, n=21), EC with aborted immunological control (AC, n=14), PWH ART-treated individuals (ART, n=24), and viremic PWH (VIR, n=18). **A**) Representative flow cytometry plots depicting the NK cell subset gating strategy from $CD3^-$ cells based on CD56 and CD16 expression (left: $CD56^+$ total, $CD56^{dim}CD16^{high}$, $CD56^{bright}$) and NKG2C and CD57 expression (right: $NKG2C^+CD57^+$ memory-like NK cells). **B**) Violin plots depicting the frequency of different NK cell populations identified by study group (left to right: $CD56^+$ total, $CD56^{dim}CD16^{high}$, $CD56^{bright}$). **C**) Violin plots showing the frequency of $NKG2C^+CD57^+$ memory-like NK cells by study group. **D**) Violin plots depicting the frequency of different NK cell markers in $CD56^+$ total NK cells by study group (left ro right: CD158b, CXCR3, KLRG1, NKG2A, NKG2D, NKp30, NKG2C, CD57). **E**) Violin plots showing the frequency of distinct NK cell receptors in expanded memory-like $NKG2C^+CD57^+$ NK cells (frequency >5% and counts >25, left to right: CD158b, CXCR3, KLRG1, NKG2A, NKG2D, NKp30). Median with range is represented. Statistical comparisons were performed using Kruskal-Wallis one-way ANOVA test followed by Dunn's multiple comparisons test. *p<0.05, **p<0<01, ***p<0.001, ****p<0.0001.

NK cells from individuals with durable control exhibit reduced natural cytotoxicity but enhanced ADCC activity against HIV-infected cells

Next, we aimed to directly elucidate the functional signatures of NK cells in all study groups. We focused on the functional response of DC participants as they represent a model for a functional cure for HIV. We performed NK cytotoxicity assays against the MHC-devoid K562 cell line, using NK cells that were either unstimulated or primed with IL-15 (gating strategy shown in **Supplementary Figure 4A**). NK cell activation, degranulation (CD107a), and IFN_{γ} secretion were measured upon stimulation (**Supplementary Figure 4B-D**). Although all study groups showed significant IFN_{γ} production and degranulation activity against target cells upon stimulation, reduced degranulation responses were observed in total $CD56^{+}$ NK cells from DC compared to HD, ART and VIR groups (**Figure 2A-C**). A trend to decreased frequencies of $CD69^{+}$ total NK cells was observed in DC compared to other groups, which was maintained upon stimulation (**Figure 2D**). Conversely, no group-based differences in HLA-DR expression were observed following stimulation (**Figure 2E**). Similarly, increased IFN_{γ} production and degranulation were observed in $CD56^{dim}CD16^{high}$ and $CD56^{bright}$ NK cell subsets upon stimulation in all study groups (**Supplementary Figure 5A-B**). Notably, the expanded memory-like NK cell population (>5% frequency) showed, in general, higher ability to produce IFN_{γ} and CD107 upon stimulation, compared to total $CD56^{+}$ NK cells (**Figure 2A-C, F-H**). A tendency towards decreased degranulation responses was observed within the memory-like NK cell population in DC, exhibiting diminished IFN_{γ} production, degranulation, and polyfunctional responses (IFN_{γ} and CD107a expression) compared to HD (**Figure 2F-H**). Conversely, no discernible differences were observed in CD69 or HLA-DR expression levels among memory-like NK cells from DC individuals relative to other groups (**Figure 2I-J**).

Subsequently, we evaluated the intrinsic natural cytotoxicity of NK cells by quantifying their killing capacity against MHC-devoid K562 cell targets. Cell killing was measured by a viability dye-based flow cytometric analysis (**Supplementary Figure 6A**). Notably, NK cells from DC individuals exhibited a significantly reduced cytotoxic response towards K562 target cells (Median killing=4.46%), in contrast to HD (Median killing=15.10%) and ART groups (Median killing=11.30%) (**Figure 2K**). Specifically, NK cells from DC demonstrated an approximate reduction of 30% in their ability to eliminate target cells compared to HD (**Figure 2K**). Importantly, and consistent with prior literature[285,426,427], our findings reveal a positive association between the frequency of $CD56^{dim}CD16^{high}$ NK cells and natural cytotoxic responses, while a negative correlation is observed with $CD56^{bright}$ frequencies (**Figure 2L**).

Of note, no significant associations were found between natural cytotoxic responses and the frequency of memory-like NK cells (**Figure 2L**).

We next evaluated the adaptive ADCC activity of NK cells towards HIV-infected cells. Briefly, ACH-2 cells were co-cultured for 4 hours with isolated NK cells from the different study groups, in the presence of plasma from a viremic HIV^+ patient containing a pool of antibodies targeting the gp120 protein. Cell killing was assessed by the lack of detection of the viral protein p24 in infected cells by flow cytometry (**Supplementary Figure 6B**). NK cells from DC performed strong ADCC responses (Median ADCC=19.09%) with an overall capacity similar to the one observed for HD (Median=29.63%), for which higher variation was observed (**Figure 2M**). Defective ADCC was observed for AC and VIR NK cells ($Median_{AC}$=7.58%, $Median_{VIR}$=1.18%), which showed significantly reduced activity compared to HD and DC (**Figure 2M**). Similarly, ADCC from NK cells derived from the ART group was reduced relative to HD ($Median_{ART}$=12.82%) (**Figure 2M**). Importantly, the enhanced capacity of NK cells from DC to kill via the ADCC mechanism was not related to the direct abundance of $CD56^{dim}CD16^{high}$ NK cells, the subset primarily implicated in ADCC response, nor to the frequencies of memory NK cells (**Figure 2N**).

Overall, all study groups exhibited elevated frequencies of activated NK cells, marked by the secretion of soluble effector molecules, such as IFN_{γ} and CD107a, upon stimulation. However, DC individuals exhibited a more limited production of these molecules compared to other groups, particularly within the memory-like NK cell subset. These functional alterations in NK cells from DC translated into lower natural cytotoxicity. Conversely, DC-NK cells demonstrated a potent ADCC response against HIV-infected cells, which was not related to the presence of any major NK subset, suggesting a distinctive feature of NK cells from DC individuals.

Figure 2

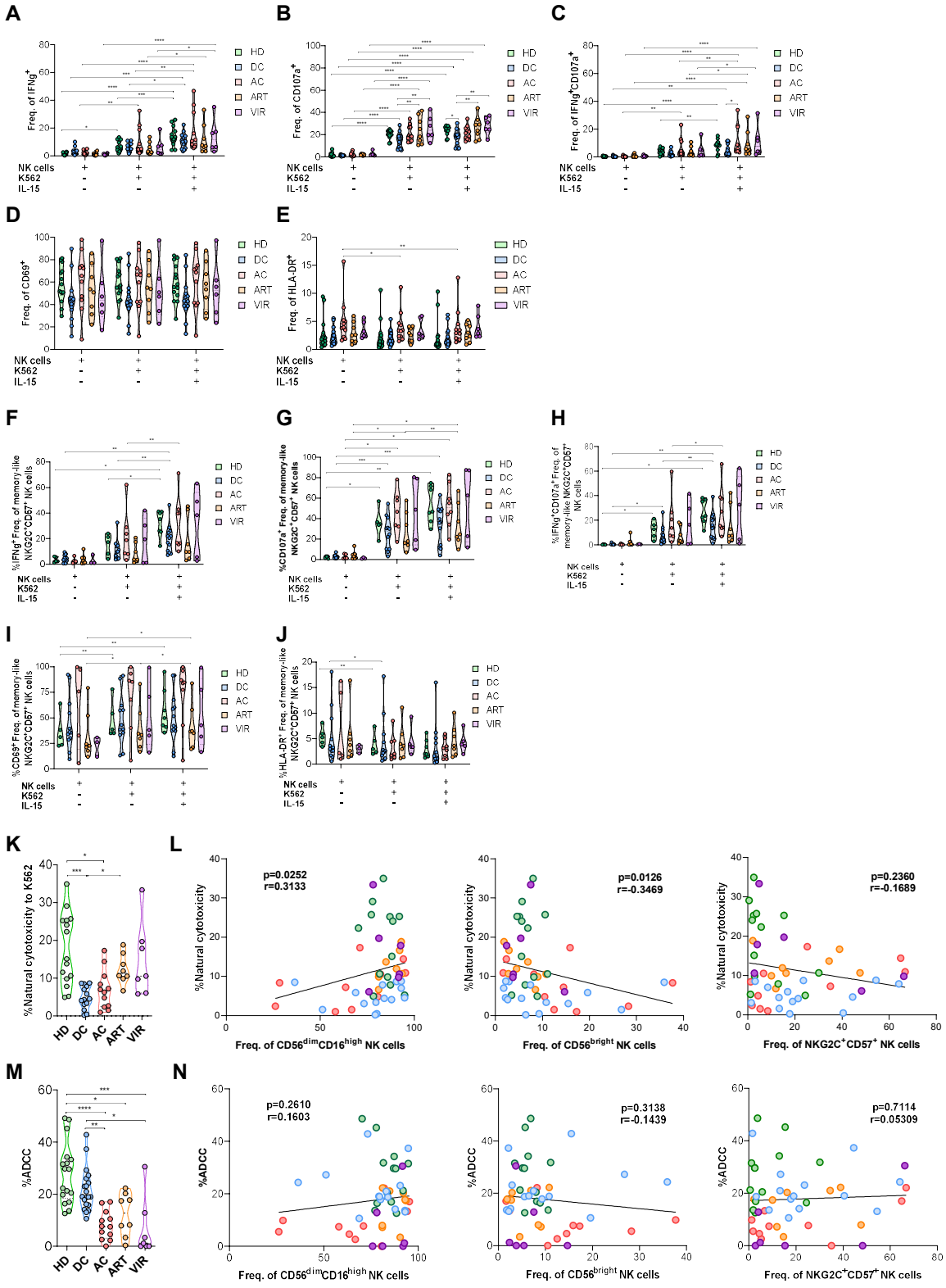


Figure 2. Functional profile of NK cells in EC. NK cell activation and cytotoxicity subsequent to stimulation were evaluated by study group. The percentages of **A**) IFNγ$^+$, **B**) CD107a$^+$, **C**) polyfunctional IFNγ$^+$CD107a$^+$, **D**) CD69$^+$, and **E**) HLA-DR$^+$ cells within the CD56$^+$ NK cell population were determined in basal conditions, following co-culture with K562 target cells, and with additional IL-15 stimulation.

Similarly, these metrics were quantified in expanded memory-like NKG2C$^+$CD57$^+$ NK cells (frequency >5%): the percentages of **F**) IFNγ$^+$, **G**), CD107a$^+$, **H**) polyfunctional IFNγ$^+$CD107a$^+$, **I**) CD69$^+$, and **J**) HLA-DR$^+$ NK cells post-stimulation were evaluated. **K**) Violin plots depicting the natural cytotoxicity exhibited by CD56$^+$ total NK cells from the different study groups following co-culture with K562 cells. **L**) Spearman correlations between natural cytotoxic responses and the frequency of distinct NK cell subsets (left to right: CD56^{dim}CD16^{high} NK cells, CD56^{bright} NK cells, and NKG2C$^+$CD57$^+$ NK cells). **M**) Violin plots showing the ADCC activity mediated by CD56$^+$ total NK cells against HIV-expressing cells by study group. **N**) Spearman correlations between ADCC responses and the frequency of different NK cell populations (left to right: CD56^{dim}CD16^{high} NK cells, CD56^{bright} NK cells, and NKG2C$^+$CD57$^+$ NK cells). For violin plots, median with range is represented. Statistical comparisons for A-J were performed using RM two-way ANOVA followed by Tukey's multiple comparisons test. Statistical comparisons for K and M were performed using the Kruskal-Wallis test. *p<0.05; **p<0.01; ***p<0.001; ****p<0.0001.

A distinctive memory-like NK population in DC is associated with enhanced ADCC responses against HIV-infected cells

Next, to uncover novel NK cell subsets linked with the functional responses observed in DC individuals, we explored the landscape of the different NK cell populations by reduction of dimensionality analysis. Unsupervised clustering analysis via the FlowSOM algorithm allowed us to identify eleven different NK cell clusters with an individual pattern of expression of the selected receptors (**Figure 3A**). Importantly, we identified clusters #C2 and #C4 as clusters of interest, as they were enriched in individuals with DC (**Figure 3B**). These clusters comprised cells expressing CD16, an important receptor to mediate ADCC, together with CXCR3, NKG2A, and CD57 (**Figure 3C**). Of note, #C4 additionally exhibited CD158b and NKG2C expression, representing a unique memory-like NK cell phenotype (**Figure 3C**).

Subsequently, we examined the relationship between functional NK cell responses and the frequency of the distinct NK cell clusters (**Figure 3D**). A significant negative correlation was observed between cluster #C6 and natural cytotoxic responses (r=-0.33, p=0.02), while a positive correlation was noted between cluster #C7 and natural cytotoxicity (r=0.30, p=0.03) (**Figure 3D-E**). Notably, there were no significant differences in the frequency of these clusters among study groups (**Figure 3B**). Both clusters prominently expressed CD158b and NKp30, while NKG2C and CD57 markers were either low or absent (**Figure 3C**). However, cluster #C7, which was associated with higher natural cytotoxicity, displayed elevated levels of CD16 and KLRG1, distinguishing it from cluster #C6, which was defined by the co-expression of CXCR3 and NKG2A (**Figure 3C**). In addition, cluster #C2 exhibited a trend for a positive correlation with ADCC responses, although no statistical significance was achieved (**Figure 3D**). Importantly, cluster #C4, predominantly composed of memory-like NK cells expressing NKG2A and CXCR3, exhibited a robust association with ADCC responses (**Figure 3D, F**). Remarkably, this correlation was particularly strong within the DC group (p=0.0082, r=0.68) (**Figure 3G**).

Overall, we identified different NK populations associated with specific functions. A $CD16^{+}$ $CD158b^{+}$ $NKp30^{+}$ $NKG2D^{dim}$ and $KLRG1^{dim}$ population correlated with better natural cytotoxicity activity, while a unique memory-like NK cell population was associated with enhanced ADCC responses, especially in DC. This memory-like NK subset was characterized by the expression of CXCR3, indicating its potential to migrate to inflamed tissues, and NKG2A, an inhibitory receptor that identifies early-differentiated NK cells. This newly identified NK cell population represents a characteristic feature of individuals exhibiting natural HIV control.

Figure 3

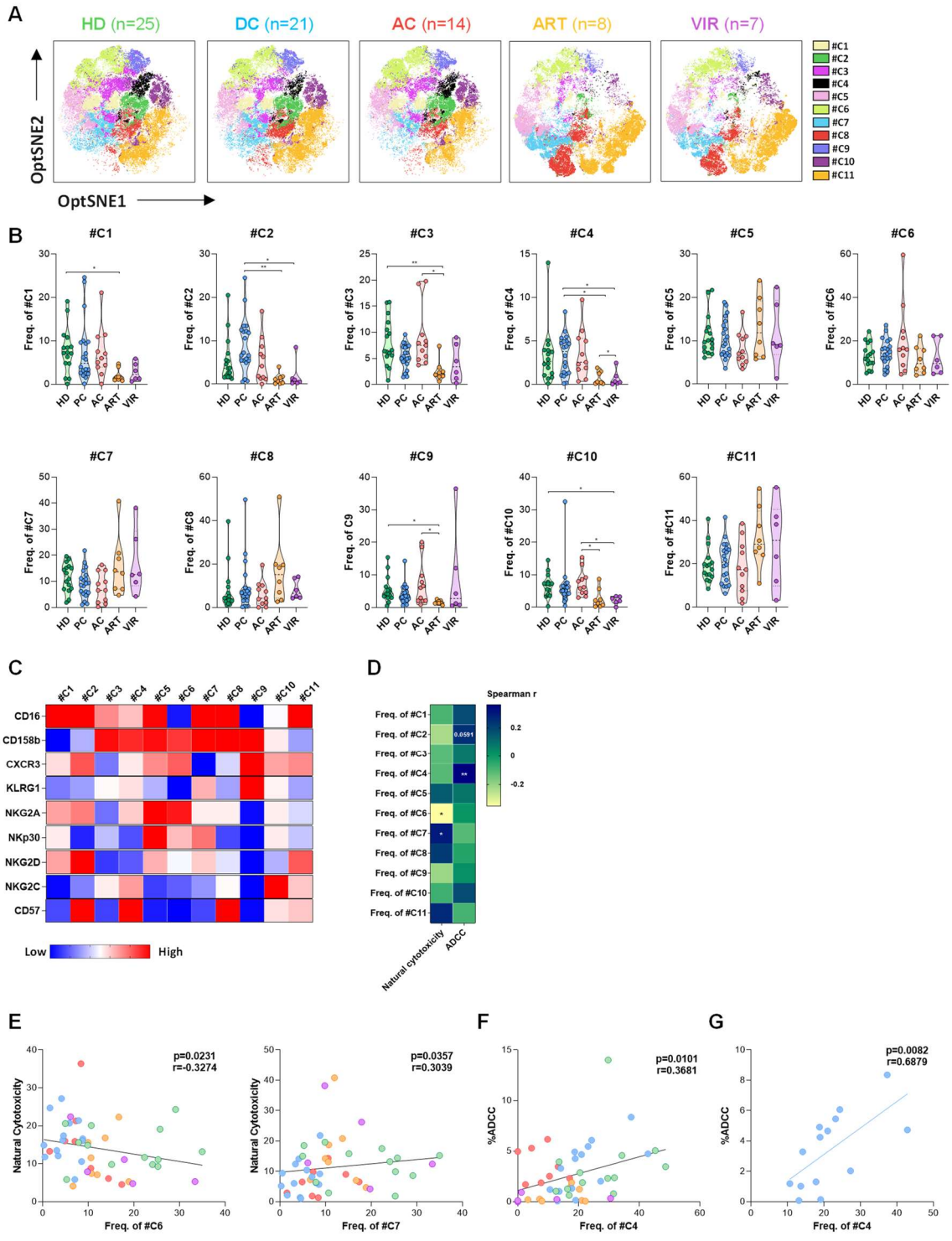


Figure 3. **Association between NK cell phenotype and functional responses in EC**. **A**) Optimized t-distributed Stochastic Neighbor Embedding (Opt-SNE) representation of distinct NK cell clusters, identified through dimensionality reduction based on the expression of the array of distinct NK cell receptors (CD16, CD158b, CXCR3, KLRG1, NKG2A, NKp30, NKG2D, NKG2C, and CD57), by study group (left to right: HD, DC, AC, ART, and VIR). **B**) Violin plots showing the frequency of each NK cell cluster in $CD56^{+}$ total NK cells by study group. **C**) Heatmap depicting the normalized median expression of the selected phenotypic NK cell markers within the cell clusters identified in Figure 2A.

D) Correlation matrix depicting Spearman correlations between the frequency of NK cell clusters identified by dimensionality reduction based on the expression of phenotypic markers and functional responses. **E**) Spearman correlations between the frequency of clusters #C6 and #C7 and natural cytotoxic responses in all study groups. **F**) Spearman correlation between the frequency of #C4 and ADCC responses in all study groups. **G**) Spearman correlation between the frequency of cluster #C4 and ADCC activity in DC group. Graphs represent medians and ranges. Each dot represents one individual of a specific cohorts, indicated by color code (HD in green; DC in blue; AC in red; ART in orange; VIR in purple). Statistical comparisons were performed using the Kruskal-Wallis test. *p<0.05; **p<0.01; ***p<0.001; ****p<0.0001.

Memory-like NK cells co-expressing NKG2A and CXCR3 exhibit heightened ADCC responses against HIV-infected cells

Next, we aimed to validate whether the memory-like NK cell population previously identified and linked to ADCC responses indeed displayed enhanced ADCC activity. We performed a functional ADCC assay using samples from 5 DC individuals. Distinct NK cell populations were isolated by FACS, based on the expression of selected receptors (**Figure 4A**). The cell numbers obtained after cell sorting are shown in **Supplementary Table S2**. Briefly, $CD16^+$ cells derived from $CD56^+$ NK cells were classified based on the expression of NKG2A, NKG2C, CD57 and CXCR3. NK cell classification included: NKA ($NKG2A^+$ $NKG2C^+$ $CD57^+$ $CXCR3^+$), NKB ($NKG2A^-$ $NKG2C^+$ $CD57^+$ $CXCR3^+$), NKC ($NKG2A^+$ $NKG2C^-$ $CD57^+$ $CXCR3^+$), and NKD ($NKG2A^-$ $NKG2C^-$ $CD57^+$ $CXCR3^+$). $CD16^-$ NK cells were designated as NKE. NK cells were then incubated with HIV^+ plasma and co-cultured with ACH-2 HIV-infected cells for 4h. We calculated cell killing as the reduction in the percentage of virally infected cells.

NKA, characterized by the co-expression of NKG2A and NKG2C, exhibited a more robust ADCC response against HIV-infected cells than any other NK population (Median ADCC=20.78%), especially compared to NK cells lacking CD16 expression (NKE, Median ADCC=1.54%), NKC (Median ADCC= 3.49%) and NKD (Median ADCC=1.38%) ($p<0.05$) (**Figure 4B**). In general, NKA exhibited the ability to eliminate approximately 50% more HIV-infected cells than the other NK cell subpopulations (Median ADCC for NKB=8.33%, NKC=3.49%, NKD=1.38%). Altogether, our findings suggest that the expression of the receptors CD16, NKG2A, NKG2C, CD57 and CXCR3 on NK cells identify a memory-like population with enhanced capacity for killing HIV-infected cells through ADCC.

Figure 4

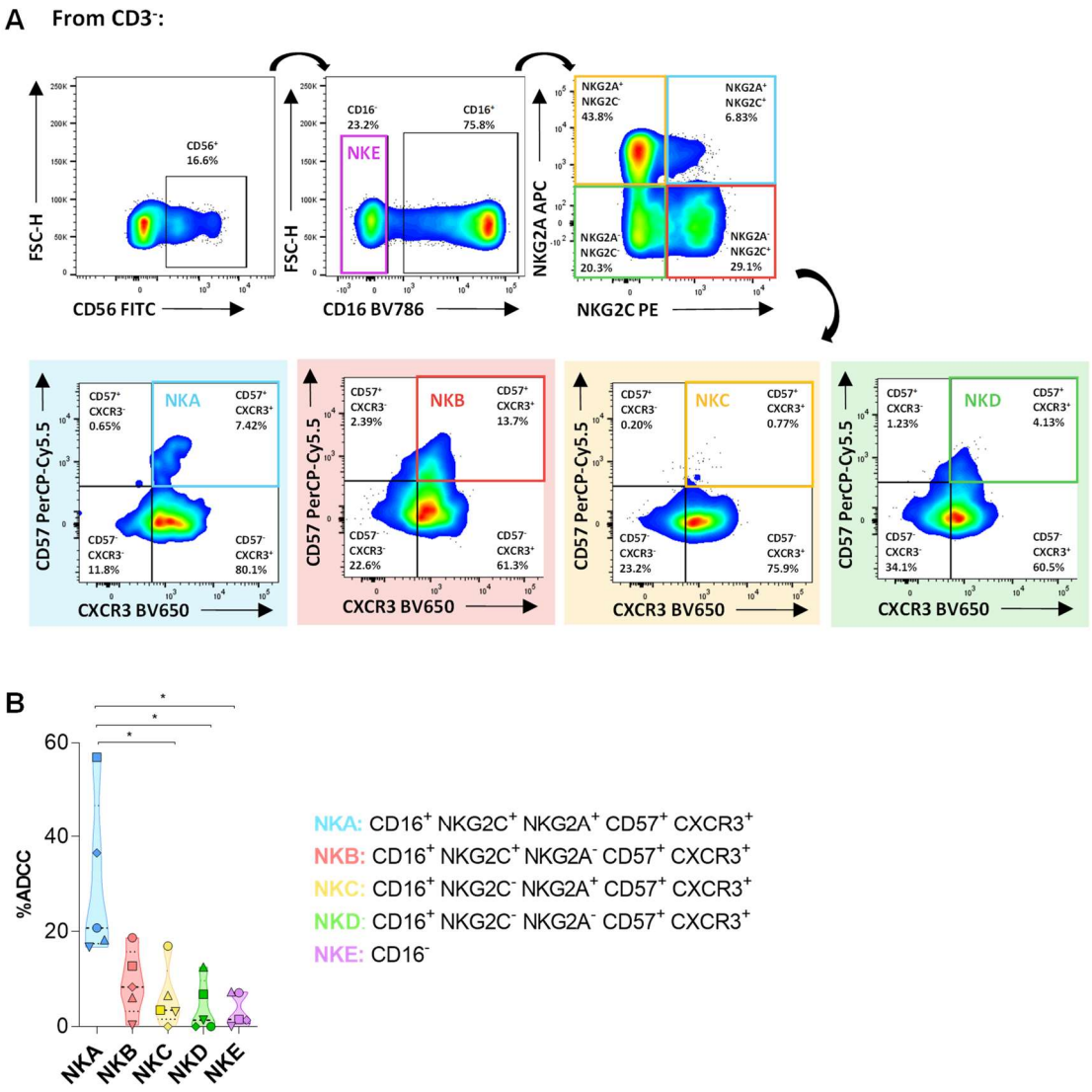


Figure 4. NK from DC enriched in specific receptors exhibit an increased ability to kill HIV-infected cells. Distinct NK cell subsets were isolated from n=5 DC individuals (Median $CD4^+$ T cell count: 1,030 cells/µl, Median viral load<40 copies HIV-1 RNA/ml) using Fluorescence-Activated Cell Sorting (FACS) based on selected receptors, and assessed for ADCC responses. **A**) Gating strategy of FACS isolated NK cell populations based on the expression of CD16, NKG2A, NKG2C, CD57, and CXCR3. Five populations were identified: NKA ($CD16^+NKG2A^+NKG2C^+CD57^+CXCR3^+$), NKB ($CD16^+NKG2A^-NKG2C^+CD57^+CXCR3^+$), NKC ($CD16^+NKG2A^+NKG2C^-CD57^+CXCR3^+$), NKD ($CD16^+NKG2A^-NKG2C^-CD57^+CXCR3^+$) and NKE ($CD16^-$). **B**) Violin plots depicting the ADCC activity mediated by each specific NK cell population based on the marker expression presented in Figure 4A. Graphs include group medians and ranges. Statistical comparisons were performed using the Friedman test followed by Dunn's multiple comparisons test. *p<0.05

Single-cell transcriptional analyses identifies NKA as a population with a unique transcriptional signature linked to increased NK cell effector functions, migration, and antiviral responses

Finally, to elucidate the molecular expression patterns associated with enhanced ADCC responses in DC individuals, we conducted single-cell RNA-seq analyses. We aimed to characterize and identify differentially expressed genes within NKA, particularly in comparison to conventional adaptive NK cells. For comparative purposes, we analyzed three related NK cell populations previously delineated in the functional ADCC analysis (NKA, NKB and NKC). All three populations were characterized by high protein expression of CD16, CXCR3, and CD57. A total of 7226, 7354, and 8180 cells were sequenced for NKA, NKB, and NKC, respectively. NKA exhibited 2618 genes and 28800 reads per cell, NKB showed 2516 genes and 26791 reads per cells, and NKC displayed 2584 genes and 24379 reads per cell. To check if data was appropriate for downstream analysis, different types of quality controls were performed, including the quality control of raw data (FastQC), the alignment and quantification of reads to described mRNAs (Cell Ranger), the number of transcripts per cell, and the percentage of counts coming from different transcript types, as previously described[428–430].

To delineate the heterogeneity of ADCC-mediating NK cells, we compared the transcriptional landscape of the distinct NK cell subsets by projecting cells into two dimensions by uniform manifold approximation and projection (UMAP) analysis. UMAP analysis unveiled NKB and NKC cell subsets as two separate populations, while NKA cells represented an intermediate state between both (**Figure 5A**). Unsupervised clustering analyses via shared neighbor (SNN) modularity optimization-based clustering algorithm resulted in the identification of 13 distinct NK cell clusters (**Figure 5B**). Of note, clustering was not significantly influenced by the cell cycle (**Supplementary Figure 7A**). Differential expression analysis identified conserved markers for each cluster, irrespective of the NK cell population (**Supplementary Table 3**). For optimization purposes, differential expression analysis only included genes with a minimum log2-fold-change above 0.25 and expressed in at least 10% of cells in either of the three populations tested.

The NKA population, defined by the co-expression of NKG2C and NKG2A, encompassed clusters #C0, #C5, #C6, and #C10 (**Figure 5B-C**). Cluster #C0, the most prevalent within the NKA population, exhibited a transcriptional profile marked by the upregulation of genes indicative of adaptive NK cell signatures, including IL32 and CD3E, while notably lacking FCER1G[414].

Additionally, it exhibited MT-CYB expression, signifying elevated metabolic demands, and IFITM2 expression, indicating an enhanced antiviral response (**Figure 5D**). Moreover, cluster #C5 displayed a transcriptomic enrichment of genes encoding soluble factors integral to NK cell effector functions, such as CCL3, CCL4, and CCL4L2, as well as XCL2, a chemokine characteristic of naïve $CD56^{bright}$ NK cells involved in the activation of the immune system and chemotaxis[431] (**Figure 5D**). Additionally, cluster #C6 demonstrated upregulation of genes implicated in actin cytoskeleton remodeling and lipid metabolism, including TRIO, PITPNC1, CASK, and APBA2 (**Figure 5D**). Importantly, cluster #C10 exhibited an upregulation of genes coding for interferon-induced proteins associated with the NK cell antiviral response, specifically MX1, MX2, ISG15, and IFI6 (**Figure 5D**). The NKB subset, characterized by high expression of NKG2C, comprised clusters #C2, #C4, and #C7 (**Figure 5B-C**). Clusters #C2 and #C4, presented the canonical transcriptional profile of adaptive NK cells, exhibiting upregulated expression of IL32 and CD3E, while lacking FCER1G and CD7 expression (**Figure 5B**). Furthermore, these clusters showed enhanced expression of genes associated with differentiation, maturation, and effector functions (THEMIS, RORA, PDE3B, CADM1) (**Figure 5B**). Notably, cluster #C7 was defined by the upregulation of genes involved in cell adhesion, activation, and differentiation (ANK3, IL7R, GZMK, NELL2) (**Figure 5B**). By contrast, the NKC subset, defined by elevated NKG2A expression, comprised clusters #C1, #C3, #C8, and #C9 (**Figure 5B-C**). Clusters #C1 and #C3 were characterized by an upregulation of genes involved in migration and cytokine production (SNX9, SGCD, IGF2R, FCE1RG) along with chemokines (CCL3, CCL4) (**Figure 5D**). Additionally, clusters #C8 and #C9 exhibited upregulated expression of genes regulating NK cell activation (NFKBIA, LINGO2) (**Figure 5D**).

Despite exhibiting adaptive NK cell traits, a direct comparison of the transcriptomic profile of the NKA subset with the conventional memory-like NKB population unveiled a heightened expression of CD7, a marker typically downregulated in adaptive NK cells. NKA cells also presented elevated gene expression levels of CCL3, CCL4, and XCL2 chemokines, known for their pivotal role in NK cell activation and recruitment (**Figure 5E**, **Supplementary Figure 7B**). Additionally, NKA exhibited heightened expression of ISG15, an interferon-induced gene pivotal in inducing IFN_{γ} in the antiviral response, and MT-CYB, a regulator of mitochondrial biogenesis and ATP synthesis, implicated in the secretion of cytolytic granules and cytokines[432] (**Figure 5E**). Of note, compared to NKB, NKA showed downregulation of RORA, a transcription factor involved in ILC2 differentiation[433] (**Figure 5E, Supplementary Figure 7B**).

Furthermore, Gene Ontology analysis revealed that the NKA subset exhibited increased pathways related with enhanced lymphocyte chemotaxis, migration, and cell regulation (**Figure F**). Moreover, relative to the NKC subset, the NKA population displayed increased expression of IL32 and THEMIS, involved in the regulation of the NK cell cytolytic response and memory NK cell differentiation (**Figure 5G, Supplementary Figure 7C**). Additionally, NKA exhibited the upregulation of GZMM and CD3E genes compared to NKA, implicated in NK cell cytotoxicity (**Figure 5G, Supplementary Figure 7C**), and compatible with the upregulation of pathways related to cell cytotoxicity, IL-2 production and response to interferon antiviral response (**Figure 5H**). Conversely to NKC, NKA exhibited downregulation of CCL3 and CCL4 chemokines, alongside FCER1G, associated to an NK-mediated regulation of the $CD8^+$ T cell response in virus control[434]. Importantly, NKA exhibited elevated expression of XCL2, CD7, MT-CYB, IFITM2 and ISG15 compared to both NKB and NKC populations, associated to NK cell migration, differentiation, cell metabolism and antiviral response (**Figure 5E-H**).

Finally, we performed a gene expression trajectory analysis to elucidate the continuum of dynamic changes occurring within these distinct NK cell clusters. A total of 5 distinct lineages, defined as ordered sets of cell clusters sharing a common starting or ending point, were identified using Slingshot (**Supplementary Table 4, Figure 5I**). Additionally, for each identified lineage, pseudotimes were determined, representing the variable indicating the transcriptional progression of each cell toward the terminal state (**Figure 5I**). Notably, irrespective of their origin, cells from all lineages transitioned through the NKA population, specifically cluster #C10, and consistently ended within cluster #C4, highly predominant in the NKB population. This observation suggests that all NK cell subsets studied transition into an intermediate population, distinguished by the expression of NKG2A and NKG2C. Furthermore, the final differentiation stage of all these identified lineages constitute cells with a differentiated and adaptive NK cell signature (**Supplementary Table 5, Figure 5I**).

Altogether, our data supports that NKA cells, expressing NKG2C and NKG2A, which are associated with higher ADCC responses in DC represent a transitional state between a less differentiated population (NKC) and a more mature and adaptive state (NKB). Importantly, these cells are characterized by upregulation of specific genes associated with enhanced effector functions, cell migration, metabolism, and antiviral responses. Overall, our data supports the potential of NKA cells to mediate strong cytotoxic pressure against HIV.

Figure 5

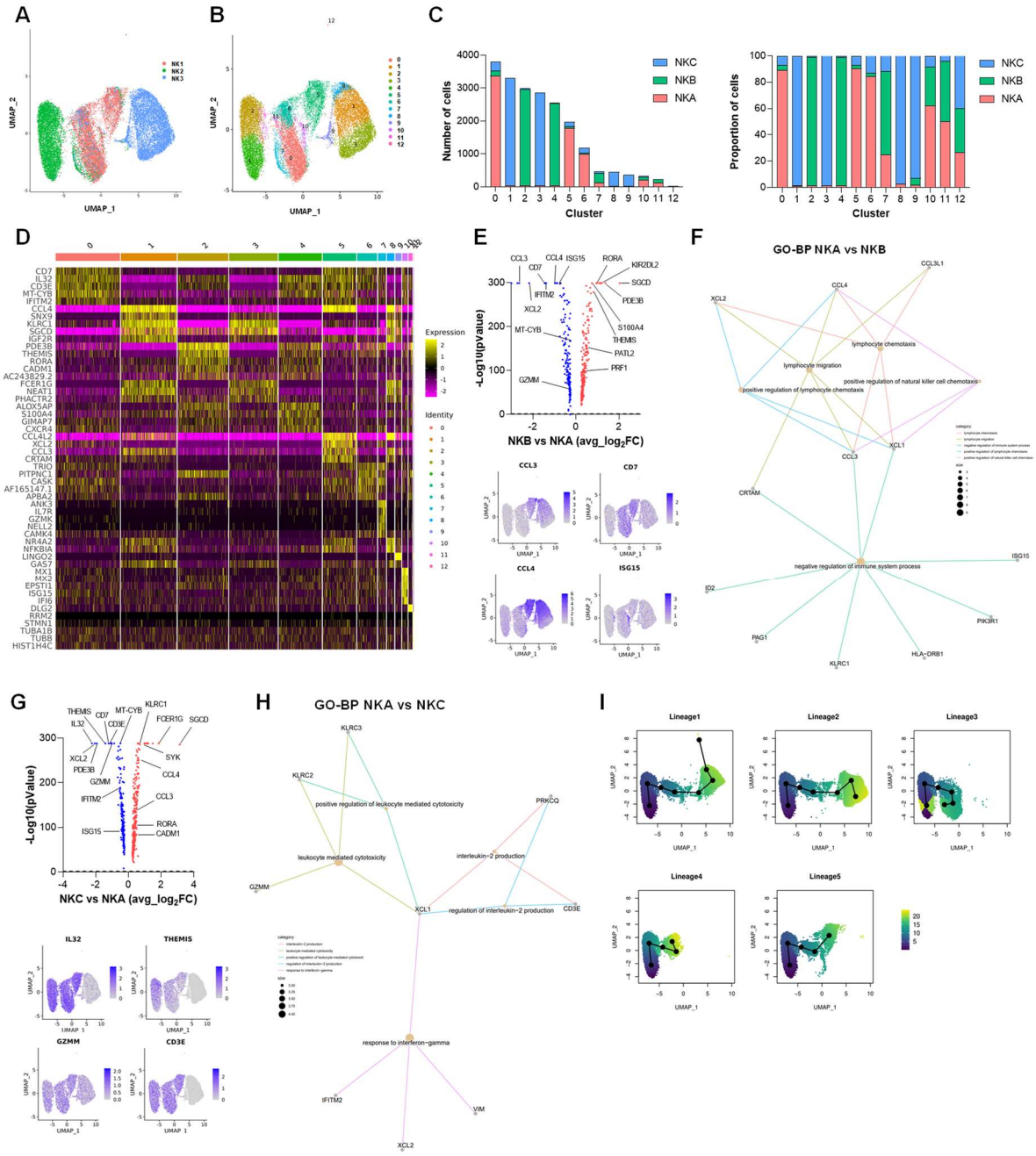


Figure 5. Unique transcriptional signatures define ADCC-mediating NK cells from DC. Gene expression analysis by single-cell RNA sequencing. **A**) Uniform Manifold Approximation and Projection (UMAP) visualization of NK cell populations sorted from DC individuals (NKA in red, NKB in green, NKC in blue). **B**) UMAP visualization of 13 distinct NK cell clusters identified from NK cell populations sorted by unsupervised hierarchical clustering. **C**) Number of cells per cluster and sample as counts (left) or proportions (right). **D**) Heatmap depicting the top 5 genes most differentially expressed (upregulated) in each NK cell cluster. **E**) Differentially expressed genes between NKB and NKA subsets (top) and representative expression patterns of characteristic NKA genes upregulated relative to NKB (bottom). **F**) Significant canonical pathways predicted by Gene Ontology Biological Process analysis (GO-BP) of differentially expressed genes in NKA vs NKB. **G**) Differentially expressed genes between NKC and NKA subsets (top) and representative expression patterns of characteristic NKA genes upregulated relative to NKC (bottom). **H**) Significant canonical pathways predicted by GO-BP of differentially expressed genes in NKA vs NKC.

I) Differentiation trajectory analysis illustrating the pseudotime inference for each NK cell cluster is shown. A total of 5 lineages were identified. UMAP plots are color-coded by inferred lineages, with the scale indicating maturation state, ranging from from yellow (least mature) to dark blue (most mature).

3.1.7 Discussion

Despite the success of ART, completely eliminating HIV from PWH remains extremely challenging due to the establishment of long-lived latent reservoirs[107]. The ability of a small number of PWH to resist disease progression and remain disease-free for prolonged periods makes these individuals attractive candidates to study and improve our understanding of the HIV pathogenesis. Although full viral elimination is not achieved, EC present undetectable levels of HIV replication by clinical assays, and therefore, represent a model of spontaneous functional cure[334,335]. Major determinants of HIV control affect HLA class I peptide presentation, implying a central role in CTL responses[401,405,435,436]. However, the role of their innate immune system in controlling HIV remains unclear. In the present study, we have characterized the phenotype, functional attributes and transcriptional signature of the NK cell repertoire of EC. We report that certain NK cell populations, especially cells with maturation and memory-like attributes, are more characteristic of people with durable viral control. Moreover, NK cells from these individuals are more refractory to cell stimulation and show a reduced natural cytotoxic activity, while showing an extraordinary ability to kill by the adaptive ADCC mechanism. Importantly, the distinctive ability to eliminate HIV-infected cells might be attributed to the presence of NK cells with a unique transcriptional landscape, associated with increased antiviral response. Thus, we add novel evidence for the importance of NK cells in HIV control.

Numerous alterations within the NK cell repertoire have been previously associated with HIV infection, including an increase of inhibitory receptors, such as KIR CD158b, and a switch from inhibitory (NKG2A) to activating NKG2 receptors expression (NKG2C)[411,437,438]. Concordantly, our study confirms these changes in NK cell populations from ART and VIR groups compared to HD. Interestingly, the distribution of these markers on DC was similar to HD, except for NKG2C, which was significantly increased in DC. This is noteworthy since this receptor is, in part, providing activating signaling upon engaging its ligand, HLA-E, expressed on the target cell. In addition, in our study NKG2C^{+}CD57^{+} NK cells appeared to be present in PWH, particularly expanded in DC and ART individuals. This phenotype has been associated with memory-like features, particularly in the context of CMV infection[419]. Moreover, CD57 is expressed in mature NK cell subsets that appear to be highly cytotoxic and its expression is consistently associated with better outcomes in cancer and autoimmune diseases[439].

Of note, in the context of HIV infection, a recent study identified CD57$^+$ NKG2C$^+$ NK cells as the predominant ADCC effector subset capable of targeting HIV-infected CD4$^+$ T cells in the presence of broadly neutralizing antibodies[421,440]. This is in agreement with the association between NKG2C$^+$-memory-like NK cells and the control of viral replication in a post-treatment controller recently reported[441].

Importantly, our study shows that although these memory-like NK cells were observed in PWH, only specific memory-like NK populations, primarily found in DC, were related to better ADCC outcomes. This indicates that the mere presence of these CD57$^+$ NKG2C$^+$ NK cells does not necessarily translate into improved NK functionality. In this regard, we found that important receptors involved in NK cell differentiation and regulation of their function, such as CD16, CD57, CXCR3, and NKG2A were enriched in DC. This observation is of significance as it suggests that NK cell subsets exhibiting varying differentiation states may potentially impact the course of HIV infection within the distinct study cohorts. Remarkably, expanded subsets in DC exhibited elevated NKG2A levels, co-expressing NKG2C, an unusual phenomenon considering their opposing functions while binding the same ligand. NKG2A, associated with inhibitory signaling, typically appears on less mature NK cell subsets, whereas NKG2C, linked to activating signals, characterizes more mature populations[295,442]. Co-expression of both markers is infrequent in healthy donor peripheral blood NK cells, but has been linked to reduced cytotoxic and pro-inflammatory responses, suggesting a role in NK cell function regulation[442,443]. Furthermore, it has been reported that despite the presence of HLA-E on HIV-infected cells, the NK cell subset most likely to respond to them is characterized by the expression of NKG2A[444]. Thus, we hypothesize that co-expression of NKG2A and NKG2C in DC-derived NK cells may denote a partially differentiated phenotype capable of balancing activating responses while maintaining a high potential to kill HIV-infected cells. In addition, these populations also showed an upregulation of the chemokine receptor CXCR3, which may facilitate the efficient recruitment of these cells to tissues[445].

Currently, it is challenging to ascertain whether the specialized expanded memory NK cells primarily observed in individuals with DC have arisen due to a prior CMV reactivation or, as recently suggested, following acute HIV infection[423]. It is worth noting that due to sample limitations, we were unable to determine the CMV serological status of our participants. However, numerous studies involving PWH have consistently indicated a significantly higher seroprevalence of CMV in this group compared to the uninfected population, with antibody levels consistently detected in more than 90% of PWH[446–448]. Hence, further studies are required to elucidate the precise timing of the generation of these NK cells and the mechanisms underlying their expansion.

HIV control is associated to ADCC, where specific antibodies bind to viral antigens on the surface of infected cells, and by Fc receptor engagement, recruit NK cells to eliminate HIV-infected targets. The importance of Fc-mediated functions was highlighted by the partially successful RV144 HIV vaccine trial, in which ADCC antibodies were associated with protection from HIV[383]. Previous studies described impairment of the NK-mediated ADCC activity during early HIV infection, indicative of premature virus-mediated NK-cell dysfunction[210,438]. In contrast, individuals with natural HIV control exhibited elevated levels of ADCC antibodies in plasma, particularly against gp120 and envelope antigens[356,449–451]. In fact, ECs that presented an HIV reservoir size below the limit of detection had significantly higher ADCC activity than those with a detectable HIV reservoir size[356]. While supporting the role of ADCC in HIV control in PWH displaying natural viral suppression, these studies predominantly investigated the functionality and diversity of ADCC antibodies in an *in vitro* model, employing NK cells from HIV-seronegative donors and CEM target cells. However, to our knowledge, existing studies have provided limited data comprehensively characterizing the ADCC potential of NK cells from HIV EC[452,453]. Our study demonstrates robust ADCC responses in NK cells from PWH exhibiting spontaneous viral control, comparable to HD, and superior to other PWH groups. These findings support the idea that NK cells in EC can effectively mediate the clearance of HIV-infected cells via ADCC, underscoring the pivotal role of this mechanism in HIV control.

NK cell activation and subsequent cytotoxicity, independent of ADCC responses, can exert a significant impact on the regulation of viral replication and HIV control. In our study, we analyzed the complexity of NK cell activation and cytotoxic responses upon stimulation with relevant targets such as K562 cells, that do not express MHC-I molecules. In agreement with previous reports, we observed that NK cells from all PWH groups preserve their cytotoxic potential, including degranulation and IFN_{γ} secretion upon stimulation[454]. However, PWH with long-term spontaneous control of HIV showed reduced capacity to produce functional molecules upon cell stimulation and a decreased ability to kill target cells. This observation is consistent with previous studies showing that NK cell populations in HIV controllers exhibit lower levels of cell activation[455,456]. In fact, NK cells can be activated through TLR stimulation, as evidenced by prior studies using HIV-derived ssRNA[457]. Consequently, the reduced expression of activation molecules in HIV controllers may be linked to a decrease in the antigen burden. Still, in the case of the reduced activation in NK cells from DC individuals, we believe that may be the result from the intricate interplay between inhibitory and activating receptors.

This balance could potentially redirect NK cell responses, favoring an HIV-specific ADCC response over nonspecific activation. Our results underscore a dynamic response of NK cells during HIV infection, potentially influencing the differential outcomes observed in PWH with distinct levels of viral control.

Single-cell RNA sequencing of ADCC-mediating NK cells revealed a unique transcriptional NK cell profile associated with enhanced NK cell metabolism, effector functions, cytokine secretion, migration, and an enhanced antiviral response. Notably, these cells exhibited pronounced upregulation of soluble factors involved in immune modulation (XCL1, XCL2), cytokines (IL32), chemokines (CCL3, CCL4), and interferon-induced genes (ISGs). XCL1 and XCL2, chemokines synthesized following NK cell activation, play a pivotal role in modulating NK cell activity and promoting antigen presentation by dendritic cells[458]. Recent studies have described that these chemokines can inhibit HIV infection by blocking viral attachment and entry by binding to the HIV Gag polyprotein[459]. In addition, IL32, a characteristic cytokine of adaptive NK cells, was initially identified as a multifunctional cytokine with inhibitory effects on HIV infection[460]. Specifically, IL-32β has been described to dampen inflammation by inducing the expression of anti-inflammatory cytokines in various cell types[461]. Furthermore, activated NK cells secrete CCL3 and CCL4, which play a crucial role in recruiting various inflammatory cells to sites of inflammation. These cytokines have also been reported to inhibit viral replication by interacting with CCR5, a coreceptor expressed on $CD4^+$ T lymphocytes and monocyte-derived macrophages that serves as an entry point for HIV into cells[124,258]. Moreover, the upregulation of ISGs in response to viral infection plays a pivotal role in inhibiting HIV replication by targeting various stages of the viral cycle. Specifically, ISG15 has been shown to interfere with the ubiquitylation of HIV gag protein, which is essential for HIV budding and release[462]. Last, HERC5 has also been reported to impede HIV assembly through ISGylation of Gag[463]. Finally, we demonstrated that these cells, characterized by enhanced effector NK cell responses, represent a transitional and intermediate state between CMV-expanded adaptive NK cells and naïve $NKG2A^+$ NK cells. These cells exhibit upregulated gene expression of canonical CMV-expanded adaptive NK cell markers (IL32, CD3E, KLRC, and lack of FCER1G) alongside CD7 and XCL2, markers previously reported to be downregulated in adaptive NK cells[414].

Overall, we found that NK cells from PWH with durable control of HIV are enriched in cells with a unique transcriptional profile that can be identified by exclusive phenotypic and functional features associated to HIV infection control.

A better understanding of the mechanism of natural control of HIV infection may have important implications for the design of new anti-HIV therapeutic strategies based on the particular functional activity of NK cells. Thus, we believe that immunotherapy approaches focused on boosting desirable NK responses, such as the ones reported here, could have potential implications in HIV cure strategies.

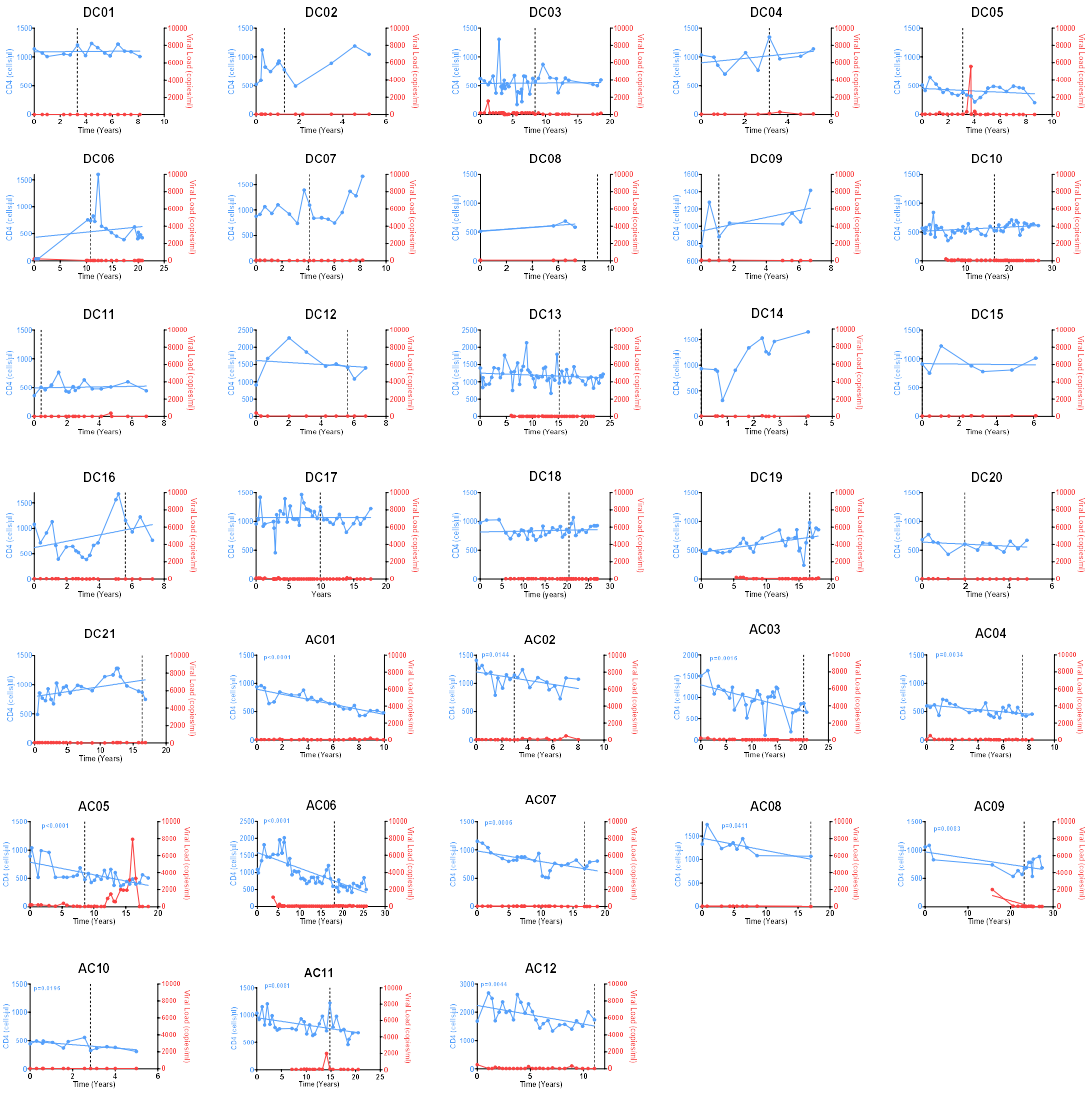
Limitations of the study

This study has some limitations. First, we did not measure the HIV reservoir, or intact HIV genomes among study samples. We attempted to quantify the total HIV DNA; however, quantities of PBMCs were very limited and we prioritized the phenotypic, functional and transcriptomics assays. Second, we measured phenotypic and functional markers from one timepoint in each study participant; longitudinal investigations will be needed to extend this analysis in the future. Third, this is a study with a limited sample size, thereby constraining the extent of functional assays conducted. However, it should be noted the scarcity of participants within these study groups, thus limiting the availability of study samples. Last, our definition of study groups could influence the generalization of our conclusions. Further, the EC group is heterogeneous, characterized by different definitions based on factors such as the length of follow-up, viremia detection limits, presence/absence of blips, and $CD4^+$ T cell counts. This inherent heterogeneity introduces variability in the study results and interpretations. Despite these limitations, we believe that this study represents a relevant contribution in the field of HIV control.

3.1.8 Supplementary Data

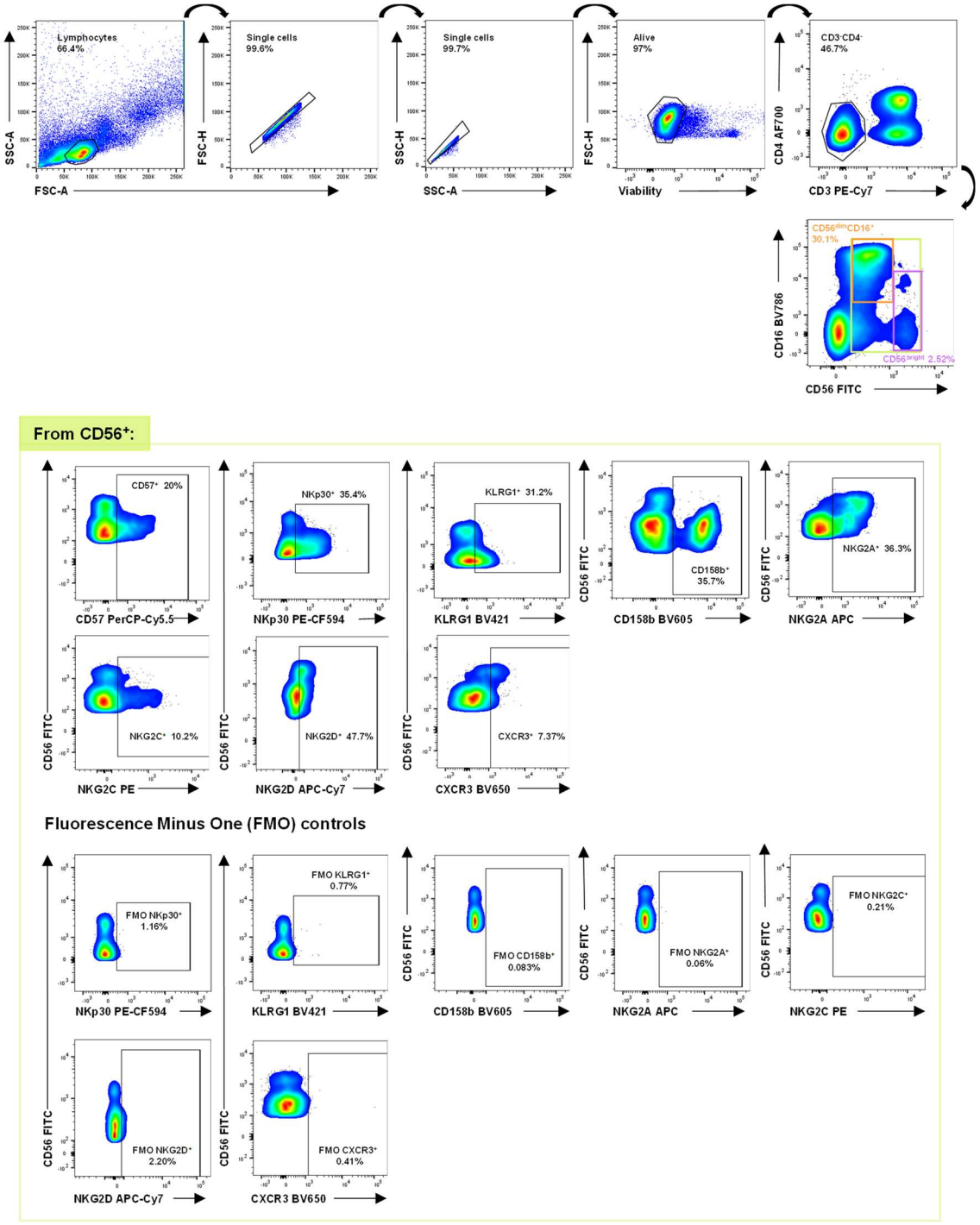
3.1.8.1 Supplementary Figures

Supplementary Figure 1



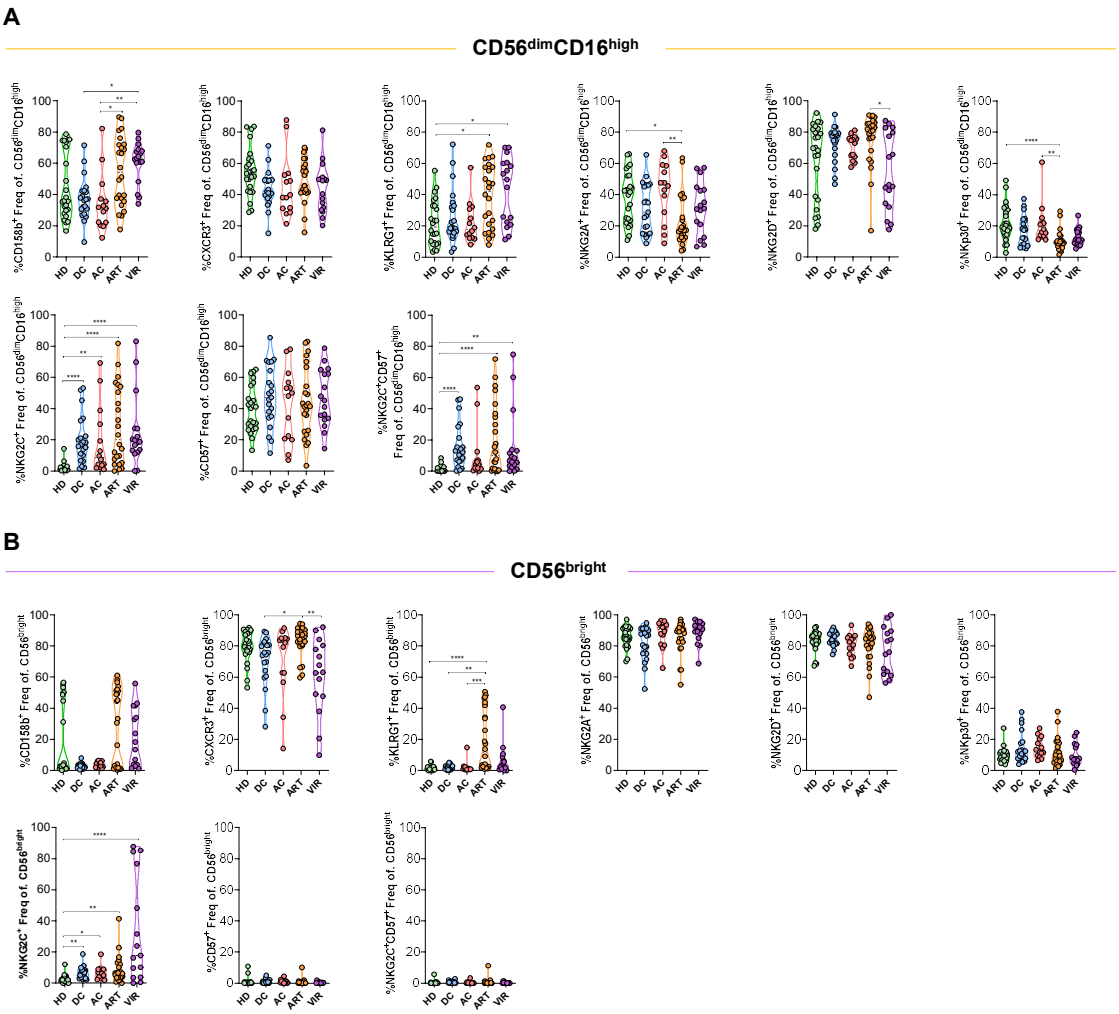
Supplementary Figure 1. Viral and immune dynamics in study participants. Viral loads (right axes) and CD4 counts (left axes) over time (x-axis) for subjects with durable (DC01 - DC21) and aborted control (AC01 - AC013). Timepoints of study sample collection are represented with dashed lines.

Supplementary Figure 2



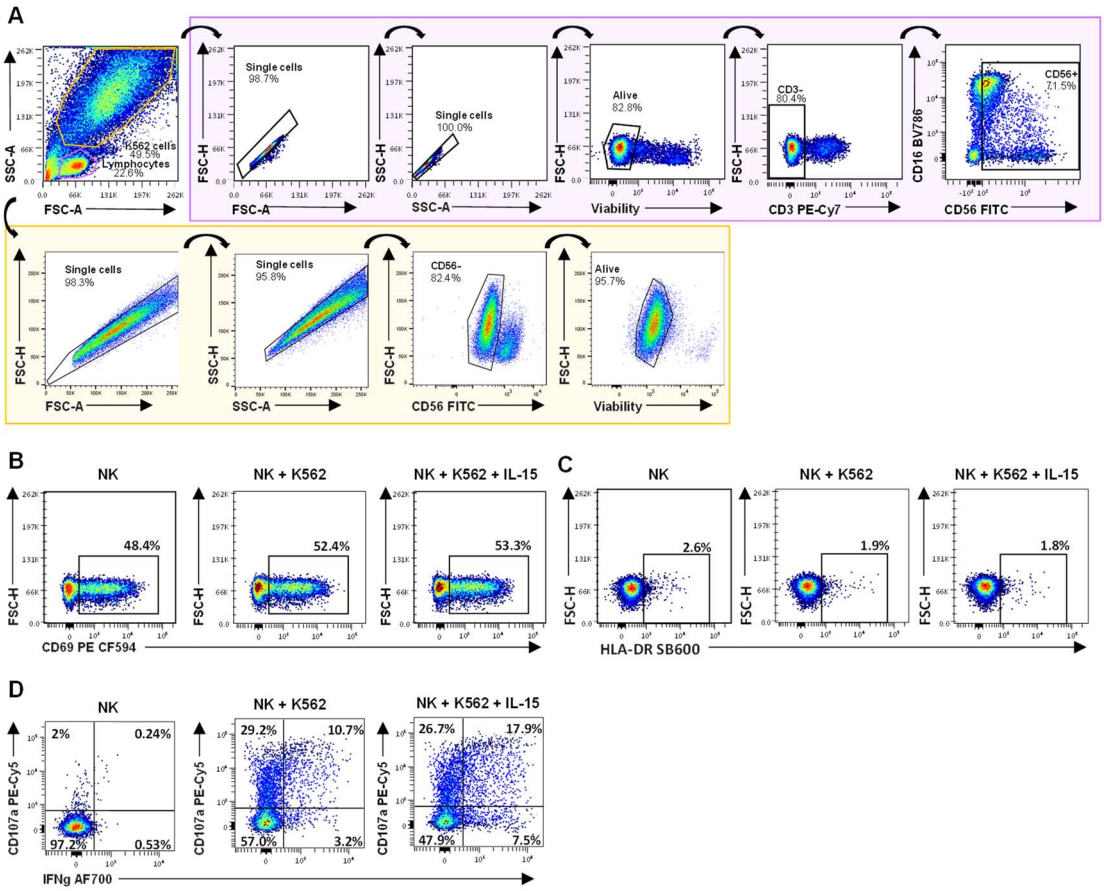
Supplementary Figure 2. Gating strategy used for the quantification of the different NK cell receptors. General gating strategy used to identify NK cell populations based on CD56 and CD16 expression from PBMC samples for phenotype and functional assays. Briefly, lymphocytes were selected based on FSC and SSC parameters, followed by doublets and dead cells exclusion. From $CD3^-$ $CD4^-$ cells, NK cells (defined as $CD3^-CD56^+$) were gated; and within NK cells, three subsets were identified in all groups: $CD56^+$, $CD56^{dim}CD16^+$ and $CD56^{bright}$. FMOs are shown for markers with continuous expression. *FSC-H, Forward Scatter-Height; FSC-A, Forward Scatter-Area; SSC-A, Side Scatter-Area.*

Supplementary Figure 3



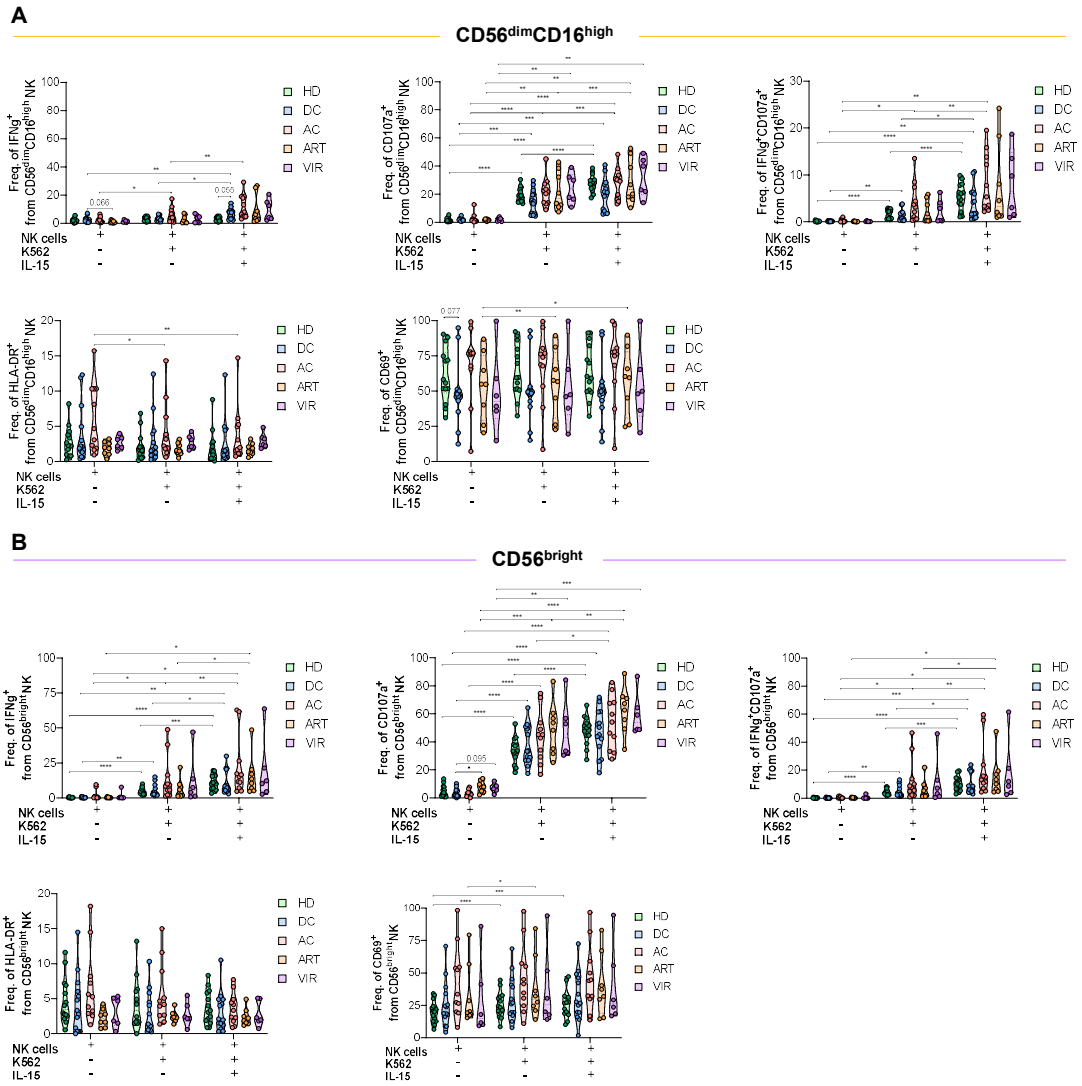
Supplementary Figure 3. **Phenotypic characterization of NK cell subsets**. **A**) Violin plots depicting the expression of distinct phenotypic NK cell markers in CD56^{dim}CD16^{high} NK cells (left to right: CD158b, CXCR3, KLRG1, NKG2A, NKG2D, NKp30, NKG2C, CD57, and the frequency of double-positive NKG2C^{+}CD57^{+} NK cells). **B**) Violin plots showing the frequency of (left to right): CD158b^{+}, CXCR3^{+}, KLRG1^{+}, NKG2A^{+}, NKG2D^{+}, NKp30^{+}, NKG2C^{+}, CD57^{+} and the frequency of double-positive NKG2C^{+}CD57^{+} CD56^{bright} NK cells. Graphs represent medians and ranges. Statistical comparisons were performed using the Kruskal-Wallis test. *p<0.05; **p<0.01; ***p<0.001; ****p<0.0001.

Supplementary Figure 4



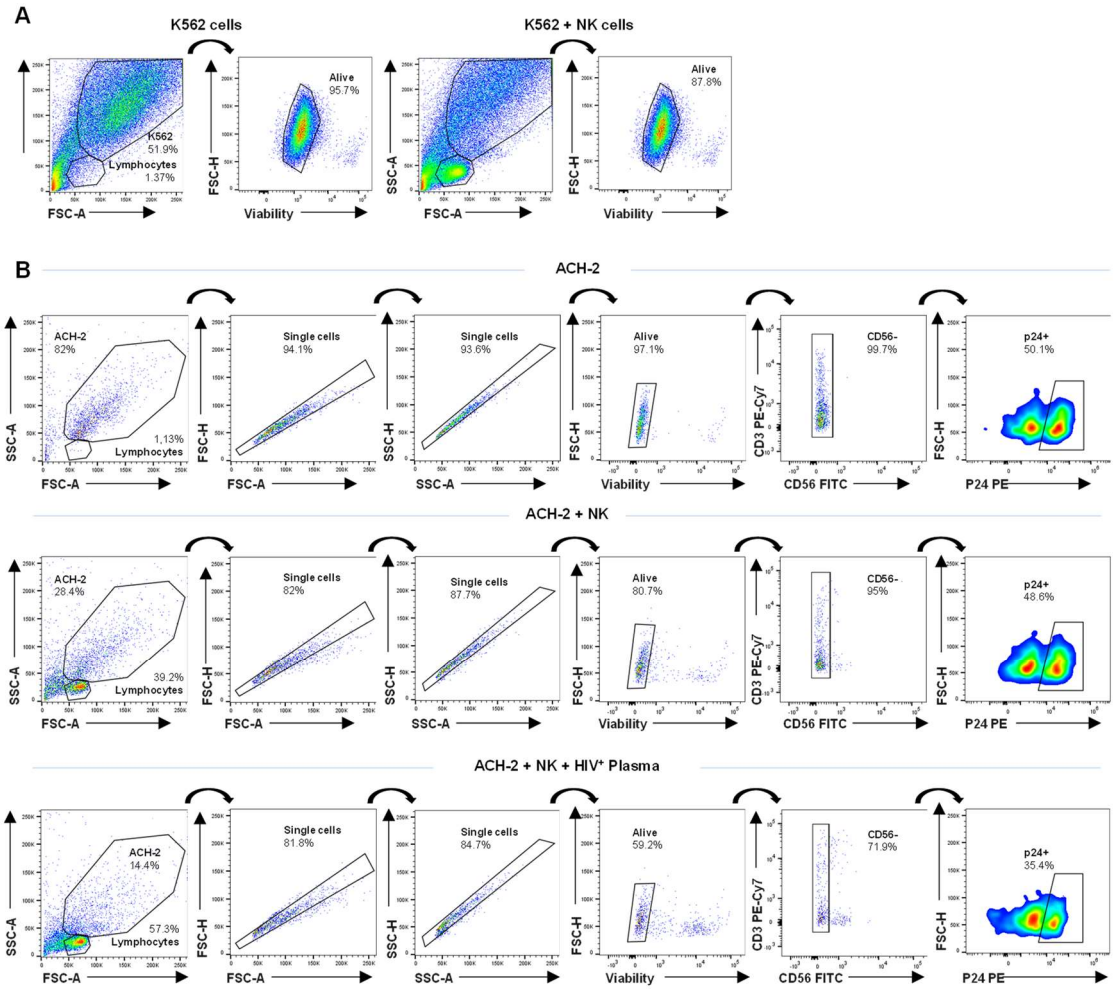
Supplementary Figure 4. **Gating strategy for NK cell activation assays. A**) General gating strategy used to identify NK cells and K562 cells in NK cell activation and cytotoxicity assays. For NK cells (labelled in purple), lymphocytes were selected based on FSC and SSC parameters, followed by doublets and dead cells exclusion. From $CD3^-$ cells, $CD56^+$ NK cells were selected. Similarly, K562 cells (labelled in yellow) were selected based on FSC and SSC parameters, followed the exclusion of doublet cells. Subsequently, $CD56^-$ cells live cells were selected. Representative flow cytometry plots illustrating the expression of **B**) CD69, **C**) HLA-DR, and **D**) $IFN\gamma^+CD107a^+$ in $CD56^+$ NK cells following stimulation with K562 and IL-15 are shown. *FSC-H, Forward Scatter-Height; FSC-A, Forward Scatter-Area; SSC-A, Side Scatter-Area.*

Supplementary Figure 5



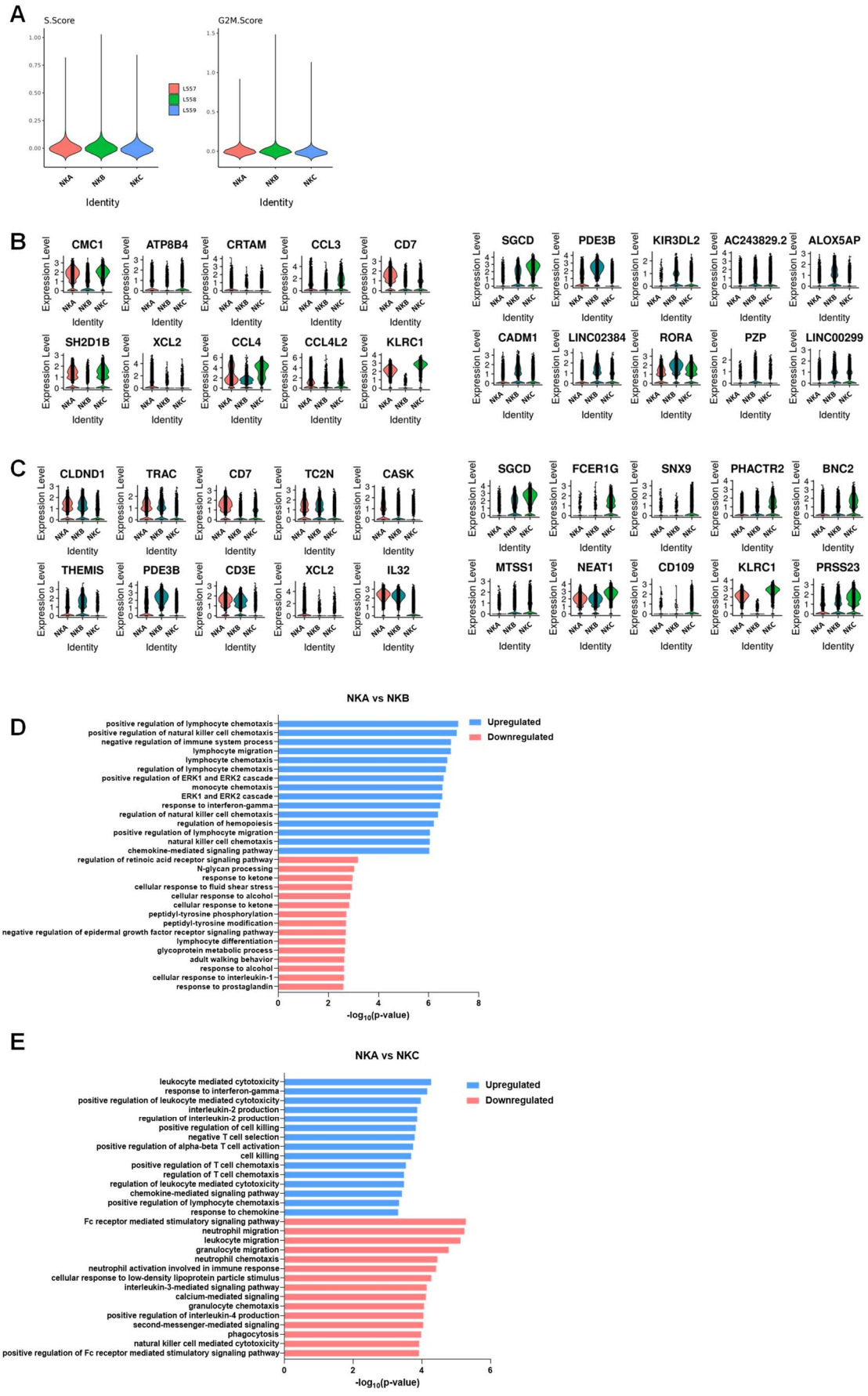
Supplementary Figure 5. Functional profile of NK cell subsets . Violin plots depicting the frequency of IFNγ$^+$, CD107a$^+$, IFNγ$^+$CD107a$^+$, HLA-DR$^+$, and CD69$^+$ cells in **A**) CD56^{dim}CD16^{high} NK cells and **B**) CD56^{bright} NK cells upon stimulation. Statistical comparisons were performed using RM two-way ANOVA followed by Tukey's multiple comparisons test. *p<0.05; **p<0.01; ***p<0.001; ****p<0.0001.

Supplementary Figure 6



Supplementary Figure 6. **Gating strategy for functional assays. A**) General gating strategy used to assess natural cytotoxicity. The viability reduction of K562 cells in co-culture with NK cells was quantified as the percentage difference between the viability of K562 cells alone and K562 cells co-cultured with NK cells. **B**) Representative flow cytometry plots showing the gating strategy used to evaluate ADCC responses. Primary NK cells were isolated and co-cultured with the p24-expressing ACH-2 cell line, with and without the addition of HIV$^+$ plasma for 4h. ACH-2 cells were gated based on SSC-A vs FSC-A plot. After doublet cell exclusion, live cells were identified based on the lack of expression of LIVE/DEAD Fixable AQUA viability cell stain. Then, p24$^+$ expression was analyzed in CD56$^-$ cells. ACH-2 cells alone, co-cultured with NK cells and with HIV$^+$ plasma are depicted below. ADCC was calculated as the fraction of cells that disappeared within the target population after the addition of HIV$^+$ plasma in comparison to the control condition with targets and NK cells, but lacking HIV$^+$ plasma. *FSC-H, Forward Scatter-Height; FSC-A, Forward Scatter-Area; SSC-A, Side Scatter-Area.*

Supplementary Figure 7



Supplementary Figure 7. Influence of cell cycle dynamics and single-cell differential gene expression analysis between NK cell populations. A) UMAP of clustering results indicating the fraction of cells within different phases of the cell cycle (S left, G2M right) across NK cell samples. Cells are colored by sample classification (NKA red, NKB green, and NKC blue). **B**) Top ten genes exhibiting upregulation (left) and downregulation (right) in NKA cells compared to NKB. **C**) Top ten genes upregulated (left) and downregulated (right) in NKA cells compared to NKC. **D-E**) Overrepresentation analysis (ORA) of the gene ontology biological process (GO-BP) analysis showing the list of biological processes upregulated or downregulated in **D**) NKA vs NKB or **E**) NKA vs NKC based on the list of genes upregulated (blue) and downregulated (red) in each comparison with an adjusted p-value below 0.05 and log2FoldChange above 0.5 (upregulated) or below -0.5 (downregulated).

3.1.8.2 Supplementary Tables

Table S1. Clinical data of PWH included in the study.

Subject characteristics		DC (n=21)	AC (n=14)	ART (n=24)	VIR (n=18)	p value between groups (test)
Sex (n, %)	Male	11 (55)	7 (50)	15 (65.2)	14 (77.7)	0.35 (Fisher's exact)
	Female	9 (45)	7 (50)	8 (34.8)	4 (22.2)	
Age (years; median, IQR)		55 (47 -59)	58 (51-61)	44 (36-52)	39 (27-46)	**<0.0001** (Kruskal-Wallis test with Dunn's post-test)
Route of transmission (n, %)	Heterosexual	6 (30)	8 (57.1)	3 (37.5)	2 (28.6)	**<0.0001** (Fisher's exact)
	MSM	4 (20)	1 (7.1)	4 (50)	5 (71.4)	
	Intravenous drug use	10 (50)	3 (21.4)	1 (12.5)	-	
	Other/unknown	-	2 (14.3)	-	-	
Protective HLA-B alleles [B*14. B*27. B*52. B*57] (n, %)		13 (72.2)	9 (69.2)	-	-	>0.99 (Fisher's exact)
CD4+ T-cell count (cells/ul; median, IQR)		846 (590.3-1109)	673 (501.8-1090)	750 (510-860)	435 (237.5-715)	**0.0005** (Kruskal-Wallis test with Dunn's post-test)
HIV viral load (log10 copies/ml; median, IQR)		<1.69	<1.69	<1.69	4.75 (4.38-5.25)	**<0.0001** (Kruskal-Wallis test with Dunn's post-test)
Time since HIV diagnosis (months; median, IQR)		87 (55.8-184.8)	132 (70.80-214.8)	74.80 (46.90-153.7)	8 (0.4-82.2)	**0.006** (Kruskal-Wallis test with Dunn's post-test)
Time on ART with VL suppressed (months; median, IQR)		N/A	N/A	53 (45-72)	N/A	

DC: Durable Control, AC: Aborted Control, ART: ART-treated PWH, VIR: Viremic PWH, IQR: Interquartile Range, MSM: Men who have sex with men; N/A not available

Table S2. Cell numbers obtained after sorting of selected NK cell populations.

	Cell population				
Sample	***NKA***	***NKB***	***NKC***	***NKD***	***NKE***
DC1	*1,043*	*5391*	*9,339*	*7,391*	*23,976*
DC2	*1,751*	*88,040*	*5,279*	*9,436*	*86,222*
DC3	*1,275*	*3,910*	*5,630*	*3,140*	*187,785*
DC4	*1,352*	*26,599*	*22,236*	*51,191*	*257,153*
DC5	*1,033*	*2,906*	*29,916*	*32,298*	*92,687*

DC: Durable Control, NKA: $CD16^{+}NKG2A^{+}NKG2C^{+}$ $CD57^{+}CXCR3^{+}$ NK cells, NKB: CD16+, $NKG2A^{+}$ $NKG2C^{-}$ $CD57^{+}$ $CXCR3^{+}$ NK cells, NKC: CD16+ $NKG2A^{-}$ $NKG2C^{+}$ $CD57^{+}$ $CXCR3^{+}$ NK cells, NKD: CD16+, $NKG2A^{-}$ $NKG2C^{-}$ $CD57^{+}$ $CXCR3^{+}$ NK cells, NKE: CD16- NK cells.

Table S3. Differentially expressed genes in each cluster.

p-val	Avg_log2FC	Pct.1	Pct.2	P_val_adj	Cluster	gene
0	0.817808347	0.864	0.517	0	0	CD7
0	0.775222722	0.993	0.666	0	0	IL32
0	0.660553583	0.905	0.51	0	0	CD3E
0	0.466822812	1	1	0	0	MT-CYB
0	0.432707859	1	1	0	0	MT-CO1
0	0.40040603	1	1	0	0	CCL5
0	0.398049407	1	1	0	0	MT-ATP6
0	0.375945164	0.348	0.096	0	0	GOLGA8M
9.3318E-300	0.420869948	1	1	2.0949E-295	0	MT-ND2
4.4041E-297	0.434556085	0.999	0.997	9.8867E-293	0	MT-ND5
6.6557E-232	0.378199728	1	1	1.4941E-227	0	RPLP1
4.6266E-229	0.380241959	0.999	0.991	1.0386E-224	0	CD52
7.2756E-211	0.449718029	0.926	0.828	1.6333E-206	0	S100A10
1.9296E-203	0.460477722	0.921	0.827	4.3318E-199	0	HOPX
6.0427E-197	0.43411818	0.549	0.293	1.3565E-192	0	CASK
1.1308E-192	0.473530087	0.894	0.772	2.5385E-188	0	IFITM2
2.0933E-182	0.368429246	0.954	0.889	4.6992E-178	0	CD63
9.9805E-166	0.451925834	0.931	0.857	2.2405E-161	0	VIM
1.7646E-164	0.393350847	0.724	0.508	3.9613E-160	0	TRAC
2.36615E-85	0.403214858	0.719	0.596	5.31178E-81	0	LGALS1
0	1.633328618	0.999	0.88	0	1	CCL4

0	1.289329938	0.621	0.101	0	1	SNX9
0	1.220976009	0.998	0.649	0	1	KLRC1
0	1.132874697	0.915	0.483	0	1	SGCD
0	1.120477702	0.947	0.637	0	1	IGF2R
0	1.108214972	0.81	0.177	0	1	FCER1G
0	0.992366798	0.835	0.506	0	1	BNC2
0	0.988083512	0.94	0.665	0	1	ZFP36L1
0	0.985956975	0.868	0.489	0	1	CCL3
0	0.985469541	0.479	0.061	0	1	CD109
0	0.907454895	0.998	0.953	0	1	NEAT1
0	0.8798496	0.756	0.386	0	1	GAS7
0	0.868009861	0.731	0.288	0	1	FAM3C
0	0.864882042	0.699	0.315	0	1	GFOD1
0	0.856125723	0.937	0.708	0	1	SLA
0	0.824201961	0.899	0.634	0	1	PTPN12
0	0.794546607	0.958	0.762	0	1	ARID5B
0	0.787932632	0.642	0.204	0	1	NR4A2
0	0.750772754	0.999	0.973	0	1	LYST
6.7483E-210	0.788017608	0.505	0.257	1.5149E-205	1	BACH2
0	1.823706877	0.978	0.441	0	2	PDE3B
0	1.263094489	0.839	0.33	0	2	THEMIS
0	0.87168551	0.971	0.785	0	2	RORA
0	0.83114146	0.73	0.39	0	2	CADM1
0	0.769260223	0.862	0.53	0	2	RHOH
0	0.765469004	0.785	0.429	0	2	LINC02384
0	0.733319968	0.68	0.269	0	2	ALOX5AP
0	0.722064739	0.488	0.1	0	2	PZP
0	0.698684046	1	0.998	0	2	CD247
0	0.68825346	0.83	0.552	0	2	NPC1
0	0.682117295	0.999	0.965	0	2	PITPNC1
0	0.667323905	0.451	0.161	0	2	PTPRM
0	0.645631081	0.447	0.085	0	2	A2M
8.074E-305	0.672478505	0.812	0.539	1.8125E-300	2	SYTL2
1.1639E-292	0.645360448	0.848	0.6	2.6128E-288	2	TTC39C
1.17E-288	0.804087199	0.642	0.32	2.6264E-284	2	AC243829.2

4.0471E-287	0.782153635	0.842	0.632	9.0853E-283	2	CCNH
3.007E-282	0.625342227	0.835	0.575	6.7504E-278	2	GRAP2
2.4488E-236	0.620100102	0.827	0.587	5.4972E-232	2	ARHGAP26
1.3003E-227	0.744190317	0.349	0.125	2.9191E-223	2	PLCB1
0	1.310533923	0.928	0.491	0	3	SGCD
0	1.020350123	0.999	0.657	0	3	KLRC1
0	0.851996852	0.762	0.2	0	3	FCER1G
0	0.648403914	0.997	0.954	0	3	NEAT1
0	0.630385784	0.602	0.197	0	3	TNFRSF18
3.9635E-264	0.715987505	0.764	0.458	8.8977E-260	3	PHACTR2
2.1781E-247	0.451740756	0.249	0.06	4.8895E-243	3	PPP1R9A
3.4671E-219	0.631636229	0.258	0.071	7.7832E-215	3	PDE7B
3.5267E-212	0.440478178	0.472	0.208	7.9171E-208	3	ATP10A
2.4169E-200	0.431192333	0.997	0.973	5.4256E-196	3	LYST
1.1135E-194	0.559088923	0.859	0.642	2.4998E-190	3	PRSS23
1.2408E-181	0.442411026	0.844	0.563	2.7856E-177	3	SH2D1B
7.42E-173	0.428603354	0.416	0.187	1.6657E-168	3	RUNX2
2.3872E-161	0.492783518	0.925	0.782	5.359E-157	3	JAZF1
2.6042E-157	0.431817175	0.851	0.691	5.8462E-153	3	DSTN
3.6564E-155	0.421338365	0.957	0.778	8.2082E-151	3	CMC1
5.5578E-141	0.418562712	0.652	0.429	1.2477E-136	3	CTBP2
2.6811E-136	0.446506569	0.947	0.866	6.0188E-132	3	TGFBR3
1.1172E-128	0.428110548	0.825	0.653	2.5079E-124	3	PTPN12
1.472E-105	0.401081651	0.533	0.339	3.3046E-101	3	GCNT1
0	0.827156839	0.691	0.277	0	4	ALOX5AP
0	0.50978675	1	1	0	4	TMSB10
0	0.505924397	0.339	0.078	0	4	KLRB1
0	0.464811142	1	1	0	4	RPL10
0	0.398258407	1	1	0	4	B2M
3.401E-288	0.511086912	0.9	0.466	7.6348E-284	4	PDE3B
9.1136E-273	0.630630634	0.987	0.689	2.0459E-268	4	IL32
4.601E-252	0.603493267	0.978	0.913	1.0329E-247	4	S100A4
1.192E-231	0.486959366	0.988	0.947	2.6759E-227	4	TRBC1
7.811E-210	0.464345096	0.548	0.26	1.7535E-205	4	KIR3DL2
3.4798E-206	0.566188233	0.891	0.733	7.8118E-202	4	GIMAP7

1.1121E-183	0.573848436	0.896	0.727	2.4966E-179	4	CXCR4
1.722E-173	0.474289563	0.967	0.896	3.8657E-169	4	FGFBP2
6.3572E-171	0.414467856	0.682	0.365	1.4271E-166	4	THEMIS
8.7425E-157	0.441105681	0.845	0.545	1.9626E-152	4	CD3E
2.6418E-151	0.556820518	0.799	0.635	5.9306E-147	4	KLF2
1.2221E-147	0.389858395	0.975	0.946	2.7435E-143	4	PLAAT4
2.5963E-144	0.453285519	0.935	0.854	5.8284E-140	4	GZMA
1.6202E-128	0.392382934	0.973	0.945	3.6371E-124	4	CRIP1
3.3547E-128	0.497308121	0.578	0.337	7.5309E-124	4	AC243829.2
0	3.029375226	0.968	0.548	0	5	CCL4L2
0	2.844960024	0.684	0.143	0	5	XCL2
0	2.193224398	0.999	0.888	0	5	CCL4
0	1.61235024	0.89	0.513	0	5	CCL3
0	1.214854957	0.659	0.17	0	5	CRTAM
0	1.06665683	0.263	0.024	0	5	XCL1
0	0.667179927	0.356	0.081	0	5	TNF
0	0.626236863	0.417	0.097	0	5	TNFSF14
1.3252E-290	0.743594841	0.878	0.549	2.9749E-286	5	CD7
2.4389E-281	1.00450589	0.719	0.394	5.4752E-277	5	CD69
2.0792E-250	0.646480621	0.995	0.953	4.6676E-246	5	ACTB
6.942E-249	0.631416175	0.585	0.241	1.5584E-244	5	NR4A2
5.9312E-241	0.650883721	0.959	0.832	1.3315E-236	5	HOPX
9.5893E-234	0.655201208	0.986	0.699	2.1527E-229	5	IL32
1.4324E-214	0.857013473	0.406	0.14	3.2156E-210	5	CCL3L1
2.8042E-211	0.624440107	0.917	0.687	6.2952E-207	5	ZFP36L1
3.4561E-196	0.612784907	0.945	0.777	7.7586E-192	5	ARID5B
3.8052E-179	0.96594882	0.88	0.725	8.5423E-175	5	NFKBIA
8.9543E-158	0.648080621	0.765	0.542	2.0101E-153	5	REL
2.41479E-98	0.776890981	0.709	0.548	5.42096E-94	5	NFKB1
5.4381E-290	0.575283585	0.498	0.121	1.2208E-285	6	GOLGA8M
1.9303E-261	0.662424704	1	0.999	4.3333E-257	6	AOAH
8.1901E-258	0.75148193	0.615	0.204	1.8386E-253	6	TRIO
3.3723E-227	0.752992823	0.997	0.969	7.5706E-223	6	PITPNC1
8.0114E-202	0.872703574	0.704	0.318	1.7985E-197	6	CASK
1.7593E-190	0.72164282	0.54	0.196	3.9495E-186	6	AF165147.1

2.4689E-175	0.572732107	0.392	0.113	5.5424E-171	6	INPP4B
1.1031E-167	0.645517643	0.987	0.871	2.4764E-163	6	ATP8A1
1.3561E-156	0.685582677	0.971	0.823	3.0443E-152	6	SAMSN1
1.5835E-152	0.729851563	0.902	0.665	3.5548E-148	6	APBA2
5.3742E-130	0.688371762	0.865	0.613	1.2065E-125	6	AUTS2
1.0018E-125	0.605279093	0.989	0.963	2.249E-121	6	ZBTB20
2.5254E-117	0.5873872	0.504	0.227	5.6693E-113	6	GNAQ
1.2E-115	0.705949306	0.67	0.386	2.6938E-111	6	NCAM1
3.9851E-114	0.56593028	0.872	0.629	8.9461E-110	6	EML4
1.5795E-111	0.575385529	0.806	0.527	3.5459E-107	6	NEK7
2.80212E-92	0.670910885	0.479	0.238	6.29047E-88	6	KIAA0825
2.90978E-92	0.660444863	0.349	0.139	6.53215E-88	6	AC008014.1
8.58516E-86	0.58042817	0.788	0.541	1.92728E-81	6	TC2N
7.03918E-84	0.565026829	0.836	0.627	1.58022E-79	6	NIBAN1
0	1.577896856	0.643	0.031	0	7	ANK3
0	1.410985374	0.474	0.019	0	7	IL7R
0	1.406842182	0.479	0.015	0	7	GZMK
0	1.02295652	0.421	0.026	0	7	NELL2
0	0.756620032	0.368	0.016	0	7	UST
2.7348E-201	1.159241933	0.609	0.131	6.1394E-197	7	CAMK4
2.1727E-170	0.59019504	0.222	0.02	4.8775E-166	7	ITGA1
1.1738E-126	1.000943985	0.801	0.33	2.635E-122	7	CASK
8.9177E-117	0.645123497	0.6	0.189	2.0019E-112	7	TCF7
4.91153E-90	0.767013262	0.571	0.213	1.10259E-85	7	LINC00996
2.91223E-78	0.797652573	0.957	0.774	6.53766E-74	7	CD44
2.38376E-77	0.704321182	0.325	0.082	5.35131E-73	7	PCAT1
2.518E-77	0.747912224	0.904	0.625	5.65266E-73	7	FAM107B
1.11362E-71	0.849051079	0.863	0.548	2.49997E-67	7	TC2N
4.56386E-71	0.895987857	0.889	0.511	1.02454E-66	7	PDE3B
1.87555E-70	0.776603334	0.776	0.438	4.21041E-66	7	EPHA4
3.32628E-68	0.569427864	0.438	0.151	7.46716E-64	7	DRAIC
2.8722E-59	0.701142124	0.515	0.221	6.44781E-55	7	TRIO
4.71156E-44	0.637324937	0.84	0.635	1.0577E-39	7	NIBAN1
2.52299E-39	0.636832516	0.425	0.195	5.66386E-35	7	LINC02446
0	0.924257664	0.613	0.081	0	8	EGR2

5.8768E-276	3.033226258	1	0.58	1.3193E-271	8	CCL4L2
1.9879E-252	2.602523572	1	0.897	4.4626E-248	8	CCL4
4.8585E-234	1.29832846	0.881	0.261	1.0907E-229	8	NR4A2
1.3786E-181	1.141913364	0.634	0.155	3.0948E-177	8	CCL3L1
1.8309E-178	1.629564091	0.982	0.734	4.1101E-174	8	NFKBIA
1.3094E-175	1.065776397	0.854	0.266	2.9394E-171	8	FCER1G
5.6504E-149	1.705998447	0.946	0.541	1.2685E-144	8	CCL3
5.4781E-139	1.169622425	0.98	0.68	1.2298E-134	8	IGF2R
1.4555E-118	0.999451311	0.769	0.333	3.2674E-114	8	RELB
1.0566E-109	0.976833704	0.825	0.416	2.3719E-105	8	CD69
2.9434E-107	0.908149985	1	0.698	6.6077E-103	8	KLRC1
9.46227E-97	0.9771762	0.939	0.746	2.12419E-92	8	RAB8B
2.04556E-94	0.989724287	0.546	0.177	4.59207E-90	8	SNX9
9.24413E-93	0.922721863	0.946	0.704	2.07522E-88	8	ZFP36L1
8.07623E-86	1.03427604	0.656	0.283	1.81303E-81	8	GABPB1
3.27598E-85	0.939141499	0.906	0.667	7.35425E-81	8	RIN3
1.73338E-72	0.947002411	0.876	0.552	3.89126E-68	8	BNC2
3.88801E-69	1.206945278	0.813	0.558	8.72818E-65	8	NFKB1
1.62839E-66	0.876516787	0.951	0.821	3.65557E-62	8	IKZF3
0	3.316054372	1	0.02	0	9	LINGO2
9.38574E-91	0.751687377	0.76	0.27	2.10701E-86	9	FCER1G
1.78856E-51	1.011644296	0.858	0.547	4.01514E-47	9	SGCD
3.70154E-50	0.61124896	0.489	0.179	8.30958E-46	9	SNX9
6.33177E-50	0.736602696	0.927	0.701	1.42142E-45	9	KLRC1
1.77093E-46	0.750053855	0.765	0.44	3.97555E-42	9	GAS7
5.73679E-44	0.675582547	0.992	0.96	1.28785E-39	9	NEAT1
7.0493E-40	0.645501827	0.891	0.673	1.5825E-35	9	PTPN12
3.83519E-36	0.648633831	0.813	0.495	8.60962E-32	9	PHACTR2
1.6998E-35	0.521556497	1	0.976	3.81588E-31	9	LYST
5.55164E-33	0.560645626	0.944	0.799	1.24629E-28	9	JAZF1
4.92347E-32	0.494913771	0.961	0.881	1.10527E-27	9	PPP3CC
1.29653E-31	0.4975575	0.556	0.288	2.91058E-27	9	MTSS1
1.27605E-30	0.512866472	0.623	0.354	2.8646E-26	9	FAM3C
4.66105E-28	0.659262186	0.883	0.683	1.04636E-23	9	IGF2R
2.69569E-25	0.503084973	0.888	0.742	6.05156E-21	9	SLA

2.36193E-23	0.561380207	0.754	0.555	5.30229E-19	9	BNC2
8.91367E-21	0.518242684	0.589	0.373	2.00103E-16	9	GFOD1
1.31209E-18	0.494561112	0.813	0.67	2.94552E-14	9	PRSS23
5.78535E-15	0.502853394	0.472	0.293	1.29875E-10	9	BACH2
0	1.949327307	0.937	0.125	0	10	MX1
0	1.193829776	0.664	0.066	0	10	RSAD2
0	1.004214767	0.648	0.073	0	10	OAS1
0	0.928347843	0.513	0.024	0	10	IFIT1
1.8952E-243	1.553929484	0.83	0.178	4.2545E-239	10	MX2
1.6296E-211	1.330930754	0.736	0.147	3.6583E-207	10	HERC5
5.6047E-181	1.610442133	0.943	0.358	1.2582E-176	10	EPSTI1
2.2394E-178	2.132782496	0.975	0.502	5.0272E-174	10	ISG15
1.8086E-175	1.138991399	0.604	0.111	4.0602E-171	10	IFIT3
3.5117E-161	1.760178096	0.862	0.327	7.8835E-157	10	IFI6
1.5437E-155	1.451133938	0.909	0.371	3.4655E-151	10	EIF2AK2
1.1268E-149	1.435897391	0.921	0.42	2.5297E-145	10	XAF1
3.6592E-129	1.109003669	0.783	0.258	8.2146E-125	10	PARP9
2.9217E-128	1.357382299	0.953	0.589	6.5589E-124	10	LY6E
5.2248E-119	1.332441308	0.94	0.591	1.1729E-114	10	ISG20
1.5007E-114	1.053621279	0.755	0.27	3.3689E-110	10	STAT1
4.156E-111	0.935869836	0.802	0.3	9.3298E-107	10	IRF9
8.3373E-100	1.05335437	0.846	0.383	1.87163E-95	10	SAMD9L
7.0726E-80	0.978220542	0.915	0.58	1.58773E-75	10	PARP14
4.97532E-63	0.962994919	0.833	0.52	1.11691E-58	10	TRIM22
0	2.720090635	1	0.086	0	11	DLG2
2.62586E-27	0.600592511	0.908	0.676	5.8948E-23	11	APBA2
6.24247E-27	0.780863835	0.729	0.4	1.40137E-22	11	THEMIS
9.6768E-23	0.506203915	1	0.97	2.17234E-18	11	PITPNC1
1.32493E-22	0.453193567	1	0.999	2.97434E-18	11	AOAH
1.25038E-19	0.713471939	0.769	0.517	2.80698E-15	11	PDE3B
2.35443E-17	0.451108302	0.974	0.938	5.28546E-13	11	CCSER2
7.32925E-16	0.417456957	0.934	0.813	1.64534E-11	11	SLFN12L
1.63337E-14	0.432436724	0.83	0.641	3.66675E-10	11	EML4
6.82471E-14	0.42445913	0.799	0.611	1.53208E-09	11	GRAP2
7.62108E-14	0.376474453	0.603	0.364	1.71086E-09	11	EPSTI1

5.92613E-13	0.381947862	0.838	0.651	1.33036E-08	11	PRKCQ
6.7003E-13	0.439167238	0.764	0.553	1.50415E-08	11	TC2N
1.34599E-12	0.42704336	0.856	0.721	3.02161E-08	11	VTI1A
1.55393E-11	0.411425113	0.856	0.735	3.48842E-07	11	SOS1
1.60467E-11	0.369180382	0.611	0.409	3.60233E-07	11	JAKMIP2
2.1816E-11	0.370616953	0.991	0.964	4.89748E-07	11	ZBTB20
2.07435E-09	0.376644605	0.703	0.529	4.65671E-05	11	LINC00342
1.27412E-06	0.372043378	0.467	0.341	0.028602742	11	ST8SIA6
1.43575E-05	0.392325663	0.52	0.407	0.322312178	11	COMMD10
0	3.509622599	1	0.001	0	12	RRM2
0	3.251782343	1	0	0	12	MKI67
0	3.113151824	1	0.001	0	12	TOP2A
0	2.413698179	0.933	0.001	0	12	ASPM
9.7155E-249	2.44902331	1	0.013	2.181E-244	12	KNL1
6.6146E-172	2.436481371	1	0.019	1.4849E-167	12	CLSPN
2.1109E-115	3.178199913	1	0.029	4.7387E-111	12	CENPF
9.43523E-80	3.34249043	1	0.043	2.11812E-75	12	NUSAP1
8.86534E-59	4.576622443	1	0.06	1.99018E-54	12	STMN1
3.85093E-33	2.552047444	1	0.115	8.64495E-29	12	PCNA
5.29793E-27	2.744176963	1	0.145	1.18933E-22	12	EZH2
6.62427E-22	2.693926888	1	0.186	1.48708E-17	12	HIST1H1C
1.1111E-20	2.775764174	1	0.214	2.49431E-16	12	NSD2
1.62738E-19	2.726007299	1	0.235	3.65331E-15	12	ATAD2
1.06619E-16	4.28484422	1	0.307	2.3935E-12	12	TUBA1B
1.37282E-16	3.548338679	1	0.311	3.08184E-12	12	TUBB
2.58171E-15	2.517699102	1	0.35	5.79569E-11	12	SMC4
2.88611E-15	5.294662325	1	0.36	6.47903E-11	12	HIST1H4C
4.1699E-13	3.072757006	1	0.521	9.361E-09	12	HMGB2
2.6373E-12	2.822979344	1	0.681	5.92048E-08	12	HMGN2

P_val: raw p-value; avg_log2FC: log2-fold-change of the average expression between the two groups (here, cluster vs all cells); pct.1: fraction of cells where the feature is detected in the cluster tested; pct.2: fraction of cells where the feature is detected in the remaining clusters; p_val_adj: adjusted p-value, based on Bonferroni correction.

Table S4. Ordering of connected clusters in each lineage.

Lineage 1	Lineage 2	Lineage 3	Lineage 4	Lineage 5
4	4	4	4	4
2	2	2	2	2
11	11	11	11	11
10	10	10	10	10
9	9	0	6	5
1	1	7		
8	3			

Lineages are identified as a set of individual cells along a path/trajectory.

3.2 Chapter 2

3.2.1 Title

NK Cell Depletion in Bispecific Antibody Therapy is Associated with Lack of HIV Control after ART interruption

3.2.2 Abstract

HIV infection remains incurable as the virus persists within a latent reservoir of $CD4^+$T cells. Novel approaches to enhance immune responses against HIV are essential for effective control and potential cure of the infection. In this study, we designed a novel tetravalent bispecific antibody (Bi-Ab32/16) to simultaneously target the gp120 viral protein on infected cells, and the CD16a receptor on NK cells. In vitro, Bi-Ab32/16 triggered a potent, specific, and polyfunctional NK-dependent response against HIV-infected cells. Moreover, addition of the Bi-Ab32/16 significantly reduced the latent HIV reservoir after viral reactivation, and mediated the clearance of cells harboring intact proviruses in samples from people with HIV (PWH). However, the *in vivo* preclinical evaluation of Bi-Ab32/16 in humanized mice expressing IL-15 (NSG-Hu-IL-15) revealed a significant decline of NK cells associated with poor virological control after ART interruption. Our study underscores the need to carefully evaluating strategies for sustained NK cell stimulation during ART withdrawal.

3.2.3 Introduction

While antiretroviral therapy (ART) effectively suppresses HIV viremia, it is unable to completely eliminate the virus that persists in anatomical and cellular reservoirs[112,464]. The latent HIV reservoir represents the main barrier to reach a cure, and is mostly constituted by resting memory $CD4^+$ T cells that do not produce viral particles, thus being invisible to the action of ART and the immune system[96,165]. Recent efforts to eliminate the latent reservoir have focused on the "shock and kill" strategy, which involves the reactivation of HIV gene expression with latency reversal agents (LRAs) followed by immune-mediated clearance of infected cells[81]. Despite progress, most LRAs are ineffective at reversing latency ex vivo, and have failed to reduce the size of the latent reservoir in vivo[372,465], especially in anatomical reservoirs where the bioavailability of the drugs is distinct from plasma[466]. Moreover, both HIV infection and treatment with specific LRAs are known to compromise the function of key immune components involved in the clearance of HIV infected cells, including $CD8^+$ T cells and natural killer (NK) cells[467,468]. Consequently, there is an urgent need for the development of novel therapeutic strategies to target persistent HIV in ART-treated individuals.

NK cells, as cytotoxic innate lymphoid cells, exhibit potent responses against infected and malignant cells[274]. Similar to $CD8^+$ T cells, NK cells experience swift and dynamic alterations during early HIV infection, exerting direct cytotoxic responses independent of HLA class I restriction[469]. NK cell activation and effector functions hinge on interactions involving germline-encoded activating or inhibitory receptors and their corresponding ligands on target cells[470,471]. Notably, the activating receptor CD16, has been described as the sole receptor capable of activating cytotoxicity and cytokine secretion independent of additional signals[472]. During HIV infection, NK cells exhibit the capacity to suppress viral replication and regulate cells harboring HIV-DNA[380]. Furthermore, recent research reveals antigen-specific memory development in human NK cells exposed to HIV, primarily dependent on the NKG2C/HLA-E axis[315]. Additionally, NK cells can kill HIV-infected cells by antibody-dependent cell-mediated cytotoxicity (ADCC), where the CD16 receptor on NK cells interacts with the Fc portion of antibodies that are bound to HIV-infected cells, leading to their activation and cytotoxic response[473,474]. These diversified functions position NK cells as attractive players for immunotherapeutic interventions aimed to target the HIV reservoir. Thus, recruiting and activation of NK cells by targeting CD16a in close proximity to infected cells could be an effective strategy against HIV-infection.

Several studies provide compelling evidence that ADCC-mediating antibodies play an important role in the context of HIV and SIV infection[388,389,475]. These studies establish a correlation between ADCC responses and lower viral loads[385], protection from infection[476,477], and improved clinical outcome in linked transmission[478]. Several non-neutralizing antibodies have been described to promote ADCC during HIV infection[479,480]. Among them, A32 is a non-neutralizing antibody isolated from an individual with HIV that has been reported to recognize a conformational epitope involving the C1 and C4 regions of HIV-gp120 present in the membrane of HIV-infected cells, following Env binding to CD4[481]. Importantly, the A32 antibody stands as a promising candidate for targeting HIV-infected cells as it presents important features, including broad reactivity against envelopes from all HIV-1 clades[482], highly conserved epitope residues[482], and no evidence of epitope escape mutations[483]. Importantly, the A32 antibody targets the earliest expressed epitope during the course of infection, a feature that may hold significance for shock and kill strategies[481].

Immune-targeted therapies based on the use of antibodies to promote NK cell mediated immune responses against HIV have been previously explored. However, antibody therapies face some limitations, including the high dosage to induce a clinical response or the need to promote an efficient cell-to-cell contact between target and effector cells. In this regard, bispecific antibodies (BiAbs) can promote the specific recruitment of effector cells by engaging its receptors to a target. BiAbs are engineered immunoglobulins that contain the specificities and properties of two different monoclonal antibodies (mAbs) into a single molecule. Thus, BiAbs can elicit synergistic activities and enhance therapeutic efficacy and/or safety compared to conventional monospecific IgGs therapies[36]. Recent studies in the field of hematological malignancies have described bispecific formats aimed at redirecting NK-mediated immune responses towards leukemia/lymphoma targets[37,38]. Of note, this approach has progressed to clinical trials involving individuals with relapsed/refractory $CD30^{+}$ malignancies (NCT01221571, NCT04101331). In addition, bispecific NK cell engagers (BiKE) have been previously developed to engage NK cells through the CD16a receptor and lyse HIV-infected cells[39–41]. Some strategies include bispecific antibodies directed to CD16a and gp41[41] or to the CD4 extracellular domain 1[39]. Further, a recent study has described two bispecific antibodies targeting the HIV envelope protein (Env) and CD16, promoting NK-mediated in vivo reduction of HIV-reservoir cells in a mouse model of HIV infection[42]. These studies provide evidence supporting the engagement of CD16a as a potent mechanism for favorably tilting the balance towards NK cell activation.

Although bispecific formats have been explored, no study up to date has assessed the role of CD16-targeting bispecific antibodies on viral recrudescence after ART interruption.

Here, to enhance the NK cell immune response against HIV-expressing cells, we engineered a tetravalent bispecific antibody (Bi-Ab32/16) targeting the gp120 HIV protein (Ab A32) and the molecule CD16a. Our study provides proof-of-concept that Bi-Ab32/16 is capable of mediating potent elimination of HIV reservoir cells ex vivo, but the in vivo administration to humanized mice infected with HIV translates into a rapid viral rebound associated with the loss of NK cells. Thus, our data contributes important clues for the development of novel immunotherapies targeting NK cells.

3.2.4 Materials and methods

Ethics statement

PBMCs from healthy donors were obtained from the Blood and Tissue Bank (Barcelona, Spain). The study protocol was approved by the Comitè d'Ètica d'Investigació Clínica (Institutional Review Board number PR(AG)350/2017) of the Hospital Universitari Vall d'Hebron (Barcelona, Spain). Samples were obtained from adults, who all provided written informed consent, and were prospectively collected and cryopreserved in the Biobank (register number C.0003590). All samples received were totally anonymous and untraceable. PBMCs from PWH were also obtained from the HIV unit of the Hospital Universitari Vall d'Hebron (Institutional Review Board number PR(AG)350/2017). All participants gave written informed consent for their participation in these studies.

Cells, antibodies, and reagents

PBMCs were isolated by Ficoll-Plaque density gradient centrifugation and cryopreserved in liquid nitrogen. PBMCs were cultured in RPMI medium (Gibco) supplemented with 10% Fetal Bovine Serum (Gibco), 100 µg/ml streptomycin (Fisher Scientific), and 100 U/ml penicillin (Fisher Scientific) (R10 medium), and maintained at 37ºC in a 5% CO_2 incubator. The cell line CEM.NKR CCR5$^+$ was obtained through the NIH AIDS Reagent Program (Division of AIDS, NIAID, NIH, from Dr. Alexandra Trkola)[484]. HIV_{BaL} gp120 recombinant protein was obtained through the NIH AIDS Reagent Program. The A32 antibody was obtained through the AIDS Research and Reference Program, NIAID, NIH (Cat#11438) from Dr. James E. Robinson[481]. The Bi-Ab32/16 antibody was designed by Dr. Maria J. Buzón and purchased at Fusion Antibodies PLC (Belfast, N. Ireland). Interleukin-2 (IL-2) was purchased from Sigma Aldrich. The anti-CD16 clone 3G8 was purchased from Stemcell. The pan-caspase inhibitor named Q-VD-OPh quinolyl-valyl-O-methylaspartyl-[–2,6-difluorophenoxy]-methyl ketone was purchased from Selleckchem.

Cell binding assays

We assessed the binding capacity of Bi-Ab32/16, A32 (anti-HIV_{gp120}) and 3G8 (anti-CD16) antibodies to their targets by flow cytometry. The bispecific antibody concentration employed in the following experiments was previously established through the determination of the effective concentration (EC_{50}) in a dose-response curve (refer to Figure 3B). Specifically, a concentration of 0.2 µg/ml of Bi-Ab32/16 was utilized. For evaluation of Bi-Ab32/16 and A32, we used the CEM.NKR CCR5$^+$ cell line.

Briefly, cells were coated with 1 µg of the HIV-1 BaL gp120 recombinant protein during 1 h at room temperature (RT). After incubation, cells were washed in ice-cold R10 medium and staining buffer (PBS containing 3% FBS). Subsequently, cells were incubated for 20 min at RT in R10 medium with Bi-Ab32/16 (0.2 µg/ml) or A32 (5 µg/ml) antibodies, and stained with an anti-human FITC-labelled secondary antibody (dil 1:100) directed to the heavy chains on human IgG (Thermo Fisher) for detection of both antibodies (20 min at RT). To assess the targeting capacity of Bi-Ab32/16 and 3G8, NK cells were obtained from PBMCs of healthy donors by negative isolation using magnetic beads (MagniSort™ Human NK cell Enrichment Kit, eBioscience). NK cells were then incubated in R10 medium containing Bi-Ab32/16 (0.2 µg/ml) or the anti-CD16 PE-labelled 3G8 antibody (5 µg/ml). For detection of Bi-Ab32/16, we used an anti-human FITC-labelled secondary antibody (dil 1:100) (ThermoFisher). Cells were then fixed with paraformaldehyde solution (PFA; Affymetrix) (2%) and acquired in an LSR Fortessa flow cytometer (Becton Dickinson). Results were analyzed with FlowJo v10 software.

NK cell phenotyping

NK cells were isolated from cryopreserved PBMCs of healthy donors using a commercial kit (MagniSort™ Human NK cell Enrichment; eBioscience). Then, cells were incubated in R10 with 0.2 µg/ml Bi-Ab32/16 for 24 hours at RT. The next day, NK cells were stained with LIVE/DEAD AQUA viability (Invitrogen) for 20 min at RT. After washing once with PBS 1X, cells were stained with anti-CXCR3-BV650 (G025H7, Biolegend) for 30 min at 37°C. Next, cells were washed with staining buffer and stained with anti-CD57-PerCP-Cy5.5 (HNK-1, Biolegend), anti-CD56-FITC (B159, Becton Dickinson), anti-CD3-PE-Cy7 (SK7, Becton Dickinson), anti-NKp30-PE-CF594 (P30-15, Biolegend), anti-NKG2C-PE (134591, R&D Systems), anti-NKG2D-APC-Cy7 (1D11, Biolegend), anti-CD4-AF700 (RPA-T4, Becton Dickinson), anti-NKG2A-APC (Z199, Beckman Coulter), anti-CD16-BV786 (3G8, Becton Dickinson), anti-CD158b-BV605 (CH-L, Becton Dickinson) and anti-KLRG1–BV421 (14C2A07, Biolegend) antibodies in brilliant stain buffer (Beckton Dickinson) for 20 min at RT. Cells were then washed with staining buffer and fixed with 2% PFA. Samples were acquired on a BD LSR Fortessa flow cytometer and data was analyzed using FlowJo V10 and OMIQ software from Dotmatics (www.omiq.ai, www.dotmatics.com).

Cell-to-cell contact assays

$CD4^+$ T cells and NK cells were isolated from cryopreserved PBMCs of healthy donors by commercial kits (MagniSort Human $CD4^+$ T Cell Enrichment; Affymetrix, and MagniSort™ Human NK cell Enrichment; eBioscience).

$CD4^+$ T cells were coated with 1 µg of recombinant gp120 protein during 1h at RT. After washing, $CD4^+$ T cells were co-cultured with NK cells in a 1:1 ratio with Bi-Ab32/16 (0.2 µg/ml) for 20 min at RT. After the incubation, cells were stained with anti-CD56 (FITC; Becton Dickinson), anti-CD3 (PE-Cy7; Becton Dickinson), anti-CD16 (PE; Biolegend) and anti-CD4 (AF700; Beckton Dickinson) antibodies for detection of $CD4^+$ T and NK cells. After 20 min incubation at RT, cells were washed and fixed with PFA (2%). Samples were then acquired on an LSR Fortessa flow cytometer (Becton Dickinson) and data were analyzed using FlowJo V10 software.

NK cell activation and functional activity assays

The activation and cytotoxic response of NK cells after stimulation with Bi-Ab32/16 was evaluated. NK cell cytotoxicity was assessed by the expression of CD107a and IFNγ. Briefly, NK cells were isolated from cryopreserved PBMCs from healthy donors by negative isolation using magnetic beads (MagniSort™ Human NK cell Enrichment Kit, eBioscience). CEM.NKR $CCR5^+$ cells were coated with 1 µg of the HIV-1 BaL gp120 during 1h at RT. Cells were then cultured at 1:1 ratio in R10 medium containing Bi-Ab32/16 (0.2 µg/ml), A32 (5 µg/ml) or 10 ng/ml PMA plus 1 µM ionomycin (positive control) for 4.5 h in a U-bottom 96-well plate at 37°C and 5% CO_2. BD GolgiPlug Protein Transport Inhibitor (Beckton Dickinson), BD GolgiStop Protein Transport Inhibitor containing monensin (Beckton Dickinson), and CD107a-PE-Cy5 (H4A3; Becton Dickinson) were also added to each well at the recommended concentrations. After incubation, cells were washed and stained with a viability dye (LIVE/DEAD Fixable Violet dead cell stain; Thermo Fisher) for 20 min at RT. Cells were washed with PBS 1X and stained with anti-CD56-FITC (B159; Becton Dickinson), anti-CD3-PE-Cy7 (SK7; Becton Dickinson), anti-CD69-PECF594 (FN50; Beckton Dickinson) and anti-HLA-DR-SB600 (LN3; eBioscience) antibodies for 20 min at RT. Cells were then fixed and permeabilized with Fixation/Permeabilization Solution (Beckton Dickinson) for 20 min at 4ºC, washed with BD Perm/Wash buffer and stained with anti-IFNγ-AF700 (Life technologies) for 30 min at 4ºC. Cells were then washed, fixed with PFA (2%) and acquired on an LSR Fortessa flow cytometer (Beckton Dickinson). Data were analyzed using FlowJo V10 and OMIQ software from Dotmatics (www.omiq.ai, www.dotmatics.com).

Antibody-dependent cell-mediated cytotoxicity (ADCC) assays

The ADCC assay was conducted as previously described with certain modifications[485]. Briefly, CEM.NKR $CCR5^+$ cells were used as target cells after being double-stained with PKH67 (Sigma-Aldrich) and eF670 (Labclinics) dyes following manufacturer's instructions.

Cells were then coated with 1 µg of the HIV-1 Bal gp120 recombinant protein for 1h at RT and extensively washed in ice-cold R10 medium. Target cells were dispensed in U-bottom 96-well plates and incubated 15 min in R10 medium containing distinct Bi-Ab32/16 or A32 antibody concentrations (0.001 µg/ml, 0.005 µg/ml, 0.01 µg/ml, 0.05 µg/ml, 0.1 µg/ml, 0.5 µg/ml, 1 µg/ml and 5 µg/mL). Plasma (1:1000 dilution) from a viremic (high viral load in blood) HIV^+ participant was used as a positive control. NK effector cells were isolated from PBMCs of healthy donors or antiretroviral therapy (ART) suppressed HIV^+ participants and added at 1:10 target/effector ratio. Plates were centrifuged and incubated for 4h at 37ºC and 5% CO_2. After washing, flow cytometry count beads (AccuCount Blank Particles, Cytognos) were added to normalize cell collection to a constant number of particles (1000 events). Finally, cells were fixed with PFA (2%) and acquired on a LSR Fortessa flow cytometer (Beckton Dickinson). Data were analyzed using FlowJo V10 software. Target cells were identified through analysis in a PKH67 versus side scatter (SSC) plot. The percentage of killing was determined by the loss of the eF670 marker in an eF670 versus PKH67 plot.

Ex vivo infection of $CD4^+$ T cells and functional ADCC assay

PBMCs from ART-suppressed PWH were thawed and incubated overnight in R10 medium containing 40U/ml of IL-2. The next day, $CD4^+$ T cells were isolated using a commercial kit (MagniSort Human $CD4^+$ T cell Enrichment; Affymetrix) and infected by spinoculation at 1200g for 2h at 37ºC with $HIV_{NL4.3}$ ($TCID_{50}$=78.125) or HIV_{BaL} ($TCID_{50}$=625) viral strains. Cells were then washed twice with PBS and cultured at 1 million/ml in a U-bottom 96-well plate with R10 containing 100 U/ml of IL-2 for the next 5 days. Five days after HIV infection, cells were placed in U-bottom 96-well plates. Autologous NK cells, previously isolated by negative selection using magnetic beads (MagniSort Human NK cell Enrichment Kit, eBioscience) from PBMCs, were then added at a 1:1 ratio. Cells were incubated in R10 medium containing 0.2 µg/ml of Bi-Ab32/16, 5 µg/ml of A32 or plasma (1:1000 dilution) from a viremic (high viral load in blood) HIV^+ participant (positive control) for 15 min at RT. Plates were then centrifuged at 400g for 3 min and incubated for 4 h at 37°C and 5% CO_2. After incubation, cells were washed with PBS and stained with a viability dye (LIVE/DEAD Fixable Violet Dead Cell Stain; Thermo Fisher) for 20 min at RT. After, cells were washed with staining buffer and stained with anti-CD56-FITC (B159; Beckton Dickinson), anti-CD3-Pe-Cy7 (SK7, Beckton Dickinson), anti-CD4-AF700 (RPA-T4, Beckton Dickinson) for 20 min at RT.

Cells were then washed with staining buffer, fixed and permeabilized with Fixation/Permeabilization Solution (Beckton Dickinson) for 20 min at 4ºC, washed with BD Perm/Wash buffer and stained with anti-p24-PE (KC57-RD1, Beckman Coulter) for 30 min on ice and 30 min at RT. Finally, cells were washed and fixed with 2% PFA. Samples were acquired in an LSR Fortessa flow cytometer (Beckton Dickinson) and analyzed using FlowJo V10 software. Target cell killing was calculated as the decrease in the population of infected ($p24^+$) cells.

Viral reactivation in ART-suppressed PWH samples

$CD4^+$ T cells from ART-suppressed PWH were isolated from PBMCs using a commercial kit (MagniSort Human $CD4^+$ T cell Enrichment; Affymetrix) and cultured in R10 medium with Q-VD-OPh (Selleckchem) for 2h in the presence of Raltegravir (1 µM), Darunavir (1 µM), and Nevirapine (1 µM) to prevent new rounds of viral infection. After 2h, PMA (Abcam; 81 nM) plus ionomycin (Abcam; 1 µM) were added to the cell culture as a latency reversal agent and left for 18h to reactivate latent HIV. After the incubation, cells were subjected to ADCC assays as described above. After, cells were stained with LIVE/DEAD Far Red viability for 20 min at RT. Cells were then washed with staining buffer and stained with anti-CD56-FITC (B159; Becton Dickinson), anti-CD3-PerCP (SK7, Becton Dickinson), and anti-CD8-APC (RPA-T8; Beckton Dickinson) for 20 min at RT. After the incubation, cells were fixed and permeabilized with Fixation/Permeabilization Solution (Beckton Dickinson) for 20 min at 4ºC, washed with BD Perm/Wash buffer and stained with anti-p24-PE (KC57-RD1, Beckman Coulter) for 30 min on ice and 30 min at RT. Finally, cells were washed and fixed with 2% PFA. Samples were acquired in a FACSCalibur (Beckton Dickinson) and AURORA (Cytek) flow cytometers.

NK killing of cells harboring intact provirus

$CD4^+$ T cells from ART-suppressed PWH were isolated from PBMCs using the Dynabeads CD4 Positive Isolation Kit (Affymetrix) and cultured in R10 medium containing Raltegravir (1 µM), Darunavir (1 µM), and Nevirapine (1 µM) to prevent new rounds of viral infection. PMA (Abcam; 81 nM) plus ionomycin (Abcam; 1 µM) were added to the cell culture as a latency reversal agent and left for 18h to reactivate latent HIV. The negative fraction of cells remaining from the $CD4^+$ T cell isolation kit were cultured overnight in R10 medium supplemented with 100 U/mL of IL-2 (Merck) at a concentration of 2 M/ml. The next day, NK cells were enriched from the CD4 negative fraction using a commercial kit (MagniSort Human NK cell Enrichment Kit, eBioscience).

Autologous NK cells were then cultured in R10 medium containing Raltegravir (1 μM), Darunavir (1 μM), and Nevirapine (1 μM) plus DNAse (100 μg/mL, Merck) and incubated in the presence of 0.2 μg of Bi-Ab32/16, 5 μg/ml of A32 or IgG2a isotype control at 0.2 μg/ml (MOPC-173, Biolegend) for 15 min at RT in U-bottom 96-well plates. After 18h, reactivated $CD4^+$ T cells were added at a 1:1 ratio and incubated for 4h at 37°C in 5% CO_2. After the incubation, the remaining viable $CD4^+$ T cells were isolated from the coculture using a combination of the EasySep Dead Cell Removal (Annexin V) Kit (StemCell Technologies) and the MagniSort Human $CD4^+$ T cell Enrichment Kit (Invitrogen). The cell pellet was then lysed with proteinase K-containing lysis buffer and incubated at 55°C overnight, followed by a 95°C incubation for 5 min, to obtain DNA for the Intact Proviral DNA Assay (IPDA) described below.

Intact proviral DNA assay (IPDA)

IPDA was performed as previously described by Bruner et al., 2019. Primers and probes specific for the Ψ HIV gene ((HIV-1 Ψ forward 5′-CAGGACTCGGCTTGCTGAAG-3′, HIV-1 Ψ reverse GCACCCATCTCTCTCCTTCTAGC and probe 5′ 6-FAM-TTTTGGCGTACTCACCAGT-MGBNFQ-3′) and env HIV gene (HIV-1 env forward 5′-AGTGGTGCAGAGAGAAAAAAGAGC-3′, HIV-1 env reverse 5′-GTCTGGCCTGTACCGTCAGC-3′, HIV-1 env intact probe 5′-VIC-CCTTGGGTTCTTGGGA-MGBNFQ-3′, and HIV-1 anti-Hypermutant env probe 5′-CCTTAGGTTCTTAGGAGC-MGBNFQ-3′) were employed. The hRPP30 gene was used for cell input normalization. Samples were analyzed in a QIAcuity One 2-plex System (Qiagen).

Animal model

All mouse experiments were conducted in a Biosafety Level 3 (BSL3) facility at the Comparative Medicine and Bioimage Centre of Catalonia (CMCiB). Hu-NSG-Tg (IL-15) NOD-*scid* IL2Rgamma^{null} (NSG) mice were procured from the Jackson Laboratory. Animal studies were performed by trained researchers, and approved and assessed by the Committee on the Ethics of Animal Experimentation from the CMCiB (CSB-22-001) and count with the authorization of the Generalitat de Catalunya (code: 11505). All procedures involving experimental animals were carried out in compliance with pertinent institutional and national animal welfare laws, guidelines, and policies. Mice were infected with $1x10^4$ $TCID_{50}$ of HIV_{BaL} strain.

Then, from 6 to 9 weeks post-infection (WPI) mice were placed on a diet combined with ART (87.5 mg/kg/day emtricitabine (FTC), 131 mg/kg/day tenofovir (TDF), and 175 mg/kg/day raltegravir (RAL) and darunavir (DRV))[80]. Subsequently, animals were randomized in three groups of n=6 animals and received 500 µg of immunotherapy intraperitoneally twice a week (A32, Bi-Ab32/16 or PBS as a vehicle control) from 8 to 10 WPI. The experimental endpoint was set at 11- and 13-WPI, at which point the mice were sacrificed. Throughout the study, mice were subjected to weekly blood extractions.

***In vivo* sample processing**

Briefly, plasma and PBMCs were isolated from blood samples by centrifugation at 2000g for 20 min at 4ºC. Plasma was collected from the supernatant and transferred to 1.5 ml conical tubes. Samples were then lysed with RAV1 buffer (Nucleospin™ RNA Virus kit, Cultek) and preserved at -80ºC for further analysis. Remaining red blood cells present in PBMCs were lysed using ACK Lysis buffer (Fisher Scientific) following manufacturer's instructions. Spleens were excised, minced into small pieces, and processed through a 70 µm cell strainer (Falcon). The obtained cells were employed for flow cytometry analysis described below.

Viral load determination

Plasma viral load (pVL) was measured weekly to evaluate the suppression of viral replication in Hu-NSG-Tg (IL-15) mice. HIV RNA was extracted from plasma using Nucleospin™ RNA Virus kit (Cultek, Macherey-Nagel) following the manufacturer's instructions. Reverse transcription of RNA to cDNA was performed with SuperScript™ III Kit (Invitrogen) in accordance with the instructions provided by the manufacturer, and cDNA was quantified by quantitative PCR (qPCR) using primers and probes specific for the 1-LTR HIV region (LTR forward 5′-TTAAGCCTCAATAAAGCTTGCC-3′ and LTR reverse 5′-GTTCGGGCGCCACTGCTAG-3′; LTR probe 5′-CCAGAGTCACACACCAGACGGGCA-3′), and TaqMan™ Gene Expression Master Mix (Thermo Fisher). Samples were analyzed in an Applied Biosystems QuantStudio5 system. Quantification of DNA was performed using a standard curve, and values were normalized to 1 million $CD4^+$ T cells.

Longitudinal analysis of immune populations and NK cell phenotype by flow cytometry in HIV-infected Hu-NSG-Tg (IL-15) mice

For immune populations evolution, lysed blood and tissue samples were transferred to a V-bottom 96 well plate, washed with PBS, and stained with a viability dye (LIVE/DEAD Fixable Aqua Dead Cell Stain; Thermo Fisher) for 20 min at RT in the dark.

After, cells were centrifuged at 2600 rpm for 5 min, washed with PBS 1X and stained in a volume of 50 ul/well with anti-CD56-FITC (B159; Beckton Dickinson), anti-CD3-PE-Cy5 (UCHT1, Biolegend), anti-CD45-AF700 (HI30, Biolegend), anti-CD8-APC (RPA-T8, BD Biosciences), anti-CD16-BV786 (3G8; Beckton Dickinson) and anti-CD4-BV605 (RPA-T4, BD Biosciences) for 20 min at RT. After the cell surface staining, cells were washed with staining buffer, fixed and permeabilized with Fixation/Permeabilization Solution (Beckton Dickinson) for 20 min at 4ºC, washed with BD Perm/Wash buffer, and stained with anti-p24 PE (KC57-RD1, Beckman Coulter) for 20 min on ice and 20 min at RT. Finally, cells were washed and fixed with 2% PFA. For NK cell phenotyping, lysed blood and tissue samples were transferred to a V-bottom 96 well plate, washed with PBS, and stained with a viability dye (LIVE/DEAD Fixable Aqua Dead Cell Stain; Thermo Fisher) for 20 min at RT in the dark. Then, cells were centrifuged at 2600 rpm for 5 min, washed with PBS 1X, and stained in a volume of 50 ul/well with anti-CD56-FITC (B159; Beckton Dickinson), anti-CD49a-PE-Cy7 (BA5b, Biolegend), anti-CD3-PE-Cy5 (UCHT1, Biolegend), anti-CD69-PE-CF594 (FN50, BD Biosciences), anti-NKG2C-PE (134591, R&D systems), anti-CD16-BV786 (3G8; Beckton Dickinson), and anti-CD45-BV605 (HI30, BD biosciences) for 20 at RT. After, cells were washed with staining buffer, fixed and permeabilized with Fixation/Permeabilization Solution (Beckton Dickinson) for 20 min at 4ªC, washed with BD Perm/Wash buffer, and stained with anti-IFNγ -AF700 (B27, Invitrogen) for 30 min at RT. Finally, cells were washed and fixed with 2% PFA. Samples were acquired in an LSR Fortessa flow cytometer (Becton Dickinson) and analyzed using FlowJo V10 and OMIQ software from Dotmatics (www.omiq.ai, www.dotmatics.com).

Dimensionality reduction analysis

Dimensionality reduction analysis of flow cytometry data was performed using the OMIQ software from Dotmatics (www.omiq.ai, www.dotmatics.com). All events within pre-gated $CD56^+$ NK cells were concatenated for each group per culture condition and analyzed. For NK cell phenotyping assays, cell clusters were identified by Flow-Self Organizing Maps (FlowSOM) artificial intelligence algorithm based on the expression of CD57, NKp30, NKG2C, NKG2D, NKG2A, CD16, CXCR3, CD158b, and KLRG1. For NK cell activation assays, FlowSOM identified cell clusters based on the expression of CD107a, IFNγ, CD69, and HLA-DR. For *in vivo* analyses, cell clusters were identified based on the expression of CD16, CD49a, CD69, and NKG2C markers. Next, optimized T-distributed stochastic neighbor embedding (optSNE) analysis was employed to depict the identified clusters. Marker expression was represented as Archsin-transformed medians within heatmaps generated via optSNE analysis.

Statistical analysis

Statistical tests were performed with GraphPad Prism software (version 8.3) and are reported within each figure legend. P values <0.05 were considered statistically significant. Volcano plots were automatically produced by the OMIQ software, and differences were regarded as statistically significant when the value of p was below 0.05. Tables were prepared using Microsoft Word.

3.2.5 Results

Bi-Ab32/16 promotes specific cell-to-cell contact between HIV-expressing CD4$^+$ T and NK cells, and shifts the NK cell phenotype

We incorporated sequences of antibodies against Env and CD16a into Bi-Ab32/16 (**Supplementary Table 1**). Bi-Ab32/16 consists of a polypeptide chain encoding the full length non-neutralizing A32 antibody (anti-HIV$_{gp120}$) combined with a single-chain variable fragment (ScFv) domain from CD16a (**Figure 1A and Supplementary Figure 1A, B**). The A32 antibody exhibits specificity towards the conformational epitopes C1 and C4 on the HIV-1 gp120 Env protein following its interaction with CD4. It has been described to recognize envelopes from all HIV-1 clades and eliminate HIV-1 infected cells through ADCC[481,482]. In addition, prior studies have indicated that CD16a plays a role in promoting NK cell activation and cytotoxicity[294].

To evaluate the binding capacity of Bi-Ab32/16 to its corresponding targets (gp120 and CD16a), we stained primary isolated CD4$^+$ T cells coated with gp120, and autologous isolated NK cells with the bispecific antibody. Parental single A32 and anti-CD16a antibodies were used as controls. Antibody binding to cell surface was detected using a secondary antibody directed to the heavy chain of human IgG, including A32 (IgG anti-HIV gp120) (**Figure 1B, C**). Bi-Ab32/16 demonstrated percentages of binding to its target molecules similar to those of monospecific antibodies, both on gp120-expressing CD4$^+$ T cells and NK cells (**Figure 1D, E**). Once the binding of the Bi-Ab32/16 were confirmed, we investigated the potential of the antibody to target both molecules at the same time, and its capacity to bring closer both gp120-expressing CD4$^+$ T and NK cells. Cell-to-cell contact experiments were performed by culturing both cell types in the presence of the Bi-Ab32/26. The frequency of double positive CD4$^+$CD16$^+$ (cell doublets) was analyzed by flow cytometry. We observed that Bi-Ab32/26 was able to induce the formation of cell-to-cell doublets, and within these doublets, we observed a considerable increase (mean 12-fold) in the frequency of specific CD4-NK doublets (**Figure 1F**). Overall, our results show that the Bi-Ab32/16 binds to both targets simultaneously and induces the formation of cell doublets among gp120-expressing CD4$^+$ T and CD16$^+$ NK cells.

Subsequently, we studied if stimulation with the Bi-Ab32/16 for 24h promoted a shift in the expression pattern of important receptors for NK cell activity. An example of the gating strategy used is shown in **Supplementary Figure 2A**.

For these analyses, we included NK receptors with activating or inhibitory potential upon interaction with ligands found on HIV-infected cells (CD16, NKG2C, NKG2A, NKG2D, NKp30, and KIR2DL2/L3 (CD158b)), the maturation marker CD57, the negative immune regulator KLRG1, and the chemokine receptor CXCR3. FMOs for markers with continuous expression are shown in **Supplementary Figure 2B**. Upon stimulation with Bi-Ab32/16, NK cells exhibited higher levels of CD16, CD57, and CD158b, as well as co-expression of both NKG2C and CD57 markers (**Supplementary Figure 3**). Reduction of dimensionality and unsupervised clustering analysis using FlowSOM algorithm allowed us to identify ten different NK cell clusters with a particular expression of the selected phenotypic markers (**Figure 1G**). Specifically, clusters #PH2 and #PH4 identified subpopulations expressing the memory-like markers CD57 and NKG2C, while exhibiting low levels of NKG2A (**Figure 1H**). Of note, cluster #PH4 presented high NKG2C levels and also expressed the chemokine receptor CXCR3, while cluster #PH2 presented dim NKG2C expression and null or low CXCR3 expression (**Figure 1H**). These populations were also characterized by an increased expression of CD16, NKG2D and the inhibitory receptor CD158b (**Figure 1H**). Interestingly, frequencies of these clusters were higher after Bi-Ab32/16 treatment (**Figure 1I**). In addition, upon Bi-Ab32/16 stimulation, higher frequencies of #PH8 were observed, which defined an NK cell $NKG2C^{dim}CD57^{-}$ memory-precursor population with high expression of CD16 and Nkp30, as well as CD158b and KLRG1 (**Figure 1H, I**). In contrast, Bi-Ab32/16 treatment resulted in the reduction of cluster #PH9, characterized by elevated NKG2A levels (**Figure 1H, I**). Overall, our results show that stimulation with Bi-Ab32/16 may promote the generation of NK cells with fully mature memory-like features ($NKG2C^{+}CD57^{+}$), high expression of the inhibitory KIR CD158b and the activating receptor NKG2D, and low levels of the inhibitory NKG2A receptor.

Figure 1

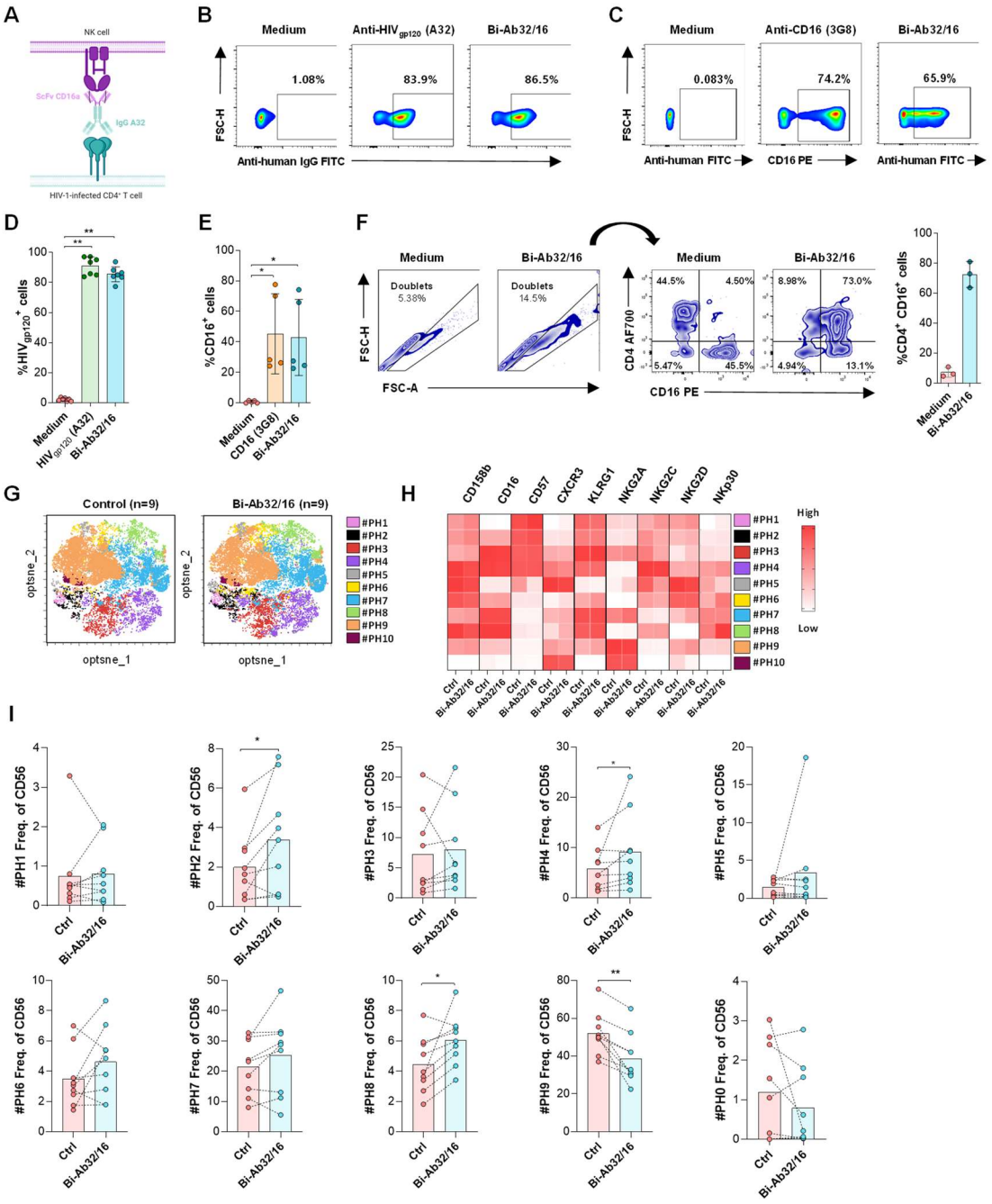


Figure 1. Binding of Bi-Ab32/16 and induced phenotypic alterations. A) Schematic illustrating the structure of the tetravalent bispecific antibody Bi-Ab32/16, comprising the IgG A32 antibody, targeting the gp120 target protein on HIV-infected CD4$^+$ T cells, and the single-chain variable fragment (ScFv) CD16a directed towards the CD16 receptor expressed on NK cells. **B)** Representative flow cytometry plots depicting the binding of anti-HIV$_{gp120}$ (A32 antibody, 5 µg/ml) and Bi-Ab32/16 (0.2 µg/ml) to CEM NKR CCR5$^+$ cells coated with the HIV-1 Bal gp120 recombinant protein after 20 minutes incubation. Recognition of the respective antigens by the antibodies was determined using an anti-human secondary antibody targeting the heavy chains on human IgG antibodies, including A32. **C**) Representative flow cytometry plots illustrating the binding of anti-CD16 (3G8 antibody) and Bi-Ab32/16 to primary isolated NK cells. The ability of the antibodies to recognize their cognate antigens was assessed using an anti-mouse secondary antibody recognizing the 3G8 antibody.

D) Summary graph of n=7 independent experiments depicting the binding of anti-HIV_{gp120} and Bi-Ab32/16 to CEM NKR $CCR5^+$ cells coated with the HIV-1 Bal gp120 recombinant protein after 20 minutes incubation. **E)** Summary graph showing the binding of anti-CD16 (3G8 antibody) and Bi-Ab32/16 to primary isolated NK cells. N=7 independent experiments are shown. **F)** Representative gating strategy employed to identify cell doublets using FSC-H and FSC-A parameters (left), and subsequent analysis of the frequency of cell doublets expressing CD4 and CD16 (right) upon incubation with Bi-Ab32/16. **G)** Optimized t-distributed stochastic neighbor embedding (opt-SNE) representations displaying the distribution of NK cell clusters based on the expression of different phenotypic markers in total ($CD56^+$) NK cells by condition. Two conditions are depicted: control (R10 medium) and Bi-Ab32/16 following 24-hour stimulation. **H)** Heatmap depicting variations in the mean fluorescence expression of distinct NK cell receptors between control (R10 medium) and Bi-Ab32/16 conditions, corresponding to the different cell clusters identified in Figure 1G and represented in different colors. **I)** Violin plots showing the frequency of the distinct NK cell clusters identified in Figure 1G among the distinct conditions. Statistical comparisons were performed using the Kruskal-Wallis test when required. Median with range (min-max) are shown. *p<0.05; **p<0.01

Bi-Ab32/16 elicits robust NK cell activation and ADCC responses in the presence of HIV-expressing cells

As a next step, we defined whether the Bi-Ab32/16 promoted the activation and induction of cytotoxic NK cells in response to HIV-expressing cells. CEM NKR $CCR5^+$ cells coated with gp120 recombinant protein were co-cultured with isolated NK cells for 4.5 hours in the presence of Bi-Ab32/16 or the parental A32 antibody. PMA/Ionomycin was used as a positive control. Distinct functional markers were measured by flow cytometry, including early (CD69) and late (HLA-DR) activation markers and cytotoxicity markers, such as proinflammatory IFNγ and surrogate marker for degranulation CD107a. In general, we observed that in the presence of the Bi-Ab32/16, primary NK cells ($CD3^-$ $CD56^+$) produced higher IFNγ and CD107a levels compared to cells treated with the A32 antibody (**Supplementary Figure 4A, B**). In addition, Bi-Ab32/16 treatment induced an increase in polyfunctional $IFN\gamma^+CD107a^+$ NK cells compared to A32 (**Supplementary Figure 4C**). Of note, Bi-Ab32/16 treatment did not significantly affect NK cell activation measured by the single expression of CD69 and HLA-DR, although a slight tendency to increased $CD69^+$ NK cell frequencies was observed upon the addition of the Bi-Ab32/16 (**Supplementary Figure 4D, E**). Dimensionality reduction analysis identified six clusters in the NK population based on the expression of activation and cytotoxicity markers. Among these activated clusters, #AC1, #AC2 and #AC5 were significantly expanded following Bi-Ab32/16 and PMA/Ionomycin stimulation (**Figure 2A, B**). These clusters comprised cells with a strong cytotoxic profile, co-expressing CD107a and IFNγ, while cluster #AC5 included the expression of the activation marker CD69 (**Figure 2C, D**). Importantly, these clusters were not present in A32-treated NK cell co-cultures, or in the presence of Bi-Ab32/16 lacking the gp120 target protein (No target condition) (**Figure 2A, E**), demonstrating that the response was specific. In summary, our findings indicate that Bi-Ab32/16 is superior to A32 inducing cytotoxic NK cell responses against gp120-coated $CD4^+$ T cells.

These results are of significance as they underscore the specificity of the bispecific antibody, which by itself remains insufficient to elicit NK cell cytotoxicity, functioning only in the context of HIV-expressing cells.

We next evaluated the ADCC activity of NK cells treated with Bi-Ab32/16 in response to HIV-expressing cells. To this end, CEM NKR CCR5^{+} cells coated with gp120 were co-cultured with primary isolated NK cells in the presence of Bi-Ab32/16 or the parental A32 antibody. Plasma from a viremic HIV^{+} participant containing a pool of antibodies targeting gp120 was used as a positive control. Cell killing was measured by the loss of the marker eFluor670 by flow cytometry (**Figure 2F and Supplementary Figure 5A**). Several antibody concentrations were employed to determine the EC_{50} value for both Bi-Ab32/16 and parental A32 antibodies in a dose-response curve. The results showed that the Bi-Ab32/16 induced a powerful ADCC response (EC_{50}=0.01 µg/ml), with an EC_{50} fifty-five times lower than the parent A32 antibody (EC_{50}=0.55 µg/ml) (**Figure 2G**). Overall, Bi-Ab32/16 induced the killing of a higher percentage of gp120-coated target cells when compared to A32 antibody (**Figure 2H**). Since NK from people with HIV (PWH) may be dysfunctional[486], we also determined the capability of the Bi-Ab32/16 to promote ADCC by NK cells from PWH. Of note, in the presence of Bi-Ab32/16, NK cells from PWH exhibited similar ADCC responses relative to healthy donors (**Figure 2H**). Therefore, our results provide evidence that Bi-Ab32/16 can effectively trigger a robust ADCC response in NK cells obtained from both healthy donors and PWH, which is far more potent than the parental A32 antibody.

Figure 2

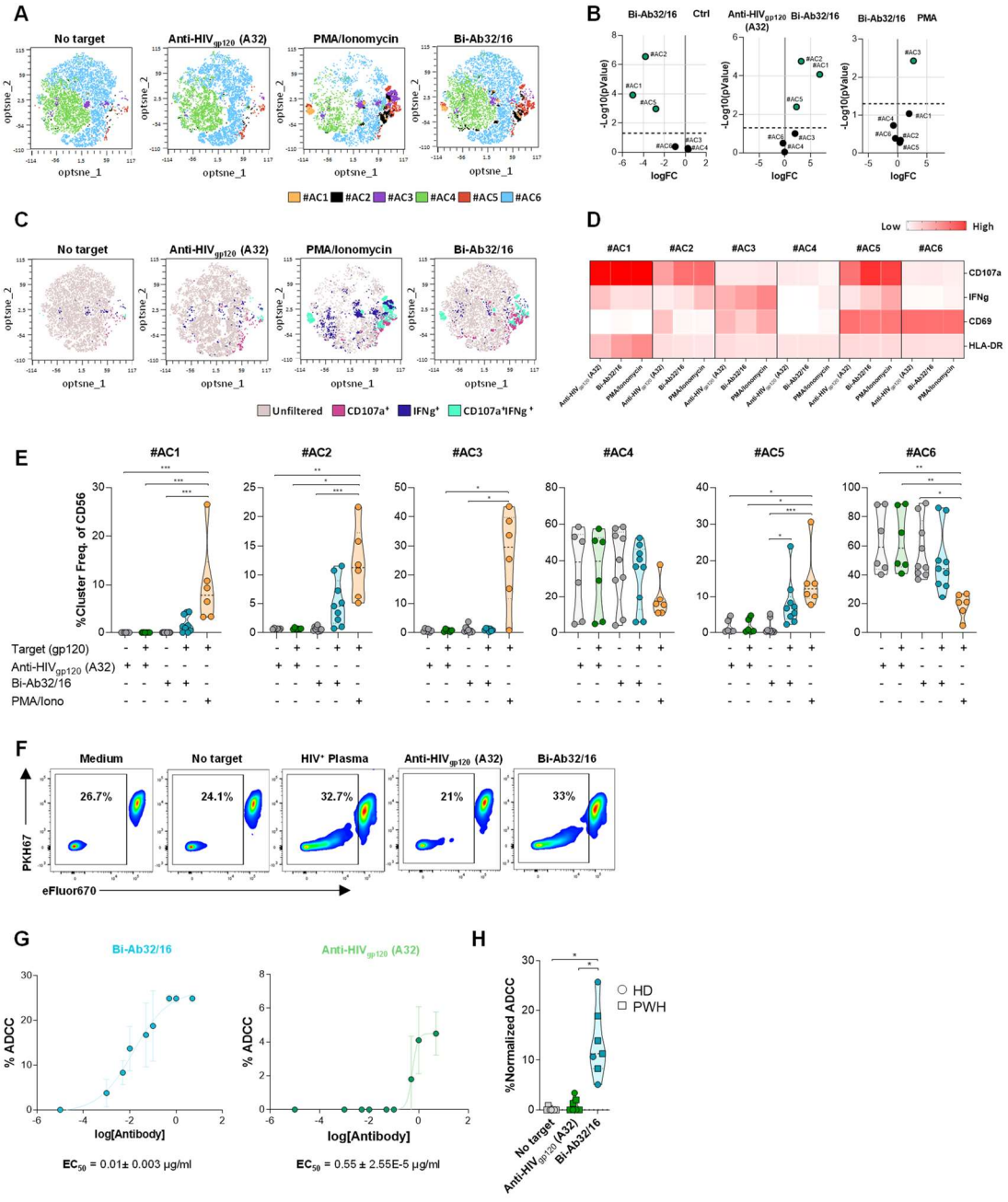


Figure 2. Functional profile and NK-mediated ADCC responses induced by Bi-Ab32/16. A) Opt-SNE representations displaying the distribution of NK cell clusters based on the expression of different activation and functional markers in total ($CD56^+$) NK cells by condition (left to right): NK cells co-cultured with $CD4^+$ T cells lacking the expression of the target protein (HIV_{gp120}) with Bi-Ab32/16 (No target), and in the presence of $CD4^+$ T cells expressing the target protein with A32, PMA/Ionomycin, and Bi-Ab32/16. **B)** Volcano plots showing the statistically significant differences in the cluster compositions between Bi-Ab32/16 and control (R10 medium), anti-HIV_{gp120} (A32) or PMA/Ionomycin conditions. **C)** Expression of CD107a and IFNγ on the different clusters identified in Figure 2A by condition. **D)** Heatmap depicting variations in the mean fluorescence expression of distinct activation and functional markers between study conditions, corresponding to the different cell clusters identified in Figure 2A. **E)** Violin plots showing the frequency of the different cell clusters of NK cells identified in Figure 2A by study condition. Statistical comparisons were performed using the Kruskal-Wallis test when required. Median with range (min-max) are shown *p<0.05; **p<0.01; ***p<0.001.

F) Representative flow cytometry plots for calculation of the ADCC activity of NK against HIV-expressing cells. CEM NKR CCR5$^+$ cells were double-stained with PKH67 and eF670, and coated with the HIV-1 Bal gp120 recombinant protein. Cells were co-cultured with primary NK for 4 h at 1:10 target/effector ratio, and in the presence of anti-HIV$_{gp120}$ (A32 antibody) or Bi-Ab32/16. Conditions without antibodies (R10 medium), without target cells (no target), and in the presence of HIV$^+$ plasma, were included as controls. Loss of the eF670 marker was used to determine the percentage of dead cells in an eF670 versus PKH67 plot. ADCC was calculated by normalizing the proportion of dead cells observed within the PKH67 versus eFluor670 plot in the co-culture conditions with antibodies to that of the co-culture without antibodies (referred to as basal killing). **G)** Dose response fitted nonlinear regression model and EC_{50} calculated values for Bi-Ab32/16 and anti-HIV$_{gp120}$ (A32). **H)** Summary graph of the ADCC activity mediated by NK cells from both healthy donors and PWH in the presence of the distinct antibodies. Statistical comparisons were performed using Wilcoxon matched-pairs signed-rank test. Median with range (min-max) are shown *p<0.05

Bi-Ab32/16 effectively binds and elicits a robust ADCC response against ex vivo HIV-infected cells

To evaluate Bi-Ab32/16 in a productive ex vivo HIV infection model, we initially assessed its binding capacity to HIV-infected cells. To this end, we performed ex vivo infection of isolated CD4$^+$ T cells with HIV$_{BaL}$ (CCR5-tropic) strain, followed by flow cytometry analysis of p24$^+$ expression after 5 days of culture. Cell surface antibody binding of Bi-Ab32/16 and A32 was detected using a secondary antibody targeting the heavy chain of human IgG. A representative gating strategy is depicted in **Figure 3A**, with distinct populations analyzed: infected CD4$^+$p24$^+$ cells (depicted in green, **Figure 3B**); infected CD4$^-$p24$^+$ cells (depicted in yellow, **Figure 3C**); and uninfected CD4$^+$p24$^-$ cells (depicted in blue, **Figure 3D**) Predominantly, p24$^+$ cells were CD4$^+$ (**Figure 3A**), and within this subset, Bi-Ab32/16 exhibited binding percentages akin to the A32 antibody alone (mean 78.7% vs 70.6%, respectively), which were significantly elevated compared to the condition without primary antibodies (**Figure 3E**). Moreover, Bi-Ab32/16 binding to p24$^+$ cells with downregulated CD4 mirrored that of A32 alone (**Figure 3E**). However, binding frequencies were lower in CD4$^-$p24$^+$ cells compared to CD4$^+$p24$^+$ cells, expected due to antibodies targeting conformational gp120 epitopes exposed upon CD4 binding, which may be less exposed when CD4 is downregulated[480]. Additionally, minimal binding of Bi-Ab32/16 and A32 antibodies was observed in uninfected CD4$^+$ T cells, suggesting a potential limited bystander killing upon treatment with either antibody (**Figure 3E**). Overall, Bi-Ab32/16 bound approximately 52% of the total p24$^+$ population, similar to A32 alone (Median binding=51%) (**Figure 3F**). Hence, Bi-Ab32/16 recognizes and binds to a significant proportion of the HIV-infected T cells.

Next, we used the ex vivo HIV infection model to validate the ability of the bispecific antibody to induce ADCC responses in a productive HIV infection system. To this end, we performed ex vivo infection of isolated CD4$^+$ T cells with two distinct viral strains: BaL (CCR5-tropic) and NL4.3 (CXCR4-tropic).

After 5 days of culture, ex vivo HIV-infected $CD4^+$ T cells were co-cultured with autologous isolated NK cells in the presence of Bi-Ab32/16 or A32 antibodies. Cell killing was assessed by the reduction of infected ($p24^+$) $CD4^+$ T cells by flow cytometry. Gating strategy is shown in **Supplementary Figure 5B**. Representative flow cytometry plots showing $CD4^+$ infection with HIV_{BaL} and $HIV_{NL4.3}$ strains over the distinct antibody conditions are depicted in **Figure 3G**. NK cells treated with Bi-Ab32/16 displayed a robust ADCC response towards $CD4^+$ T cells productively infected with HIV_{BaL} or $HIV_{NL4.3}$ compared to cells alone or to the A32 antibody condition (**Figure 3H**). Specifically, Bi-Ab32/16 was able to reduce HIV infection by 75% for HIV_{BaL}, and 62% for $HIV_{NL4.3}$ (**Figure 3H**). Overall, our findings support the potential of Bi-Ab32/16 in eliciting a robust ADCC-mediated elimination of HIV-infected cells, surpassing the effects achieved by the A32 antibody alone.

Figure 3

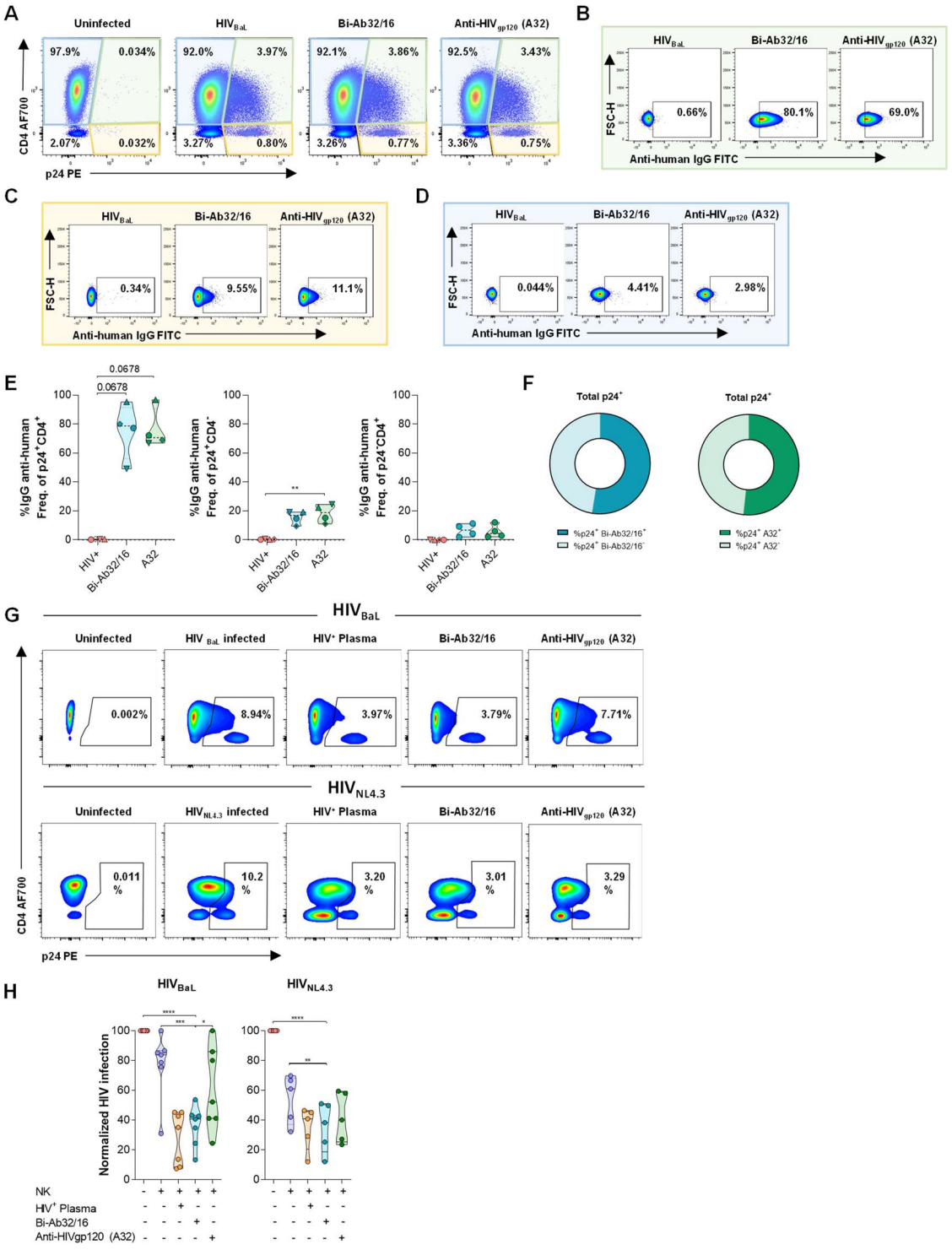


Figure 3. Characterization of Bi-Ab32/16 binding and ADCC responses against ex vivo HIV infected CD4⁺ T cells. A) Representative flow cytometry plots depicting ex vivo HIV_{BaL} infection of $CD4^+$ T cells through the detection of the viral protein p24. Plots demonstrate the expression of p24 and CD4 in uninfected, infected, Bi-Ab32/16-treated, or anti-HIV_{gp120} (A32)-stimulated cells. Three distinct cell populations are analyzed: $CD4^+p24^-$ cells (depicted in blue), $CD4^+p24^+$ cells (depicted in green), and $CD4^-p24^+$ cells (depicted in yellow). **B)** Representative flow cytometry plots illustrating the gating of anti-human IgG-expressing cells within the $CD4^+p24^+$ cell population under distinct conditions (from left to right): infected, treated with Bi-Ab32/16, or treated with A32.

Similar plots are shown for **C)** $CD4^-p24^+$ cells and **D)** $CD4^+p24^-$ cells. **E)** Violin plots depicting the frequency of anti-human IgG^+ cells quantified across various experimental conditions, including infected, Bi-Ab32/16-treated, or A32-stimulated cells, within the distinct cell populations analyzed (from left to right): $CD4^+p24^+$ cells, $CD4^-p24^+$ cells, and $CD4^+p24^-$ cells. Statistical comparisons were performed using ANOVA Friedman test. Median with range (min-max) are shown. *p<0.05; **p<0.01. **F)** Pie charts illustrating the median frequency of total $p24^+$ HIV-infected cells bound to Bi-Ab32/16 (represented by dark blue) or A32 (represented by dark green) antibodies. **G)** Representative flow cytometry plots showing HIV infection, as determined by the detection of the viral protein p24, following a 6-day infection period with HIV_{Bal} (upper) and $HIV_{NL4.3}$ (lower) strains. Plots show the reduction of p24 expression upon co-culture of infected $CD4^+$ T cells with NK cells stimulated with Bi-Ab32/16 or anti-HIV_{gp120} (A32) antibodies. HIV^+ plasma was included as a positive control. **H)** Violin plots depicting the reduction in p24 expression after co-culturing ex vivo HIV_{Bal} (left) or $HIV_{NL4.3}$ (right) infected $CD4^+$ T cells with NK cells previously treated with Bi-Ab32/16 or anti-HIV_{gp120} (A32) antibodies. Statistical comparisons were performed using 2way ANOVA followed by Dunn's multiple comparison test. Median with range (min-max) are shown. *p<0.05; **p<0.01; ***p<0.001; ****p<0.0001.

Bi-Ab32/16 enhances the NK-mediated killing of latently HIV-infected cells from PWH following viral reactivation

Next, we assessed if treatment with Bi-Ab32/16 induced an NK-mediated cytotoxic response against viral-reactivated cells from the persistent natural HIV reservoir. Isolated $CD4^+$ T cells from PWH with non-detectable viremia (2-6 years ART-treated) were subjected to PMA/Ionomycin reactivation, and subsequently incubated with autologous isolated NK cells. As previously reported, viral reactivation was measured by the intracellular expression of the viral protein p24 by flow cytometry[453,487]. NK cells stimulated with the Bi-Ab32/16 were able to reduce the pool of reactivated cells by a median of 55%, compared to NK cells alone (**Figure 4A**). By contrast, cells treated with A32 presented a reduction of 12%, relative to NK cells alone. Moreover, we quantified the intact proviral DNA in $CD4^+$ T cells following pharmacological reactivation in the presence of Bi-Ab32/16 and autologous NK cells in another set of PWH with non-detectable viremia. Reduction in the intact proviruses was observed in three out of five samples tested (**Figure 4B**). Our results are consistent with a recent study describing the impact of two CD16-specific antibodies in promoting the NK-mediated elimination of cells harboring intact proviral DNA, observed in approximately 70% of the samples tested[488]. Overall, we show that the Bi-Ab32/16 enhances the killing of productively and reactivated HIV-infected cells via ADCC and, in some individuals, reduces the intact HIV reservoir after viral reactivation. Therefore, the properties of our Bi-Ab32/16 hold potential significance within the context of emerging shock and kill strategies.

Figure 4

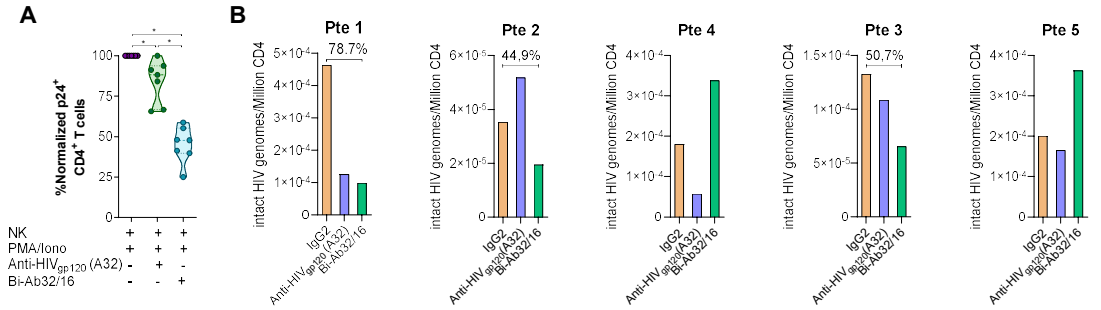


Figure 4. NK-mediated elimination of HIV-infected cells subsequent to viral reactivation of the natural HIV reservoir, and impact in intact provirus. A) Violin plot showing the reduction in p24 expression in CD4⁺ T cells from ART-treated PWH upon latency reversal with PMA/Ionomycin and co-culture with NK cells treated with anti-HIV_{gp120} (A32) or Bi-Ab32/16. Statistical comparisons were performed using the Wilcoxon matched-pairs signed-rank test. *p<0.05. **B)** Intact proviral DNA assay (IPDA) in samples from five ART-treated PWH after performing the NK killing assay with primary *ex vivo* reactivated CD4⁺ T cells with PMA and ionomycin and autologous isolated NK cells. IgG2 was added as an isotype control.

Evaluation of the Bi-Ab32/16 in a humanized mice model expressing IL-15

We next performed the preclinical evaluation of the Bi-Ab32/16 using the Hu-NSG-Tg (IL-15) mouse model[489] (**Figure 5A**). A total of n=33 Hu-NSG-Tg (IL-15) mice were challenged with 10^4 $TCID_{50}$ (50% tissue culture infectious dose) of HIV_{BaL} strain. Mice received ART from week 6 to 9 post-infection (WPI). From 8 to 10 WPI, they were randomized in three groups of animals (n=6/group) that received A32 or Bi-Ab32/16 (500 µg/mouse) twice a week, or PBS as a vehicle control, a protocol selected based on prior evaluation of the plasma pharmacokinetics of Bi-Ab32/16 after a single injection (**Supplementary Figure 6A, B**). Immune cell subsets and time to viral rebound were monitored from 11 until 13 WPI (**Figure 5A**). Of note, mice did not show any evidence of toxicity, measured by changes in weight, during the course of the study (**Supplementary Figure 6C**). As previously described, hCD3⁺ and hCD56⁺ cells represented relatively low frequencies among the total hCD45⁺ cell population at baseline, in contrast to hCD19⁺ cells, which constituted the predominant proportion[489] (**Supplementary Figure 6D**). NK cells, identified by CD56 expression, constituted a mean of 6% of the overall hCD45⁺ cell population, mirroring the ranges in human blood (2-18%) previously described[424]. Furthermore, NK cells exhibited a standard subset distribution at baseline, where the $CD56^{dim}CD16^{high}$ subset predominated in peripheral blood, consistent with the pattern observed in human blood[46] (**Supplementary Figure 6E**).

Based on previous reports[489], we analyzed parameters associated with HIV infection at 3-6 WPI. Although HIV viral loads were detected at 3 WPI, ranging from 10^3 to 10^5 copies/ml, in 24 out of 34 animals (**Supplementary Figure 6F**), all HIV-challenged Hu-NSG-Tg (IL-15) mice experienced a significant depletion of circulating $hCD45^+$ and $hCD4^+$ cells at 4 WPI, followed by a reduction in the CD4/CD8 ratio (**Supplementary Figure 6G-J**). By contrast, an increase in $CD56^+$ NK cell frequencies were observed at 3-5 WPI (**Figure 5B**). Further, all these parameters were normalized at 9 WPI, after ART treatment administration (**Figure 5B**, **Supplementary Figure 6G-J**). Thus, we speculate that failure to detect HIV load in 10 animals before ART was due to the low numbers of $CD4^+$ T cells, which most likely precluded the production of detectable viral particles. Consistent with this hypothesis is the observed dynamics of the immune cells, which is compatible with HIV infection in animals with undetectable viral load.

Subsequently, we monitored the time to viral rebound after treatment discontinuation (until 13 WPI). We observed that the entire group of animals treated with Bi-Ab32/16 (n=6) presented viral rebound, with a mean rebound time of 16 days after ART interruption. In contrast, only 4 out of 6 A32-treated mice experienced viral rebound, with a mean duration of 22 days. All vehicle-treated animals (n=5) showed viral rebound, occurring at a mean of 15 days (**Figure 5C**). Further, after Bi-Ab32/16 administration, reduced percentages of $CD56^+$ NK cells were observed in mice compared to A32 or vehicle control conditions (**Figure 5B**). Additionally, $CD56^+$ NK cell frequencies negatively correlated with HIV infection levels at the end of the experiment (**Figure 5D**), while no significant associations were observed between CD4 frequencies and HIV infection levels (**Supplementary Figure 6K**). Of note, to enhance data integrity and reliability, CD16 expression was excluded from the analyses due to potential interference from the Bi-Ab32/16 in CD16 staining (**Supplementary Figure 6L**). Collectively, our data indicate that in vivo treatment with Bi-Ab32/16 fosters a decline in $CD56^+$ NK cells, a phenomenon that is inversely associated with HIV infection, thus negatively impacting viral rebound.

Figure 5

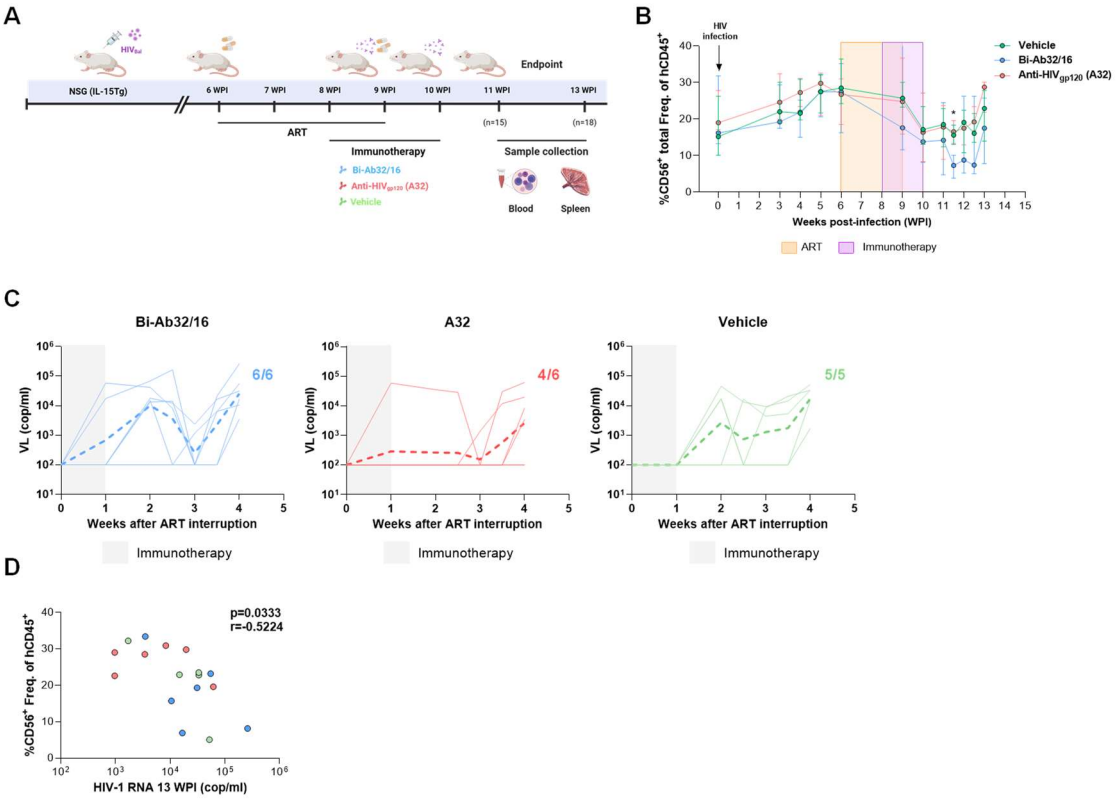


Figure 5. Preclinical evaluation of Bi-Ab32/16 in Hu-NSG-Tg (IL-15) mice. **A)** Schematic representation of the experimental design. 33 Hu-NSG-Tg (IL-15) mice were infected with 10,000 $TCID_{50}$ of HIV_{Bal}, administered ART from weeks 6-9 post infection (WPI), randomized and injected intraperitoneally with 500 µg of Bi-Ab32/16, anti-HIV_{gp120} (A32) or vehicle from weeks 8 to 10, sampled for peripheral blood weekly, and euthanized in two groups at weeks 11 and 13 for collection of blood and splenic tissue. **B)** Evolution of the frequency of $CD56^+$ NK cells from peripheral blood of HIV-infected mice by condition. **C)** Time to viral rebound expressed by HIV-1 RNA copies per ml of plasma from 0 to 4 weeks after ART interruption in Hu-NSG-Tg (IL-15) treated with Bi-Ab32/16, anti-HIV_{gp120} (A32) or vehicle. Data are shown as individual values (thin lines) and average values (dashed and thicker lines). **D)** Spearman correlation between the frequency of $CD56^+$ NK cells and viral load expressed as HIV-1 RNA copies/ml at 13 WPI. Statistical comparisons were performed using Mann-Whitney test. Median with range (min-max) are shown. *p<0.05

Bi-Ab32/16 modulates NK cell dynamics in vivo

To better understand correlates of time to viral rebound in the three groups of challenged mice, we analyzed by flow cytometry the phenotype of both blood and splenic NK cells at 11 and 13 WPI. Reduction of dimensionality and unsupervised clustering analysis using FlowSOM algorithm allowed us to identify seven different NK cell clusters with a particular expression of the selected receptors in peripheral blood (**Figure 6A**). In blood, clusters #BC1 and #BC2 exhibited an activated memory-like phenotype, marked by the expression of NKG2C, and the activation markers CD69 and IFNγ (**Figure 6B)**. Cluster #BC1 presented elevated NKG2C levels and constituted a minor cluster at 11 WPI, with no significant inter-group differences in frequency (**Figure 6C**).

Conversely, at 13 WPI, Bi-Ab32/16 mice showed lower #BC1 frequencies compared to A32 and control groups (**Supplementary Figure 7A**). Cluster #BC2 presented slightly reduced frequencies in Bi-Ab32/16 treated mice, was defined by dim NKG2C expression and higher IFNγ levels compared to A32 and control conditions, and was inversely associated with HIV infection across all groups (**Figure 6B-D**). Conversely, Bi-Ab32/16 treated mice presented slightly elevated #BC3 frequencies at 11 WPI, characterized by CD69 expression, absence of IFNγ, and a positive association with HIV infection, compared to A32 and control groups (**Figure 6B-D**). Although group differences were not evident at 13 WPI, #BC3 frequencies positively correlated with HIV-1 RNA levels (**Supplementary Figure 7B**). Moreover, clusters #BC5 and #BC6 exhibited dim IFNγ expression, and were inversely associated with HIV control (**Figure 6B, -D**). Notably, cluster #BC7, characterized by robust CD69 expression, exhibited lower frequencies in Bi-Ab32/16 treated mice compared to the A32 group at 11 WPI (**Figure 6C**).

Similarly, reduction of dimensionality and unsupervised clustering analysis on NK cells derived from splenic tissue allowed us to identify eight distinct NK cell subpopulations (**Figure 6E, F**). Although no statistically significant differences were observed in the frequency of these clusters among the study groups at 11 WPI, a subtle tendency towards lower frequencies of spleen clusters #SC2 and #SC8 was noted in the Bi-Ab32/16 treated group compared to the A32 group (**Figure 6G**). Both clusters exhibited a tissue-resident NK cell phenotype, characterized by the expression of CD49a, CD69, and NKG2C, and lacked IFNγ expression (**Figure 6F**). Notably, cluster #SC8 displayed strong NKG2C expression (**Figure 6F**). In addition, at 13 WPI clusters #SC5 and #SC7 were found in higher frequencies in the Bi-Ab32/16 treated group compared to A32 and control groups, respectively (**Supplementary Figure 7C**). Cluster #SC5 was defined by elevated expression of the tissue-resident markers CD49a and CD69, while cluster #SC7 exhibited high CD49a expression while lacking CD69 (**Figure 6F**). Furthermore, cluster #SC7 presented high levels of IFNγ expression (**Figure 6F**). Importantly, at 13 WPI, the presence of cluster #SC8 inversely correlated with HIV infection (**Supplementary Figure 7D**).

Collectively, our findings suggest that the administration of Bi-Ab32/16 to Hu-NSG-Tg (IL-15) mice perturbs the NK cell landscape. Specific NK cell subsets expressing NKG2C and CD69 exhibit an inverse correlation with HIV infection in both blood and spleen, underscoring their potential role in HIV control in vivo.

Figure 6

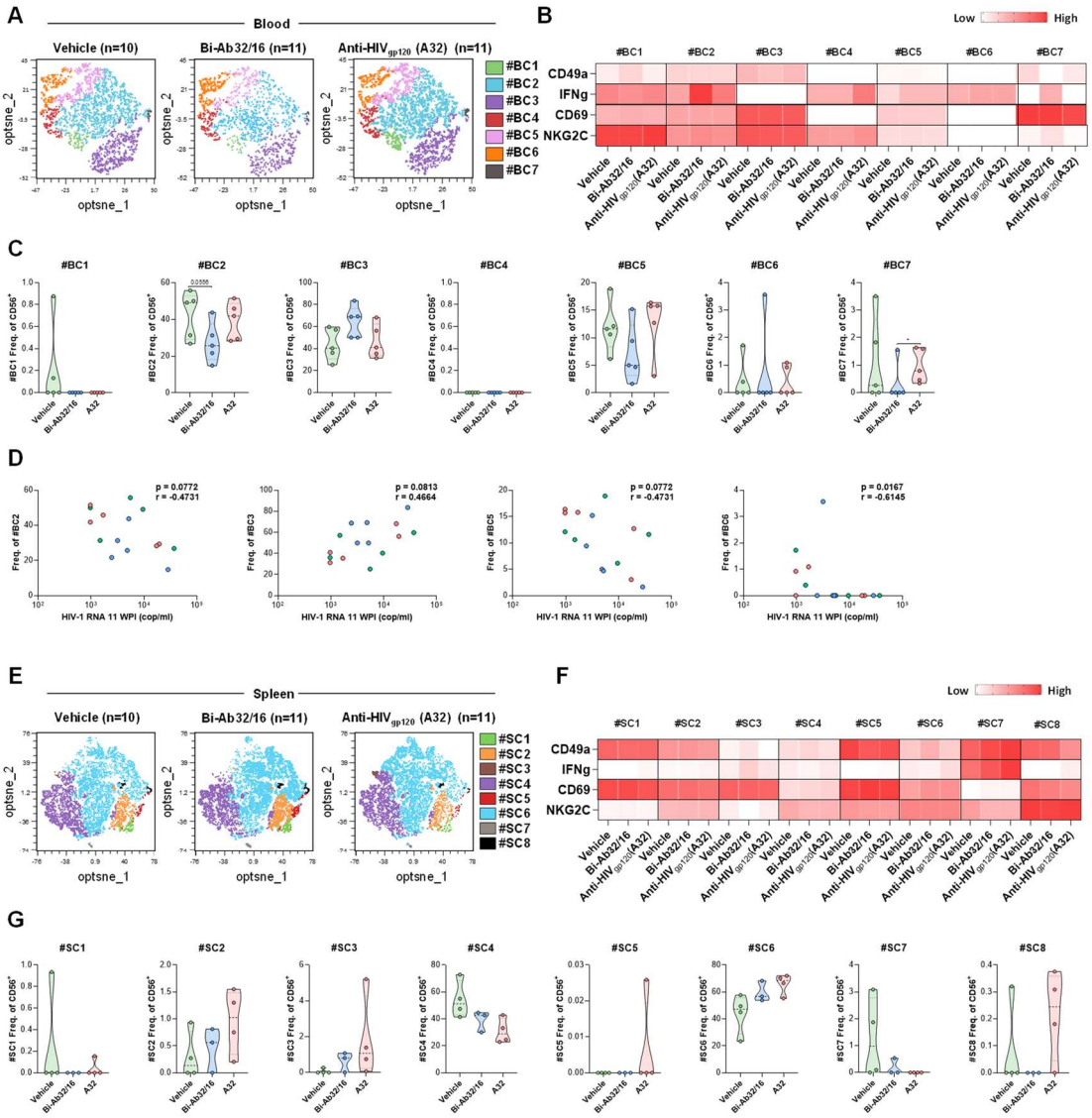


Figure 6. Characterization of the NK cell repertoire in blood and splenic tissue from Hu-NSG-Tg (IL-15) mice following Bi-Ab32/16 administration. **A)** Opt-SNE representations showing the distribution of peripheral blood NK cell clusters, based on the expression of diverse phenotypic and functional markers in total ($CD56^+$) NK cells by condition (left to right: vehicle, Bi-Ab32/16, and A32). **B)** Heatmap depicting variations in the mean fluorescence expression of distinct NK cell phenotypic and functional markers, including CD49a, IFNγ, CD69, and NKG2C, between study conditions, corresponding to the different cell clusters identified in Figure 5A. **C)** Violin plots showing the frequency of the different cell clusters of NK cells identified in Figure 5A by study condition. **D)** Spearman correlations between the frequency of clusters (left to right): #BC2, #BC3, #BC5, and #BC6 in total ($CD56^+$) NK cells and viral load expressed as RNA copies per ml of plasma. **E)** Reduction of dimensionality representations showing the distribution of splenic tissue NK cell clusters, based on the expression of distinct tissue and functional markers in total ($CD56^+$) NK cells by condition. **F)** Heatmap depicting variations in the mean fluorescence expression of the different tissue and functional markers between study conditions, corresponding to the distinct cell clusters identified in Figure 5E. **G)** Violin plots depicting the frequency of the different cell clusters identified in 5E by study condition. Statistical comparisons were performed using Mann-Whitney test. Median with range (min-max) are shown. *p<0.05; **p<0.01.

3.2.6 Discussion

The development of novel therapeutic strategies aimed at eradicating the latent HIV reservoir represents a current priority in the pursuit of an effective HIV cure. In this study, we have shown that Bi-Ab32/16, a tetravalent bispecific antibody directed against CD16a on NK cells and the gp120 HIV protein (Ab A32) on HIV-infected cells, boosts NK cell cytotoxicity and mediates elimination of HIV reservoir cells in vitro. Our analyses revealed that Bi-Ab32/16 was able to significantly enhance the generation of NK-target cell conjugates, and activate NK cells to induce a potent and cytotoxic response against HIV infected cells. Importantly, Bi-Ab32/16 efficiently reduced the pool of latent HIV-infected cells after pharmacological viral reactivation, supporting its application in future "shock-and-kill" strategies. However, despite these promising in vitro results, a lack of HIV control was observed in vivo when Bi-Ab32/16 was infused to HIV challenged humanized NSG hu-IL-15 mice. Bi-Ab32/16 influenced specific NK cell populations, reducing total $CD56^+$ NK numbers, negatively impacting HIV control. Consequently, we believe that Bi-Ab32/16 may be more suitable for ex vivo cell therapies or for administration at different stages of the infection, rather than direct infusion of the bispecific format in the context of ART interruption.

NK cells exhibit a diverse array of inhibitory and activating cell receptors, and the induction of a cytotoxic immune response is contingent upon a precise equilibrium in the expression of these receptors. Among them, CD16 has been reported to mediate ADCC activity[440]. We proved that CD16 stimulation by Bi-Ab32/16 promotes a shift on the phenotype of NK cells in vitro, resulting in a marked increase in the expression of CD16, together with the NKG2C and CD57 receptors. Prior studies provide substantial support for the crucial involvement of ADCC in regulating HIV infection as well as impacting the composition of the viral reservoir during treated infection[383,453]. Additionally, NKG2C receptor plays a key role in modulating the tolerance or reactivity of NK cells towards target cells[295]. Further, the preferential expression of CD57 by a subset of NK cells with a mature phenotype implies that this molecule may identify clonally expanded NK cells due to infections[296,443,490]. Of note, the expression of both NKG2C and CD57 has been associated with memory-like features, particularly evident in the context of CMV infection[296]. We speculate that these cells may represent subsets of activated NK cells with memory-like features, suggesting that the expansion of such cells could confer potential benefits for the control of HIV during the course of HIV infection.

We demonstrated that direct CD16 engagement by Bi-Ab32/16 achieved a potent anti-HIV cytotoxic response in NK cells from PWH. Additionally, the elicited response was specific, as it was exclusively generated in the presence of the target protein gp120.

This observation is significant, as persistent HIV infection has been associated with the emergence of dysfunctional NK cells characterized by a reduced capacity to eliminate cellular targets[491]. Notably, this NK cell exhaustion endures even in the presence of ART[210,492,493]. Therefore, these features position Bi-Ab32/16 as an appealing tool capable of redirecting and enhancing NK cell responses towards the mitigation of HIV infection. Importantly, in vitro, Bi-Ab32/16 was able to promote a NK-mediated clearance of HIV-latently infected cells following pharmacological reactivation, mimicking “shock-and-kill” assays. Latently HIV-infected cells are expected to undergo efficient elimination by the immune system upon viral reactivation. However, the reactivation of viral expression alone has proven insufficient for the complete eradication of cellular reservoirs[372,494]. Hence, optimal potentiation of the immune system is needed for the complete elimination of the latent reservoir. Previous studies have proposed that NK cells could contribute to the comprehensive clearance of viral-reactivated cells[380,383,495,496]. Our study provides evidence that Bi-Ab32/16 significantly diminishes the pool of reactivated latently infected cells through the induction of a robust NK cell immune response. Moreover, Bi-Ab32/16 treatment can impact the natural HIV reservoir, as evidenced by the decrease in intact proviruses within samples derived from PWH subsequent to viral reactivation. This is of relevance since the majority (>90%) of latent viruses have been reported to harbor cytotoxic T lymphocyte (CTL) escape mutations, resulting in infected cells that are unresponsive to CTLs targeting common epitopes[497–500].

The predominant approach in preclinical HIV studies involves the utilization of well-established humanized mouse models such as the BLT mice[501,502]. However, these models exhibit limited support for robust development of human NK cells derived from human hematopoietic stem cells engraftment[503]. A major obstacle to effective human NK cell reconstitution is the absence of signaling through human interleukin-15 (IL-15), given the suboptimal stimulation provided by murine IL-15 to the human IL-15 receptor[504]. In this study, the selected animal model was NSG mice expressing a transgene encoding human IL-15, resulting in mice with physiological levels of human IL-15, which facilitates engraftment of human NK cells. Notably, this model has been previously characterized to sustain HIV infection, leading to elicited human NK cell responses in HIV-infected mice[489]. Consequently, this model stands as a robust and innovative platform for investigating NK cell responses in the context of HIV. In our study, we observed a slight delay in HIV rebound after treatment interruption in A32-treated mice. Since A32 is a non-neutralizing antibody that binds gp120 after encounter with the CD4 receptor, this effect is likely the result of a NK-mediated ADCC. Thus, our results support the contribution of non-neutralizing antibodies in the control of HIV.

Unexpectedly, despite its excellent in vitro performance, Bi-Ab32/16 did not improve HIV control in treated mice. Notably, we detected a reduction in total $CD56^+$ NK cells following prolonged Bi-Ab32/16 stimulation (two weeks). Furthermore, a direct inverse correlation between the presence of $CD56^+$ NK cells and viral load was observed in HIV-infected mice, providing evidence for the substantial role of NK cells in HIV infection control. As previously described, CD16 engagement is a strong activator of NK cell function, facilitating antigen-specific recruitment of NK cell responses[505]. Moreover, CD16 binds to the constant Fc domain of IgG antibodies, thereby triggering the ADCC response. Our results are consistent with previous reports that describe the association between NK cell-mediated ADCC responses and diminished viral set points in PWH[383,388,505,506]. However, the observations presented in our study are noteworthy, suggesting that sustained in vivo stimulation with Bi-Ab32/16, in the context of detectable viremia, may lead to an unexpected adverse impact on NK cells. This stands in contrast to in vitro studies, where CD16 stimulation by the Bi-Ab32/16 elicits an increase in receptor expression.

A recent study evaluating the efficacy of two bispecific antibodies based on broadly neutralizing antibodies targeting Env and CD16, revealed robust and specific NK cell activation and subsequent reduction of HIV-infected cells in vitro[488]. These findings align with the results presented in our study. By contrast, preclinical evaluation of one of the bispecific antibodies in a Hu-NSG-Tg (IL-15) mice model, soon after ART initiation, demonstrated increased NK cell activity and reduced reservoir size. The opposite outcomes observed in vivo between this study and the present study raise questions regarding the optimal timing of intervention and whether the interruption of ART presents an adequate context for the successful targeting of NK cells. Furthermore, in *Board et al*., study, discerning between effector functions driven by CD16 engagement and neutralizing functions of the bispecific antibody during the non-suppressive ART period may be challenging. We hypothesize that the concurrent presence of viral replication after ART interruption, together with the sustained CD16 stimulation by the Bi-Ab32/16, may have influenced NK cell dynamics. This modulation could potentially induce prolonged immune activation, consequently resulting in a reduction in CD16 expression and cytotoxic function, thus leading to an ineffective clearance of HIV-infected cells. Furthermore, the utilization of the IL-15 NSG mice model, incorporating implanted human fetal thymic and liver tissue fragments in the aforementioned study, fully reconstituted the immune environment, which may have positively influenced NK cell functionality during the study.

Comparative analyses with other models, such as the SHIV-AD8 infected non-human primate model, where NK-mediated control of viral rebound is evident at the time of ART interruption, offer valuable insights into the intricate dynamics of NK cell-mediated therapeutic strategies[507]. In addition, some studies have indicated that the conformational state of Env glycoprotein significantly influences both antibody recognition and ADCC responses[508–510]. Engagement of CD4 receptor leads to a transition of Env to an “open” conformation, thereby sensitizing HIV-infected cells to ADCC responses mediated by non-neutralizing CD4-induced antibodies. However, HIV restricts Env-CD4 interaction by reducing CD4 expression and limiting Env accumulation on the surface of infected cells. In this regard, small CD4-mimetic compounds (CD4mc) have been identified to alter Env conformation on HIV-infected cell surfaces, thereby exposing CD4-induced epitopes on viral particles and enhancing susceptibility of infected cells to ADCC by non-neutralizing antibodies. Recent investigations have demonstrated that co-administration of CD4-induced non-neutralizing antibodies or HIV^+ plasma with CD4mc in HIV-infected humanized mice resulted in notable reductions in viral reservoir size across various tissues and delayed viral rebound[509].

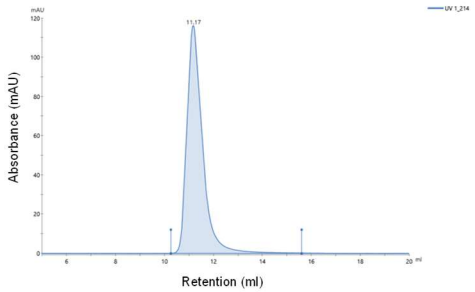
Overall, we hypothesize that strategies involving intermittent administration of the antibody upon ART withdrawal, ex vivo preloading of NK cells with Bi-Ab32/16, followed by the infusion of the complexed product into the person with HIV, or the co-administration of this bispecific format with NK cells during ART interruption, along with the addition of CD4mc could mitigate NK cell depletion, enhance ADCC responses, and potentially lead to optimal NK cell-mediated killing of HIV-infected cells. Our results underscore the relevance of avoiding in vivo NK cell overstimulation to attain more favorable biological outcomes. Still, the results presented here provide evidence for the beneficial effects of the Bi-Ab32/16 platform in the elimination of HIV-infected cells in vitro, reinforcing the role of CD16 NK cells in the control of HIV and the value of therapies directed to enhance their function.

3.2.7 Supplementary Data

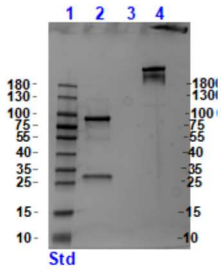
3.2.7.1 Supplementary Figures

Supplementary Figure 1

A



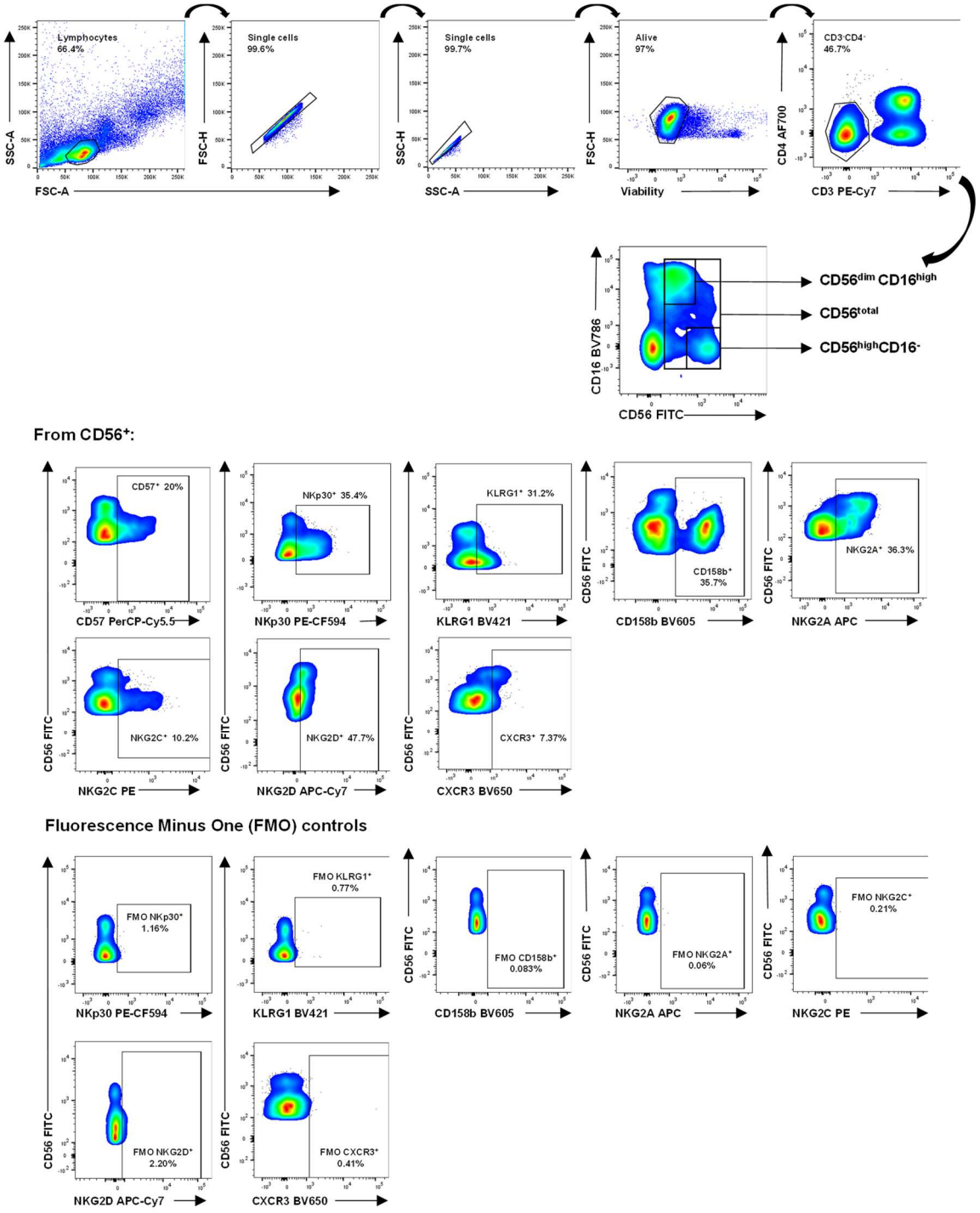
B



Lane Number	Sample	Lot	Amount (µg)	Conditions
1	PageRuler (Thermo Fisher)	NA	NA	Reducing
2	Ab1258	081020	2	Reducing
3	Blank	-	-	-
4	Ab1258	081020	2	Non-reducing

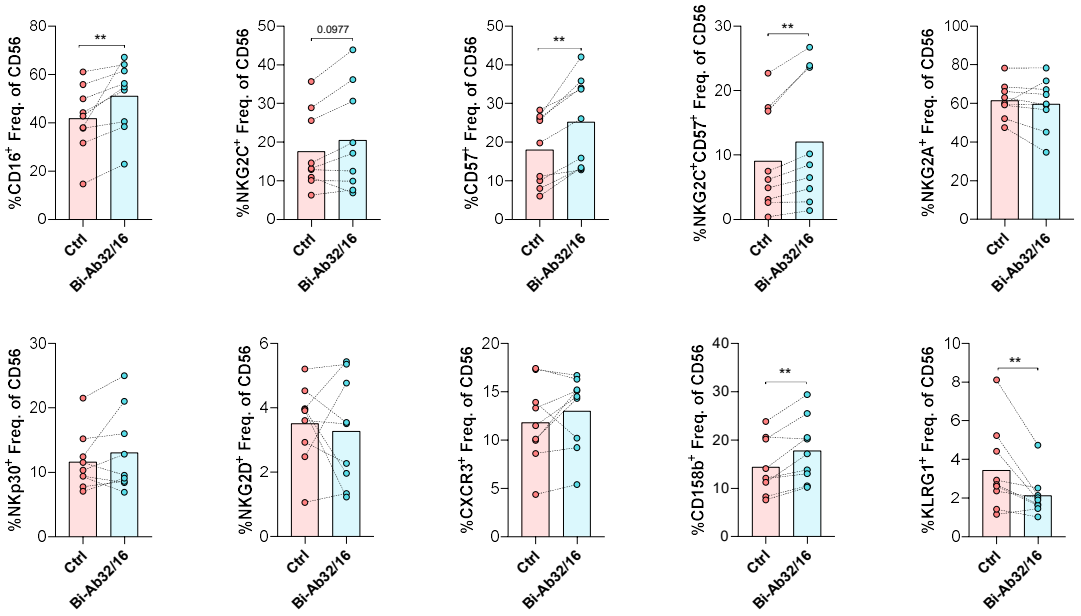
Supplementary Figure 1. A) Bi-Ab32/16 purity after size-exclusion chromatography. The peak retention time is indicated above the chromatogram. **B**) SDS-PAGE analysis of Bi-Ab32/16. 4-20% denaturing (1), reducing (2), blank (3), and non-reducing (4) conditions are shown. Molecular weight markers are shown in kilodaltons.

Supplementary Figure 2



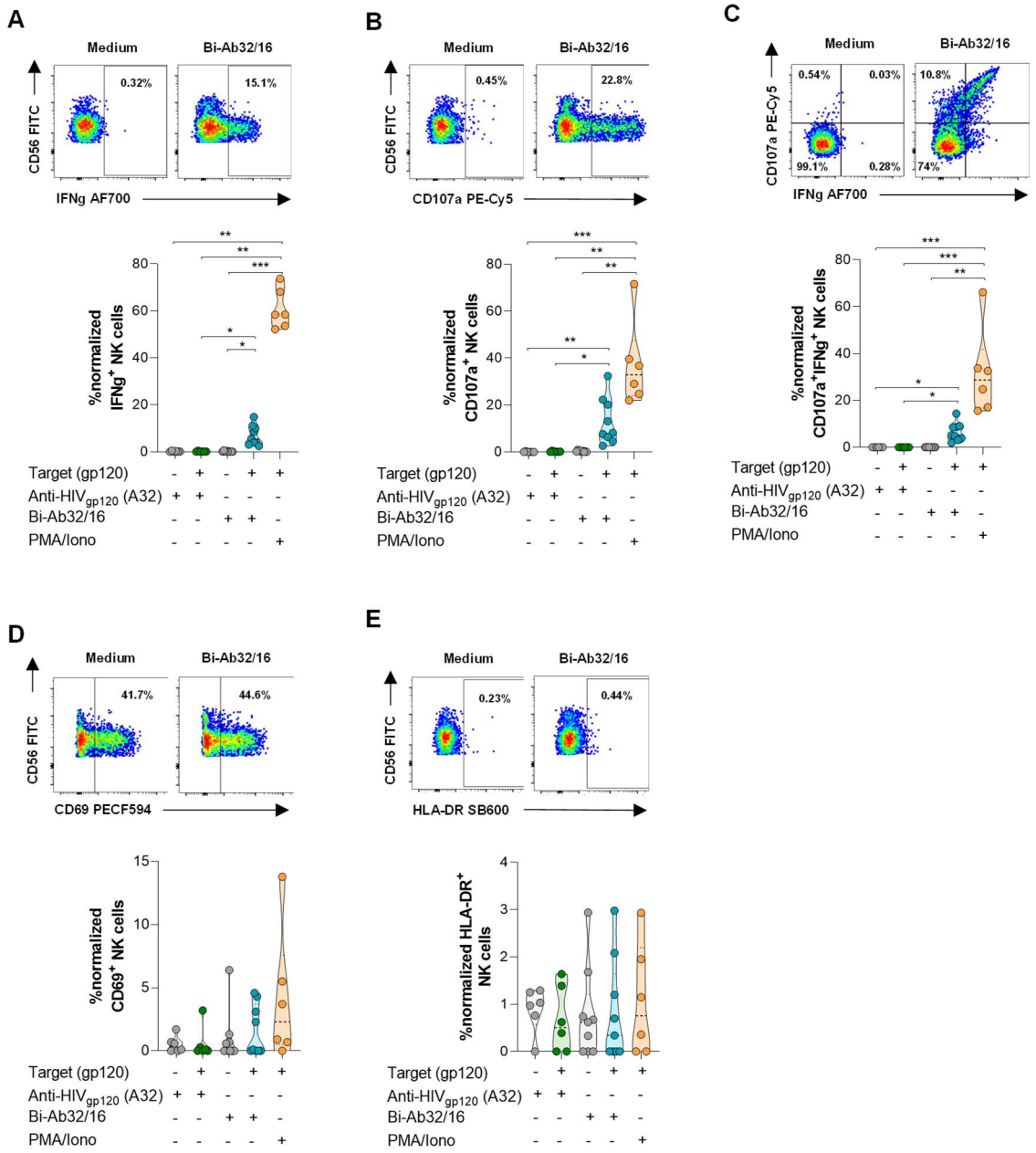
Supplementary Figure 2. Gating strategy used for the quantification of the different NK cell receptors. FMOs are shown for markers with continuous expression.

Supplementary Figure 3



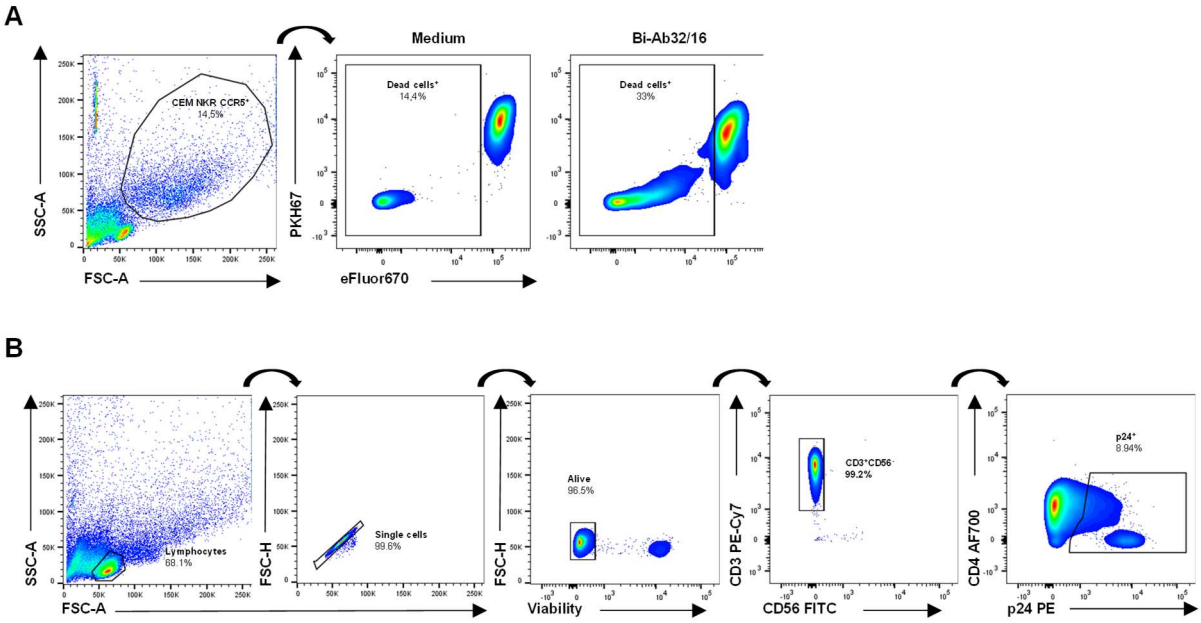
Supplementary Figure 3. Phenotypic characterization of NK cells upon Bi-Ab32/16 stimulation. The expression of different phenotypic NK cell markers following Bi-Ab32/16 stimulation was assessed by flow cytometry in healthy donors (HD, n=9). All graphs represent median with range (min-max) for each condition. Statistical analyses were performed using Wilcoxon matched-pairs signed-rank test. *p<0.05; **p<0.01.

Supplementary Figure 4



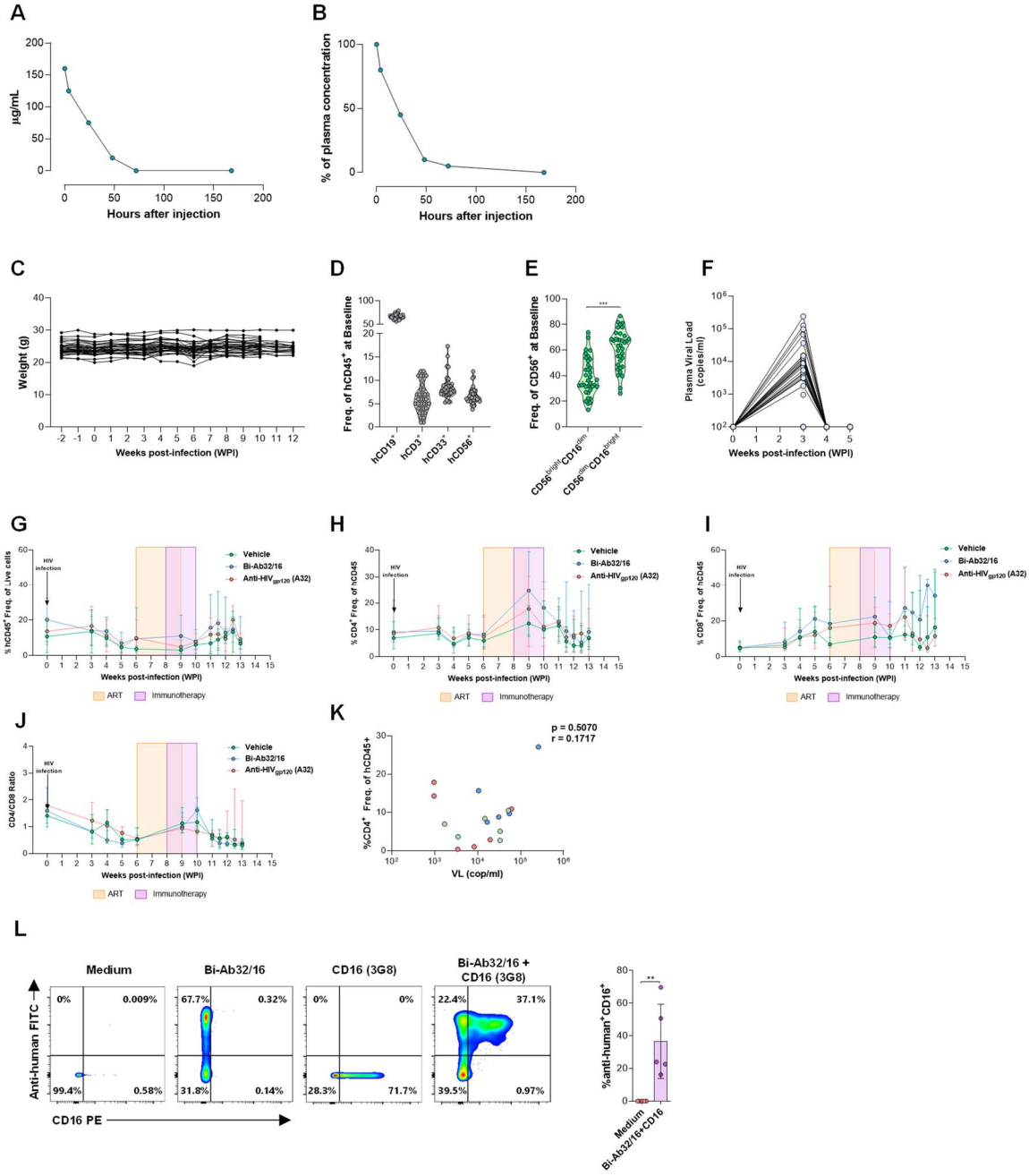
Supplementary Figure 4. Assessment of NK cell activation induced by Bi-Ab32/16. Representative flow cytometry plots and summary graphs of different markers of NK cell activation and function after co-culturing NK cells for 4.5h with CEM NKR CCR5$^+$ cells coated with the HIV Bal gp120 recombinant protein in the presence of Bi-Ab32/16 or anti-HIV$_{gp120}$ (A32) antibodies. Positive controls consisted in adding PMA (10 ng/ml) and ionomycine (1,5 µM) to the culture. **A**) Percentage of IFNγ$^+$ cells. **B**) Percentage of CD107a$^+$ cells. **C**) Percentage of polyfunctional IFNγ$^+$CD107a$^+$ cells. **D**) Percentage of CD69$^+$ cells. **E**) Percentage of HLA-DR$^+$ cells. All graphs represent median with range (min-max) for each condition. Statistical analyses were performed using Kruskal-Wallis test. *p<0.05; **p<0.01; ***p<0.001.

Supplementary Figure 5



Supplementary Figure 5. Gating strategies used in ADCC assays. **A**) Gating strategy used to measure ADCC in CEM NKR CCR5^{+} cells coated with HIV Bal gp120 recombinant protein. Loss of the eF670 marker was used to determine the percentage of dead cells in an eF670 versus PKH67 plot. **B**) Gating strategy used for the detection of p24^{+} CD4^{+} T cells after *ex vivo* viral infection.

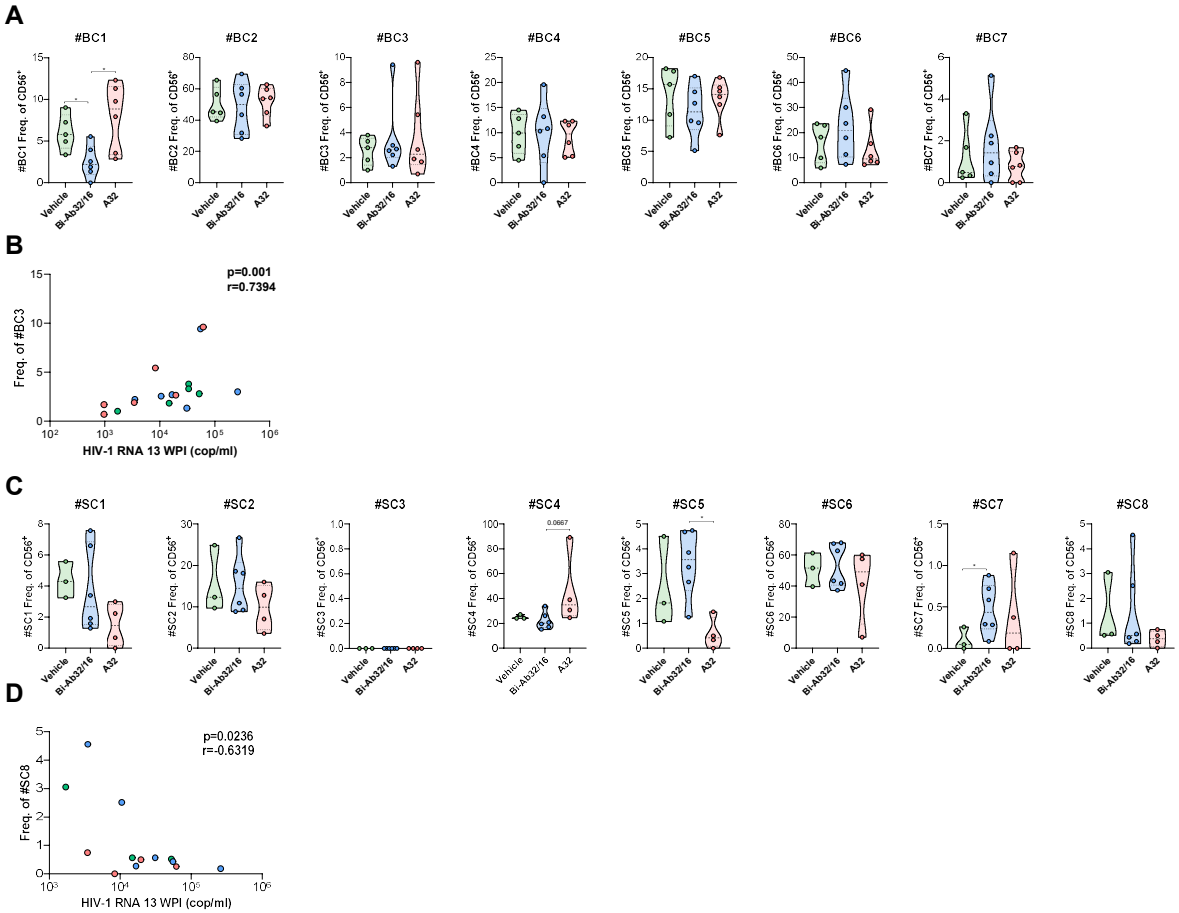
Supplementary Figure 6



Supplementary Figure 6. Hu-NSG-Tg (IL-15) mice model. A-B) Bi-Ab32/16 plasma pharmacokinetics in Hu-NSG-Tg (IL-15) mice. Mice received a single 500 µg intraperitoneal injection of Bi-Ab32/16 and antibody plasma concentrations were assessed at 24, 48, 72, 96, 120, 144, 168, and 198 hours after injection. Plasma concentrations are represented as **A**) µg/ml, and **B**) percentage of plasma concentration. **C**) Tolerability of Bi-Ab32/16 and anti-HIV_{gp120} (A32) in Hu-NSG-Tg (IL-15) mice. Body weight of the mice is reported in grams. Changes in body weights compared to day 0 at any time point are determined by two-way ANOVA. **D**) Frequencies of human $CD19^+$, $CD3^+$, $CD33^+$, and $CD56^+$ cells in the peripheral blood of Hu-NSG-Tg (IL-15) mice after reconstitution of the $CD34^+$ hematopoietic stem cell engraftment. **E**) Frequency distribution of $CD56^+$ NK cells at baseline into $CD56^{bright}CD16^{dim}$ and $CD56^{dim}CD16^{bright}$ NK cell subsets. Median with range (min-max) are represented. Statistical analyses were performed using Wilcoxon matched-pairs signed-rank test. *p<0.05; **p<0.01; ***p<0.001. **F**) Viral load expressed as HIV-1 RNA copies per ml of plasma from 1 to 5 weeks post-infection (WPI). Longitudinal dynamics in the percentages of **G**) $CD45^+$, **H**) $CD4^+$, **I**) $CD8^+$ cells, and **J)** CD4/CD8 Ratio, from 0 to 13 WPI on Hu-NSG-Tg (IL-15) mice by condition. All graphs represent median with range (min-max) for each condition.

Statistical comparisons were performed using Mann-Whitney test. **K**) Spearman correlation between the frequency of CD4⁺ T cells and viral load expressed as HIV-1 RNA copies/ml at 13 WPI. **L**) Representative flow cytometry plots (left) and summary graph (right) showing the detection of NK cells bound to both Bi-Ab32/16 and anti-CD16 (3G8). Median with range (min-max) are represented. Statistical analyses were performed using Wilcoxon matched-pairs signed-rank test. *p<0.05; **p<0.01.

Suplementary Figure 7



Supplementary Figure 7. NK cell cluster frequency distribution in peripheral blood and splenic tissue. **A**) Violin plots showing the frequency of the different cell clusters of peripheral blood NK cells identified in Figure 6A at 13 WPI by study condition. **B**) Spearman correlation between the frequency of cluster #BC3 in blood and viral load expressed as HIV-1 RNA copies per ml of plasma. **C**) Violin plots depicting the frequency of the different splenic NK cell clusters identified in Figure 6E at 13 WPI by study condition. **D**) Spearman correlation between the frequency of cluster #SC8 in splenic tissue and viral load expressed as HIV-1 RNA copies per ml of plasma. Statistical comparisons were performed using Mann-Whitney test. Median with range (min-max) are shown. *p<0.05; **p<0.01.

3.2.7.2 Supplementary Tables

Table S1. Sequences of the V_H and V_L regions for Bi-Ab32/16.

Antigen	V_H	V_L
Human CD16	QVQLVQSGAEVKKPGESLKVSCKASGYTFT SYYMHWVRQAPGQGLEWMGIINPSGGSTS YAQKFQGRVTMTRDTSTSTVYMELSSLRSE DTAVYYCARGSAYYYDFADYWGQGTLVTVS S	SYVLTQPSSVSVAPGQTATISCGGHNIGSKN VHWYQQRPGQSPVLVIYQDNKRPSGIPERF SGSNSGNTATLTISGTQAMDEADYYCQVW DNYSVLFGGGTKLTVL
HIV-1 Env (gp120)	QVQLQQWGPGLVKPSQTLSLSCTVSGGSSS SGAHYWSWIRQYPGKGLEWIGYIHYSGNTY YNPSLKSRITISQHTSENQFSLKLNSVTVADT AVYYCARGTRLRTLRNAFDIWGQGTTVTVS S	QSALTQPPSASGSPGQSVTISCTGTSSDVG GYNYVSWYQHHPGKAPKLIISEVNNRPSGV PDRFSGSKSGNTASLTVSGLQAEDEAEYYC SSYTDIHNFVFGGGTKVTVL

Table S2: Purification summary of Bi-Ab32/16.

Sample	Lot	Concentration (mg/ml)	Volume (ml)	Total (mg)	Purity (%)	Monomer (%)	Endotoxin (EU/mg)
Bi-Ab32/16	081020	1.52	33.30	50.62	>95	>98	<1.00

Table S3: Characteristics of the study participants.

Participant ID	Age (years)	Gender	Race	Time since diagnosis (months)	ART regimen	Time on ART (months)	Time on suppressive ART (months)
1	37,972603	M	-	184	CBV, RPV	92	89
2	43,59726	M	Caucasian	71	FTC, RPV, TAF	63	61
3	40,273973	M	Caucasian	113	BIC, FTC, TAF	94	87
4	57,265753	M	Caucasian	322	COB, DRV, RTG	259	145
5	43,59726	M	Caucasian	71	FTC, RPV, TAF	63	61
6	28,19726	M	Caucasian	101	ETV, FTC, TDF	91	75
7	22,583562	F	Black	30	3TC, ABV, DTG	28	24
8	34,079452	F	-	76	3TC, DTG	66	68
9	43,320548	M	Caucasian	98	DRV, FTC, RTV, TDF	97	70
10	48,243836	M	Caucasian	180	CBV, RPV	38	18
11	46,484932	M	Caucasian	32	3TC, ABV, DTG	30	24
12	45,693151	F	Caucasian	68	3TC, DTG	63	61
13	52,619178	M	Caucasian	55	3TC, DTG	53	51
14	44,09589	F	Caucasian	270	BIC, FTC, TAF	120	100
15	51,635616	F	Caucasian	249	COB, DRV, FTC, TAF	69	66
16	45,356164	M	-	66	BIC, FTC, TAF	59	58
17	31,673973	M	Caucasian	147	ETV, FTC, TDF	133	117

4. DISCUSSION

4 Discussion

The discovery of HIV in the 1980s marked the onset of a global health crisis, leading to the deaths of millions of people. However, the development of ART stands as a significant milestone in HIV research. ART has demonstrated remarkable efficacy in suppressing plasma viremia to undetectable levels, restoring immune function, reducing both mortality and morbidity rates, and mitigating the risk of viral transmission[90,511].

To date, achieving complete elimination of HIV infection through ART remains elusive, largely attributed to the formation of viral reservoirs within the host. Early initiation of ART has been described to limit the establishment of HIV reservoirs[512]. Some studies suggest that ART initiation during the acute phase of HIV infection may attenuate reservoir seeding by facilitating the clearance of HIV-infected target cells[513]. However, despite such early intervention, ART fails to prevent the establishment of a latent and persistent HIV reservoir, thus resulting in viral rebound upon treatment interruption[201,514,515]. Viral rebound underscores the resilience of the virus within stable latent reservoirs, primarily found in resting $CD4^+$ T cells, thereby posing a significant barrier to HIV cure initiatives[515]. Consequently, lifelong administration of ART remains necessary. Hence, there is a compelling need for the development of therapeutic strategies aimed at achieving the cure of HIV infection.

However, the advancement of novel strategies requires a comprehensive understanding of the immune-mediated mechanisms involved in HIV control, alongside the development of tailored approaches aimed at enhancing these immune responses to ensure HIV elimination. In this context, this thesis endeavors to enhance our understanding of the immune responses underlying HIV control in Elite Controllers, while also exploring a novel immunotherapeutic approach to bolster immune-mediated responses against HIV-infected cells.

Chapter 1: Co-expression of NKG2C and NKG2A Defines a Highly Functional Antiviral NK Population in Spontaneous HIV Control

Achieving a cure for HIV infection represents a complex endeavor that will require to overcome multiple barriers in order to eliminate HIV reservoirs, encompassing mechanisms that sustain HIV latency, clonal expansion, and dysfunctional immune responses. To date, six cases of HIV cure have been documented, notably the Berlin, City of Hope, Düsseldorf, London, New York, and Geneva patients[516]. These cases resulted from high-risk hematopoietic stem cell transplantation from donors harboring a mutation in the CCR5 gene, rendering cells largely resistant to HIV infection by R5-tropic viruses.

Nonetheless, stem cell transplantation remains viable for only a select few individuals with both HIV and specific blood cancers. Additionally, cases of transient HIV control following prompt initiation of HIV treatment have been observed, exemplified by the Mississippi child, born to an HIV-positive mother, who received ART for the initial 18 months of life and subsequently discontinued treatment. Upon re-engagement with medical care five months later, the child exhibited undetectable HIV viral load, although viral rebound occurred after two years of ART cessation[516]. Furthermore, findings presented at the 2024 Conference on Retroviruses and Opportunistic Infections (CROI) unveiled the potential of early treatment in reducing the HIV reservoir and establishing a foundation for a functional cure, particularly in pediatric cases[517]. Infants acquiring HIV in utero who promptly initiated ART within 48 hours of birth achieved sustained HIV remission for up to a year following closely monitored treatment interruption[517]. Moreover, exceptional elite controllers, exemplified by individuals such as the Esperanza and San Francisco patients, showcase prolonged control of HIV replication, absence of immune dysfunction, and minimal disease progression for over three decades[516]. The elucidation of methods to optimize or enhance the immune system's functionality could represent a pivotal step toward inducing treatment-free control of HIV.

Multiple studies have underscored the shared influence of both host and viral factors on the progression of HIV infection, with the activation status of innate immunity emerging as a critical factor[518,519]. While extensive research has elucidated the adaptive immune mechanisms in individuals naturally controlling HIV infection, our understanding of innate immunity remains limited. Serving as the primary line of defense against pathogenic incursions, innate immunity not only acts independently but also serves as a conduit for eliciting effective adaptive immune responses. Collectively, innate immune components form a rapid-response system against infection, thereby impeding its dissemination[406]. Consequently, a further understanding of innate immune mechanisms in EC of HIV infection holds promise for identifying novel therapeutic targets and theoretical frameworks essential for advancing strategies for functional cure, prevention, and control of HIV, aimed at replicating the EC phenotype in HIV-infected progressors[356].

In **Chapter 1** of this thesis, we hypothesized that HIV EC exhibit distinctive innate immunological features that facilitate the elimination or containment of HIV-infected cells. Our primary aim was to characterize the NK cell repertoire in individuals capable of sustained HIV control in the absence of ART, whom we designated as durable control (DC) EC.

Through a comprehensive phenotypic and functional analysis, we compared NK cell subsets in DC with those in other cohorts of PWH: aborted control (AC) EC, characterized by undetectable viral loads but a progressive decline in $CD4^+$ T cell counts; ART-suppressed PWH (ART); and viremic individuals (VIR). Our findings revealed an enrichment of NK cell populations expressing memory markers such as NKG2C and CD57, in conjunction with CD16, NKG2A, and CXCR3, in DC individuals. Notably, these cells demonstrated robust ADCC responses against HIV-infected cells. Subsequently, we conducted a transcriptional profiling of these cells, unveiling a distinct transcriptional signature associated with cell metabolism, migration, chemotaxis, activation, chemokine secretion, and antiviral responses. This discovery is significant as it suggests the identification of a pivotal NK cell subset with potent antiviral immune capabilities in PWH exhibiting sustained viral control.

Numerous reports have described disruptions within the NK cell compartment in the context of HIV infection, encompassing reductions in absolute cell counts, impaired IFNγ production, and compromised cytotoxicity against MHC class I negative targets[437,492,520]. These alterations include heightened proportions of NK cells bearing inhibitory receptors of the KIR family, along with diminished populations expressing activating NCRs. Among the overall decline in the expression of inhibitory receptors in NK cells, a reduction in the proportion of NK cells bearing the inhibitory NKG2A receptor has been described during chronic HIV infection[322,437]. Our findings align with these reports, as we observed similar changes in NK cell profiles among ART-treated and VIR individuals compared to HD. Notably, while the distribution of NK cell receptors remained similar between DC and HD individuals, the expression of the activating NKG2C receptor was significantly elevated in DC, reaching frequencies akin to those observed in PWH without natural control of HIV infection. This observation is of particular significance, given that NKG2C receptor has been associated with memory-like features, particularly in the context of CMV infection. Memory-like NK cells expressing NKG2C may exhibit epigenetic modifications conductive to increased IFNγ secretion and ADCC activity compared to conventional NK cells[410]. Moreover, the presence of $NKG2C^+$ memory-like NK cells has been previously linked to HIV control[441]. A recent study found elevated NKG2C expression concurrent with enrichment of H3K4me3, a histone modification indicative of chromatin accessibility associated with active gene transcription, specifically at the promoter locus of the KLRC2 gene, responsible for encoding NKG2C, in HIV EC[521]. The deposition of this histone mark at promoters of immune-related genes serves as a characteristic feature of sustained innate immune memory, also termed as trained immunity.

This association suggests a potential correlation between enhanced antiviral control in ECs and the induction of trained immunity[521].

Our phenotypic analysis revealed a significant expansion of an NK cell subset expressing NKG2C, CD16, CD57, NKG2A, and CXCR3 in DC individuals compared to non-controllers. CD16, a potent activator of NK cell function, plays a pivotal role in controlling HIV infection by facilitating ADCC[406]. Furthermore, CD57 serves as a marker of terminally mature NK cells, and its co-expression with NKG2C has been linked to the presence of memory-like NK cells[423]. Notably, recent findings have identified $NKG2C^{+}CD57^{+}$ NK cells as the predominant subset mediating ADCC against HIV-infected $CD4^{+}$ T cells in the presence of broadly neutralizing antibodies[421,440]. Additionally, we observed co-expression of NKG2C and NKG2A receptors on DC-expanded NK cells, a phenomenon that is infrequent given their opposing functions while binding the same ligand. Prior studies have underscored the pivotal role of NK cells expressing NKG2A in the immunological control of HIV[522]. In particular, augmented HLA-A expression has been implicated in upregulating HLA-E expression, thereby augmenting NKG2A-mediated NK cell inhibition, and impeding the clearance of HIV-infected cells[522]. However, it is noteworthy that NKG2C also interacts with HLA-E, potentially contributing to antiviral responses[522]. While signaling through NKG2A typically dominates and suppresses NKG2C signaling, co-expression of these receptors by NK cells has been observed, leading to dampened pro-inflammatory responses and suggesting a regulatory role in NK cell function[295,442,443]. We postulate that the co-expression of NKG2C alongside NKG2A in NK cells derived from DC may signify a partially differentiated phenotype capable of modulating activating responses. Additionally, the expression of CXCR3 within this subset may indicate their proficient migratory capacity towards infected tissues[445].

Substantial evidence supports the pivotal role of cellular immunity in controlling HIV replication in a significant proportion of HIV EC, characterized by the overrepresentation of protective HLA alleles, robust HIV-specific CD8 T cell responses with suppressive capabilities, and preservation of memory $CD4^{+}$ T cells[341,347,523–526]. While HIV-specific $CD8^{+}$ T cell responses in controllers exhibit greater polyfunctionality and are more inclined to degranulate and release perforin and granzyme B upon stimulation compared to those in non-controllers[341,342,410,527], we do not observe such phenomenon in NK cells. Consistent with prior findings, our results support the maintenance of cytotoxic potential in NK cells across all groups of PWH following stimulation, characterized by IFNγ production and degranulation[454–456].

However, comparative analysis revealed diminished frequencies of NK cell subsets displaying a cytotoxic profile in DC individuals relative to HD and non-controllers. Lower levels of cell activation in DC could be attributed to a decrease in the antigen burden, as suggested by previous studies[457].

By contrast, our data reveals that DC individuals exhibit robust ADCC responses against HIV-infected cells, comparable to those observed in HD, and superior to non-controllers. These findings align with previous studies suggesting that HIV controllers generate antibodies with enhanced efficacy in driving ADCC[388,449,475,528–531]. Additionally, ADCC has been linked to lower viral load in untreated HIV progressors and conferred protection against HIV infection in the RV144 vaccine trial[356]. Moreover, ADCC responses have been associated with reduced reservoir size in HIV EC[356]. These observations hold significance as a considerable proportion of EC lack protective HLA alleles and may exert control over HIV infection via non-CTL mechanisms[403]. In this regard, EC were found to exhibit higher ADCC-antibody titers compared to viremic individuals, with non-protective HLA-bearing EC demonstrating even higher ADCC titers than their protective HLA counterparts[525]. This observation suggests that ADCC responses may represent a predominant immune mechanism contributing to HIV control in these individuals[525]. This finding holds significance for functional cure strategies, as it underscores the considerable heterogeneity within the EC population and suggests that coordinated CD8-NK cell responses may be crucial for effective HIV control. Indeed, some studies support this hypothesis, as EC with robust CD8 suppressive activity were found to have higher ADCC antibody titers compared to weak responders[525]. One plausible explanation could be that cellular-mediated suppressive activity diminishes immune activation levels, thereby influencing antibody glycosylation profiles that in turn impact Fc receptor (FcR)-binding antibody functions such as ADCC[532–534]. Additionally, ADCC has been positively correlated with plasma HIV RNA levels, implying that low viral replication levels may stimulate ADCC responses[525]. These low viral replication levels, combined with functional HIV-specific $CD4^+$ T cells and preserved B cell compartments, may contribute to the production of high ADCC antibody titers in HIV EC[525]. Further support for this hypothesis comes from studies in SIV models[385]. Thus, our findings are consistent with prior literature, indicating that ADCC responses may represent a pivotal element in HIV control, highlighting their potential significance as a focal point for vaccine development. This is of importance given that the majority of the general population does not present protective HLA alleles[525].

Single-cell RNA sequencing analysis of ADCC-mediating NK cell subsets revealed a distinct transcriptional profile associated with heightened cell activation, cytokine secretion, and an augmented antiviral response. These cells exhibited significant upregulation of soluble factors involved in immune modulation (i.e. XCL1, XCL2), cytokines (i.e. IL-32), chemokines (i.e. CCL3, CCL4), and interferon-induced genes (ISGs). Our transcriptomic findings align with previous research describing a unique transcriptional signature in HIV-specific $CD8^+$ T cells from lymph nodes of ECs[345]. These cells were enriched in genes associated with homeostasis (i.e. IL-7R) and various chemokines/cytokines (i.e. CCL5 and IL-32), indicative of a highly functional memory phenotype[345]. Further, LN-derived $CD8^+$ T cells exhibited upregulation of genes encoding predicted secreted factors such as TNF, CCL5, and IL-32, known to suppress HIV replication[345]. These features likely signify a protective immune signature, as $CD8^+$ T cells from the LNs of ART-treated individuals failed to acquire these characteristics even in the absence of viremia. Further, other studies suggest that CCR5 is downregulated in $CD4^+$ T cells from ECs compared to ART-suppressed individuals[350], consequently reducing susceptibility to CCR5-dependent HIV entry. The diminished expression of CCR5 in HIV-specific $CD4^+$ T cells from ECs may arise from genetic factors or be influenced by increased expression of the β-chemokines CCL5 and CCL3, which could induce CCR5 downregulation following robust TCR stimulation. Cases of bi-allelic CCR5 mutations, such as homozygous deletions in CCR5Δ32, or the combination of CCR5Δ32 deletion with a C101X nonsense mutation, have been reported in highly exposed uninfected individuals[535,536]. In this regard, a recent study elucidated that efficient deletion of CCR5 by CRISPR/Cas9 in a xenograft mice model conferred complete protection against CCR5-tropic HIV strains[537]. Importantly, if $CD8^+$ T cells and NK cells also secrete CCL3, CCL4, and CCL5 chemokines that bind to the CCR5 co-receptor, they may collaborate in inhibiting CCR5-mediated HIV entry into the cell, thereby directly contributing to the establishment of HIV control.

Together, these observations underscore the considerable heterogeneity among ECs and suggest that HIV control is a multifaceted process, wherein NK cells may play a pivotal role, collaborating with CTLs to execute coordinated functions. These findings may serve as a foundation for the development of novel immunotherapeutic strategies aimed at eliciting potent ADCC responses and enhancing virus clearance, thereby promoting sustained HIV control of viral replication, also referred to as functional cure of HIV infection[449].

Chapter 2: NK Cell Depletion in Bispecific Antibody Therapy is Associated with Lack of HIV Control after ART interruption

Substantial progress has been made in elucidating the mechanisms underlying virus reactivation from latency. However, initial expectations regarding the efficacy of latency reversal as a standalone approach for reducing infected cell reservoirs, whether through viral cytopathic effects or innate immune responses, have yet to be realized. It is increasingly apparent that effective strategies for latency reversal must be supplemented with interventions that enhance immune recognition and clearance of cells hosting reactivated virus[538].

In this regard, a growing body of research has highlighted the presence of broadly neutralizing antibodies (bNAbs) with broad and potent HIV-neutralizing capabilities, offering promise for immunotherapeutic interventions[539–541]. Currently, bNAbs represent a leading strategy for achieving undetectable viral loads in infected humanized mice and rhesus macaques, as well as prolonging the time to viral rebound in humans[540,542]. In vivo administration of bNAbs has been shown to confer protection against infection in multiple studies[541,543–546]. Notably, in a study led by Dan H. Barouch et al., the combination of certain LRAs with bNAb treatment significantly suppressed viral rebound for more than six months following interruption of ART in half of SIV-infected macaques[547]. However, it is important to acknowledge that all known bNAbs are vulnerable to viral escape mutations, which may arise from HIV reverse transcriptase activity or immunological pressure-induced mutations, presenting challenges to the therapeutic efficacy of bNAb monotherapies for HIV prevention and treatment[543]. Despite the improved efficacy of bNAb cocktails for viral control in vivo, the presence of pre-existing or post-infusion resistant viral strains poses a significant obstacle to this therapeutic approach[543,548–551]. Resistance to single antibody regimens often emerges through immune evasion mechanisms, as viruses adapt to evade host immune responses[543]. Furthermore, given that most symptoms of viral infections manifest after the peak of viremia, early administration of monoclonal antibody (mAb) therapy is essential, often preceding the onset of clinical symptoms. However, HIV presents a rapid viral evolution, and the emergence of escape mutations may compromise the efficacy of mAb therapy[543].

Immunotherapeutic approaches based on the use of BiAbs to enhance immune-mediated responses against infected cells have been explored[552]. The use of BiAbs compared to monoclonal Abs has demonstrated notable advantages, such as enhanced efficacy and safety profiles by simultaneously targeting and binding two distinct antigenic epitopes, thereby uniquely redirecting cytotoxic effector cells[553].

In this regard, in **Chapter 2** of this thesis, we present the findings from the evaluation of a BiAb (Bi-Ab32/16) designed to enhance NK-mediated responses against HIV-infected cells. Specifically, Bi-Ab32/16 comprises a polypeptide chain encoding the full-length non-neutralizing A32 antibody (targeting HIVgp120) fused with a single-chain variable fragment (ScFv) domain from CD16a. As previously described, the A32 antibody demonstrates specificity towards the conformational epitopes C1 and C4 on the HIV_{gp120} Env protein subsequent to its interaction with CD4, while CD16 facilitates the redirection and activation of NK cell cytotoxic responses[481]. Previous studies have underscored A32 as a promising candidate for HIV-infected cell targeting, as it recognizes epitopes rapidly expressed in virions bound to target cells, exhibits reactivity against envelopes from all HIV clades, and lacks evidence of epitope escape mutations[483,554,555]. Our study demonstrates that Bi-Ab32/16 promotes cell-to-cell interactions between NK cells and HIV-infected $CD4^+$ T cells, eliciting a specific, potent, and multifunctional cytotoxic NK cell response. Furthermore, Bi-Ab32/16 substantially diminishes the latent HIV reservoir following viral reactivation, and mediates the elimination of cells harboring intact proviruses in samples from PWH. However, preclinical evaluation of Bi-Ab32/16 in a humanized mouse model of HIV infection revealed a significant reduction in NK cell populations associated with poor virological control following ART interruption.

In our study, we demonstrated that Bi-Ab32/16 elicits a robust anti-HIV cytotoxic response in NK cells from PWH. This finding holds particular significance, as HIV infection is associated with the expansion of dysfunctional NK cell populations, which lose their ability to eliminate HIV-infected targets, even in the presence of ART. Notably, this effect was contingent upon the presence of the target protein, demonstrating specificity. These characteristics position Bi-Ab32/16 as an attractive molecular tool capable of redirecting and amplifying NK cell-mediated responses against HIV-infected cells. Our observations were consistent across various HIV infection settings, including ex vivo infection with distinct HIV strains and upon latency reversal, akin to “shock and kill” strategies. Thus, our results provide compelling evidence that Bi-Ab32/16 exerts an impact on the natural HIV reservoir. This finding is particularly relevant given that the majority of latent viruses have been reported to harbor CTL escape mutations, rendering HIV-infected cells unresponsive to CTLs targeting common epitopes. Our results align with previous studies evaluating non-neutralizing BiAbs designed to engage NK cells via CD16a. For instance, a recent study described improved NK-mediated killing of autologous HIV-infected $CD4^+$ T cells using a non-neutralizing BiAb targeting the gp41 region of HIV Env alongside CD16[556].

Furthermore, another study revealed that a BiAb molecule targeting HIV Env and CD16 effectively redirected NK cells from cord blood to eliminate HIV-infected cells, and that this killing activity could significantly increase with IL-15 treatment[557]. These studies collectively underscore CD16a engagement as a potent mechanism for enhancing NK cell activation. However, they did not investigate the impact of these BiAbs upon latency reversal of the HIV reservoir and its subsequent effect on viral reservoir dynamics. In addition, our results are consistent with a recent study describing the impact of two BiAbs directed against the HIV Env protein and CD16, elucidating their role in promoting an NK-mediated reduction in HIV reservoir cells, contingent upon latency reversal[488].

In addition, we conducted the preclinical evaluation of Bi-Ab32/16 in a humanized mice model of HIV infection. Traditional preclinical studies in HIV research often rely on well-established humanized mouse models such as BLT mice[501,502]. However, these models present limited support for robust human NK cell development derived from engrafted human hematopoietic stem cells[558]. Alternatively, humanized NOD.Cg-Prkdcscid Il2rgtm1Wjl/SzJ (NSG) mice infected with HIV exhibit virological and immunological characteristics akin to HIV infection and latency in humans[552,559]. Nonetheless, due to complete IL-2Rg knockout, human NK cell engraftment and maturation are markedly low in this mouse strain. Further, NSG mice engineered to express a transgene encoding human IL-15 (NSG-Tg(IL-15)) exhibit physiological levels of human IL-15 and support long-term engraftment of human NK cells upon transplantation with human umbilical-cord-blood-derived hematopoietic stem cells. Hu-NSG-Tg(IL-15) mice manifest robust and sustained reconstitution with human immune cells without developing graft-versus-host disease (GvHD), thereby facilitating extended studies of human NK cells. Moreover, these mice sustain HIV infection, eliciting human NK cell responses in HIV-infected hosts, rendering them a robust and innovative model for investigating NK cell responses to HIV[489]. In our study, we opted to utilize the Hu-NSG-Tg(IL-15) animal model for the in vivo preclinical evaluation of Bi-Ab32/16.

We observed a modest delay in the time to viral rebound following treatment interruption in mice treated with A32 mAb. Given that A32 is a non-neutralizing antibody that targets gp120 upon interaction with the CD4 receptor, this delay is likely attributed to NK-mediated ADCC. However, despite exhibiting excellent performance in vitro, Bi-Ab32/16 failed to enhance HIV control in treated mice. We observed a decline in total $CD56^{+}$ NK cells following two weeks of Bi-Ab32/16 stimulation, which correlated inversely with viral load, thereby providing evidence for the involvement of NK cells in HIV infection control. We posit that sustained CD16 stimulation induced by Bi-Ab32/16, amidst detectable viremia, may inadvertently elicit adverse effects on NK cells.

A recent study published by Nathan et al. evaluating two distinct BiAbs, based on bNAbs targeting Env and CD16, yielded comparable in vitro outcomes to our study[488]. However, their preclinical evaluation of one antibody in the same animal model demonstrated augmented NK cell activity and reduced reservoir size. Both studies employed bispecific formats targeting identical epitopes in the same animal model. Yet, their experimental design did not include an ART interruption period. Findings from both studies prompt inquiries into the optimal timing of intervention and whether ART interruption provides a conducive environment for effective NK cell targeting. Furthermore, their study incorporated two conditions: one with the bispecific antibody, and another with an irrelevant isotype control against a mutant p53 epitope present on HLA-A*02:01, combined with a CD16 antibody[488]. However, the absence of a control condition with the bNAb alone complicates the discernment between effector functions driven by CD16 engagement and the neutralizing properties of the bispecific antibody. We postulate that the concurrent viral replication following ART interruption, along with sustained CD16 stimulation by Bi-Ab32/16, may have influenced NK cell dynamics in our study.

Furthermore, previous studies have demonstrated that the density of Env surface proteins plays a pivotal role in determining the elimination of HIV-infected cells by distinct Env-specific immunotherapeutic approaches, including BiAbs[560]. Achieving robust elimination of reservoir cells in vivo with Env-directed therapeutics will likely require single or combination therapies incorporating LRAs with increased potency. Moreover, recent studies have highlighted the significant impact of the conformational state of Env glycoprotein on both antibody recognition and ADCC responses[508–510]. The engagement of the CD4 receptor triggers a transition of Env to an “open” conformation, thereby sensitizing HIV-infected cells to ADCC responses mediated by non-neutralizing antibodies. However, HIV has evolved mechanisms to restrict Env-CD4 interaction. Evidence strongly suggests that HIV infection modulates Env-CD4 interaction to protect infected cells against ADCC by downregulating CD4 expression via viral proteins such as Nef, Vpu, and Env[479,510,561,562]. In this context, small CD4-mimetic compounds (CD4mc) have been described to modulate Env conformation on the surface of HIV-infected cells, inducing the CD4-bound conformation of HIV envelope glycoproteins. These changes expose CD4-induced epitopes (CD4i), effectively sensitizing HIV-infected $CD4^+$ T cells to ADCC mediated by CD4i-antibodies present in biological fluids from PWH[563]. Recent findings have demonstrated that combining CD4mc with two families of CD4i-antibodies significantly reduces HIV replication, viral reservoir size, and viral rebound after ART interruption in a SRG-15 model of humanized mice[509].

In this regard, we have shown in our study that Bi-Ab32/16 binds approximately 50% of total HIV-infected cells. We hypothesize that the overall percentage of HIV-infected cells exhibiting CD4 downregulation may vary depending on the viral strain used or the activation status of the cell prior to infection. However, we posit that strategies involving the co-administration of the bispecific format with CD4mc could enhance ADCC responses and, therefore, requires further investigation.

Further, considering that similar immunotherapeutic strategies centered on adoptive BiAb-NK cell therapies are presently undergoing clinical trials for hematological malignancies[564,565] (NCT04074746), we posit that ex vivo priming of NK cells with Bi-Ab32/16 followed by an infusion of the complexed product into PWH could represent an interesting strategy to effectively mediate NK-mediated clearance of HIV-infected cells. Additionally, co-administration of this bispecific format with NK cells during ART interruption may mitigate NK cell depletion, enhance ADCC responses, and potentially optimize NK-mediated killing of HIV-infected cells. Our findings provide evidence for the beneficial effects of the Bi-Ab32/16 platform in vitro, underscoring the role of NK cells in HIV control and the value of therapies aimed at enhancing their function.

In vivo studies of HIV infection faithfully reproduce critical aspects of the disease and are indispensable to HIV cure research. These studies facilitate comprehensive examination of diverse anatomic reservoirs and enable manipulation of various immune cell populations to elucidate their roles in HIV infection and persistence. Specifically, the Hu-NSG-Tg(IL-15) in vivo model provides a platform for investigating NK cell responses to HIV infection and evaluating strategies aimed at enhancing their effector functions. However, in vivo HIV studies present limitations, including constraints such as the limited volume of blood plasma available for viral load analysis, the restricted amount of peripheral blood accessible for in vitro functional assessments, and the time-intensive nature of working with animal models. Moreover, a limitation of our humanized mouse model lies in the likelihood that the reduction in infected $CD4^+$ T cells predominantly reflects the elimination of productively infected $CD4^+$ T cells, which constitute the majority of the infected cell population during the early stages of HIV infection, rather than the elimination of latently-infected $CD4^+$ T cells. Further studies involving the administration of a combination of BiAbs and LRAs during prolonged viral suppression will be essential to directly assess the BiAb-mediated clearance of latent reservoir cells.

In summary, bispecific antibodies offer unique properties that are not found in monoclonal antibodies alone, representing a compelling avenue for enhancing NK-mediated responses against HIV-infected cells. However, several aspects must be addressed for the successful implementation of these strategies.

These include the short half-life of NK cells in vivo, challenges in accessing certain tissues, and limitations in expanding NK cell populations in vitro[566]. Future investigations should focus on expanding, activating, and redirecting distinct NK cell subsets with enhanced ADCC responses, such as memory-like NK cells, which hold promise for combating HIV infection. Specifically, strategies aimed at improving and expanding the memory NK cell phenotype observed in EC could facilitate viral reservoir elimination. In this regard, our group is currently exploring the generation, expansion, and enhancement of function of two distinct subsets of memory-like NK cells from PWH: cytokine-induced memory-like (CIML) NK cells and CIML NK cells with tissue-resident (TR) characteristics. Additionally, we are also investigating the role of cord blood-derived NK cells (CB-NKs) in HIV infection to expand and refine ex vivo immunotherapeutic approaches based on CB-NKs for HIV reservoir elimination.

5. CONCLUSIONS

5 Conclusions

1. NK cells from individuals with prolonged HIV control exhibit a **phenotypically distinct NK cell repertoire** compared to other groups of PWH.

2. Individuals exhibiting durable HIV control present elevated frequencies of **memory-like NK cells** expressing the inhibitory NKG2A marker.

3. NK cells from individuals with durable HIV control show **diminished natural cytotoxic responses** upon non-specific target interaction or cytokine stimulation.

4. Memory-like NK cells expressing NKG2A and CXCR3 display **heightened ADCC responses** against HIV targets in individuals with durable HIV control.

5. ADCC-mediating NK cells from individuals with prolonged HIV control have a **unique transcriptional signature**, marked by the upregulation of genes associated with NK cell metabolism, migration, effector functions, and antiviral responses.

6. A **bispecific antibody** platform designed to engage $CD16^+$ NK cells with gp120-expressing HIV-infected $CD4^+$ T cells (Bi-Ab32/16) enhances **cell-to-cell contact** between both cells, facilitating targeted immune responses.

7. Bi-Ab32/16 induces robust and specific **anti-HIV cytotoxic responses** in NK cells from PWH against in vitro and ex vivo HIV-infected cells, demonstrating its potential efficacy in viral suppression.

8. Bi-Ab32/16 enhances the **NK-mediated clearance of latently HIV-infected cells** and cells harboring intact proviral DNA from PWH following viral reactivation.

9. **In vivo** evaluation of Bi-Ab32/16 unveils a reduction in the total pool of $CD56^+$ NK cells, which is **inversely associated with HIV control** following sustained Bi-Ab32/16 stimulation.

10. Prolonged in vivo administration of Bi-Ab32/16 **disrupts the NK cell landscape** in both blood and splenic tissue, leading to a decrease in IFNγ-producing cells, which may impact overall immune function.

6. REFERENCES

6 References

1. (U.S.), C. for D. C. and P. Morbidity and Mortality Weekly Report. *Epidemiologic Notes and Reports* Vol. 30, (1981).

2. Friedman-Kien, A. E. Disseminated Kaposi's sarcoma syndrome in young homosexual men. *J. Am. Acad. Dermatol.* 5, 468–471 (1981).

3. Greene, W. C. A history of AIDS: Looking back to see ahead. *Eur. J. Immunol.* 37, S94–S102 (2007).

4. Cock, K. M. D., Jaffe, H. W. & Curran, J. W. Reflections on 30 Years of AIDS - Volume 17, Number 6—June 2011 - Emerging Infectious Diseases journal - CDC. *Emerg. Infect. Dis.* 17, 1044–1048 (2011).

5. Barré-Sinoussi, F. *et al.* Isolation of a T-Lymphotropic Retrovirus from a Patient at Risk for Acquired Immune Deficiency Syndrome (AIDS). *Science* 220, 868–871 (1983).

6. Gallo, R. C. *et al.* Frequent Detection and Isolation of Cytopathic Retroviruses (HTLV-III) from Patients with AIDS and at Risk for AIDS. *Science* 224, 500–503 (1984).

7. Popovic, M., Sarngadharan, M. G., Read, E. & Gallo, R. C. Detection, Isolation, and Continuous Production of Cytopathic Retroviruses (HTLV-III) from Patients with AIDS and Pre-AIDS. *Science* 224, 497–500 (1984).

8. Schüpbach, J. *et al.* Serological Analysis of a Subgroup of Human T-Lymphotropic Retroviruses (HTLV-III) Associated with AIDS. *Science* 224, 503–505 (1984).

9. Coffin, J. *et al.* What to call the AIDS virus? *Nature* 321, 10–10 (1986).

10. Institutet, T. N. A. at K. *The Nobel Prize in Physiology or Medicine 2008*. (2008).

11. Perelson, A. S. *et al.* Decay characteristics of HIV-1-infected compartments during combination therapy. *Nature* 387, 188–191 (1997).

12. UNAIDS. UNAIDS Epidemiological Estimates 2023.

13. Eisinger, R. W., Dieffenbach, C. W. & Fauci, A. S. HIV Viral Load and Transmissibility of HIV Infection. *JAMA* 321, 451–452 (2019).

14. Coffin, J. *et al.* ICTV Virus Taxonomy Profile: Retroviridae 2021. *J. Gen. Virol.* 102, 001712 (2021).

15. Ryu, W.-S. Molecular Virology of Human Pathogenic Viruses. *Part IV: RT Viruses* 227–246 (2017) doi:10.1016/b978-0-12-800838-6.00017-5.

16. Kannangai, R., David, S. & Sridharan, G. Human immunodeficiency virus type-2—A milder, kinder virus: An update. *Indian J. Méd. Microbiol.* 30, 6–15 (2012).

17. Clavel, F. *et al.* Isolation of a New Human Retrovirus from West African Patients with AIDS. *Science* 233, 343–346 (1986).

18. Marlink, R. *et al.* Reduced Rate of Disease Development After HIV-2 Infection as Compared to HIV-1. *Science* 265, 1587–1590 (1994).

19. Campbell-Yesufu, O. T. & Gandhi, R. T. Update on Human Immunodeficiency Virus (HIV)-2 Infection. *Clin. Infect. Dis.* 52, 780–787 (2011).

20. Hahn, B. H., Shaw, G. M., De, K. M., Cock & Sharp, P. M. AIDS as a Zoonosis: Scientific and Public Health Implications. *Science* 287, 607–614 (2000).

21. Keele, B. F. *et al.* Chimpanzee Reservoirs of Pandemic and Nonpandemic HIV-1. *Science* 313, 523–526 (2006).

22. Worobey, M. *et al.* Island Biogeography Reveals the Deep History of SIV. *Science* 329, 1487–1487 (2010).

23. Gao, F. *et al.* Origin of HIV-1 in the chimpanzee Pan troglodytes troglodytes. *Nature* 397, 436–441 (1999).

24. Silvestri, G., Paiardini, M., Pandrea, I., Lederman, M. M. & Sodora, D. L. Understanding the benign nature of SIV infection in natural hosts. *J. Clin. Investig.* 117, 3148–3154 (2007).

25. Chahroudi, A., Bosinger, S. E., Vanderford, T. H., Paiardini, M. & Silvestri, G. Natural SIV Hosts: Showing AIDS the Door. *Science* 335, 1188–1193 (2012).

26. Briggs, J. A. G. *et al.* The stoichiometry of Gag protein in HIV-1. *Nat. Struct. Mol. Biol.* 11, 672–675 (2004).

27. Coffin, J. M., Hughes, S. H. & Varmus, and H. E. *Retroviruses*. (1997).

28. Arthur, L. O. *et al.* Cellular Proteins Bound to Immunodeficiency Viruses: Implications for Pathogenesis and Vaccines. *Science* 258, 1935–1938 (1992).

29. Muesing, M. A. *et al.* Nucleic acid structure and expression of the human AIDS/lymphadenopathy retrovirus. *Nature* 313, 450–458 (1985).

30. Kingsman, S. M. & Kingsman, A. J. The Regulation of Human Immunodeficiency Virus Type-1 Gene Expression. *Eur. J. Biochem.* 240, 491–507 (1996).

31. Sanyaolu, A. *et al.* The Mechanism of HIV-1 Latency and Therapeutic Implication. *Madridge J. Immunol.* 3, 78–83 (2019).

32. Turner, B. G. & Summers, M. F. Structural biology of HIV 1 1 Edited by P. E. Wright. *J. Mol. Biol.* 285, 1–32 (1999).

33. Sierra, S., Kupfer, B. & Kaiser, R. Basics of the virology of HIV-1 and its replication. *J. Clin. Virol.* 34, 233–244 (2005).

34. Watts, J. M. *et al.* Architecture and secondary structure of an entire HIV-1 RNA genome. *Nature* 460, 711–716 (2009).

35. Feinberg, M. B. & Greene, W. C. Molecular insights into human immunodeficiency virus type 1 pathogenesis. *Curr. Opin. Immunol.* 4, 466–474 (1992).

36. Vaishnav, Y. N. & Wong-Staal, F. The Biochemistry of Aids. *Annu. Rev. Biochem.* 60, 577–630 (1991).

37. Malim, M. H. & Emerman, M. HIV-1 Accessory Proteins—Ensuring Viral Survival in a Hostile Environment. *Cell Host Microbe* 3, 388–398 (2008).

38. Maddon, P. J. *et al.* The T4 gene encodes the AIDS virus receptor and is expressed in the immune system and the brain. *Cell* 47, 333–348 (1986).

39. Dalgleish, A. G. *et al.* The CD4 (T4) antigen is an essential component of the receptor for the AIDS retrovirus. *Nature* 312, 763–767 (1984).

40. Chen, B. Molecular Mechanism of HIV-1 Entry. *Trends Microbiol.* 27, 878–891 (2019).

41. Deng, H. *et al.* Identification of a major co-receptor for primary isolates of HIV-1. *Nature* 381, 661–666 (1996).

42. Rizzuto, C. D. *et al.* A Conserved HIV gp120 Glycoprotein Structure Involved in Chemokine Receptor Binding. *Science* 280, 1949–1953 (1998).

43. Simmons, G. *et al.* Primary, syncytium-inducing human immunodeficiency virus type 1 isolates are dual-tropic and most can use either Lestr or CCR5 as coreceptors for virus entry. *J. Virol.* 70, 8355–8360 (1996).

44. Burdick, R. C. *et al.* HIV-1 uncoating requires long double-stranded reverse transcription products. *Sci. Adv.* 10, eadn7033 (2024).

45. Hu, W.-S. & Hughes, S. H. HIV-1 Reverse Transcription. *Cold Spring Harb. Perspect. Med.* 2, a006882 (2012).

46. Smyth, R. P., Davenport, M. P. & Mak, J. The origin of genetic diversity in HIV-1. *Virus Res.* 169, 415–429 (2012).

47. Ferguson, M. R., Rojo, D. R., Lindern, J. J. von & O'Brien, W. A. HIV-1 replication cycle. *Clin. Lab. Med.* 22, 611–635 (2002).

48. Engelman, A., Mizuuchi, K. & Craigie, R. HIV-1 DNA integration: Mechanism of viral DNA cleavage and DNA strand transfer. *Cell* 67, 1211–1221 (1991).

49. Dwivedi, R., Prakash, P., Kumbhar, B. V., Balasubramaniam, M. & Dash, C. HIV-1 capsid and viral DNA integration. *mBio* 15, e00212-22 (2023).

50. Marini, B. *et al.* Nuclear architecture dictates HIV-1 integration site selection. *Nature* 521, 227–231 (2015).

51. Schröder, A. R. W. *et al.* HIV-1 Integration in the Human Genome Favors Active Genes and Local Hotspots. *Cell* 110, 521–529 (2002).

52. Engelman, A. & Cherepanov, P. The structural biology of HIV-1: mechanistic and therapeutic insights. *Nat. Rev. Microbiol.* 10, 279–290 (2012).

53. Peterlin, B. M. & Price, D. H. Controlling the Elongation Phase of Transcription with P-TEFb. *Mol. Cell* 23, 297–305 (2006).

54. Karn, J. & Stoltzfus, C. M. Transcriptional and Posttranscriptional Regulation of HIV-1 Gene Expression. *Cold Spring Harb. Perspect. Med.* 2, a006916 (2012).

55. Jolly, C. & Sattentau, Q. J. Human Immunodeficiency Virus Type 1 Assembly, Budding, and Cell-Cell Spread in T Cells Take Place in Tetraspanin-Enriched Plasma Membrane Domains. *J. Virol.* 81, 7873–7884 (2007).

56. Sundquist, W. I. & Kräusslich, H.-G. HIV-1 Assembly, Budding, and Maturation. *Cold Spring Harb. Perspect. Med.* 2, a006924 (2012).

57. Das, S. R. & Jameel, S. Biology of the HIV Nef protein. *Indian J. Méd. Res.* 121, 315–32 (2005).

58. Kleinpeter, A. B. & Freed, E. O. HIV-1 Maturation: Lessons Learned from Inhibitors. *Viruses* 12, 940 (2020).

59. Hill, M., Tachedjian, G. & Mak, J. The Packaging and Maturation of the HIV-1 Pol Proteins. *Curr. HIV Res.* 3, 73–85 (2005).

60. Epstein, F. H., Pantaleo, G., Graziosi, C. & Fauci, A. S. The Immunopathogenesis of Human Immunodeficiency Virus Infection. *N. Engl. J. Med.* 328, 327–335 (1993).

61. Chen, Q. *et al.* Different transmission routes and the risk of advanced HIV disease: A systematic review and network meta-analysis of observational studies. *EClinicalMedicine* 16, 121–128 (2019).

62. Cardenas, M. C. *et al.* Prevention of the Vertical Transmission of HIV; A Recap of the Journey so Far. *Viruses* 15, 849 (2023).

63. Maartens, G., Celum, C. & Lewin, S. R. HIV infection: epidemiology, pathogenesis, treatment, and prevention. *Lancet* 384, 258–271 (2014).

64. Wu, L. & KewalRamani, V. N. Dendritic-cell interactions with HIV: infection and viral dissemination. *Nat. Rev. Immunol.* 6, 859–868 (2006).

65. Turville, S. G. *et al.* Diversity of receptors binding HIV on dendritic cell subsets. *Nat. Immunol.* 3, 975–983 (2002).

66. Mehandru, S. *et al.* Primary HIV-1 Infection Is Associated with Preferential Depletion of CD4+ T Lymphocytes from Effector Sites in the Gastrointestinal Tract. *J. Exp. Med.* 200, 761–770 (2004).

67. Hofer, U. & Speck, R. F. Disturbance of the gut-associated lymphoid tissue is associated with disease progression in chronic HIV infection. *Semin. Immunopathol.* 31, 257–266 (2009).

68. Keele, B. F. *et al.* Characterization of the Follicular Dendritic Cell Reservoir of Human Immunodeficiency Virus Type 1. *J. Virol.* 82, 5548–5561 (2008).

69. Fiebig, E. W. *et al.* Dynamics of HIV viremia and antibody seroconversion in plasma donors. *AIDS* 17, 1871–1879 (2003).

70. Cohen, M. S., Shaw, G. M., McMichael, A. J. & Haynes, B. F. Acute HIV-1 Infection. *N. Engl. J. Med.* 364, 1943–1954 (2011).

71. Kahn, J. O. & Walker, B. D. Acute Human Immunodeficiency Virus Type 1 Infection. *N. Engl. J. Med.* 339, 33–39 (1998).

72. Vanhems, P. *et al.* Severity and Prognosis of Acute Human Immunodeficiency Virus Type 1 Illness: A Dose-Response Relationship. *Clin. Infect. Dis.* 26, 323–329 (1998).

73. Keet, I. P. M. *et al.* Predictors of rapid progression to AIDS in HIV-1 seroconverters. *AIDS* 7, 51–58 (1993).

74. Buttò, S., Raimondo, M., Fanales-Belasio, E. & Suligoi, B. Suggested strategies for the laboratory diagnosis of HIV infection in Italy. *Ann. dell'Ist. Super. di sanita* 46, 34–41 (2010).

75. Pantaleo, G. & Fauci, A. S. IMMUNOPATHOGENESIS OF HIV INFECTION1. *Annu. Rev. Microbiol.* 50, 825–854 (1996).

76. Ford, E. S., Puronen, C. E. & Sereti, I. Immunopathogenesis of asymptomatic chronic HIV Infection: the calm before the storm. *Curr. Opin. HIV AIDS* 4, 206–214 (2009).

77. Koup, R. A. *et al.* Temporal association of cellular immune responses with the initial control of viremia in primary human immunodeficiency virus type 1 syndrome. *J. Virol.* 68, 4650–4655 (1994).

78. Letvin, N. L. & Walker, B. D. Immunopathogenesis and immunotherapy in AIDS virus infections. *Nat. Med.* 9, 861–866 (2003).

79. Stamatatos, L., Morris, L., Burton, D. R. & Mascola, J. R. Neutralizing antibodies generated during natural HIV-1 infection: good news for an HIV-1 vaccine? *Nat. Med.* 15, 866–870 (2009).

80. Forthal, D. N. & Finzi, A. Antibody-dependent cellular cytotoxicity in HIV infection. *AIDS* 32, 2439–2451 (2018).

81. Sengupta, S. & Siliciano, R. F. Targeting the Latent Reservoir for HIV-1. *Immunity* 48, 872–895 (2018).

82. Fanales-Belasio, E., Raimondo, M., Suligoi, B. & Buttò, S. HIV virology and pathogenetic mechanisms of infection: a brief overview. *Ann. dell'Ist. Super. di sanita* 46, 5–14 (2010).

83. Furman, P. A. & Barry, D. W. Spectrum of antiviral activity and mechanism of action of zidovudine. An overview. *Am. J. Med.* 85, 176–81 (1988).

84. Broder, S. The development of antiretroviral therapy and its impact on the HIV-1/AIDS pandemic. *Antivir. Res.* 85, 1–18 (2010).

85. Deeks, S. G., Overbaugh, J., Phillips, A. & Buchbinder, S. HIV infection. *Nat. Rev. Dis. Prim.* 1, 15035 (2015).

86. Lee, N. E. & Sutherland, R. K. Lenacapavir and the novel HIV-1 capsid inhibitors: an emerging therapy in the management of multidrug-resistant HIV-1 virus. *Curr. Opin. Infect. Dis.* 36, 15–19 (2023).

87. Flexner, C., Owen, A., Siccardi, M. & Swindells, S. Long-acting drugs and formulations for the treatment and prevention of HIV infection. *Int. J. Antimicrob. Agents* 57, 106220 (2021).

88. Tang, M. W. & Shafer, R. W. HIV-1 Antiretroviral Resistance. *Drugs* 72, e1–e25 (2012).

89. Staszewski, S. *et al.* Virological and immunological analysis of a triple combination pilot study with loviride, lamivudine and zidovudine in HIV-1-infected patients. *AIDS* 10, F1–F7 (1996).

90. Arts, E. J. & Hazuda, D. J. HIV-1 Antiretroviral Drug Therapy. *Cold Spring Harb. Perspect. Med.* 2, a007161 (2012).

91. Palella, F. J. *et al.* Declining Morbidity and Mortality among Patients with Advanced Human Immunodeficiency Virus Infection. *N. Engl. J. Med.* 338, 853–860 (1998).

92. Palella, F. J. *et al.* Factors associated with mortality among persistently viraemic triple-antiretroviral-class-experienced patients receiving antiretroviral therapy in the HIV Outpatient Study (HOPS)*. *J. Antimicrob. Chemother.* 69, 2826–2834 (2014).

93. Rodger, A. J. *et al.* Risk of HIV transmission through condomless sex in serodifferent gay couples with the HIV-positive partner taking suppressive antiretroviral therapy (PARTNER): final results of a multicentre, prospective, observational study. *Lancet* 393, 2428–2438 (2019).

94. O'Brien, M. & Markowitz, M. Should We Treat Acute HIV Infection? *Curr. HIVAIDS Rep.* 9, 101–110 (2012).

95. Wong, J. K. *et al.* Recovery of Replication-Competent HIV Despite Prolonged Suppression of Plasma Viremia. *Science* 278, 1291–1295 (1997).

96. Finzi, D. *et al.* Identification of a Reservoir for HIV-1 in Patients on Highly Active Antiretroviral Therapy. *Science* 278, 1295–1300 (1997).

97. Chun, T.-W. *et al.* Presence of an inducible HIV-1 latent reservoir during highly active antiretroviral therapy. *Proc. Natl. Acad. Sci.* 94, 13193–13197 (1997).

98. Margolis, A. M., Heverling, H., Pham, P. A. & Stolbach, A. A Review of the Toxicity of HIV Medications. *J. Méd. Toxicol.* 10, 26–39 (2014).

99. Chun, T.-W. *et al.* In vivo fate of HIV-1-infected T cells: Quantitative analysis of the transition to stable latency. *Nat. Med.* 1, 1284–1290 (1995).

100. Blankson, J. N., Persaud, D. & Siliciano, R. F. THE CHALLENGE OF VIRAL RESERVOIRS IN HIV-1 INFECTION. *Annu. Rev. Med.* 53, 557–593 (2002).

101. Davey, R. T. *et al.* HIV-1 and T cell dynamics after interruption of highly active antiretroviral therapy (HAART) in patients with a history of sustained viral suppression. *Proc. Natl. Acad. Sci.* 96, 15109–15114 (1999).

102. Chun, T.-W., Davey, R. T., Engel, D., Lane, H. C. & Fauci, A. S. Re-emergence of HIV after stopping therapy. *Nature* 401, 874–875 (1999).

103. Barton, K., Winckelmann, A. & Palmer, S. HIV-1 Reservoirs During Suppressive Therapy. *Trends Microbiol.* 24, 345–355 (2016).

104. Ghosn, J. *et al.* Despite being highly diverse, immunovirological status strongly correlates with clinical symptoms during primary HIV-1 infection: a cross-sectional study based on 674 patients enrolled in the ANRS CO 06 PRIMO cohort. *J. Antimicrob. Chemother.* 65, 741–748 (2010).

105. Buzon, M. J. *et al.* HIV-1 persistence in CD4+ T cells with stem cell–like properties. *Nat. Med.* 20, 139–142 (2014).

106. Parisi, S. G. *et al.* Baseline Cellular HIV DNA Load Predicts HIV DNA Decline and Residual HIV Plasma Levels during Effective Antiretroviral Therapy. *J. Clin. Microbiol.* 50, 258–263 (2012).

107. Eisele, E. & Siliciano, R. F. Redefining the Viral Reservoirs that Prevent HIV-1 Eradication. *Immunity* 37, 377–388 (2012).

108. Vanhamel, J., Bruggemans, A. & Debyser, Z. Establishment of latent HIV-1 reservoirs: what do we really know? *J. virus Erad.* 5, 3–9 (2019).

109. Astorga-Gamaza, A. & Buzon, M. J. The active human immunodeficiency virus reservoir during antiretroviral therapy: emerging players in viral persistence. *Curr. Opin. HIV AIDS* 16, 193–199 (2021).

110. Serra-Peinado, C. *et al.* Expression of CD20 after viral reactivation renders HIV-reservoir cells susceptible to Rituximab. *Nat. Commun.* 10, 3705 (2019).

111. Abdel-Mohsen, M. *et al.* CD32 is expressed on cells with transcriptionally active HIV but does not enrich for HIV DNA in resting T cells. *Sci. Transl. Med.* 10, (2018).

112. Finzi, D. *et al.* Latent infection of CD4+ T cells provides a mechanism for lifelong persistence of HIV-1, even in patients on effective combination therapy. *Nat. Med.* 5, 512–517 (1999).

113. Chomont, N. *et al.* HIV reservoir size and persistence are driven by T cell survival and homeostatic proliferation. *Nat. Med.* 15, 893–900 (2009).

114. Chun, T.-W. *et al.* Quantification of latent tissue reservoirs and total body viral load in HIV-1 infection. *Nature* 387, 183–188 (1997).

115. Kulpa, D. A. *et al.* Differentiation into an Effector Memory Phenotype Potentiates HIV-1 Latency Reversal in CD4+ T Cells. *J. Virol.* 93, e00969-19 (2019).

116. Mahnke, Y. D., Brodie, T. M., Sallusto, F., Roederer, M. & Lugli, E. The who's who of T-cell differentiation: Human memory T-cell subsets. *Eur. J. Immunol.* 43, 2797–2809 (2013).

117. Grau-Expósito, J. *et al.* A Novel Single-Cell FISH-Flow Assay Identifies Effector Memory CD4+ T cells as a Major Niche for HIV-1 Transcription in HIV-Infected Patients. *mBio* 8, e00876-17 (2017).

118. Wonderlich, E. R. *et al.* Effector memory differentiation increases detection of replication-competent HIV-l in resting CD4+ T cells from virally suppressed individuals. *PLoS Pathog.* 15, e1008074 (2019).

119. Zerbato, J. M., McMahon, D. K., Sobolewski, M. D., Mellors, J. W. & Sluis-Cremer, N. Naive CD4+ T Cells Harbor a Large Inducible Reservoir of Latent, Replication-competent Human Immunodeficiency Virus Type 1. *Clin. Infect. Dis.* 69, 1919–1925 (2019).

120. Rullo, E. V. *et al.* Persistence of an intact HIV reservoir in phenotypically naive T cells. *JCI Insight* 5, e133157 (2020).

121. Ostrowski, M. A. *et al.* Both Memory and CD45RA + /CD62L + Naive CD4 + T Cells Are Infected in Human Immunodeficiency Virus Type 1-Infected Individuals. *J. Virol.* 73, 6430–6435 (1999).

122. Vrisekoop, N. *et al.* Sparse production but preferential incorporation of recently produced naïve T cells in the human peripheral pool. *Proc. Natl. Acad. Sci.* 105, 6115–6120 (2008).

123. Turner, D. L. & Farber, D. L. Mucosal Resident Memory CD4 T Cells in Protection and Immunopathology. *Front. Immunol.* 5, 331 (2014).

124. Cantero-Pérez, J. *et al.* Resident memory T cells are a cellular reservoir for HIV in the cervical mucosa. *Nat. Commun.* 10, 4739 (2019).

125. Kulpa, D. A. & Chomont, N. HIV persistence in the setting of antiretroviral therapy: when, where and how does HIV hide? *J. virus Erad.* 1, 59–66 (2015).

126. Sallusto, F. Heterogeneity of Human CD4+ T Cells Against Microbes. *Annu. Rev. Immunol.* 34, 317–334 (2016).

127. Lee, G. Q. *et al.* Clonal expansion of genome-intact HIV-1 in functionally polarized Th1 CD4+ T cells. *J. Clin. Investig.* 127, 2689–2696 (2017).

128. Romagnani, S. *et al.* Role of TH1/TH2 Cytokines in HIV Infection. *Immunol. Rev.* 140, 73–92 (1994).

129. Orlova-Fink, N. *et al.* Preferential susceptibility of Th9 and Th2 CD4+ T cells to X4-tropic HIV-1 infection. *AIDS* 31, 2211–2215 (2017).

130. Wacleche, V. S. *et al.* New insights into the heterogeneity of Th17 subsets contributing to HIV-1 persistence during antiretroviral therapy. *Retrovirology* 13, 59 (2016).

131. Gong, J., Zhan, H., Liang, Y., He, Q. & Cui, D. Role of Th22 Cells in Human Viral Diseases. *Front. Med.* 8, 708140 (2021).

132. Chevalier, M. F. & Weiss, L. The split personality of regulatory T cells in HIV infection. *Blood* 121, 29–37 (2013).

133. Dunay, G. A. *et al.* Assessment of the HIV-1 reservoir in CD4+ regulatory T cells by a Droplet Digital PCR based approach. *Virus Res.* 240, 107–111 (2017).

134. Perreau, M. *et al.* Follicular helper T cells serve as the major CD4 T cell compartment for HIV-1 infection, replication, and production. *J. Exp. Med.* 210, 143–156 (2013).

135. García, M. *et al.* Peripheral T follicular helper Cells Make a Difference in HIV Reservoir Size between Elite Controllers and Patients on Successful cART. *Sci. Rep.* 7, 16799 (2017).

136. Hendricks, C. M., Cordeiro, T., Gomes, A. P. & Stevenson, M. The Interplay of HIV-1 and Macrophages in Viral Persistence. *Front. Microbiol.* 12, 646447 (2021).

137. Coleman, C. M. & Wu, L. HIV interactions with monocytes and dendritic cells: viral latency and reservoirs. *Retrovirology* 6, 51 (2009).

138. Kandathil, A. J., Sugawara, S. & Balagopal, A. Are T cells the only HIV-1 reservoir? *Retrovirology* 13, 86 (2016).

139. Ellery, P. J. *et al.* The CD16+ Monocyte Subset Is More Permissive to Infection and Preferentially Harbors HIV-1 In Vivo. *J. Immunol.* 178, 6581–6589 (2007).

140. Cribbs, S. K., Lennox, J., Caliendo, A. M., Brown, L. A. & Guidot, D. M. Healthy HIV-1-Infected Individuals on Highly Active Antiretroviral Therapy Harbor HIV-1 in Their Alveolar Macrophages. *AIDS Res. Hum. Retroviruses* 31, 64–70 (2015).

141. Honeycutt, J. B. *et al.* Macrophages sustain HIV replication in vivo independently of T cells. *J. Clin. Investig.* 126, 1353–1366 (2016).

142. Trillo-Pazos, G. *et al.* Detection of HIV-1 DNA in Microglia/ Macrophages, Astrocytes and Neurons Isolated from Brain Tissue with HIV-1 Encephalitis by Laser Capture Microdissection. *Brain Pathol.* 13, 144–154 (2003).

143. Zalar, A. *et al.* Macrophage HIV-1 infection in duodenal tissue of patients on long term HAART. *Antivir. Res.* 87, 269–271 (2010).

144. Ganor, Y. *et al.* HIV-1 reservoirs in urethral macrophages of patients under suppressive antiretroviral therapy. *Nat. Microbiol.* 4, 633–644 (2019).

145. Manches, O., Frleta, D. & Bhardwaj, N. Dendritic cells in progression and pathology of HIV infection. *Trends Immunol.* 35, 114–122 (2014).

146. Westermann, J. & Pabst, R. Distribution of lymphocyte subsets and natural killer cells in the human body. *Clin. Investig.* 70, 539–544 (1992).

147. Yukl, S. A. *et al.* The Distribution of HIV DNA and RNA in Cell Subsets Differs in Gut and Blood of HIV-Positive Patients on ART: Implications for Viral Persistence. *J. Infect. Dis.* 208, 1212–1220 (2013).

148. Chaillon, A. *et al.* HIV persists throughout deep tissues with repopulation from multiple anatomical sources. *J. Clin. Investig.* 130, 1699–1712 (2020).

149. Wong, J. K. & Yukl, S. A. Tissue reservoirs of HIV. *Curr. Opin. HIV AIDS* 11, 362–370 (2016).

150. Cavert, W. *et al.* Kinetics of Response in Lymphoid Tissues to Antiretroviral Therapy of HIV-1 Infection. *Science* 276, 960–964 (1997).

151. Pantaleo, G. *et al.* HIV infection is active and progressive in lymphoid tissue during the clinically latent stage of disease. *Nature* 362, 355–358 (1993).

152. Folkvord, J. M., Armon, C. & Connick, E. Lymphoid Follicles Are Sites of Heightened Human Immunodeficiency Virus Type 1 (HIV-1) Replication and Reduced Antiretroviral Effector Mechanisms. *AIDS Res. Hum. Retroviruses* 21, 363–370 (2005).

153. Kohler, S. L. *et al.* Germinal Center T Follicular Helper Cells Are Highly Permissive to HIV-1 and Alter Their Phenotype during Virus Replication. *J. Immunol.* 196, 2711–2722 (2016).

154. Bronnimann, M. P., Skinner, P. J. & Connick, E. The B-Cell Follicle in HIV Infection: Barrier to a Cure. *Front. Immunol.* 9, 20 (2018).

155. Li, S. *et al.* Simian Immunodeficiency Virus-Producing Cells in Follicles Are Partially Suppressed by CD8 + Cells In Vivo. *J. Virol.* 90, 11168–11180 (2016).

156. Miles, B. *et al.* Follicular Regulatory CD8 T Cells Impair the Germinal Center Response in SIV and Ex Vivo HIV Infection. *PLoS Pathog.* 12, e1005924 (2016).

157. Fletcher, C. V. *et al.* Persistent HIV-1 replication is associated with lower antiretroviral drug concentrations in lymphatic tissues. *Proc. Natl. Acad. Sci.* 111, 2307–2312 (2014).

158. Klatt, N. R., Funderburg, N. T. & Brenchley, J. M. Microbial translocation, immune activation, and HIV disease. *Trends Microbiol.* 21, 6–13 (2013).

159. Mehandru, S. *et al.* Lack of Mucosal Immune Reconstitution during Prolonged Treatment of Acute and Early HIV-1 Infection. *PLoS Med.* 3, e484 (2006).

160. Yukl, S. A. *et al.* A comparison of methods for measuring rectal HIV levels suggests that HIV DNA resides in cells other than CD4+ T cells, including myeloid cells. *AIDS* 28, 439–442 (2014).

161. Belmonte, L. *et al.* The intestinal mucosa as a reservoir of HIV-1 infection after successful HAART. *AIDS* 21, 2106–2108 (2007).

162. Ellis, R. J. *et al.* Cerebrospinal fluid HIV RNA originates from both local CNS and systemic sources. *Neurology* 54, 927–936 (2000).

163. Kumar, A. M., Borodowsky, I., Fernandez, B., Gonzalez, L. & Kumar, M. Human immunodeficiency virus type 1 RNA Levels in different regions of human brain: Quantification using real-time reverse transcriptase-polymerase chain reaction. *J. NeuroVirology* 13, 210–224 (2007).

164. Peluso, M. J. *et al.* Cerebrospinal fluid HIV escape associated with progressive neurologic dysfunction in patients on antiretroviral therapy with well controlled plasma viral load. *AIDS* 26, 1765–1774 (2012).

165. Siliciano, R. F. & Greene, W. C. HIV Latency. *Cold Spring Harb. Perspect. Med.* 1, a007096 (2011).

166. Ananworanich, J. *et al.* HIV DNA Set Point is Rapidly Established in Acute HIV Infection and Dramatically Reduced by Early ART. *EBioMedicine* 11, 68–72 (2016).

167. Castro-Gonzalez, S., Colomer-Lluch, M. & Serra-Moreno, R. Barriers for HIV Cure: The Latent Reservoir. *AIDS Res. Hum. Retroviruses* 34, 739–759 (2018).

168. Colin, L. & Lint, C. V. Molecular control of HIV-1 postintegration latency: implications for the development of new therapeutic strategies. *Retrovirology* 6, 111 (2009).

169. Chun, T.-W. *et al.* Gene expression and viral prodution in latently infected, resting CD4+ T cells in viremic versus aviremic HIV-infected individuals. *Proc. Natl. Acad. Sci.* 100, 1908–1913 (2003).

170. Shan, L. *et al.* Transcriptional Reprogramming during Effector-to-Memory Transition Renders CD4+ T Cells Permissive for Latent HIV-1 Infection. *Immunity* 47, 766-775.e3 (2017).

171. Zack, J. A. *et al.* HIV-1 entry into quiescent primary lymphocytes: Molecular analysis reveals a labile, latent viral structure. *Cell* 61, 213–222 (1990).

172. Pierson, T. C. *et al.* Molecular Characterization of Preintegration Latency in Human Immunodeficiency Virus Type 1 Infection. *J. Virol.* 76, 8518–8531 (2002).

173. Siliciano, J. D. *et al.* Long-term follow-up studies confirm the stability of the latent reservoir for HIV-1 in resting CD4+ T cells. *Nat. Med.* 9, 727–728 (2003).

174. Coiras, M., López-Huertas, M. R., Pérez-Olmeda, M. & Alcamí, J. Understanding HIV-1 latency provides clues for the eradication of long-term reservoirs. *Nat. Rev. Microbiol.* 7, 798–812 (2009).

175. Richman, D. D. *et al.* The Challenge of Finding a Cure for HIV Infection. *Science* 323, 1304–1307 (2009).

176. Festenstein, R. *et al.* Modulation of Heterochromatin Protein 1 Dynamics in Primary Mammalian Cells. *Science* 299, 719–721 (2003).

177. Han, Y. *et al.* Resting CD4 + T Cells from Human Immunodeficiency Virus Type 1 (HIV-1)-Infected Individuals Carry Integrated HIV-1 Genomes within Actively Transcribed Host Genes. *J. Virol.* 78, 6122–6133 (2004).

178. Battistini, A. & Sgarbanti, M. HIV-1 Latency: An Update of Molecular Mechanisms and Therapeutic Strategies. *Viruses* 6, 1715–1758 (2014).

179. Cary, D. C., Fujinaga, K. & Peterlin, B. M. Molecular mechanisms of HIV latency. *J. Clin. Investig.* 126, 448–454 (2016).

180. Blazkova, J. *et al.* CpG Methylation Controls Reactivation of HIV from Latency. *PLoS Pathog.* 5, e1000554 (2009).

181. Kauder, S. E., Bosque, A., Lindqvist, A., Planelles, V. & Verdin, E. Epigenetic Regulation of HIV-1 Latency by Cytosine Methylation. *PLoS Pathog.* 5, e1000495 (2009).

182. Lusic, M., Marcello, A., Cereseto, A. & Giacca, M. Regulation of HIV-1 gene expression by histone acetylation and factor recruitment at the LTR promoter. *EMBO J.* 22, 6550–6561 (2003).

183. Li, Z. *et al.* The KAT5-Acetyl-Histone4-Brd4 axis silences HIV-1 transcription and promotes viral latency. *PLoS Pathog.* 14, e1007012 (2018).

184. Jiang, C. *et al.* Distinct viral reservoirs in individuals with spontaneous control of HIV-1. *Nature* 585, 261–267 (2020).

185. Donahue, D. A. & Wainberg, M. A. Cellular and molecular mechanisms involved in the establishment of HIV-1 latency. *Retrovirology* 10, 11 (2013).

186. Lenasi, T., Contreras, X. & Peterlin, B. M. Transcriptional Interference Antagonizes Proviral Gene Expression to Promote HIV Latency. *Cell Host Microbe* 4, 123–133 (2008).

187. Han, Y. *et al.* Orientation-Dependent Regulation of Integrated HIV-1 Expression by Host Gene Transcriptional Readthrough. *Cell Host Microbe* 4, 134–146 (2008).

188. Einkauf, K. B. *et al.* Intact HIV-1 proviruses accumulate at distinct chromosomal positions during prolonged antiretroviral therapy. *J. Clin. Investig.* 129, 988–998 (2019).

189. Pasternak, A. O. & Berkhout, B. The Splice of Life: Does RNA Processing Have a Role in HIV-1 Persistence? *Viruses* 13, 1751 (2021).

190. Moron-Lopez, S. *et al.* Human splice factors contribute to latent HIV infection in primary cell models and blood CD4+ T cells from ART-treated individuals. *PLoS Pathog.* 16, e1009060 (2020).

191. Lassen, K. G., Ramyar, K. X., Bailey, J. R., Zhou, Y. & Siliciano, R. F. Nuclear Retention of Multiply Spliced HIV-1 RNA in Resting CD4+ T Cells. *PLoS Pathog.* 2, e68 (2006).

192. Ne, E., Palstra, R.-J. & Mahmoudi, T. Chapter Six Transcription: Insights From the HIV-1 Promoter. *Int. Rev. Cell Mol. Biol.* 335, 191–243 (2018).

193. McManus, W. R. *et al.* HIV-1 in lymph nodes is maintained by cellular proliferation during antiretroviral therapy. *J. Clin. Investig.* 129, 4629–4642 (2019).

194. Wiegand, A. *et al.* Single-cell analysis of HIV-1 transcriptional activity reveals expression of proviruses in expanded clones during ART. *Proc. Natl. Acad. Sci.* 114, E3659–E3668 (2017).

195. Hermankova, M. *et al.* Analysis of Human Immunodeficiency Virus Type 1 Gene Expression in Latently Infected Resting CD4 + T Lymphocytes In Vivo. *J. Virol.* 77, 7383–7392 (2003).

196. Kearney, M. F. *et al.* Origin of Rebound Plasma HIV Includes Cells with Identical Proviruses That Are Transcriptionally Active before Stopping of Antiretroviral Therapy. *J. Virol.* 90, 1369–1376 (2016).

197. Wagner, T. A. *et al.* Proliferation of cells with HIV integrated into cancer genes contributes to persistent infection. *Science* 345, 570–573 (2014).

198. Simonetti, F. R. *et al.* Clonally expanded CD4+ T cells can produce infectious HIV-1 in vivo. *Proc. Natl. Acad. Sci.* 113, 1883–1888 (2016).

199. Maldarelli, F. *et al.* Specific HIV integration sites are linked to clonal expansion and persistence of infected cells. *Science* 345, 179–183 (2014).

200. Cohn, L. B. *et al.* HIV-1 Integration Landscape during Latent and Active Infection. *Cell* 160, 420–432 (2015).

201. Henrich, T. J. *et al.* HIV-1 persistence following extremely early initiation of antiretroviral therapy (ART) during acute HIV-1 infection: An observational study. *PLoS Med.* 14, e1002417 (2017).

202. Palmer, S. *et al.* Low-level viremia persists for at least 7 years in patients on suppressive antiretroviral therapy. *Proc. Natl. Acad. Sci.* 105, 3879–3884 (2008).

203. Palmer, S. *et al.* New Real-Time Reverse Transcriptase-Initiated PCR Assay with Single-Copy Sensitivity for Human Immunodeficiency Virus Type 1 RNA in Plasma. *J. Clin. Microbiol.* 41, 4531–4536 (2003).

204. Lorenzo-Redondo, R. *et al.* Persistent HIV-1 replication maintains the tissue reservoir during therapy. *Nature* 530, 51–56 (2016).

205. Walker, B. & McMichael, A. The T-Cell Response to HIV. *Cold Spring Harb. Perspect. Med.* 2, a007054 (2012).

206. Balasubramaniam, M. *et al.* HIV-1 mutants that escape the cytotoxic T-lymphocytes are defective in viral DNA integration. *PNAS Nexus* 1, pgac064 (2022).

207. Yang, O. O. *et al.* Determinants of HIV-1 Mutational Escape From Cytotoxic T Lymphocytes. *J. Exp. Med.* 197, 1365–1375 (2003).

208. Kahan, S. M., Wherry, E. J. & Zajac, A. J. T cell exhaustion during persistent viral infections. *Virology* 479, 180–193 (2015).

209. Nabatanzi, R. *et al.* Aberrant natural killer (NK) cell activation and dysfunction among ART-treated HIV-infected adults in an African cohort. *Clin. Immunol.* 201, 55–60 (2019).

210. Lichtfuss, G. F. *et al.* Virologically Suppressed HIV Patients Show Activation of NK Cells and Persistent Innate Immune Activation. *J. Immunol.* 189, 1491–1499 (2012).

211. Zhang, Z.-Q. *et al.* Kinetics of CD4+ T cell repopulation of lymphoid tissues after treatment of HIV-1 infection. *Proc. Natl. Acad. Sci.* 95, 1154–1159 (1998).

212. Strain, M. C. *et al.* Effect of Treatment, during Primary Infection, on Establishment and Clearance of Cellular Reservoirs of HIV-1. *J. Infect. Dis.* 191, 1410–1418 (2005).

213. Sahu, G. K., Sarria, J. C. & Cloyd, M. W. Recovery of Replication-Competent Residual HIV-1 from Plasma of a Patient Receiving Prolonged, Suppressive Highly Active Antiretroviral Therapy. *J. Virol.* 84, 8348–8352 (2010).

214. Tosiano, M. A., Jacobs, J. L., Shutt, K. A., Cyktor, J. C. & Mellors, J. W. A Simpler and More Sensitive Single-Copy HIV-1 RNA Assay for Quantification of Persistent HIV-1 Viremia in Individuals on Suppressive Antiretroviral Therapy. *J. Clin. Microbiol.* 57, (2019).

215. Amendola, A. *et al.* Standardization and performance evaluation of “modified” and “ultrasensitive” versions of the Abbott RealTime HIV-1 assay, adapted to quantify minimal residual viremia. *J. Clin. Virol.* 52, 17–22 (2011).

216. Cillo, A. R. *et al.* Improved Single-Copy Assays for Quantification of Persistent HIV-1 Viremia in Patients on Suppressive Antiretroviral Therapy. *J. Clin. Microbiol.* 52, 3944–3951 (2014).

217. Williams, J. P. *et al.* HIV-1 DNA predicts disease progression and post-treatment virological control. *eLife* 3, e03821 (2014).

218. Yerly, S. *et al.* Proviral HIV-DNA predicts viral rebound and viral setpoint after structured treatment interruptions. *AIDS* 18, 1951–1953 (2004).

219. Rouzioux, C., Mélard, A. & Avéttand-Fénoël, V. Human Retroviruses, Methods and Protocols. *Methods Mol. Biol.* 1087, 261–270 (2013).

220. Hindson, B. J. *et al.* High-Throughput Droplet Digital PCR System for Absolute Quantitation of DNA Copy Number. *Anal. Chem.* 83, 8604–8610 (2011).

221. Strain, M. C. *et al.* Highly Precise Measurement of HIV DNA by Droplet Digital PCR. *PLoS ONE* 8, e55943 (2013).

222. Bosman, K. J. *et al.* Comparison of digital PCR platforms and semi-nested qPCR as a tool to determine the size of the HIV reservoir. *Sci. Rep.* 5, 13811 (2015).

223. Rozera, G. *et al.* Comparison of real-time PCR methods for measurement of HIV-1 proviral DNA. *J. Virol. Methods* 164, 135–138 (2010).

224. Eriksson, S. *et al.* Comparative Analysis of Measures of Viral Reservoirs in HIV-1 Eradication Studies. *PLoS Pathog.* 9, e1003174 (2013).

225. Koelsch, K. K. *et al.* Dynamics of Total, Linear Nonintegrated, and Integrated HIV-1 DNA In Vivo and In Vitro. *J. Infect. Dis.* 197, 411–419 (2008).

226. O'Doherty, U., Swiggard, W. J., Jeyakumar, D., McGain, D. & Malim, M. H. A Sensitive, Quantitative Assay for Human Immunodeficiency Virus Type 1 Integration. *J. Virol.* 76, 10942–10950 (2002).

227. Liszewski, M. K., Yu, J. J. & O'Doherty, U. Detecting HIV-1 integration by repetitive-sampling Alu-gag PCR. *Methods* 47, 254–260 (2009).

228. Bruner, K. M. *et al.* Defective proviruses rapidly accumulate during acute HIV-1 infection. *Nat. Med.* 22, 1043–1049 (2016).

229. Bruner, K. M. *et al.* A quantitative approach for measuring the reservoir of latent HIV-1 proviruses. *Nature* 566, 120–125 (2019).

230. Kinloch, N. N. *et al.* HIV-1 diversity considerations in the application of the Intact Proviral DNA Assay (IPDA). *Nat. Commun.* 12, 165 (2021).

231. Imamichi, H. *et al.* Defective HIV-1 proviruses produce novel protein-coding RNA species in HIV-infected patients on combination antiretroviral therapy. *Proc. Natl. Acad. Sci.* 113, 8783–8788 (2016).

232. Procopio, F. A. *et al.* A Novel Assay to Measure the Magnitude of the Inducible Viral Reservoir in HIV-infected Individuals. *EBioMedicine* 2, 874–883 (2015).

233. Zhang, W., Akusjärvi, S. S., Sönnerborg, A. & Neogi, U. Characterization of Inducible Transcription and Translation-Competent HIV-1 Using the RNAscope ISH Technology at a Single-Cell Resolution. *Front. Microbiol.* 9, 2358 (2018).

234. Chang, L. *et al.* Single molecule enzyme-linked immunosorbent assays: Theoretical considerations. *J. Immunol. Methods* 378, 102–115 (2012).

235. Rissin, D. M. *et al.* Single-molecule enzyme-linked immunosorbent assay detects serum proteins at subfemtomolar concentrations. *Nat. Biotechnol.* 28, 595–599 (2010).

236. Richter, E. *et al.* CROI 2024 - Ultra-Low Level HIV p24 Production as a Driver of Immune Activation in Individuals Treated with ART. (2024).

237. Baxter, A. E. *et al.* Single-Cell Characterization of Viral Translation-Competent Reservoirs in HIV-Infected Individuals. *Cell Host Microbe* 20, 368–380 (2016).

238. Siliciano, J. D. & Siliciano, R. F. Human Retrovirus Protocols, Virology and Molecular Biology. *Methods Mol. Biol. (Clifton, NJ)* 304, 3–15 (2005).

239. Abdel-Mohsen, M. *et al.* Recommendations for measuring HIV reservoir size in cure-directed clinical trials. *Nat. Med.* 26, 1339–1350 (2020).

240. Laird, G. M. *et al.* Rapid Quantification of the Latent Reservoir for HIV-1 Using a Viral Outgrowth Assay. *PLoS Pathog.* 9, e1003398 (2013).

241. Ho, Y.-C. *et al.* Replication-Competent Noninduced Proviruses in the Latent Reservoir Increase Barrier to HIV-1 Cure. *Cell* 155, 540–551 (2013).

242. Pate, K. A. M. *et al.* A Murine Viral Outgrowth Assay to Detect Residual HIV Type 1 in Patients With Undetectable Viral Loads. *J. Infect. Dis.* 212, 1387–1396 (2015).

243. Altfeld, M. & Jr, M. G. Innate immunity against HIV-1 infection. *Nat. Immunol.* 16, 554–562 (2015).

244. Rustagi, A. & Gale, M. Innate Antiviral Immune Signaling, Viral Evasion and Modulation by HIV-1. *J. Mol. Biol.* 426, 1161–1177 (2014).

245. Loo, Y.-M. & Gale, M. Immune Signaling by RIG-I-like Receptors. *Immunity* 34, 680–692 (2011).

246. Kawai, T. & Akira, S. The role of pattern-recognition receptors in innate immunity: update on Toll-like receptors. *Nat. Immunol.* 11, 373–384 (2010).

247. Iwasaki, A. & Medzhitov, R. Regulation of Adaptive Immunity by the Innate Immune System. *Science* 327, 291–295 (2010).

248. Jakobsen, M. R. *et al.* IFI16 senses DNA forms of the lentiviral replication cycle and controls HIV-1 replication. *Proc. Natl. Acad. Sci.* 110, E4571–E4580 (2013).

249. Gao, D. *et al.* Cyclic GMP-AMP Synthase Is an Innate Immune Sensor of HIV and Other Retroviruses. *Science* 341, 903–906 (2013).

250. Mogensen, T. H., Melchjorsen, J., Larsen, C. S. & Paludan, S. R. Innate immune recognition and activation during HIV infection. *Retrovirology* 7, 54 (2010).

251. Schoggins, J. W. *et al.* A diverse range of gene products are effectors of the type I interferon antiviral response. *Nature* 472, 481–485 (2011).

252. Stetson, D. B. & Medzhitov, R. Type I Interferons in Host Defense. *Immunity* 25, 373–381 (2006).

253. Monroe, K. M. *et al.* IFI16 DNA Sensor Is Required for Death of Lymphoid CD4 T Cells Abortively Infected with HIV. *Science* 343, 428–432 (2014).

254. Akira, S., Uematsu, S. & Takeuchi, O. Pathogen Recognition and Innate Immunity. *Cell* 124, 783–801 (2006).

255. Iwasaki, A. Innate Immune Recognition of HIV-1. *Immunity* 37, 389–398 (2012).

256. Chang, J. J. & Altfeld, M. Innate Immune Activation in Primary HIV-1 Infection. *J. Infect. Dis.* 202, S297–S301 (2010).

257. Tomescu, C., Chehimi, J., Maino, V. C. & Montaner, L. J. NK Cell Lysis of HIV-1-Infected Autologous CD4 Primary T Cells: Requirement for IFN-Mediated NK Activation by Plasmacytoid Dendritic Cells. *J. Immunol.* 179, 2097–2104 (2007).

258. Flórez-Álvarez, L., Hernandez, J. C. & Zapata, W. NK Cells in HIV-1 Infection: From Basic Science to Vaccine Strategies. *Front. Immunol.* 9, 2290 (2018).

259. McMichael, A. J., Borrow, P., Tomaras, G. D., Goonetilleke, N. & Haynes, B. F. The immune response during acute HIV-1 infection: clues for vaccine development. *Nat. Rev. Immunol.* 10, 11–23 (2010).

260. Kazer, S. W., Walker, B. D. & Shalek, A. K. Evolution and Diversity of Immune Responses during Acute HIV Infection. *Immunity* 53, 908–924 (2020).

261. Tomaras, G. D. *et al.* Initial B-Cell Responses to Transmitted Human Immunodeficiency Virus Type 1: Virion-Binding Immunoglobulin M (IgM) and IgG Antibodies Followed by Plasma Anti-gp41 Antibodies with Ineffective Control of Initial Viremia. *J. Virol.* 82, 12449–12463 (2008).

262. Schmitz, J. E. *et al.* Effect of Humoral Immune Responses on Controlling Viremia during Primary Infection of Rhesus Monkeys with Simian Immunodeficiency Virus. *J. Virol.* 77, 2165–2173 (2003).

263. McMichael, A. J. & Rowland-Jones, S. L. Cellular immune responses to HIV. *Nature* 410, 980–987 (2001).

264. Yue, F. Y. *et al.* Virus-Specific Interleukin-17-Producing CD4 + T Cells Are Detectable in Early Human Immunodeficiency Virus Type 1 Infection. *J. Virol.* 82, 6767–6771 (2008).

265. Arthos, J. *et al.* HIV-1 envelope protein binds to and signals through integrin α4β7, the gut mucosal homing receptor for peripheral T cells. *Nat. Immunol.* 9, 301–309 (2008).

266. Walker, C. M., Moody, D. J., Stites, D. P. & Levy, J. A. CD8+ Lymphocytes Can Control HIV Infection in Vitro by Suppressing Virus Replication. *Science* 234, 1563–1566 (1986).

267. Miedema, F. T cell dynamics and protective immunity in HIV infection: a brief history of ideas. *Curr. Opin. HIV AIDS* 1, 1–2 (2006).

268. Demers, K. R. *et al.* Temporal Dynamics of CD8+ T Cell Effector Responses during Primary HIV Infection. *PLoS Pathog.* 12, e1005805 (2016).

269. Lichterfeld, M. *et al.* HIV-1 Nef is preferentially recognized by CD8 T cells in primary HIV-1 infection despite a relatively high degree of genetic diversity. *AIDS* 18, 1383–1392 (2004).

270. Cocchi, F. *et al.* Identification of RANTES, MIP-1α, and MIP-1β as the Major HIV-Suppressive Factors Produced by CD8+ T Cells. *Science* 270, 1811–1815 (1995).

271. Liu, J. *et al.* IL-10-Producing B Cells Are Induced Early in HIV-1 Infection and Suppress HIV-1-Specific T Cell Responses. *PLoS ONE* 9, e89236 (2014).

272. Eller, M. A. *et al.* Expansion of Inefficient HIV-Specific CD8 T Cells during Acute Infection. *J. Virol.* 90, 4005–4016 (2016).

273. Caligiuri, M. A. Human natural killer cells. *Blood* 112, 461–469 (2008).

274. Vivier, E., Tomasello, E., Baratin, M., Walzer, T. & Ugolini, S. Functions of natural killer cells. *Nat. Immunol.* 9, 503–510 (2008).

275. Carrega, P. & Ferlazzo, G. Natural killer cell distribution and trafficking in human tissues. *Front. Immunol.* 3, 347 (2012).

276. Klose, C. S. N. & Artis, D. Innate lymphoid cells control signaling circuits to regulate tissue-specific immunity. *Cell Res.* 30, 475–491 (2020).

277. Spits, H. & Santo, J. P. D. The expanding family of innate lymphoid cells: regulators and effectors of immunity and tissue remodeling. *Nat. Immunol.* 12, 21–27 (2011).

278. Blum, K. S. & Pabst, R. Lymphocyte numbers and subsets in the human blood Do they mirror the situation in all organs? *Immunol. Lett.* 108, 45–51 (2007).

279. Tognarelli, E. I. *et al.* Natural Killer T Cell Diversity and Immunotherapy. *Cancers* 15, 5737 (2023).

280. Freud, A. G., Yu, J. & Caligiuri, M. A. Human natural killer cell development in secondary lymphoid tissues. *Semin. Immunol.* 26, 132–137 (2014).

281. Cichocki, F., Grzywacz, B. & Miller, J. S. Human NK Cell Development: One Road or Many? *Front. Immunol.* 10, 2078 (2019).

282. Yu, J., Freud, A. G. & Caligiuri, M. A. Location and cellular stages of natural killer cell development. *Trends Immunol.* 34, 573–582 (2013).

283. Ran, G. he *et al.* Natural killer cell homing and trafficking in tissues and tumors: from biology to application. *Signal Transduct. Target. Ther.* 7, 205 (2022).

284. Michel, T. *et al.* Human CD56bright NK Cells: An Update. *J. Immunol.* 196, 2923–2931 (2016).

285. Cooper, M. A., Fehniger, T. A. & Caligiuri, M. A. The biology of human natural killer-cell subsets. *Trends Immunol.* 22, 633–640 (2001).

286. Ferlazzo, G. & Münz, C. NK Cell Compartments and Their Activation by Dendritic Cells. *J. Immunol.* 172, 1333–1339 (2004).

287. Anfossi, N. *et al.* Human NK Cell Education by Inhibitory Receptors for MHC Class I. *Immunity* 25, 331–342 (2006).

288. Moretta, L. Dissecting CD56dim human NK cells. *Blood* 116, 3689–3691 (2010).

289. Sivori, S. *et al.* IL-21 induces both rapid maturation of human CD34+ cell precursors towards NK cells and acquisition of surface killer Ig-like receptors. *Eur. J. Immunol.* 33, 3439–3447 (2003).

290. Horowitz, A. *et al.* Genetic and Environmental Determinants of Human NK Cell Diversity Revealed by Mass Cytometry. *Sci. Transl. Med.* 5, 208ra145 (2013).

291. Shankar, K., Capitini, C. M. & Saha, K. Genome engineering of induced pluripotent stem cells to manufacture natural killer cell therapies. *Stem Cell Res. Ther.* 11, 234 (2020).

292. Quatrini, L. *et al.* Human NK cells, their receptors and function. *Eur. J. Immunol.* 51, 1566–1579 (2021).

293. Sivori, S. *et al.* Human NK cells: surface receptors, inhibitory checkpoints, and translational applications. *Cell. Mol. Immunol.* 16, 430–441 (2019).

294. Ochoa, M. C. *et al.* Antibody-dependent cell cytotoxicity: immunotherapy strategies enhancing effector NK cells. *Immunol. Cell Biol.* 95, 347–355 (2017).

295. Siemaszko, J., Marzec-Przyszlak, A. & Bogunia-Kubik, K. Activating NKG2C Receptor: Functional Characteristics and Current Strategies in Clinical Applications. *Arch. Immunol. Ther. Exp.* 71, 9 (2023).

296. Lopez-Vergès, S. *et al.* Expansion of a unique CD57+NKG2Chi natural killer cell subset during acute human cytomegalovirus infection. *Proc. Natl. Acad. Sci.* 108, 14725–14732 (2011).

297. Gang, M., Wong, P., Berrien-Elliott, M. M. & Fehniger, T. A. Memory-like natural killer cells for cancer immunotherapy. *Semin. Hematol.* 57, 185–193 (2020).

298. Kim, S. *et al.* Licensing of natural killer cells by host major histocompatibility complex class I molecules. *Nature* 436, 709–713 (2005).

299. Colonna, M. & Samaridis, J. Cloning of Immunoglobulin-Superfamily Members Associated with HLA-C and HLA-B Recognition by Human Natural Killer Cells. *Science* 268, 405–408 (1995).

300. Dębska-Zielkowska, J. *et al.* KIR Receptors as Key Regulators of NK Cells Activity in Health and Disease. *Cells* 10, 1777 (2021).

301. Moradi, S. *et al.* The Structure of the Atypical Killer Cell Immunoglobulin-like Receptor, KIR2DL4*. *J. Biol. Chem.* 290, 10460–10471 (2015).

302. Middleton, D. & Gonzelez, F. The extensive polymorphism of KIR genes. *Immunology* 129, 8–19 (2010).

303. Braud, V. M. *et al.* HLA-E binds to natural killer cell receptors CD94/NKG2A, B and C. *Nature* 391, 795–799 (1998).

304. André, P. *et al.* Anti-NKG2A mAb Is a Checkpoint Inhibitor that Promotes Anti-tumor Immunity by Unleashing Both T and NK Cells. *Cell* 175, 1731-1743.e13 (2018).

305. Shannon, M. J. & Mace, E. M. Natural Killer Cell Integrins and Their Functions in Tissue Residency. *Front. Immunol.* 12, 647358 (2021).

306. Spriel, A. B. van *et al.* Mac-1 (CD11b/CD18) is essential for Fc receptor–mediated neutrophil cytotoxicity and immunologic synapse formation. *Blood* 97, 2478–2486 (2001).

307. Zwirner, N. W. & Ziblat, A. Regulation of NK Cell Activation and Effector Functions by the IL-12 Family of Cytokines: The Case of IL-27. *Front. Immunol.* 8, 25 (2017).

308. Hawke, L. G., Mitchell, B. Z. & Ormiston, M. L. TGF-β and IL-15 Synergize through MAPK Pathways to Drive the Conversion of Human NK Cells to an Innate Lymphoid Cell 1-like Phenotype. *J. Immunol. (Baltim., Md : 1950)* 204, 3171–3181 (2019).

309. Metkar, S. S. *et al.* Cytotoxic Cell Granule-Mediated Apoptosis Perforin Delivers Granzyme B-Serglycin Complexes into Target Cells without Plasma Membrane Pore Formation. *Immunity* 16, 417–428 (2002).

310. Krzewski, K., Gil-Krzewska, A., Nguyen, V., Peruzzi, G. & Coligan, J. E. LAMP1/CD107a is required for efficient perforin delivery to lytic granules and NK-cell cytotoxicity. *Blood* 121, 4672–4683 (2013).

311. Cohnen, A. *et al.* Surface CD107a/LAMP-1 protects natural killer cells from degranulation-associated damage. *Blood* 122, 1411–1418 (2013).

312. Alter, G., Malenfant, J. M. & Altfeld, M. CD107a as a functional marker for the identification of natural killer cell activity. *J. Immunol. Methods* 294, 15–22 (2004).

313. Fauriat, C., Long, E. O., Ljunggren, H.-G. & Bryceson, Y. T. Regulation of human NK-cell cytokine and chemokine production by target cell recognition. *Blood* 115, 2167–2176 (2010).

314. Mah, A. Y. & Cooper, M. A. Metabolic Regulation of Natural Killer Cell IFN-γ Production. *Crit. Rev. Immunol.* 36, 131–147 (2016).

315. Jost, S. *et al.* Antigen-specific memory NK cell responses against HIV and influenza use the NKG2/HLA-E axis. *Sci. Immunol.* 8, eadi3974 (2023).

316. Stary, V. & Stary, G. NK Cell-Mediated Recall Responses: Memory-Like, Adaptive, or Antigen-Specific? *Front. Cell. Infect. Microbiol.* 10, 208 (2020).

317. Fauci, A. S., Mavilio, D. & Kottilil, S. NK cells in HIV infection: Paradigm for protection or targets for ambush. *Nat. Rev. Immunol.* 5, 835–843 (2005).

318. BANDYOPADHYAY, S. *et al.* Natural killer cell-mediated lysis of T cell lines chronically infected with HIV-1. *Clin. Exp. Immunol.* 79, 430–435 (1990).

319. Oliva, A. *et al.* Natural killer cells from human immunodeficiency virus (HIV)-infected individuals are an important source of CC-chemokines and suppress HIV-1 entry and replication in vitro. *J. Clin. Investig.* 102, 223–231 (1998).

320. Flores-Villanueva, P. O. *et al.* Control of HIV-1 viremia and protection from AIDS are associated with HLA-Bw4 homozygosity. *Proc. Natl. Acad. Sci.* 98, 5140–5145 (2001).

321. Martin, M. P. *et al.* Epistatic interaction between KIR3DS1 and HLA-B delays the progression to AIDS. *Nat. Genet.* 31, 429–434 (2002).

322. Mavilio, D. *et al.* Natural killer cells in HIV-1 infection: Dichotomous effects of viremia on inhibitory and activating receptors and their functional correlates. *Proc. Natl. Acad. Sci.* 100, 15011–15016 (2003).

323. Kottilil, S. *et al.* Expression of Chemokine and Inhibitory Receptors on Natural Killer Cells: Effect of Immune Activation and HIV Viremia. *J. Infect. Dis.* 189, 1193–1198 (2004).

324. Maria, A. D. *et al.* The impaired NK cell cytolytic function in viremic HIV-1 infection is associated with a reduced surface expression of natural cytotoxicity receptors (NKp46, NKp30 and NKp44). *Eur. J. Immunol.* 33, 2410–2418 (2003).

325. Mavilio, D. *et al.* Characterization of CD56–/CD16+ natural killer (NK) cells: A highly dysfunctional NK subset expanded in HIV-infected viremic individuals. *Proc. Natl. Acad. Sci.* 102, 2886–2891 (2005).

326. Kottilil, S. *et al.* Innate Immunity in Human Immunodeficiency Virus Infection: Effect of Viremia on Natural Killer Cell Function. *J. Infect. Dis.* 187, 1038–1045 (2003).

327. Jost, S. & Altfeld, M. Evasion from NK cell-mediated immune responses by HIV-1. *Microbes Infect.* 14, 904–915 (2012).

328. Ahmad, A. & Menezes, J. Antibody-dependent cellular cytotoxicity in HIV infections. *FASEB J.* 10, 258–266 (1996).

329. Chung, A. W. *et al.* Immune escape from HIV-specific antibody-dependent cellular cytotoxicity (ADCC) pressure. *Proc. Natl. Acad. Sci.* 108, 7505–7510 (2011).

330. Madhavi, V. *et al.* Antibody-Dependent Effector Functions Against HIV Decline in Subjects Receiving Antiretroviral Therapy. *J. Infect. Dis.* 211, 529–538 (2015).

331. Hartana, C. A. & Yu, X. G. Immunological effector mechanisms in HIV-1 elite controllers. *Curr. Opin. HIV AIDS* 16, 243–248 (2021).

332. Lambotte, O. *et al.* HIV Controllers: A Homogeneous Group of HIV-1--Infected Patients with Spontaneous Control of Viral Replication. *Clin. Infect. Dis.* 41, 1053–1056 (2005).

333. O'Connell, K. A. *et al.* Control of HIV-1 in Elite Suppressors despite Ongoing Replication and Evolution in Plasma Virus. *J. Virol.* 84, 7018–7028 (2010).

334. Deeks, S. G. & Walker, B. D. Human Immunodeficiency Virus Controllers: Mechanisms of Durable Virus Control in the Absence of Antiretroviral Therapy. *Immunity* 27, 406–416 (2007).

335. Autran, B., Descours, B., Avettand-Fenoel, V. & Rouzioux, C. Elite controllers as a model of functional cure. *Curr. Opin. HIV AIDS* 6, 181–187 (2011).

336. Walker, B. D. & Yu, X. G. Unravelling the mechanisms of durable control of HIV-1. *Nat. Rev. Immunol.* 13, 487–498 (2013).

337. Study, I. H. C. *et al.* The Major Genetic Determinants of HIV-1 Control Affect HLA Class I Peptide Presentation. *Science* 330, 1551–1557 (2010).

338. Chan, H. Y. *et al.* A T Cell Receptor Sequencing-Based Assay Identifies Cross-Reactive Recall CD8+ T Cell Clonotypes Against Autologous HIV-1 Epitope Variants. *Front. Immunol.* 11, 591 (2020).

339. Gaiha, G. D. *et al.* Structural topology defines protective CD8+ T cell epitopes in the HIV proteome. *Science* 364, 480–484 (2019).

340. Collins, D. R., Gaiha, G. D. & Walker, B. D. CD8+ T cells in HIV control, cure and prevention. *Nat. Rev. Immunol.* 20, 471–482 (2020).

341. Migueles, S. A. *et al.* HIV-specific CD8+ T cell proliferation is coupled to perforin expression and is maintained in nonprogressors. *Nat. Immunol.* 3, 1061–1068 (2002).

342. Betts, M. R. *et al.* HIV nonprogressors preferentially maintain highly functional HIV-specific CD8+ T cells. *Blood* 107, 4781–4789 (2006).

343. Shasha, D. *et al.* Elite controller CD8+ T cells exhibit comparable viral inhibition capacity, but better sustained effector properties compared to chronic progressors. *J. Leukoc. Biol.* 100, 1425–1433 (2016).

344. Monel, B. *et al.* HIV Controllers Exhibit Effective CD8+ T Cell Recognition of HIV-1-Infected Non-activated CD4+ T Cells. *Cell Rep.* 27, 142-153.e4 (2019).

345. Nguyen, S. *et al.* Elite control of HIV is associated with distinct functional and transcriptional signatures in lymphoid tissue CD8+ T cells. *Sci. Transl. Med.* 11, (2019).

346. Angin, M. *et al.* Metabolic plasticity of HIV-specific CD8+ T cells is associated with enhanced antiviral potential and natural control of HIV-1 infection. *Nat. Metab.* 1, 704–716 (2019).

347. Potter, S. J. *et al.* Preserved Central Memory and Activated Effector Memory CD4 + T-Cell Subsets in Human Immunodeficiency Virus Controllers: an ANRS EP36 Study. *J. Virol.* 81, 13904–13915 (2007).

348. Laher, F. *et al.* HIV Controllers Exhibit Enhanced Frequencies of Major Histocompatibility Complex Class II Tetramer + Gag-Specific CD4 + T Cells in Chronic Clade C HIV-1 Infection. *J. Virol.* 91, (2017).

349. Vingert, B. *et al.* HIV Controller CD4+ T Cells Respond to Minimal Amounts of Gag Antigen Due to High TCR Avidity. *PLoS Pathog.* 6, e1000780 (2010).

350. Claireaux, M. *et al.* Low CCR5 expression protects HIV-specific CD4+ T cells of elite controllers from viral entry. *Nat. Commun.* 13, 521 (2022).

351. Morou, A. *et al.* Altered differentiation is central to HIV-specific CD4+ T cell dysfunction in progressive disease. *Nat. Immunol.* 20, 1059–1070 (2019).

352. Thobakgale, C. & Jost, S. Editorial: Innate immune responses in HIV controllers. *Front. Immunol.* 14, 1159278 (2023).

353. Coindre, S. *et al.* Mass Cytometry Analysis Reveals Complex Cell-State Modifications of Blood Myeloid Cells During HIV Infection. *Front. Immunol.* 10, 2677 (2019).

354. Pohlmeyer, C. W. *et al.* Identification of NK Cell Subpopulations That Differentiate HIV-Infected Subject Cohorts with Diverse Levels of Virus Control. *J. Virol.* 93, (2019).

355. Kant, S. *et al.* Quantifying Anti-HIV Envelope-Specific Antibodies in Plasma from HIV Infected Individuals. *Viruses* 11, 487 (2019).

356. Kant, S. *et al.* Polyfunctional Fc Dependent Activity of Antibodies to Native Trimeric Envelope in HIV Elite Controllers. *Front. Immunol.* 11, 583820 (2020).

357. Gasca-Capote, C. *et al.* The HIV-1 reservoir landscape in persistent elite controllers and transient elite controllers. *J. Clin. Investig.* (2024) doi:10.1172/jci174215.

358. Veenhuis, R. T. *et al.* Long-term remission despite clonal expansion of replication-competent HIV-1 isolates. *JCI Insight* 3, e122795 (2018).

359. Caetano, D. G. *et al.* Next-generation sequencing analyses of the emergence and maintenance of mutations in CTL epitopes in HIV controllers with differential viremia control. *Retrovirology* 15, 62 (2018).

360. Salgado, M. *et al.* Evolution of the HIV-1 nefgene in HLA-B*57 Positive Elite Suppressors. *Retrovirology* 7, 94 (2010).

361. Cruz, N. V. G., Amorim, R., Oliveira, F. E., Speranza, F. A. C. & Costa, L. J. Mutations in the nef and vif genes associated with progression to AIDS in elite controller and slow-progressor Patients. *J. Méd. Virol.* 85, 563–574 (2013).

362. Mann, J. K. *et al.* Ability of HIV-1 Nef to downregulate CD4 and HLA class I differs among viral subtypes. *Retrovirology* 10, 100 (2013).

363. Sabin, C. A. & Lundgren, J. D. The natural history of HIV infection. *Curr. Opin. HIV AIDS* 8, 311–317 (2013).

364. Colomer-Lluch, M., Ruiz, A., Moris, A. & Prado, J. G. Restriction Factors: From Intrinsic Viral Restriction to Shaping Cellular Immunity Against HIV-1. *Front. Immunol.* 9, 2876 (2018).

365. Grevenynghe, J. van *et al.* Transcription factor FOXO3a controls the persistence of memory CD4+ T cells during HIV infection. *Nat. Med.* 14, 266–274 (2008).

366. Archin, N. M. *et al.* Administration of vorinostat disrupts HIV-1 latency in patients on antiretroviral therapy. *Nature* 487, 482–485 (2012).

367. Gay, C. L. *et al.* Stable Latent HIV Infection and Low-level Viremia Despite Treatment With the Broadly Neutralizing Antibody VRC07-523LS and the Latency Reversal Agent Vorinostat. *J. Infect. Dis.* 225, 856–861 (2021).

368. Gruell, H. *et al.* Effect of 3BNC117 and romidepsin on the HIV-1 reservoir in people taking suppressive antiretroviral therapy (ROADMAP): a randomised, open-label, phase 2A trial. *Lancet Microbe* 3, e203–e214 (2022).

369. Gutiérrez, C. *et al.* Bryostatin-1 for latent virus reactivation in HIV-infected patients on antiretroviral therapy. *AIDS* 30, 1385–1392 (2016).

370. Kroon, E. D. M. B. *et al.* A randomized trial of vorinostat with treatment interruption after initiating antiretroviral therapy during acute HIV-1 infection. *J. Virus Erad.* 6, 100004 (2020).

371. McMahon, D. K. *et al.* A Phase 1/2 Randomized, Placebo-Controlled Trial of Romidespin in Persons With HIV-1 on Suppressive Antiretroviral Therapy. *J. Infect. Dis.* 224, 648–656 (2020).

372. Rasmussen, T. A. *et al.* Panobinostat, a histone deacetylase inhibitor, for latent-virus reactivation in HIV-infected patients on suppressive antiretroviral therapy: a phase 1/2, single group, clinical trial. *Lancet HIV* 1, e13–e21 (2014).

373. Marsden, M. D. *et al.* In vivo activation of latent HIV with a synthetic bryostatin analog effects both latent cell “kick” and “kill” in strategy for virus eradication. *PLoS Pathog.* 13, e1006575 (2017).

374. Yuan, Z. CROI 2024 Blockade of IFN-beta Reactivates HIV Reservoir in ART-Suppressed HIV-Infected BLT Humanized Mice. (2024).

375. Pernas, M. *et al.* Factors Leading to the Loss of Natural Elite Control of HIV-1 Infection. *J. Virol.* 92, (2018).

376. Siliciano, J. D. & Siliciano, R. F. HIV cure: The daunting scale of the problem. *Science* 383, 703–705 (2024).

377. Santos, J. d. CROI 2024 Trained Immunity in Monocytes Is Associated With Persistent Elite Controller Status. (2024).

378. Scott-Algara, D. *et al.* Cutting Edge: Increased NK Cell Activity in HIV-1-Exposed but Uninfected Vietnamese Intravascular Drug Users. *J. Immunol.* 171, 5663–5667 (2003).

379. Tomescu, C. *et al.* Impact of protective killer inhibitory receptor/human leukocyte antigen genotypes on natural killer cell and T-cell function in HIV-1-infected controllers. *AIDS* 26, 1869–1878 (2012).

380. Marras, F. *et al.* Control of the HIV-1 DNA Reservoir Is Associated In Vivo and In Vitro with NKp46/NKp30 (CD335 CD337) Inducibility and Interferon Gamma Production by Transcriptionally Unique NK Cells crossm. *Journal of Virology* 91, (2017).

381. Hua, S. *et al.* Pegylated Interferon-α–Induced Natural Killer Cell Activation Is Associated With Human Immunodeficiency Virus-1 DNA Decline in Antiretroviral Therapy–Treated HIV-1/Hepatitis C Virus–Coinfected Patients. *Clin. Infect. Dis.* 66, 1910–1917 (2017).

382. Papasavvas, E. *et al.* NK Response Correlates with HIV Decrease in Pegylated IFN-α2a–Treated Antiretroviral Therapy–Suppressed Subjects. *J. Immunol.* 203, 705–717 (2019).

383. F., H. B. *et al.* Immune-Correlates Analysis of an HIV-1 Vaccine Efficacy Trial. *N. Engl. J. Med.* 366, 1275–1286 (2012).

384. Barouch, D. H. *et al.* Protective efficacy of adenovirus/protein vaccines against SIV challenges in rhesus monkeys. *Science* 349, 320–324 (2015).

385. Alpert, M. D. *et al.* ADCC Develops Over Time during Persistent Infection with Live-Attenuated SIV and Is Associated with Complete Protection against SIVmac251 Challenge. *PLoS Pathog.* 8, e1002890 (2012).

386. Yates, N. L. *et al.* Vaccine-Induced Env V1-V2 IgG3 Correlates with Lower HIV-1 Infection Risk and Declines Soon After Vaccination. *Sci. Transl. Med.* 6, 228ra39 (2014).

387. Banks, N. D., Kinsey, N., Clements, J. & Hildreth, J. E. K. Sustained Antibody-Dependent Cell-Mediated Cytotoxicity (ADCC) in SIV-Infected Macaques Correlates with Delayed Progression to AIDS. *AIDS Res. Hum. Retroviruses* 18, 1197–1205 (2002).

388. Baum, L. L. *et al.* HIV-1 gp120-specific antibody-dependent cell-mediated cytotoxicity correlates with rate of disease progression. *J. Immunol.* 157, 2168–2173 (1996).

389. BROLIDEN, K. *et al.* Antibody-dependent cellular cytotoxicity and neutralizing activity in sera of HIV-1-infected mothers and their children. *Clin. Exp. Immunol.* 93, 56–64 (1993).

390. Cao, Y., Qin, L., Zhang, L., Safrit, J. & Ho, D. D. Virologic and Immunologic Characterization of Long-Term Survivors of Human Immunodeficiency Virus Type 1 Infection. 65–76 (1995) doi:10.1159/000424936.

391. Pantaleo, G. *et al.* Studies in Subjects with Long-Term Nonprogressive Human Immunodeficiency Virus Infection. *N. Engl. J. Med.* 332, 209–216 (1995).

392. Mens, H. *et al.* HIV-1 Continues To Replicate and Evolve in Patients with Natural Control of HIV Infection. *J. Virol.* 84, 12971–12981 (2010).

393. Miura, T. *et al.* Impaired Replication Capacity of Acute/Early Viruses in Persons Who Become HIV Controllers. *J. Virol.* 84, 7581–7591 (2010).

394. Casado, C. *et al.* Permanent control of HIV-1 pathogenesis in exceptional elite controllers: a model of spontaneous cure. *Sci. Rep.* 10, 1902 (2020).

395. Fellay, J. *et al.* A Whole-Genome Association Study of Major Determinants for Host Control of HIV-1. *Science* 317, 944–947 (2007).

396. Navarrete-Muñoz, M. A., Restrepo, C., Benito, J. M. & Rallón, N. Elite controllers: A heterogeneous group of HIV-infected patients. *Virulence* 11, 889–897 (2020).

397. Grabar, S. *et al.* Prevalence and comparative characteristics of long-term nonprogressors and HIV controller patients in the French Hospital Database on HIV. *AIDS* 23, 1163–1169 (2009).

398. Hatano, H. *et al.* Evidence for Persistent Low-Level Viremia in Individuals Who Control Human Immunodeficiency Virus in the Absence of Antiretroviral Therapy. *J. Virol.* 83, 329–335 (2009).

399. Pereyra, F. *et al.* Persistent Low-Level Viremia in HIV-1 Elite Controllers and Relationship to Immunologic Parameters. *J. Infect. Dis.* 200, 984–990 (2009).

400. Bailey, J. R., Williams, T. M., Siliciano, R. F. & Blankson, J. N. Maintenance of viral suppression in HIV-1–infected HLA-B*57+ elite suppressors despite CTL escape mutations. *J. Exp. Med.* 203, 1357–1369 (2006).

401. Altfeld, M. *et al.* Influence of HLA-B57 on clinical presentation and viral control during acute HIV-1 infection. *AIDS* 2581–2591 (2003).

402. May, M. E. *et al.* Combined Effects of HLA-B*57/5801 Elite Suppressor CD8+ T Cells and NK Cells on HIV-1 Replication. *Front. Cell. Infect. Microbiol.* 10, 113 (2020).

403. Emu, B. *et al.* HLA class I-restricted T-cell responses may contribute to the control of human immunodeficiency virus infection, but such responses are not always necessary for long-term virus control. *J. Virol.* 82, 5398–407 (2008).

404. Jansen, C. A. *et al.* High responsiveness of HLA-B57-restricted Gag-specific CD8+ T cells in vitro may contribute to the protective effect of HLA-B57 in HIV-infection. *Eur. J. Immunol.* 35, 150–158 (2005).

405. Collins, D. R. *et al.* Functional impairment of HIV-specific CD8+ T cells precedes aborted spontaneous control of viremia. *Immunity* 54, 2372-2384.e7 (2021).

406. Shi, Y. *et al.* The Role of Innate Immunity in Natural Elite Controllers of HIV-1 Infection. *Front. Immunol.* 13, 780922 (2022).

407. Sugawara, S., Reeves, R. K. & Jost, S. Learning to Be Elite: Lessons From HIV-1 Controllers and Animal Models on Trained Innate Immunity and Virus Suppression. *Front. Immunol.* 13, 858383 (2022).

408. Lanier, L. L. Up on the tightrope: natural killer cell activation and inhibition. *Nat. Immunol.* 9, 495–502 (2008).

409. Mikulak, J., Oriolo, F., Zaghi, E., Vito, C. D. & Mavilio, D. Natural killer cells in HIV-1 infection and therapy. *AIDS* 31, 2317–2330 (2017).

410. Bernard, N. F., Kant, S., Kiani, Z., Tremblay, C. & Dupuy, F. P. Natural Killer Cells in Antibody Independent and Antibody Dependent HIV Control. *Front. Immunol.* 13, 879124 (2022).

411. Martin, M. P. *et al.* Innate partnership of HLA-B and KIR3DL1 subtypes against HIV-1. *Nat. Genet.* 39, 733–740 (2007).

412. Martin, M. P. *et al.* Killer cell immunoglobulin-like receptor 3DL1 variation modifies HLA-B*57 protection against HIV-1. *J. Clin. Investig.* 128, 1903–1912 (2018).

413. Gumá, M. *et al.* Imprint of human cytomegalovirus infection on the NK cell receptor repertoire. *Blood* 104, 3664–3671 (2004).

414. Rückert, T., Lareau, C. A., Mashreghi, M.-F., Ludwig, L. S. & Romagnani, C. Clonal expansion and epigenetic inheritance of long-lasting NK cell memory. *Nat. Immunol.* 23, 1551–1563 (2022).

415. O'Connor, G. M., Holmes, A., Mulcahy, F. & Gardiner, C. M. Natural Killer cells from long-term non-progressor HIV patients are characterized by altered phenotype and function. *Clin. Immunol.* 124, 277–283 (2007).

416. Zhang, Z. *et al.* Changes in NK Cell Subsets and Receptor Expressions in HIV-1 Infected Chronic Patients and HIV Controllers. *Front. Immunol.* 12, 792775 (2021).

417. Davis-Gardner, M. E., Gardner, M. R., Alfant, B. & Farzan, M. eCD4-Ig promotes ADCC activity of sera from HIV-1-infected patients. *PLoS Pathog.* 13, e1006786 (2017).

418. Braanker, H. den, Bongenaar, M. & Lubberts, E. How to Prepare Spectral Flow Cytometry Datasets for High Dimensional Data Analysis: A Practical Workflow. *Front. Immunol.* 12, 768113 (2021).

419. Barnes, S., Schilizzi, O., Audsley, K. M., Newnes, H. V. & Foley, B. Deciphering the Immunological Phenomenon of Adaptive Natural Killer (NK) Cells and Cytomegalovirus (CMV). *Int. J. Mol. Sci.* 21, 8864 (2020).

420. Lopez-Vergès, S. *et al.* CD57 defines a functionally distinct population of mature NK cells in the human CD56dimCD16+ NK-cell subset. *Blood* 116, 3865–3874 (2010).

421. Gondois-Rey, F. *et al.* A Mature NK Profile at the Time of HIV Primary Infection Is Associated with an Early Response to cART. *Front. Immunol.* 8, 54 (2017).

422. Muntasell, A., Vilches, C., Angulo, A. & López-Botet, M. Adaptive reconfiguration of the human NK-cell compartment in response to cytomegalovirus: A different perspective of the host-pathogen interaction. *Eur. J. Immunol.* 43, 1133–1141 (2013).

423. Hearps, A. C. *et al.* Adaptive NK Cells Rapidly Expand during Acute HIV Infection and Persist Despite Early Initiation of Antiretroviral Therapy. *J. Immunol.* (2024) doi:10.4049/jimmunol.2300523.

424. Angelo, L. S. *et al.* Practical NK cell phenotyping and variability in healthy adults. *Immunol. Res.* 62, 341–356 (2015).

425. Kaulfuss, M. *et al.* The NK cell checkpoint NKG2A maintains expansion capacity of human NK cells. *Sci. Rep.* 13, 10555 (2023).

426. Jacobs, R. *et al.* CD56bright cells differ in their KIR repertoire and cytotoxic features from CD56dim NK cells. *Eur. J. Immunol.* 31, 3121–3126 (2001).

427. Poli, A. *et al.* CD56bright natural killer (NK) cells: an important NK cell subset. *Immunology* 126, 458–465 (2009).

428. Andrews, S. *et al.* FastQC. *FasQC.* https://qubeshub.org/resources/fastqc (2012).

429. Butler, A., Hoffman, P., Smibert, P., Papalexi, E. & Satija, R. Integrating single-cell transcriptomic data across different conditions, technologies, and species. *Nat. Biotechnol.* 36, 411–420 (2018).

430. Ewels, P., Magnusson, M., Lundin, S. & Käller, M. MultiQC: summarize analysis results for multiple tools and samples in a single report. *Bioinformatics* 32, 3047–3048 (2016).

431. Yang, C. *et al.* Heterogeneity of human bone marrow and blood natural killer cells defined by single-cell transcriptome. *Nat. Commun.* 10, 3931 (2019).

432. Kim, S.-H. *et al.* Enhancement of the Anticancer Ability of Natural Killer Cells through Allogeneic Mitochondrial Transfer. *Cancers* 15, 3225 (2023).

433. Cherrier, D. E., Serafini, N. & Santo, J. P. D. Innate Lymphoid Cell Development: A T Cell Perspective. *Immunity* 48, 1091–1103 (2018).

434. Duhan, V. *et al.* NK cell–intrinsic FcεRIγ limits CD8+ T-cell expansion and thereby turns an acute into a chronic viral infection. *PLoS Pathog.* 15, e1007797 (2019).

435. Altfeld, M. *et al.* HLA Alleles Associated with Delayed Progression to AIDS Contribute Strongly to the Initial CD8+ T Cell Response against HIV-1. *PLoS Med.* 3, e403 (2006).

436. Sáez-Cirión, A. *et al.* HIV controllers exhibit potent CD8 T cell capacity to suppress HIV infection ex vivo and peculiar cytotoxic T lymphocyte activation phenotype. *Proc. Natl. Acad. Sci.* 104, 6776–6781 (2007).

437. Mela, C. M. *et al.* Switch from inhibitory to activating NKG2 receptor expression in HIV-1 infection: lack of reversion with highly active antiretroviral therapy. *AIDS* 19, 1761–1769 (2005).

438. Pace, M. *et al.* Impact of antiretroviral therapy in primary HIV infection on natural killer cell function and the association with viral rebound and HIV DNA following treatment interruption. *Front. Immunol.* 13, 878743 (2022).

439. Nielsen, C. M., White, M. J., Goodier, M. R. & Riley, E. M. Functional Significance of CD57 Expression on Human NK Cells and Relevance to Disease. *Front. Immunol.* 4, 422 (2013).

440. Tomescu, C. *et al.* Identification of the predominant human NK cell effector subset mediating ADCC against HIV-infected targets coated with BNAbs or plasma from PLWH. *Eur. J. Immunol.* 51, 2051–2061 (2021).

441. Climent, N. *et al.* Immunological and virological findings in a patient with exceptional post-treatment control: a case report. *Lancet HIV* 10, e42–e51 (2023).

442. Kusumi, M. *et al.* Expression patterns of lectin-like natural killer receptors, inhibitory CD94/NKG2A, and activating CD94/NKG2C on decidual CD56bright natural killer cells differ from those on peripheral CD56dim natural killer cells. *J. Reprod. Immunol.* 70, 33–42 (2006).

443. Béziat, V. *et al.* Human NKG2A overrides NKG2C effector functions to prevent autoreactivity of NK cells. *Blood* 117, 4394–4396 (2011).

444. Davis, Z. B. *et al.* A Conserved HIV-1-Derived Peptide Presented by HLA-E Renders Infected T-cells Highly Susceptible to Attack by NKG2A/CD94-Bearing Natural Killer Cells. *PLoS Pathog.* 12, e1005421 (2016).

445. Ali, A. *et al.* Natural killer cell immunosuppressive function requires CXCR3-dependent redistribution within lymphoid tissues. *J Clin Invest*.

446. Hoehl, S., Berger, A., Ciesek, S. & Rabenau, H. F. Thirty years of CMV seroprevalence—a longitudinal analysis in a German university hospital. *Eur. J. Clin. Microbiol. Infect. Dis.* 39, 1095–1102 (2020).

447. Grønborg, H. L., Jespersen, S., Hønge, B. L., Jensen-Fangel, S. & Wejse, C. Review of cytomegalovirus coinfection in HIV-infected individuals in Africa. *Rev. Méd. Virol.* 27, e1907 (2017).

448. Albasanz-Puig, A. *et al.* Low frequency of cytomegalovirus (CMV) disease despite high prevalence of CMV viraemia in patients with advanced HIV infection: a clinical and immunological 48-week follow-up study. *HIV Med.* 22, 682–689 (2021).

449. Ackerman, M. E. *et al.* Polyfunctional HIV-Specific Antibody Responses Are Associated with Spontaneous HIV Control. *PLoS Pathog.* 12, e1005315 (2016).

450. Lambotte, O. *et al.* Heterogeneous neutralizing antibody and antibody-dependent cell cytotoxicity responses in HIV-1 elite controllers. *AIDS* 23, 897–906 (2009).

451. Wren, L. H. *et al.* Specific antibody-dependent cellular cytotoxicity responses associated with slow progression of HIV infection. *Immunology* 138, 116–123 (2013).

452. Kammers, K. *et al.* HIV Antibody Profiles in HIV Controllers and Persons With Treatment-Induced Viral Suppression. *Front. Immunol.* 12, 740395 (2021).

453. Astorga-Gamaza, A. *et al.* Identification of HIV-reservoir cells with reduced susceptibility to antibody-dependent immune response. *eLife* 11, e78294 (2022).

454. Vieillard, V., Fausther-Bovendo, H., Samri, A., Debré, P. & Group, F. A. à L. T. (ALT) A.-C. S. Specific Phenotypic and Functional Features of Natural Killer Cells From HIV-Infected Long-Term Nonprogressors and HIV Controllers. *JAIDS J. Acquir. Immune Defic. Syndr.* 53, 564–573 (2010).

455. Kuri-Cervantes, L., Oca, G. S., Ávila-Ríos, S., Hernández-Juan, R. & Reyes-Terán, G. Activation of NK cells is associated with HIV-1 disease progression. *J. Leukoc. Biol.* 96, 7–16 (2014).

456. Naranbhai, V. *et al.* Changes in Natural Killer Cell Activation and Function during Primary HIV-1 Infection. *PLoS ONE* 8, e53251 (2013).

457. Alter, G. *et al.* Single-Stranded RNA Derived from HIV-1 Serves as a Potent Activator of NK Cells. *J. Immunol.* 178, 7658–7666 (2007).

458. Fox, J. C. *et al.* Structural and agonist properties of XCL2, the other member of the C-chemokine subfamily. *Cytokine* 71, 302–311 (2015).

459. Guzzo, C. *et al.* The CD8-Derived Chemokine XCL1/Lymphotactin Is a Conformation-Dependent, Broad-Spectrum Inhibitor of HIV-1. *PLoS Pathog.* 9, e1003852 (2013).

460. Rasool, S. T. *et al.* Increased level of IL-32 during human immunodeficiency virus infection suppresses HIV replication. *Immunol. Lett.* 117, 161–167 (2008).

461. Ribeiro-Dias, F., Gomes, R. S., Silva, L. L. L., Santos, J. C. & Joosten, L. A. B. Interleukin 32: a novel player in the control of infectious diseases. *J. Leukoc. Biol.* 101, 39–52 (2017).

462. Jurczyszak, D. *et al.* ISG15 deficiency restricts HIV-1 infection. *PLoS Pathog.* 18, e1010405 (2022).

463. Mathieu, N. A., Paparisto, E., Barr, S. D. & Spratt, D. E. HERC5 and the ISGylation Pathway: Critical Modulators of the Antiviral Immune Response. *Viruses* 13, 1102 (2021).

464. Vittinghoff, E. *et al.* Combination Antiretroviral Therapy and Recent Declines in AIDS Incidence and Mortality. *J. Infect. Dis.* 179, 717–720 (1999).

465. Grau-Expósito, J. *et al.* Latency reversal agents affect differently the latent reservoir present in distinct CD4+ T subpopulations. *PLoS Pathog.* 15, e1007991 (2019).

466. Rothenberger, M. K. *et al.* Large number of rebounding/founder HIV variants emerge from multifocal infection in lymphatic tissues after treatment interruption. *Proc. Natl. Acad. Sci.* 112, E1126–E1134 (2015).

467. Jones, R. B. *et al.* Histone Deacetylase Inhibitors Impair the Elimination of HIV-Infected Cells by Cytotoxic T-Lymphocytes. *PLoS Pathog.* 10, e1004287 (2014).

468. Pace, M. *et al.* Histone Deacetylase Inhibitors Enhance CD4 T Cell Susceptibility to NK Cell Killing but Reduce NK Cell Function. *PLoS Pathog.* 12, e1005782 (2016).

469. Alrubayyi, A., Rowland-Jones, S. & Peppa, D. Natural killer cells during acute HIV-1 infection: clues for HIV-1 prevention and therapy. *AIDS* 36, 1903–1915 (2022).

470. Rezvani, K., Rouce, R., Liu, E. & Shpall, E. Engineering Natural Killer Cells for Cancer Immunotherapy. *Mol. Ther.* 25, 1769–1781 (2017).

471. D'Andrea, A. & Lanier, L. L. Specificity, Function, and Development of NK Cells, NK Cells: The Effector Arm of Innate Immunity. *Curr. Top. Microbiol. Immunol.* 230, 25–39 (1998).

472. Bryceson, Y. T., March, M. E., Ljunggren, H.-G. & Long, E. O. Synergy among receptors on resting NK cells for the activation of natural cytotoxicity and cytokine secretion. *Blood* 107, 159–66 (2006).

473. Horwitz, J. A. *et al.* Non-neutralizing Antibodies Alter the Course of HIV-1 Infection In Vivo. *Cell* 170, 637-648.e10 (2017).

474. Wang, W., Erbe, A. K., Hank, J. A., Morris, Z. S. & Sondel, P. M. NK Cell-Mediated Antibody-Dependent Cellular Cytotoxicity in Cancer Immunotherapy. *Front. Immunol.* 6, 368 (2015).

475. Gómez-Román, V. R. *et al.* Vaccine-Elicited Antibodies Mediate Antibody-Dependent Cellular Cytotoxicity Correlated with Significantly Reduced Acute Viremia in Rhesus Macaques Challenged with SIVmac251. *J. Immunol.* 174, 2185–2189 (2005).

476. Hessell, A. J. *et al.* Fc receptor but not complement binding is important in antibody protection against HIV. *Nature* 449, 101–104 (2007).

477. Hidajat, R. *et al.* Correlation of Vaccine-Elicited Systemic and Mucosal Nonneutralizing Antibody Activities with Reduced Acute Viremia following Intrarectal Simian Immunodeficiency Virus SIV mac251 Challenge of Rhesus Macaques. *J. Virol.* 83, 791–801 (2009).

478. Tuen, M. *et al.* Immune Correlates of Disease Progression in Linked HIV-1 Infection. *Front. Immunol.* 10, 1062 (2019).

479. Ding, S. *et al.* A Highly Conserved Residue of the HIV-1 gp120 Inner Domain Is Important for Antibody-Dependent Cellular Cytotoxicity Responses Mediated by Anti-cluster A Antibodies. *J. Virol.* 90, 2127–2134 (2016).

480. Veillette, M. *et al.* The HIV-1 gp120 CD4-Bound Conformation Is Preferentially Targeted by Antibody-Dependent Cellular Cytotoxicity-Mediating Antibodies in Sera from HIV-1-Infected Individuals. *J. Virol.* 89, 545–551 (2015).

481. Ferrari, G. *et al.* An HIV-1 gp120 Envelope Human Monoclonal Antibody That Recognizes a C1 Conformational Epitope Mediates Potent Antibody-Dependent Cellular Cytotoxicity (ADCC) Activity and Defines a Common ADCC Epitope in Human HIV-1 Serum. *J. Virol.* 85, 7029–7036 (2011).

482. Tolbert, W. D. *et al.* Paring Down HIV Env: Design and Crystal Structure of a Stabilized Inner Domain of HIV-1 gp120 Displaying a Major ADCC Target of the A32 Region. *Structure* 24, 697–709 (2016).

483. Lewis, G. K., Pazgier, M. & DeVico, A. L. Survivors Remorse: antibody-mediated protection against HIV-1. *Immunol. Rev.* 275, 271–284 (2017).

484. Trkola, A., Matthews, J., Gordon, C., Ketas, T. & Moore, J. P. A Cell Line-Based Neutralization Assay for Primary Human Immunodeficiency Virus Type 1 Isolates That Use either the CCR5 or the CXCR4 Coreceptor. *J. Virol.* 73, 8966–8974 (1999).

485. Gómez-Román, V. R. *et al.* A simplified method for the rapid fluorometric assessment of antibody-dependent cell-mediated cytotoxicity. *J. Immunol. Methods* 308, 53–67 (2006).

486. Nabatanzi, R., Cose, S., Joloba, M., Jones, S. R. & Nakanjako, D. Effects of HIV infection and ART on phenotype and function of circulating monocytes, natural killer, and innate lymphoid cells. *AIDS Res. Ther.* 15, 7 (2018).

487. Astorga-Gamaza, A. *et al.* KLRG1 expression on natural killer cells is associated with HIV persistence, and its targeting promotes the reduction of the viral reservoir. *Cell Rep. Med.* 4, 101202 (2023).

488. Board, N. L. *et al.* Bispecific antibodies promote natural killer cell-mediated elimination of HIV-1 reservoir cells. *Nat. Immunol.* 1–9 (2024) doi:10.1038/s41590-023-01741-5.

489. Abeynaike, S. A. *et al.* Human Hematopoietic Stem Cell Engrafted IL-15 Transgenic NSG Mice Support Robust NK Cell Responses and Sustained HIV-1 Infection. *Viruses* 15, 365 (2023).

490. Björkström, N. K. *et al.* Expression patterns of NKG2A, KIR, and CD57 define a process of CD56dim NK-cell differentiation uncoupled from NK-cell education. *Blood* 116, 3853–3864 (2010).

491. Bi, J. & Tian, Z. NK Cell Exhaustion. *Front. Immunol.* 8, 760 (2017).

492. Azzoni, L. *et al.* Sustained Impairment of IFN-γ Secretion in Suppressed HIV-Infected Patients Despite Mature NK Cell Recovery: Evidence for a Defective Reconstitution of Innate Immunity. *J. Immunol.* 168, 5764–5770 (2002).

493. Chehimi, J. *et al.* Baseline Viral Load and Immune Activation Determine the Extent of Reconstitution of Innate Immune Effectors in HIV-1-Infected Subjects Undergoing Antiretroviral Treatment. *J. Immunol.* 179, 2642–2650 (2007).

494. Elliott, J. H. *et al.* Activation of HIV Transcription with Short-Course Vorinostat in HIV-Infected Patients on Suppressive Antiretroviral Therapy. *PLoS Pathog.* 10, e1004473 (2014).

495. Søgaard, O. S. *et al.* The Depsipeptide Romidepsin Reverses HIV-1 Latency In Vivo. *PLoS Pathog.* 11, e1005142 (2015).

496. Astorga-Gamaza, A. *et al.* Antibody cooperative adsorption onto AuNPs and its exploitation to force natural killer cells to kill HIV-infected T cells. *Nano Today* 36, 101056 (2021).

497. Borrow, P. *et al.* Antiviral pressure exerted by HIV-l-specific cytotoxic T lymphocytes (CTLs) during primary infection demonstrated by rapid selection of CTL escape virus. *Nat. Med.* 3, 205–211 (1997).

498. Deng, K. *et al.* Broad CTL response is required to clear latent HIV-1 due to dominance of escape mutations. *Nature* 517, 381–385 (2015).

499. Liu, M. K. P. *et al.* Vertical T cell immunodominance and epitope entropy determine HIV-1 escape. *J. Clin. Investig.* 123, 380–393 (2013).

500. Phillips, R. E. *et al.* Human immunodeficiency virus genetic variation that can escape cytotoxic T cell recognition. *Nature* 354, 453–459 (1991).

501. Karpel, M. E., Boutwell, C. L. & Allen, T. M. BLT humanized mice as a small animal model of HIV infection. *Curr. Opin. Virol.* 13, 75–80 (2015).

502. Denton, P. W. *et al.* Generation of HIV Latency in Humanized BLT Mice. *J. Virol.* 86, 630–634 (2012).

503. Wu, Y., Tian, Z. & Wei, H. Developmental and Functional Control of Natural Killer Cells by Cytokines. *Front. Immunol.* 8, 930 (2017).

504. Eisenman, J. *et al.* INTERLEUKIN-15 INTERACTIONS WITH INTERLEUKIN-15 RECEPTOR COMPLEXES: CHARACTERIZATION AND SPECIES SPECIFICITY. *Cytokine* 20, 121–129 (2002).

505. Scully, E. & Alter, G. NK Cells in HIV Disease. *Curr. HIVAIDS Rep.* 13, 85–94 (2016).

506. Chen, X. *et al.* The Early Antibody-Dependent Cell-Mediated Cytotoxicity Response Is Associated With Lower Viral Set Point in Individuals With Primary HIV Infection. *Front. Immunol.* 9, 2322 (2018).

507. Goyal, A. *et al.* Estimation of the in vivo neutralization potency of eCD4Ig and conditions for AAV-mediated production for SHIV long-term remission. *Sci. Adv.* 8, eabj5666 (2022).

508. Fritschi, C. J. *et al.* Indoline CD4-mimetic compounds mediate potent and broad HIV-1 inhibition and sensitization to antibody-dependent cellular cytotoxicity. *Proc. Natl. Acad. Sci. United States Am.* 120, e2222073120 (2023).

509. Rajashekar, J. K. *et al.* Modulating HIV-1 envelope glycoprotein conformation to decrease the HIV-1 reservoir. *Cell Host Microbe* 29, 904-916.e6 (2021).

510. Laumaea, A. *et al.* Small CD4 mimetics sensitize HIV-1-infected macrophages to antibody-dependent cellular cytotoxicity. *Cell Rep.* 42, 111983 (2023).

511. Williams, B. G., Lima, V. & Gouws, E. Modelling the Impact of Antiretroviral Therapy on the Epidemic of HIV. *Curr. HIV Res.* 9, 367–382 (2011).

512. Massanella, M. *et al.* Long-term effects of early antiretroviral initiation on HIV reservoir markers: a longitudinal analysis of the MERLIN clinical study. *Lancet Microbe* 2, e198–e209 (2021).

513. Leyre, L. *et al.* Abundant HIV-infected cells in blood and tissues are rapidly cleared upon ART initiation during acute HIV infection. *Sci. Transl. Med.* 12, (2020).

514. Colby, D. J. *et al.* Rapid HIV RNA rebound after antiretroviral treatment interruption in persons durably suppressed in Fiebig I acute HIV infection. *Nat. Med.* 24, 923–926 (2018).

515. Siliciano, J. D. & Siliciano, R. F. In Vivo Dynamics of the Latent Reservoir for HIV-1: New Insights and Implications for Cure. *Annu. Rev. Pathol.: Mech. Dis.* 17, 1–24 (2021).

516. amfAR. Curing HIV—How Far Have We Come? https://www.amfar.org/news/how-many-have-been-cured/.

517. Persaud, D. CROI 2024 ART-Free HIV-1 Remission in Very Early Treated Children: Results From IMPAACT P1115. (2024).

518. Wang, B. Viral Factors in Non-Progression. *Front. Immunol.* 4, 355 (2013).

519. Zaunders, J. & Bockel, D. van. Innate and Adaptive Immunity in Long-Term Non-Progression in HIV Disease. *Front. Immunol.* 4, 95 (2013).

520. Plaeger-Marshall, S. *et al.* Alterations in cytotoxic and phenotypic subsets of natural killer cells in acquired immune deficiency syndrome (AIDS). *J. Clin. Immunol.* 7, 16–23 (1987).

521. Santos, J. C. D. CROI 2023 Trained immunity features in NK cells of HIV-1 Elite Controllers. (2023).

522. Ramsuran, V. *et al.* Elevated HLA-A expression impairs HIV control through inhibition of NKG2A-expressing cells. *Sci. (N. York, NY)* 359, 86–90 (2018).

523. Sáez-Cirión, A. *et al.* Heterogeneity in HIV Suppression by CD8 T Cells from HIV Controllers: Association with Gag-Specific CD8 T Cell Responses. *J. Immunol.* 182, 7828–7837 (2009).

524. Pereyra, F. *et al.* Genetic and Immunologic Heterogeneity among Persons Who Control HIV Infection in the Absence of Therapy. *J. Infect. Dis.* 197, 563–571 (2008).

525. Lambotte, O. *et al.* High Antibody-Dependent Cellular Cytotoxicity Responses Are Correlated with Strong CD8 T Cell Viral Suppressive Activity but Not with B57 Status in HIV-1 Elite Controllers. *PLoS ONE* 8, e74855 (2013).

526. Gaiha, G. CROI 2023 Elite Controllers with distinct viral reservoir have robust CTL to networked epitopes. (2023).

527. Almeida, J. R. *et al.* Superior control of HIV-1 replication by CD8+ T cells is reflected by their avidity, polyfunctionality, and clonal turnover. *J. Exp. Med.* 204, 2473–2485 (2007).

528. Aasa-Chapman, M. M. I. *et al.* Detection of Antibody-Dependent Complement-Mediated Inactivation of both Autologous and Heterologous Virus in Primary Human Immunodeficiency Virus Type 1 Infection. *J. Virol.* 79, 2823–2830 (2005).

529. Tyler, D. S. *et al.* Alterations in antibody-dependent cellular cytotoxicity during the course of HIV-1 infection. Humoral and cellular defects. *J. Immunol. (Baltim., Md : 1950)* 144, 3375–84 (1990).

530. Ljunggren, K. *et al.* Antibodies Mediating Cellular Cytotoxicity and Neutralization Correlate with a Better Clinical Stage in Children Born to Human Immunodeficiency Virus-Infected Mothers. *J. Infect. Dis.* 161, 198–202 (1990).

531. Ahmad, R. *et al.* Evidence for a Correlation Between Antibody-Dependent Cellular Cytotoxicity-Mediating Anti-HIV-1 Antibodies and Prognostic Predictors of HIV Infection. *J. Clin. Immunol.* 21, 227–233 (2001).

532. Wada, R., Matsui, M. & Kawasaki, N. Influence of N-glycosylation on effector functions and thermal stability of glycoengineered IgG1 monoclonal antibody with homogeneous glycoforms. *mAbs* 11, 350–372 (2019).

533. Ackerman, M. E. *et al.* Natural variation in Fc glycosylation of HIV-specific antibodies impacts antiviral activity. *J. Clin. Investig.* 123, 2183–2192 (2013).

534. Peipp, M. *et al.* Antibody fucosylation differentially impacts cytotoxicity mediated by NK and PMN effector cells. *Blood* 112, 2390–2399 (2008).

535. Brelot, A. & Chakrabarti, L. A. CCR5 Revisited: How Mechanisms of HIV Entry Govern AIDS Pathogenesis. *J. Mol. Biol.* 430, 2557–2589 (2018).

536. Quillent, C. *et al.* HIV-1-resistance phenotype conferred by combination of two separate inherited mutations of CCR5 gene. *Lancet* 351, 14–18 (1998).

537. Claiborne, D. CROI 2020 Efficient deletion of CCR5 provides complete protection against HIV in xenograft mice. (2020).

538. Singh, V., Dashti, A., Mavigner, M. & Chahroudi, A. Latency Reversal 2.0: Giving the Immune System a Seat at the Table. *Curr. HIVAIDS Rep.* 18, 117–127 (2021).

539. Mascola, J. R. & Haynes, B. F. HIV-1 neutralizing antibodies: understanding nature's pathways. *Immunol. Rev.* 254, 225–244 (2013).

540. Barouch, D. H. *et al.* Therapeutic efficacy of potent neutralizing HIV-1-specific monoclonal antibodies in SHIV-infected rhesus monkeys. *Nature* 503, 224–228 (2013).

541. Lynch, R. M. *et al.* Virologic effects of broadly neutralizing antibody VRC01 administration during chronic HIV-1 infection. *Sci. Transl. Med.* 7, 319ra206 (2015).

542. Mendoza, P. *et al.* Combination therapy with anti-HIV-1 antibodies maintains viral suppression. *Nature* 561, 479–484 (2018).

543. Fabozzi, G., Pegu, A., Koup, R. A. & Petrovas, C. Bispecific antibodies: Potential immunotherapies for HIV treatment. *Methods* 154, 118–124 (2019).

544. Lu, C.-L. *et al.* Enhanced clearance of HIV-1–infected cells by broadly neutralizing antibodies against HIV-1 in vivo. *Science* 352, 1001–1004 (2016).

545. Moldt, B. *et al.* Highly potent HIV-specific antibody neutralization in vitro translates into effective protection against mucosal SHIV challenge in vivo. *Proc. Natl. Acad. Sci.* 109, 18921–18925 (2012).

546. Pegu, A. *et al.* Neutralizing antibodies to HIV-1 envelope protect more effectively in vivo than those to the CD4 receptor. *Sci. Transl. Med.* 6, 243ra88 (2014).

547. Borducchi, E. N. *et al.* Antibody and TLR7 agonist delay viral rebound in SHIV-infected monkeys. *Nature* 563, 360–364 (2018).

548. Shingai, M. *et al.* Passive transfer of modest titers of potent and broadly neutralizing anti-HIV monoclonal antibodies block SHIV infection in macaques. *J. Exp. Med.* 211, 2061–2074 (2014).

549. Shingai, M. *et al.* Antibody-mediated immunotherapy of macaques chronically infected with SHIV suppresses viraemia. *Nature* 503, 277–280 (2013).

550. Halper-Stromberg, A. *et al.* Broadly Neutralizing Antibodies and Viral Inducers Decrease Rebound from HIV-1 Latent Reservoirs in Humanized Mice. *Cell* 158, 989–999 (2014).

551. Scheid, J. F. *et al.* HIV-1 antibody 3BNC117 suppresses viral rebound in humans during treatment interruption. *Nature* 535, 556–560 (2016).

552. Huang, Y. *et al.* Engineered Bispecific Antibodies with Exquisite HIV-1-Neutralizing Activity. *Cell* 165, 1621–1631 (2016).

553. Sun, Y. *et al.* Bispecific antibodies in cancer therapy: Target selection and regulatory requirements. *Acta Pharm. Sin. B* 13, 3583–3597 (2023).

554. Mengistu, M., Ray, K., Lewis, G. K. & DeVico, A. L. Antigenic Properties of the Human Immunodeficiency Virus Envelope Glycoprotein Gp120 on Virions Bound to Target Cells. *PLoS Pathog.* 11, e1004772 (2015).

555. Moore, J. P. *et al.* Exploration of antigenic variation in gp120 from clades A through F of human immunodeficiency virus type 1 by using monoclonal antibodies. *J. Virol.* 68, 8350–8364 (1994).

556. Ramadoss, N. S. *et al.* Enhancing natural killer cell function with gp41-targeting bispecific antibodies to combat HIV infection. *AIDS* 34, 1313–1323 (2020).

557. Pollara, J. *et al.* Redirection of Cord Blood T Cells and Natural Killer Cells for Elimination of Autologous HIV-1-Infected Target Cells Using Bispecific DART® Molecules. *Front. Immunol.* 11, 713 (2020).

558. Kim, J. T., Bresson-Tan, G. & Zack, J. A. Current Advances in Humanized Mouse Models for Studying NK Cells and HIV Infection. *Microorganisms* 11, 1984 (2023).

559. Adams, P. *et al.* CD32+CD4+ memory T cells are enriched for total HIV-1 DNA in tissues from humanized mice. *iScience* 24, 101881 (2021).

560. Herzig, E. *et al.* Attacking Latent HIV with convertibleCAR-T Cells, a Highly Adaptable Killing Platform. *Cell* 179, 880-894.e10 (2019).

561. Veillette, M. *et al.* Interaction with Cellular CD4 Exposes HIV-1 Envelope Epitopes Targeted by Antibody-Dependent Cell-Mediated Cytotoxicity. *J. Virol.* 88, 2633–2644 (2014).

562. Prévost, J. *et al.* Influence of the Envelope gp120 Phe 43 Cavity on HIV-1 Sensitivity to Antibody-Dependent Cell-Mediated Cytotoxicity Responses. *J. Virol.* 91, (2017).

563. Richard, J. *et al.* CD4 mimetics sensitize HIV-1-infected cells to ADCC. *Proc. Natl. Acad. Sci.* 112, E2687–E2694 (2015).

564. Nieto, Y. *et al.* Innate Cell Engager AFM13 Combined with Preactivated and Expanded Cord Blood-Derived NK Cells for Patients with Double Refractory CD30+ Lymphoma. *Blood* 140, 415–416 (2022).

565. Kerbauy, L. N. *et al.* Combining AFM13, a Bispecific CD30/CD16 Antibody, with Cytokine-Activated Blood and Cord Blood–Derived NK Cells Facilitates CAR-like Responses Against CD30+ Malignancies. *Clin. Cancer Res.* 27, 3744–3756 (2021).

566. Phung, C. D., Tran, T. H. & Kim, J. O. Engineered nanoparticles to enhance natural killer cell activity towards onco-immunotherapy: a review. *Arch. Pharmacal Res.* 43, 32–45 (2020).

7. PUBLICATIONS

7 Publications

Grau-Expósito J*, **Sánchez-Gaona N***, Massana N, et al. Peripheral and lung resident memory T cell responses against SARS-CoV-2. *Nat Commun*. 2021;12(1):3010. Published 2021 May 21. doi: 10.1038/s41467-021-23333-3.

Álvarez-Sierra D, **Sánchez-Gaona N**, Cruz M, et al. Thyroid cells from normal and autoimmune thyroid glands suppress T lymphocytes proliferation upon contact revealing a new regulatory inhibitory type of interaction independent of PD1/PDL1. *J Autoimmun*. 2023 Apr:136:103013. Published 2023 February 27. doi: 10.1016/j.jaut.2023.103013.

Astorga-Gamaza A, Perea D, **Sánchez-Gaona N**, et al. KLRG1 expression on natural killer cells is associated with HIV persistence, and its targeting promotes the reduction of the viral reservoir. *Cell Rep Med*. 2023 Oct 17;4(10):101202. Published 2023 October 17. doi: 10.1016/j.xcrm.2023.101202.